

**Role of IL-10 and β -catenin signaling
in dendritic cells
during acute and latent mCMV infection**

Dissertation

zur Erlangung des akademischen Grades

doctor rerum naturalium

(Dr. rer. nat.)

am Fachbereich Biologie der
Johannes Gutenberg-Universität Mainz

vorgelegt von

Josephin Schwarz

geboren am 02.06.1988 in Torgau

Mainz, Juli 2022

Die vorliegende Arbeit wurde am [REDACTED]
[REDACTED] in der Zeit vom Oktober 2018 bis Dezember 2021 unter
der Leitung von [REDACTED] angefertigt.

Dekan:

1. Berichterstatter:
2. Berichterstatter:

Tag der mündlichen Prüfung:

Für meine Eltern!

In Liebe und Dankbarkeit!

Table of contents

Table of contents	i
Summary	iii
Zusammenfassung	v
List of Abbreviations	vii
1 Introduction	1
1.1 Cytomegalovirus	1
1.1.1 Morphology and replication	1
1.1.2 Latency and reactivation	3
1.1.3 Clinical relevance of hCMV infection	4
1.1.4 mCMV infection as model system as hCMV	5
1.1.5 Immunological control of mCMV infection	5
1.1.6 Immune evasion strategies	6
1.2 Dendritic cells and their role in immune response	7
1.2.1 Characterizing DC in lung, lymph node and spleen	8
1.2.2 DC in mCMV infection	11
1.3 Importance of CD8 ⁺ T cells	12
1.3.1 Differentiation of CD8 ⁺ T cells	13
1.4 Relation of Treg and mCMV infection	16
1.4.1 Development and function of Treg	16
1.4.2 CD4 Treg	17
1.4.3 CD8 Treg	18
1.4.4 Treg in mCMV infection	19
1.5 IL-10 function	20
1.5.1 IL-10 receptor and signaling	21
1.5.2 IL-10 in infectious disease	22
1.6 β -catenin/Wnt signaling pathway	23
1.6.1 β -catenin signaling in DC shape the immune response	24
1.7 Objectives	25
2 Materials and Methods	27
2.1 Chemicals and buffers	27
2.2 Molecular biology	28
2.2.1 Isolation of genomic DNA from biopsies	28
2.2.2 Polymerase Chain Reaction (PCR)	28
2.2.3 Agarose gel electrophoresis	30
2.2.4 Isolation of viral DNA	30
2.2.5 Quantification of DNA	30
2.2.6 Quantitative PCR (qPCR)	30
2.3 Cell biology	32
2.3.1 Preparation of single cell suspensions from lung and lymphoid organs	32
2.3.2 Preparation of blood cells	32
2.3.3 Cell counting	33
2.3.4 Flow cytometry	33
2.3.5 mCMV	34
2.4 Mouse experiments	35

2.4.1	Mice.....	35
2.4.2	Infection with mCMV.....	35
2.4.3	Statistical analysis and software.....	36
3	Results	37
3.1	Establishment of intranasal mCMV infection model	37
3.2	The influence of IL-10 on DC during mCMV infection	38
3.2.1	IL-10 production by DC does not play an essential role during acute mCMV infection	39
3.2.2	IL-10 signaling in DC has no impact on acute mCMV infection	45
3.3	The role of β -catenin in DC during mCMV infection	52
3.3.1	Deletion of β -catenin in DC does not play a crucial role during acute mCMV infection.....	53
3.3.2	Intranasal mCMV infection results in reduced splenic DC numbers in β -cat ^{CD11c/EX3} mice accompanied by an expansion of XCR-1 ⁺ cDC1	60
3.4	mCMV latency.....	67
3.4.1	IL-10 signaling in DC reveals unaltered memory CD8 ⁺ T cell inflation during latent mCMV infection.....	67
3.4.2	β -catenin signaling impacts the virus-specific memory CD8 ⁺ T cell response accompanied by an expansion of Treg during latent infection.....	81
4	Discussion and Outlook.....	96
4.1	Intranasal infection route	96
4.2	The role of IL-10 in DC during mCMV infection.....	98
4.2.1	IL-10 production during acute mCMV infection.....	98
4.2.2	IL-10R signaling during latent mCMV infection	101
4.3	The role of β -catenin in DC during mCMV infection	102
4.3.1	β -catenin signaling during acute mCMV infection.....	102
4.3.2	β -catenin signaling during latent mCMV infection	106
5	Supplement	110
6	References	119
7	Curriculum Vitae.....	163
8	Scientific Achievements.....	164
9	Acknowledgements	165
10	Eidesstattliche Erklärung.....	166

Summary

Dendritic cells (DC) are the most important antigen-presenting cells of the immune system and play a central role in the initiation of an anti-viral immune response by driving effector T cell (Teff) activation and regulatory T cell (Treg) induction. IL-10 is an essential regulatory cytokine during mutual interaction between Teff, Treg and DC during immunity to infection. During latent mCMV infection IL-10 limited the CD8⁺ T cell expansion but to what extent DC are targets or relevant sources of IL-10 during mCMV infection remains elusive. Another pathway associated with a tolerogenic DC function is the β -catenin signaling pathway. The stabilization of β -catenin in DC mediated a pro-inflammatory function and promoted the development of CD8⁺ T cell responses in the context of a viral infection but whether and to what extent β -catenin signaling in DC affects the immunity and persistence of mCMV is not known. To investigate the role of IL-10 production by DC and IL-10 as well as β -catenin signaling in DC during acute and latent mCMV infection, we used transgenic mice with a CD11c-specific deficiency of IL-10, IL-10R and β -catenin or expression of a stabilized form of β -catenin in CD11c⁺ cells (referred to as IL-10^{ACD11c}, IL-10R^{ACD11c}, β -cat^{ACD11c} and β -cat^{ACD11c/EX3} mice).

First, we established an intranasal (i.n.) mCMV infection model more closely reflecting the natural route of infection. For this purpose, we determined the CD8⁺ T cell response by MHC-I-specific Tetramer staining and observed a maximum frequency of M38 Tetramer binding mCMV-specific CD8⁺ T cells at 14 days post infection (p.i.), while the M45 Tetramer response was much weaker and peaked at 7 days p.i.. Based on these findings, we examined the role of DC in β -catenin and IL-10 signaling during acute mCMV infection 14 days p.i. using the M38 Tetramer. After acute mCMV infection, no significant differences in the magnitude of the mCMV-specific CD8⁺ T cell responses and Treg differentiation were detected in IL-10^{ACD11c} and IL-10R^{ACD11c} mice. Moreover, latently infected IL-10R^{ACD11c} mice showed neither an influence nor a memory inflation (MI) of mCMV-specific CD8⁺ T cells. These results indicate that DC IL-10 production and signaling does not play an essential role in the regulation of anti-viral CD8⁺ T cell responses during acute and/or latent mCMV infection. Furthermore, the deletion of β -catenin in CD11c⁺ cells did not affect the mCMV-specific CD8⁺ T cell response and Treg differentiation, while the stabilization of β -catenin in CD11c⁺ cells resulted in a significant expansion of FoxP3⁺ CD4 Treg in the steady state as well as during acute mCMV infection. This expansion of Treg numbers was due to higher numbers of thymus-derived FoxP3⁺ CD4 Treg. In β -cat^{CD11c/EX3}, splenic DC exhibited a shift toward

increased XCR-1⁺ cDC1 and diminished CD172 α ⁺ cDC2. The mCMV-specific CD8⁺ T cell response showed similar expansion in β -cat^{CD11c/EX3} and control mice, whereas the mCMV-specific CD8⁺ T cell subpopulations revealed a modification in the distribution of pulmonary effector memory CD8⁺ T cells. Therefore, we investigated the impact of β -catenin signaling in latently infected β -cat^{CD11c/EX3} mice. The mCMV-specific CD8⁺ T cell response was comparable in β -cat^{CD11c/EX3} compared to control mice and revealed no MI, while the further fractionation into subpopulations displayed a shift toward increased conventional effector memory T cells (cTEM) and reduced double-positive effector T cells (DPEC) in lung and spleen of β -cat^{CD11c/EX3} mice, associated by increased FoxP3⁺ CD4 Treg. These data suggest an important role of β -catenin in DC for the induction of FoxP3⁺ CD4 Treg and possibly CD8⁺ memory T cells during mCMV infection.

Zusammenfassung

Dendritische Zellen (DC) sind die wichtigsten Antigen-präsentierenden Zellen des Immunsystems und spielen eine zentrale Rolle bei der Initiierung einer antiviralen Immunantwort, indem sie die Aktivierung von Effektor T Zellen und die Induktion von regulatorischen T Zellen (Treg) vorantreiben. IL-10 ist ein essentielles regulatorisches Zytokin bei der gegenseitigen Interaktion zwischen Teff, Treg und DC während der Immunität gegen Infektionen. Während einer latenten mCMV Infektion begrenzte IL-10 die CD8⁺ T Zell-Expansion, aber inwieweit DC während einer mCMV Infektion Zielzellen oder relevante Quellen von IL-10 sind, ist jedoch unklar. Ein weiterer Signalweg, der mit einer tolerogenen DC-Funktion assoziiert ist, ist der β -Catenin Signalweg. Die Stabilisierung von β -Catenin in DC vermittelte eine proinflammatorische Funktion und förderte die Entwicklung der CD8⁺ T Zellantworten im Kontext einer viralen Infektion, aber ob und in welchem Ausmaß die β -Catenin Signalgebung in DC die Immunität und Persistenz von mCMV beeinflusst, ist nicht bekannt. Um die Rolle der IL-10 Produktion von DC und der IL-10 und der β -Catenin Signalisierung in DC während der akuten und latenten mCMV-Infektion zu untersuchen, haben wir transgene Mäuse analysiert, in denen die Expression von IL-10, IL-10R und β -Catenin auf CD11c⁺ Zellen ausgeschaltet oder eine stabilisierte Form von β -Catenin in CD11c⁺ Zellen exprimiert wurde (benannt als IL-10^{ACD11c}, IL-10R^{ACD11c}, β -cat^{ACD11c} und β -cat^{ACD11c/EX3} Mäuse).

Zunächst etablierten wir ein intranasales (i.n.) mCMV-Infektionsmodell, welches die natürliche Infektionsroute widerspiegelt. Zu diesem Zweck bestimmten wir die CD8⁺ T Zellantwort mit Hilfe der MHC-I-spezifischen Tetramer-Färbung und beobachteten eine maximale Frequenz von M38 Tetramer-bindenden mCMV-spezifischen CD8⁺ T Zellen 14 Tage nach der Infektion, während die M45 Tetramer-Antwort geringer war und ihr Maximum 7 Tage nach der Infektion erreichte. Aufgrund dieser Ergebnisse untersuchten wir die Rolle der IL-10 und β -Catenin Signalisierung in DC während der akuten mCMV Infektion 14 Tage nach der Infektion unter der Verwendung des M38 Tetramers. Nach der akuten mCMV-Infektion wurden keine signifikanten Unterschiede in der mCMV-spezifischen CD8⁺ T Zellantwort und der Treg Differenzierung in IL-10^{ACD11c} und IL-10R^{ACD11c} Mäusen festgestellt. Zudem zeigten latent infizierte IL-10^{ACD11c} Mäuse weder eine 'memory inflation' noch einen Einfluss auf die mCMV-spezifische CD8⁺ T Zellantwort. Diese Ergebnisse deuten darauf hin, dass die DC IL-10 Produktion und Signalisierung in der akuten und/oder latenten Immunantwort keine wesentliche Rolle spielen. Des Weiteren hatte die Deletion von β -Catenin in CD11c⁺ Zellen

keinen Einfluss auf die mCMV-spezifische CD8⁺ T Zellantwort und die Treg Differenzierung, wohingegen die Stabilisierung von β -Catenin in CD11c⁺ Zellen zu einem erheblichen Anstieg der FoxP3⁺ CD4 Treg sowohl in nicht-infizierten als auch in akut mCMV-infizierten Mäusen führte. Die Zunahme dieser Treg war auf eine höhere Anzahl von FoxP3⁺ CD4 Treg aus dem Thymus zurückzuführen. In den β -cat^{ΔCD11c/EX3} Mäusen wiesen die DC in der Milz eine Verschiebung zu mehr XCR-1⁺ cDC1 und weniger CD172α⁺ cDC2 auf. Zudem zeigte die mCMV-spezifische CD8⁺ T Zellantwort einen ähnlichen Verlauf in β -cat^{ΔCD11c/EX3} und Kontrollmäusen, während die mCMV-spezifischen CD8⁺ T Subpopulationen eine Veränderung in der Verteilung der pulmonalen Effektor-Gedächtnis CD8⁺ T Zellen aufwiesen. Aufgrund dessen untersuchten wir den Einfluss von β -Catenin in latent infizierten β -cat^{ΔCD11c/EX3} Mäusen. Die mCMV-spezifische CD8⁺ T Zellantwort war bei den β -cat^{ΔCD11c/EX3} und Kontrollmäusen vergleichbar und zeigte keine 'memory inflation', während eine weitere Fraktionierung der Subpopulationen eine Verschiebung zu mehr konventionellen Effektor-Gedächtnis T Zellen (cTEM) und weniger doppelt positiven Effektor T Zellen (DPEC) in der Lunge und Milz von β -cat^{ΔCD11c/EX3} Mäusen aufwies, was mit einer Zunahme von FoxP3⁺ CD4 Treg einherging. Die Daten deuten auf eine wichtige Rolle von β -Catenin in DC für die Induktion von FoxP3⁺ CD4 Treg und möglicherweise CD8⁺ Gedächtnis T Zellen während einer mCMV Infektion hin.

List of Abbreviations

AAD	allergic airway disease
Ag	antigen
AIDS	acquired immunodeficiency syndrome
AM	alveolar macrophage
APC	antigen-presenting cell or Adenomatous Polyposis Coli
Batf	basic leucine zipper ATF-like
BM	bone marrow
BMDC	bone marrow-derived dendritic cell
BMT	bone marrow transplant
bp	base pair
BSA	bovine serum albumin
°C	temperature in celsius degrees
CCR	chemokine receptor type
CD	cluster differentiation
cDC	conventional dendritic cell
CDP	common DC precursor
CK	casein kinase
CMP	common myeloid progenitor
CMV	cytomegalovirus
cTEM	conventional effector memory T cell
CTLL	cytolytic T-lymphocyte line
Cre	causing recombination
DC	dendritic cell
DKK1	Dikkopf-1
DNA	deoxyribonucleic acid
DPEC	double-positive effector T cell
DSS	dextran-sodium-sulfate
E	early
EAE	experimental autoimmune encephalitis
EDTA	ethylenediaminetetraacetic acid
EEC	early effector cell
EGFR	epithelial growth factor receptor
ER	endoplasmatic reticulum
<i>et al.</i>	<i>et alii</i>
EtOH	ethanol
FACS	fluorescence-activated cell sorting
FCS	fetal calf serum
Fig.	figure
FSC	forward scatter
Flt3L	Fms-like tyrosine kinase 3 ligand
FoxP3	forkhead box transcription factor
GM-CSF	granulocyte-macrophage colony-stimulating factor
GMP	granulocyte macrophage progenitor
GSK	glycogen synthase kinase
GvHD	graft versus host disease
h	hour
hCMV	human cytomegalovirus
HCT	hematopoietic cell transplantation
HEV	high endothelial venules

HSC	hematopoietic stem cell
HSPG	heparan sulfate proteoglycan
HSV-1	herpes simplex virus 1
IAV	influenza A virus
IE	immediate early
IL	interleukin
IM	interstitial macrophage
IDO	indoleamine 2,3-dioxygenase
i.n.	intranasal
i.p.	intraperitoneal
IPEX	immune dysregulation, polyendocrinopathy, enteropathy, X-linked syndrome
IRF	interferon regulatory factor
i.v.	intravenously
iTEM	inflationary effector memory T cell
ITIM	immunoreceptor tyrosine-based inhibitory motife
Jak1	Janus tyrosine kinase-1
Klf4	krüppel-like factor 4
KLRG-1	killer cell lectin-like receptor subfamily G member 1
L	late
LCMV	lymphocytic choriomeningitis virus infection
LN	lymph node
LPS	lipopolysaccharide
LT	lymphotoxin
M	molar
mCMV	murine cytomegalovirus
MHC	major histocompability complex
MI	memory inflation
min	minute
ml	milliliter
mM	millimolar
MPP	multipotent progenitor
MuHV-4	murid herpesvirus-4
MZ	marginal zone
Nfil	nuclear factor interleukin
ng	nanogram
nm	nanomolar
Notch2	notch homolog protein 2
NK	natural killer
OD	optical density
o/n	over night
ORF	open reading frame
OVA	ovalbumin
PBMC	peripheral blood mononuclear cell
PBS	phosphate buffered saline
PCR	polymerase chain reaction
pDC	plasmacytoid DC
PFU	plaque forming unit
p.i.	post infection
pre-cDC	DC-committed progenitor
PRR	pattern recognition receptor
rpm	revolutions per minute

RT	room temperature
SCID	severe combined immunodeficiency
SCT	stem cell transplantation
sec	second
SG	salivary gland
SLEC	short-lived effector cell
SSC	sideward scatter
STAT3	signal transducer and activator of transcription 3
TAE	Tris-Acetate-EDTA
TCM	central memory T cell
Tcov	conventional T cell
TCR	T cell receptor
Teff	effector T cells
TEM	effector memory T cell
Th	T helper
TLR	Toll-like receptor
TNF	tissue necrosis factor
Treg	regulatory T cell
Tyk-2	tyrosine kinase-2
U	Units
μg	microgram
μl	microliter
μM	micromolar
V	volt
vRAP	viral regulators of antigen presentation
v/v	volume per volume
Wnt	Wingless-Int
WP	white pulp
WT	wild type
w/v	weight per volume
× g	times gravity
3'	three prime end of DNA sequences
5'	five prime end of DNA sequences

1 Introduction

1.1 Cytomegalovirus

Cytomegalovirus (CMV) belongs to the family of *Herpesviridae*. Members of the *Herpesviridae* have a double-stranded linear DNA genome and an icosahedral capsid in common, which is surrounded by a lipid bilayer (Connolly et al., 2021; Plummer, 1967; Roizman et al., 1992). During primary infection, progeny viruses are produced by lytic infection and are able to establish latency in the host (Roizman and Baines, 1991). Due to their replication rate, the pathogenicity and the cell tropism, they are classified into three subfamilies: α -, β - and γ -*Herpesviridae* (Roizman, 1979; Roizman et al., 1981). CMV is a member of the β -*Herpesviridae*, has a long replication cycle and is strictly species-specific (Schottstedt et al., 2010; Tang et al., 2006).

1.1.1 Morphology and replication

CMV virions have a diameter of 150-200 nm and show morphological characteristics of herpesviruses (**Fig. 1**) (Butcher et al., 1998; Chen et al., 1999). The DNA-protein-complex, which is located inside the virus, is embedded by an icosahedral capsid of approximately 120 nm diameter, consisting of 162 capsomeres. The capsid is surrounded by a tegument containing at least 27 different viral phosphoproteins but also a number of cellular and viral RNA (Mocarski and Courcelle, 2001; Terhune et al., 2004). The envelope is a lipid bilayer (Tooze et al., 1993) containing both viral and cellular glycoproteins (Streblow et al., 2006). Viral glycoproteins mediate viral attachment to the host cell as well as pH-independent fusion of the viral envelope with the cellular membrane (penetration) (Compton et al., 1992). Viral glycoproteins have important functions in virion maturation and induction of the CMV-specific humoral immune response (Feire and Compton, 2013).

Human CMV (hCMV) has the largest genome with a length of approximately 240 kb with regards to the other viruses of the *Herpesviridae* family (Davison et al., 2003). The genome size of the murine CMV (mCMV) is approximately 230 kbp (Rawlinson et al., 1996) and contains about 170 open reading frames (ORF) (Cheng et al., 2010; Tang et al., 2006), whereas hCMV encodes 165-252 ORF (Chee et al., 1990; Davison et al., 2003; Murphy et al., 2003). In 2012 Stern-Ginossar *et al.* used ribosome profiling and transcript analysis to define hCMV

translation products and identified up to 751 translated ORF in hCMV (Stern-Ginossar et al., 2012).

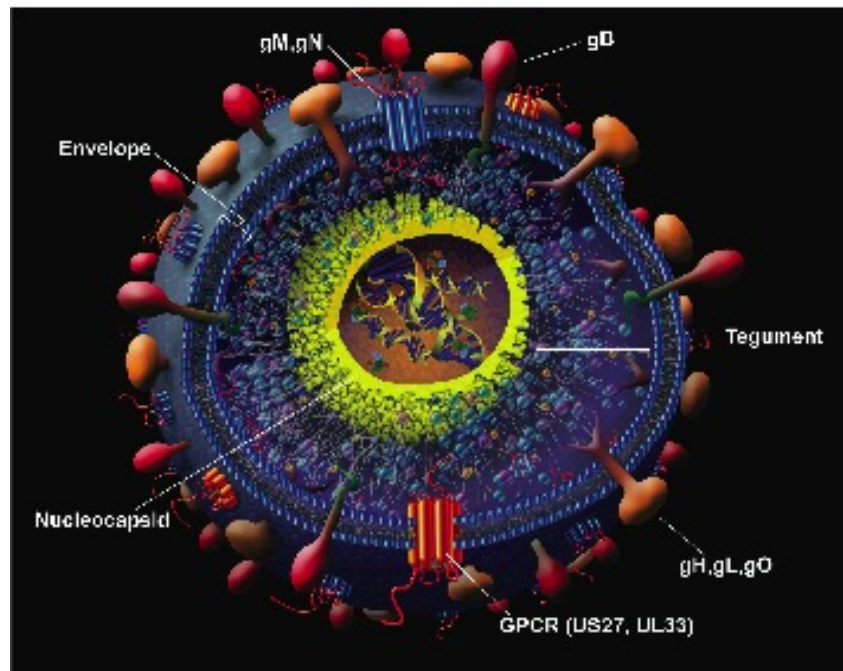


Figure 1: Structure of CMV.

The nucleocapsid is the first layer and contains the double-stranded viral genome, which is embedded in the tegument. The outer layer of the virion is a host-derived lipid bilayer studded with viral glycoproteins (gM, gN, gB, gH, gL, gO) (Streblow et al., 2006).

The first step of CMV infection is the binding and entry of the virus into the cells (Boyle and Compton, 1998). The attachment of the virion to the host cell membrane is initiated by binding of viral glycoproteins gB and gM/gN to cellular heparan sulfate proteoglycans (HSPG) (Boyle and Compton, 1998; Compton et al., 1992; Mocarski, 1996). To stabilize the first attachment of the virion, further viral proteins interact and bind cellular receptors (docking) (Compton et al., 1993; Feire and Compton, 2013). Different cellular receptors involved in the docking process like epithelial growth factor receptor (EGFR), Annexin II, CD13 or integrins are yet to be discussed (Feire et al., 2004; Giugni et al., 1996; Soderberg et al., 1993; Wright et al., 1994). The process of attachment is followed by pH-independent penetration (Compton et al., 1993; Mocarski, 1996). Both capsid and tegument enter the cytoplasm and the capsid is transported to the nucleus via microtubules (Ogawa-Goto et al., 2003). The viral genome enters the nucleoplasm through a nuclear pore and circulates to an episome (Mocarski, 1996; Ojala et al., 2000).

Gene expression of viral DNA is highly regulated in a cascade-dependent manner and can be separated into three phases: immediate early (IE), early (E) and late (L) (Mocarski 1996). IE gene expression occurs immediately after the viral DNA enters the nucleus. The IE proteins activate the viral replication cycle and viral gene expression. Additionally, they control the intrinsic and innate cellular immune response (Meier and Stinski, 2013). Two hours after infection, the regulatory function of IE proteins in CMV initiates the E phase, which is essential for viral DNA replication (Keil et al., 1984). E proteins regulate host cell responses and establish the viral replication (Compton and Feire, 2007). DNA synthesis takes place according to the rolling circle mechanism and results in a single DNA strand containing multiple virus genome copies (Mocarski, 1996). In the L phase predominantly structural proteins are synthesized, which are needed for the assembly of new viral particles (Isomura et al., 2011; Mocarski, 1996). The assembly of herpesviruses takes place in the nucleus. In primary envelopment, nucleocapsids are transported through the inner nuclear membrane into the perinuclear space. After fusion of the viral membrane with the outer nuclear membrane, naked capsids enter the cytoplasm (Buser et al., 2007; Mocarski, 1996). In secondary envelopment, the capsids receive a double membrane at the cytoplasmic cisterna. Finally, fusion with the plasma membrane of the cells leads to the release of viral particles with a single envelope membrane (Mocarski, 1996; Sanchez et al., 2000).

1.1.2 Latency and reactivation

Latency is defined as the persistence of functional viral genomes in a non-replicative state in the host after the control of primary infection (Bain et al., 2006; Griessl et al., 2021). Latent viral genomes have the ability to reactivate at any time in response to stimuli, resulting in recurrence of infectious viruses (Roizmans and Sears, 1987). During latent hCMV infection, viral DNA is detectable in various organs such as lung, liver, heart, kidney, and pancreas (Koffron et al., 1997). mCMV establishes latency in lung, spleen, kidney, brain, salivary glands (SG) and heart (Balthesen et al., 1993; Collins et al., 1993). Previous studies also found hCMV in cells of myeloid origin such as granulocytes, monocytes, macrophages (M Φ) and dendritic cells (DC) (Hahn et al., 1998; Sinclair and Sissons, 2006; Soderberg et al., 1993; Soderberg-Naucler and Nelson, 1999). Interestingly, viral genomes have not been detected in B and T cells (Mocarski et al., 2007; Taylor-Wiedeman et al., 1993; Taylor-Wiedeman et al., 1991). In addition, endothelial cells came into the focus as putative latency sites (Koffron et al., 1998;

Quirici et al., 2001) and were described by Seckert *et al.* as a place of latency in the liver (Seckert et al., 2009).

Reactivation after latency results in productive infection with new infectious virions, which is a high risk factor for immunocompromised patients after stem cell or organ transplantation (Baltesen et al., 1994; Reddehase et al., 1994). Reactivation could be achieved by immunosuppression, such as total body irradiation (Kurz and Reddehase, 1999; Reddehase et al., 1994) or depletion of lymphoid cells using antibodies (Bevan et al., 1996; Polic et al., 1998), leading to impaired CD8⁺ T cell control. Moreover, reactivation can be induced by cell differentiation and activation of myeloid cells by pro-inflammatory cytokines (Hahn et al., 1998; Hertel et al., 2003; Kondo et al., 1994). The transcription factor TNF- α plays an important role on the molecular site in reactivation. Both studies of mCMV and hCMV confirmed the involvement of TNF- α of reactivation of the virus (Docke et al., 1994; Prosch et al., 2002). Cook *et al.* also demonstrated the influence of TNF- α on the reactivation in an mCMV sepsis model (Cook et al., 2006).

1.1.3 Clinical relevance of hCMV infection

The rate of hCMV transmission is highly dependent on geographic location and social status. While up to 100% of the human population living in metropolitan areas and in third world countries carry the virus, only 40-70% of the population are infected in central Europe and North America (Ho, 2008; Schottstedt et al., 2010). hCMV can be transmitted either horizontally or vertically. During the horizontal transmission, the virus is transmitted through direct contact, such as saliva, urine, tear fluid, breast milk or genital secretions (Mocarski 1996; Schottstedt et al., 2010). Moreover, it can also be transmitted via blood transfusion or organ transplantation. Vertical transmission takes place transplacentally or during birth from mother to child. Additionally, the transmission to the newborn can occur via breast milk.

Both, primary infections and reactivation of hCMV, are usually unapparent in immunocompetent individuals. Occasionally, primary CMV infection can lead to mononucleosis with symptoms such as fever, fatigue, nausea and headache (Lancini et al., 2014; Rubin, 1990). In immunocompromised patients the clinical manifestation of hCMV has a broad range of symptoms such as asymptomatic infection or multi-organ disease accompanied by mortality and morbidity (Dioverti and Razonable, 2016). This group includes patients with congenital (severe combined immunodeficiency, SCID) or acquired (acquired

immunodeficiency syndrome, AIDS) immunodeficiency, recipients of stem cell or organ transplants, as well as patients undergoing chemotherapy and congenitally infected fetuses (Dioverti and Razonable, 2016; Neiman et al., 1977; Singh et al., 1988). In recipients of organ and bone marrow transplantations, the serological status plays a crucial role (Miller et al., 1991; Boeckh et al., 2003).

1.1.4 mCMV infection as model system as hCMV

All cytomegaloviruses are strict species-specific, therefore it is not possible to study hCMV in animal models. However, due to their similar structure, genetics and development of adaptations, the murine model of mCMV infection is widely used (Rawlinson et al., 1996; Reddehase, 2002). In both, hCMV and mCMV, the immune control has similar kinetics and is mediated mainly by CD8⁺ T cells (Holtappels et al., 2006; Reddehase and Lemmermann, 2018; Reddehase et al., 2002). After primary infection, both viruses develop a lifelong latency in the same organs such as lung, SG or spleen (Baltesen et al., 1993; Krmpotic et al., 2003; Reddehase, 2002; Reddehase et al., 1994). Moreover, the murine model has been established for the analysis of viral immune evasion mechanisms (Reddehase et al., 2002) and the discovery of ‘memory inflation’ (Holtappels et al., 2000), as well as latency (Seckert et al., 2012). The murine model could also contribute to the description of effector T cell populations mediating immunological control of infection (Holtappels et al., 2006; Simon et al., 2006).

1.1.5 Immunological control of mCMV infection

Control of primary CMV infection occurs in two phases and begins immediately after infection with the activation of the innate immune system, while the activation of the adaptive immune response occurs later (Bukowski and Welsh, 1985; Welsh et al., 1991). Innate immune cells such as MΦ, DC and natural killer cells (NK) are involved in the defense and control upon CMV infection (Bukowski and Welsh, 1985; Arase et al., 2002; Jonjić, et al., 2006). These cells are equipped with pattern recognition receptors (PRR) enabling them to detect conserved pathogen- or damage-associated molecular patterns (PAMP, DAMP) such as LPS and bacterial DNA (Janeway and Medzhitov, 2002; Hartmann et al., 1999). In addition, these cells secrete anti-viral cytokines such interferons, interleukins and chemokines and support the initiation of

the adaptive immune response, which is essential for long-term control of infection (Goodbourn et al., 2000; Grandvaux et al., 2002; Welsh et al., 1991).

The adaptive immune response consists of a humoral and cellular component. The latter is essentially mediated by virus-specific CD8⁺ T cells (also known as cytotoxic CD8⁺ T cells). They terminate productive infection in organs and mediate long-term control through inhibiting CMV replication in the acute phase (Griessel et al., 2021; La Rosa and Diamond, 2012; Reddehase, 2002; Sylwester et al., 2005). Previous studies have shown that the transfer of anti-viral CD8⁺ T cells control CMV disease after transplantation (Riddell et al., 1992). CD4⁺ T cells (also known as T helper cells- T_H) also contribute to the anti-viral immune response. They can limit viral replication during chronic infection through cytolytic activities and secretion of cytokines, in particular IFN- γ (Jonjic et al., 1990; Jeitziner et al., 2013; Verma et al., 2016). The humoral response includes the secretion of virus-specific antibodies by B lymphocytes. Their contribution to the control of primary infection is small, but they perform a protective function against secondary infection and limit spread in the virus reactivation (Klenovsek et al., 2007; Reddehase et al., 1994; Wirtz et al., 2008).

1.1.6 Immune evasion strategies

mCMV evolves strategies to interfere with DC to affect the anti-viral immune response, which are called immune evasion strategies. These different immune evasion strategies include components of the innate and adaptive immunity. It is known that CMV encodes proteins which are involved in modifying and mimicking MHC protein function, leukocyte migration, activation and cytokine responses (Mocarski, 2002; Reddehase, 2002). Four mCMV (m138, m145, m152 and m155) proteins reduce the expression of natural killer group 2D receptor (NKG2D), which leads to a reduced NK cell response (Hasan et al., 2005; Krmpotic et al., 2005; Lenac et al., 2006; Lodoen et al., 2003). Some other immune evasion proteins affect the CD8⁺ T cell response, because they inhibiting antigen (Ag) presentation via MHC-I. These proteins, namely m04, m06 and m152, are known as vRAPs (viral regulators of antigen presentation) (Holtappels et al., 2006). Virus mutants without these genes showed a higher virus-specific CD8⁺ T cell response (Doom and Hill, 2008; Hengel et al., 1999; Holtappels et al., 2006; Reddehase, 2002).

1.2 Dendritic cells and their role in immune response

DC are a heterogeneous population, which belongs to the group of antigen-presenting cells (APC) (Mildner and Jung, 2014; Ueno et al., 2007). Originally, they were discovered in 1973 by Steinman and Cohn as an undefined cell type in a mouse spleen, which were named as “dendritic cell” due to their extended cytoplasmic processes (Chen et al., 2016; Steinman and Cohn, 1973). DC are present in almost every tissue of the body, e.g. in the skin, mucosa, lymph nodes (LN), spleen, lung and thymus (Steinman and Cohn, 1973).

DC develop from hematopoietic stem cells (HSC) of the bone marrow (BM) in a stepwise manner. HSC generate common myeloid progenitor (CMP), which differentiate through a series of precursors into common DC precursors (CDP) (Hettinger et al., 2013; Liu and Nussenzweig, 2010; Manz et al., 2001; Onai et al., 2013; Sichien et al., 2017). They subsequently differentiate into plasmacytoid DC (pDC) or precursor conventional DC (pre-cDC) (Naik et al., 2007; Onai et al., 2013). Latter leave the BM into the bloodstream and migrate to different tissues where they differentiate into conventional type 1 DC (cDC1) dependent of different transcription factors and type 2 DC (cDC2) (Diao et al., 2006; Sichien et al., 2017).

DC are different in their phenotype and function and therefore referred to immature and mature DC (Schuler and Steinman, 1985). Newly generated immature DC migrate to peripheral tissues via the bloodstream and can accumulate within a short time at sites where pathogens occur. Circulating DC are attracted by chemokines, secreted as a result of a pathogen-induced inflammatory response (McWilliam et al., 1996). Immature DC take up Ag through the PRR such as Toll-like receptor (TLR) (Meylan et al., 2006). Subsequently, the ability of DC to take up further Ag rapidly decreases and the DC migration and maturation is initiated (Bancherau et al., 2000). The maturation process is accompanied by increased expression of MHC-II molecules, co-stimulatory molecules such as CD80, CD86 and CD40, and a change in their morphology (Mellman and Steinman, 2001; Wallet et al., 2005). DC migrate to the T cell zones in draining lymph nodes (dLN) in a chemokine receptor type 7 (CCR7)-dependent manner (Ohl et al., 2004; Saban, 2014). In dLN, mature DC present Ag to naïve T cells. Chemokines attract both mature DC and naïve T cells, favoring the encounter of antigen-presenting DC with antigen-specific T cells (Gunn et al., 1998; Saeki et al., 1999). Upon Ag presentation, proliferation and polarization of naïve T cells into antigen-specific effector (Teff) or regulatory T cells is induced (Treg) (Sichien et al., 2017; Zanna et al., 2021). These activated T cells home to the tissue of DC origin and orchestrate the immune response through the production of

immunomodulatory cytokines, including IL-17, IFN- γ , IL-4, IL-5, and IL-10 (Banchereau and Steinman, 1998; Merad et al., 2013).

DC process the Ag for presentation on their cell surface using MHC for recognition by the TCR on T cells (Bancherau et al., 2000). They are able to present both exogenous and endogenous Ag. The exogenous Ag is taken up, processed in the endosome and presented on MHC-II-molecules, resulting in the activation of antigen-specific CD4⁺ T cells (Guermonprez et al., 2002). MHC-I presentation of pathogenic Ag and the additional interaction of co-stimulatory cytokines activates CD8⁺ T cells (Rudolph et al., 2006). Depending on the origin of the peptide, two types of Ag presentation are known, direct presentation and cross-presentation. The former describes the presentation of peptides derived from intracellularly synthesized and processed proteins (endogenous Ag), e.g. produced in the cytoplasm of DC. The peptide is presented on MHC-I molecules and activates the antigen-specific CD8⁺ T cells (Rammensee et al., 1993; Rock et al., 2002; Suh et al., 1994). DC can also present exogenous Ag via micropinocytosis/endocytosis on MHC-I molecules, a process known as cross-presentation (Joffre et al., 2012; Sallusto et al., 1995). cDC1 are most efficient for CD8⁺ T cell priming via cross-presentation. They play an important role in defense against cancer and against intracellular pathogens including mCMV (Busche et al., 2013, Dalod et al., 2003).

1.2.1 Characterizing DC in lung, lymph node and spleen

DC can be classified into conventional DC (cDC) and plasmacytoid DC (pDC). The latter secretes high amounts of type I interferons (IFN-I) during viral infections, which is important in anti-viral immune responses, but pDC have a restricted potential to prime T cells (Nakano et al., 2001; Sapozhnikov et al., 2007; Swiecki and Colonna, 2015). cDC can be characterized by the expression of the integrin CD11c and MHC-II (Sichien et al., 2017; Zanna et al., 2021). Based on their surface phenotype, developmental transcription factors and function, cDC are classified into cDC1 and cDC2 (Guilliams et al., 2014). Both cDC subsets present pathogenic Ag to naïve T cells and initiate the adaptive immune response (Lambrecht and Hammad, 2012). They can be found in secondary lymphoid organs and parenchymal tissues, where they have a sentinel function (Mildner and Jung, 2014).

In the **lung**, the three main DC subsets (cDC1, cDC2 and pDC) are present in the steady state (**Fig. 2 a**) (Lambrecht and Hammad, 2012). cDC express high levels of CD11c, while pDC

express Siglec-H and low levels of CD11c. cDC subsets can be further distinguished by the expression of CD103 and CD11b. The CD11c^{hi} CD103⁺ cDC1 belong to the CD8 α type and express XCR-1, whereas the CD11c^{hi} CD11b⁺ cDC2 express CD172 α . In the lung, a network of cDC1 is found in the epithelial layer. They form dendrites and penetrate the epithelial cell layer to gain access to the airway lumen (Guilliams et al., 2013). Pulmonary cDC1 are specialized in cross-presenting Ag to CD8⁺ T cells (Guilliams et al., 2013; Mildner and Jung, 2014). Thus, cDC1 are important for immune defense against intracellular pathogens including mCMV (Alexandre et al., 2014). In comparison, cDC2 are found in the lamina propria (Neyt and Lambrecht, 2013). These cells are potent activators of CD4⁺ T cells and inducers of T_H2 and T_H17 responses, and promote the humoral immunity (Alexandre et al., 2014; Mildner and Jung, 2014; Neyt and Lambrecht, 2013). Furthermore, pulmonary cDC2 trigger the activation of cytotoxic T lymphocytes (CTL) after influenza infection and remain in draining LN (dLN). During a respiratory virus infection an additional subpopulation, the CD11b⁺ monocyte-derived DC (moDC), are recruited to the lung (**Fig. 2 b**). These cells maintain the pro-inflammatory microenvironment by secreting cytokines (Lambrecht and Hammad, 2012).

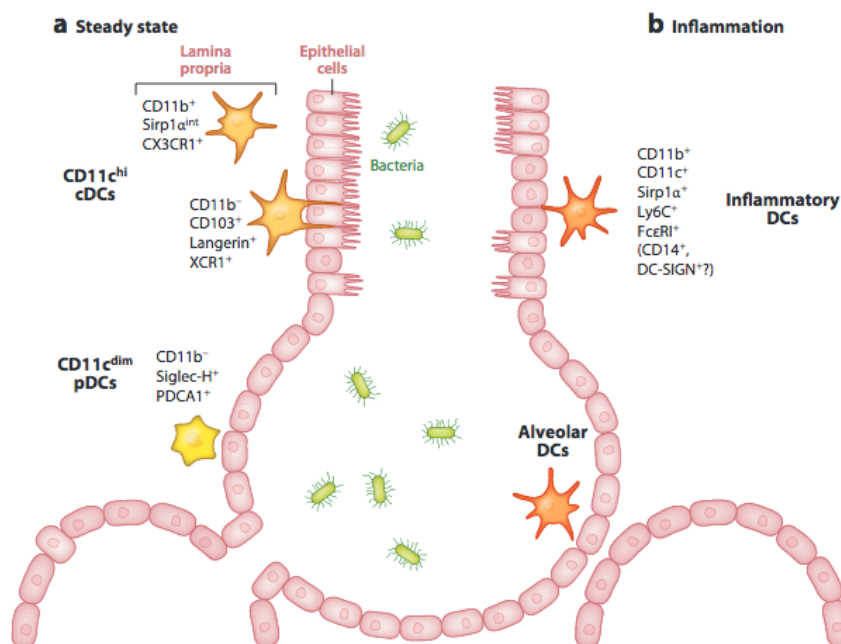


Figure 2: Characterization of DC subsets in the lung of mice.

Two subsets of CD11c^{hi} cDC were identified in steady state (**a**). CD103⁺ cDC1 are found in the epithelial layer of the larger airways of the lung, whereas CD11b⁺ cDC2 are predominantly encountered in the lamina propria. A third population of pDC can be found in the epithelial layer. During inflammation, CD11b⁺ monocyte-derived DC are induced and recruited to the lung (**b**) (adapted from Lambrecht and Hammad, 2012).

In the LN, DC can be subdivided into resident and migratory cells. Resident DC can be distinguished from migratory DC by the expression levels of MHC-II and CD11c. In steady state of mice, resident DC are CD11c^{hi} MHCII^{int}, while migratory DC are CD11c^{int} MHCII^{hi} in LN (Ohl et al., 2004). Similar to the lung, resident cDC in the LN can be subdivided into CD103⁺ cDC1 and CD11b⁺ cDC2. Despite the name, resident DC, are able to migrate through different areas within secondary lymphoid organs. They continuously enter the LN from the blood and acquire Ag by lymphatic drainage or by transfer from other cells. The acquired Ag is used for CD4 and CD8 T cell priming (Allan et al., 2006; Ersland et al., 2010; Gurevich et al., 2017). In contrast, migratory DC reside in the parenchymal tissue and must migrate to LN via afferent lymphatics in a CCR7-dependent fashion to interact with naïve T cells (Mildner and Jung, 2014; Ohl et al., 2004). Migratory DC carry Ag from the periphery to CD8⁺ resident DC in the LN for cross-presentation (Allan et al., 2006).

The **spleen** predominately harbors cDC, which can be further classified into CD8 α ⁺ (cDC1) and CD8 α ⁻ (cDC2) subsets. cDC1 are phenotypically characterized as CD11b⁻ CD8 α ⁺ XCR-1⁺ (also known as CD103⁺ cDC1), while cDC2 are CD11b⁺ CD8 α ⁻ CD172 α ⁺ cells (Sichien et al., 2017; Vremec et al., 2000). The two subsets differ in immune function, cytokine production and their ability to cross-present Ag (Hochrein et al., 2001). It has been published, that cDC1 are localized in the marginal zone (MZ) of the spleen and take up lymph- and blood-born Ag and pathogens (Idoyaga et al., 2009). Moreover, they are involved in the maintenance of tolerance to self-antigens, which is due to their close proximity to resting T cells and their ability of cross-presentation (De Smedt et al., 1996; Steinman et al., 1997). cDC1 predominately produce interleukin 12 (IL-12) which is crucial for the CD8⁺ T cell proliferation (Heath et al., 2004). On the other hand, cDC2 are more heterogeneous than cDC1 and have a low cross-priming capacity (De Smedt et al., 1996). A study used *in vivo* labelling to identify the localization of cDC2 and discovered, that half of these cells were exposed to Ag in the MZ of the spleen (Calabro et al., 2016). The other half of cDC2 is suggested to be in the white pulp (WP) and thus have no access to large blood-derived Ag. Therefore, these cells cannot present viral Ag to naïve CD4 T cells and initiate the adaptive immune response. After lipopolysaccharide (LPS) stimulation, cDC2 migrate into the T cell areas and secrete inflammatory cytokines (De Smedt et al., 1996).

1.2.2 DC in mCMV infection

DC are an important link between the innate and adaptive immune system (Sichien et al., 2017; Zanna et al., 2021). The main function of these cells is to capture pathogen Ag, initiating and modulating the adaptive immune response by activating CD4⁺ and CD8⁺ T cells. During infection, DC recognize mCMV DNA mainly through the TLR-9. These receptor triggers a distinct signaling pathway and result in the production of pro-inflammatory cytokines such as IFN-I (Brinkmann et al., 2015; Puttur et al., 2016).

CD11c is a typical marker to characterize DC, which can also be found on the surface of other immune cells, such as T cells (Liao et al., 2017). Pulmonary immune cells express CD11c and most of them are cDC expressing high levels of CD86 and MHC-II after 3 days of mCMV infection. A few years ago, the group of Sacher showed remarkable amounts of EGFP-virus in most organs of CD11c-Cre mice and thus the main part of the virus replicated in CD11c⁺ cells, probably cDC (Sacher et al., 2008). This suggests that cDC contribute to virus replication and disseminate across tissues during infection. Additionally, it is known that mCMV can infect DC. Already after 36-48 h of mCMV infection mainly cDC1 were infected (Dalod et al., 2003). In contrast to cDC2, splenic cDC1 do not produce infectious virus after 18 h of infection (Busche et al., 2013). In spleen and liver of Batf3^{-/-} mice virus titers were not affected despite the absence of cDC1 (Torti et al., 2011b). However, cDC are not involved in the establishment of latency and occurs in the absence of cDC1 (Daley-Bauer et al., 2014; Torti et al., 2011a). Non-classical monocytes (CX₃CR1^{hi}) are important for the establishment of latency. These cells become infected and serve as immune vehicles to spread the virus to distant organs such as the SG after footpad infection (Daley-Bauer et al., 2014). Usually an mCMV infection occurs via mucosal membranes and the virus transmits via the respiratory tract. Therefore, the intranasal (i.n.) infection route seems to be the most likely natural route. After i.n. infection CD11c⁺ DC migrate from the lungs to the mediastinal lymph nodes (mLN), then enter the blood and reach the SG (Farrell et al., 2017). In lung, mCMV-infected DC exit the LN by a distinct route to lymphocytes, entering high endothelial venules (HEV) and evade the efferent lymph. This exit depends on CD44 and the viral M33 chemokine receptor (G-protein-dependent signaling), because in the absence of both, CD44 and M33, infected DC accumulate in the LN and reduce the viral spread. These findings suggest a virus-driven DC recirculation. Moreover, natural CMV infection of the respiratory tract is associated with exposure to environmental Ag in the air (Reddehase, 2019). In a mouse model Reuter *et al.* investigated the simultaneously respiratory exposure to CMV and ovalbumin (OVA), which is a well-studied environmental Ag with low allergenic potential. The airway infection combined with the OVA sensitization

was more receptive for an allergic airway disease (AAD), while the mCMV infection or exposure to OVA by itself did not sensitize to AAD. Both, cDC2 and cDC1 are activated by mCMV in the airway mucosa where they take up OVA, migrate to tracheal lymph node (tLN) and present Ag. This AAD was driven by CD4⁺ T helper cells (T_H2) type 2 in lung and accompanied by the production of IL-4, IL-5, IL-9 and IL-25 (Reuter et al., 2019). DC derived from BM in presence of GM-CSF are permissive to mCMV *in vitro* and infected DC are weak activators of T cells (Andrews et al., 2001; Loewendorf et al., 2004).

1.3 Importance of CD8⁺ T cells

T lymphocytes, especially virus-specific CD8⁺ T cells, are the major mediator of the adaptive immune response during CMV infection to limit the viral replication (Reddehase, 2002; Wills et al. 2013). The immune response by CMV-specific CD8⁺ T cells begins 2-3 days after infection and reaches its maximum at approximately 10 days (Bohm et al., 2008; Quinnan et al., 1978).

T cells originate in the bone marrow (BM) and mature in the thymus. Mature naïve T cells leave the thymus and circulate throughout the body until they recognize their specific Ag on the surface of APC and are activated in secondary lymphoid organs (Randolph et al., 2005). The activation of CD8⁺ T cells occurs through binding of its TCR to the peptide-loaded MHC-I complex. Simultaneously, co-stimulatory molecules and signals from inflammatory cytokines, in particular IL-12 and IFN- γ , control the activation of T cells (Harty and Badovinac, 2008; Harty et al., 2000; Mescher et al., 2006). After activation, effector CD8⁺ T cells migrate via efferent lymphatic vessels to the peripheral sites of infection. There, they can kill infected cells by secreting perforin and granzyme B and recruit other effector cells through cytokine production.

During primary infection, CD8⁺ T cells undergo four stages: activation, expansion, contraction, and the memory phase. Following activation, rapid cell expansion and effector cell differentiation occur (Blattman et al., 2002; Busch et al., 1998; Butz and Bevan, 1998; Murali-Krishna et al., 1998). Effector functions of CD8⁺ T cells compromise cytolytic activity and secretion of cytokines such as TNF and IFN- γ and chemokines (Doherty, 1993; Harty et al., 2000). This mediates the control of infection by the CD8⁺ T cells and promotes clearance of the virus. The CD8⁺ T cell response is essential for the control of mCMV infection and has been confirmed in several studies (Bohm et al., 2008; Holtappels et al., 2006; Holtappels et al., 2000;

Pahl-Seibert et al., 2005). An adoptive transfer of T lymphocytes from mCMV-infected donor mice to susceptible immune suppressed mCMV-infected recipient mice has been shown to protect these mice. In the contraction phase, 90-95% of T cells undergo apoptosis and only long-lived memory T cells survive (Kaech et al., 2002). In contrast to other virus infections, CMV-specific memory T cells increases with time. This phenomenon is called ‘memory inflation’ (MI) and is boosted by repeated reactivation of CMV over lifetime (Holtappels et al., 2020; Holtappels et al., 2000; Holtappels et al., 2002; Karrer et al., 2003; Kim et al., 2015).

1.3.1 Differentiation of CD8⁺ T cells

After activation, naïve CD8⁺ T cells develop into effector cells and remain as memory T cells after surviving an infection (Weninger et al., 2002). Originally, these memory T cells were differentiated into two major subtypes, the central memory T cells (TCM) and effector memory T cells (TEM) (Hamann et al., 1997; Stemberger et al., 2009). TCM are localized in the LN but can also migrate to peripheral organs upon inflammatory signals (Weninger et al., 2002; Wherry et al., 2003). In contrast, TEM are not found in LN and are restricted to the peripheral tissue (Masopust et al., 2001; Wherry et al., 2003).

Recent publications show that two different kinetic patterns of CD8⁺ T cell responses are induced after mCMV infection (**Fig. 3**) (Munks et al., 2006). The main group of CD8⁺ T cells are the ‘conventional CD8⁺ T cells’, which follow the classical contraction, expansion and memory. They are stably maintained at low levels in the latency phase by cytokine-induced homeostatic proliferation. The conventional memory pool is characterized by CD8⁺ T cells, which are specific for e.g. epitopes M45 and M57 in C57/BL6 mice. In contrast, mCMV-specific ‘inflationary CD8⁺ T cells’ continuously expand after the control of primary infection and are stabilized at high numbers in peripheral tissues during latency phase. In C57/BL6 mice, the epitopes M38, m139 and IE3 also follow the inflationary response and expanded over 8-12 weeks after infection. During latency phase, these inflationary CD8⁺ T cells are maintained at high levels (Munks et al., 2006; Snyder et al., 2008; Torti and Oxenius, 2012). In this work, the two Tetramers M38 and M45 were used to study the virus-specific T cell response of conventional and inflationary CD8⁺ T cells during acute and latent mCMV infection.

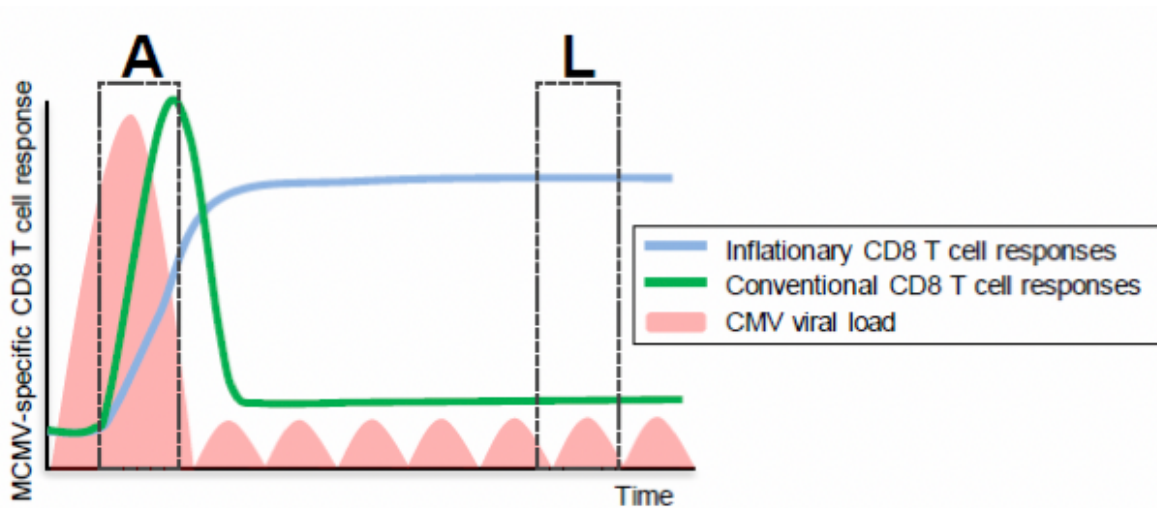


Figure 3: Kinetic patterns of CD8⁺ T cells responses during mCMV infection.

The acute infection (A) is controlled by innate immune cells and CD8⁺ T cells and is followed by the latency phase (L). During the acute infection ‘conventional CD8⁺ T cells’ undergo the classical expansion, contraction and memory phase (green line), which is accompanied with high lytic viral replications (pink areas). The ‘inflationary CD8⁺ T cell response’ expand after acute infection and are maintained at high levels during latent infection (blue line). The viral loads show local reactivation events, which are rapidly controlled during the latency phase (Torti and Oxenius, 2012).

Based on a recent publication by Griessel *et al.*, CD8⁺ T cells were classified into following subpopulations using surface markers CD127, KLRG-1 and CD62L (Griessel *et al.*, 2021):

early effector cells (EEC)	CD127 ⁻ KLRG-1 ⁻ CD62L ⁻
inflationary effector memory T cells (iTEM)	CD127 ⁻ KLRG-1 ⁺ CD62L ⁻
double-positive effector T cells (DPEC)	CD127 ⁺ KLRG-1 ⁺ CD62L ⁻
conventional effector memory T cells (cTEM)	CD127 ⁺ KLRG-1 ⁻ CD62L ⁻
central memory T cells (TCM)	CD127 ⁺ KLRG-1 ⁻ CD62L ⁺ .

CD127 also known as IL-7R α is a subunit of the interleukin-7 receptor and is expressed on DPEC, cTEM and TCM (Bachmann *et al.*, 2005; Griessel *et al.*, 2021; Wherry and Ahmed, 2004). The presence of CD127 correlates with increased expression of anti-apoptotic molecules, such as Bcl-2 (Kaech *et al.*, 2003; Schluns *et al.*, 2000). KLRG-1 (killer cell lectin-like receptor subfamily G member 1) is a transmembrane protein with an immunoreceptor tyrosine-based inhibitory motif (ITIM). This protein interacts with E-cadherin and inhibits cell proliferation and cyclin production, as well as phosphorylation of Akt, a kinase involved in cell survival (Henson *et al.*, 2009; Tessmer *et al.*, 2007). Furthermore, KLRG-1 inhibits the IL-2 production of T cells, which affects the magnitude and duration of effector phase (Banh *et al.*, 2009). CD62L is a homing marker, which is expressed only by TCM and

enables the migration to secondary lymphoid organs (Torti and Oxenius, 2012; Wherry et al., 2003).

The development of EEC is induced by cytokines such as IL-12, IL-15, and IFN- α/β , which subsequently develop into terminally differentiated short-lived effector cells – SLEC (above classified as iTEM) or memory T cells (Obar et al., 2011; Obar and Lefrancois, 2010a; Xiao et al., 2009). IL-2 and IL-12 are important inflammatory cytokines to induce the iTEM population. In addition, these two cytokines regulate transcription factors such as T-bet, Eomes, Blimp1 and Bcl6, which are important for cell differentiation (Joshi et al., 2007; Obar et al., 2011; Takemoto et al., 2006). IFN- γ regulates the proliferation and survival of CD8⁺ T cells, promotes IL-12 production and iTEM differentiation (Obar et al., 2011; Obar and Lefrancois, 2010b). iTEM has an extended life span due to increased expression of the anti-apoptotic protein Bcl-2 mediated by IL-15, resulting in a memory cell-like appearance (Baumann et al., 2018; Holtappels et al., 2020). This expanding CD8⁺ T cell population was originally classified as SLEC with cell surface marker phenotype KLRG-1⁺ CD62L⁻. However, based on the memory cell-like characterization, they were renamed as iTEM. The inclusion of the marker molecule CD127 allows a further distinction between iTEM (CD127⁻ KLRG-1⁺ CD62L⁻), cTEM (CD127⁺ KLRG-1⁻ CD62L⁻) and DPEC (CD127⁺ KLRG-1⁺ CD62L⁻) (Griessler et al., 2021). In a cell culture experiment, cells of cytolytic T-lymphocyte line (CTL) showed a DPEC phenotype after a long-term infection. This observation suggests, that repeated Ag re-stimulation by latently infected cells could generate CTL *in vivo* (Ebert et al., 2012). However, the investigation of MI, 6 months after hematopoietic cell transplantation (HCT) and mCMV infection, revealed low contribution from DPEC in lungs (Griessler et al., 2021).

A study characterizing the lineage relationship of the CD8⁺ T cell subsets during viral infections showed that CD62L⁻ CD127⁺ T cells (new classified as cTEM) develop first after Ag priming (Bachmann et al., 2005). During mCMV latency, inflationary CD8⁺ T cells with effector memory phenotype (iTEM) are stabilized at high numbers in peripheral tissues (Torti et al., 2011a). Moreover, these mCMV-specific CD8⁺ T cells express low levels of co-stimulatory molecules CD27 and CD28 (Snyder et al., 2008). In the LN the MI is induced by additional mCMV Ag recognition of latent infected non-hematopoietic cells (Seckert et al., 2011; Torti et al., 2011a). The inflationary CD8⁺ T cells include a central memory phenotype (TCM) and are re-stimulated to proliferate. Afterwards, these cells obtain an effector phenotype and migrate to peripheral tissues, where they are critical in controlling latency or reactivation of a mCMV infection (Torti and Oxenius, 2012).

1.4 Relation of Treg and mCMV infection

As mentioned before (chapter 1.3) hCMV and mCMV infections are controlled by the adaptive immune response, in particular the virus-specific CD8⁺ T cells. However, the virus cannot be eliminated and establishes a lifelong latent infection (Roizman and Baines, 1991). So far, it is unclear which immunological mechanisms are responsible for the control of latency. Treg are able to suppress the innate and adaptive immune response and thus they are able to regulate the self-tolerance of the immune system (Berod et al., 2012; Lindenberg et al., 2014; Mayer et al., 2012). It has been demonstrated that the depletion of CD4 Treg after mCMV infection has an impact on latent mCMV infection (Almanan et al., 2017). CD4 Treg are associated with viral reactivation, but the mechanisms contributing to the control of latent mCMV are still not clear. It is known that innate and adaptive immunity can be modulated by CD4 Treg, while the importance and subgroup of CD8 Treg remain still controversial (Niederlova et al., 2021; Vieyra-Lobato et al., 2018).

1.4.1 Development and function of Treg

Treg can suppress the innate and adaptive immune system and thereby maintain homeostasis and peripheral self-tolerance (Belkaid and Rouse, 2005; Fehervari and Sakaguchi, 2004; Sakaguchi, 2004). Moreover, they prevent autoimmune disease and allergies. In addition, Treg inhibit exaggerated T cell responses during infection (Lanteri et al., 2009; Suvas et al., 2004), enhance Teff differentiation and memory formation toward pathogens (Laidlaw et al., 2015; Pandiyan et al., 2011), and inhibit tumor immunity (Shimizu et al., 1999).

Until the early 2000s, the characterization of Treg was a problem due to the lack of phenotypic Treg markers, the diversity of suppressive mechanisms, and the difficulty of generating antigen-specific Treg clones for cellular and molecular analysis (Almeida et al., 2002; Shevyrev and Tereshchenko, 2019). Later it has been shown that IL-2 and its receptors (IL-2R α and IL-2R β) are critical for the development and maintenance of Treg (Almeida et al., 2002; Malek et al., 2002).

Treg are a heterogeneous population in terms of TCR repertoire and function. The development of Treg is defined by their ontogeny. Primarily, they developed in the thymus (tTreg), but can also develop in the periphery (pTreg) (Feurer et al., 2009; Sakaguchi et al., 2008; Shevyrev and Tereshchenko, 2019). tTreg are mainly found in the bloodstream as well as in the LN, and play an essential role in providing tolerance to autoantigens. While tTreg develops in the thymus,

pTreg are induced from conventional T cells (Tconv) affected by IL-2 and TGF- β and they are converted to cells with suppressive capacity in peripheral tissues. pTreg are predominantly located in peripheral barrier tissue and are involved in prevention of local inflammation in the presence of exogenous Ag (Shevyrev and Tereshchenko, 2019; Zheng et al., 2007). The transcription factor Helios is used to discriminate between CD4 tTreg and pTreg. tTreg express high amounts of Helios, whereas pTreg express low levels of Helios. In mice with a deletion of Helios, CD8 Treg were not able to control the Teff responses and thus exemplify the role of Helios in suppressive functions, differentiation and survival of Treg. The transcription factor Helios appears to be involved in stabilization of CD8 Treg in an inflammatory context (Kim and Sejnowski, 2021; Sebastian et al., 2016).

Treg have different mechanisms to inhibit proliferation and activation of Teff. These mechanisms can be classified into four groups: 1) the suppression by inhibitory cytokines, 2) cytolysis, 3) metabolic perturbation and 4) and the modulation of DC maturation (Vignali et al., 2008).

1.4.2 CD4 Treg

To date, CD4 Treg are the most characterized Treg subtype. It was identified that CD4 Treg express the IL-2R α chain (CD25) (Li et al., 2015; Nigam et al., 2010). CD4⁺ CD25⁺ Treg are hyporesponsive after activation via their TCR and suppress the proliferation of Teff (Sakaguchi et al., 1995; Shevach et al., 2001). However, CD25 is also highly expressed on activated Teff with considerably activity (Li et al., 2015). Several studies have shown that a population of CD4⁺ CD25⁺ cells derive from CD4⁺ CD25⁻ cells, which suppress the proliferation of other cells *in vitro* (Annacker et al., 2001; Furtado et al., 2002; Gavin et al., 2002). The CD4⁺ CD25⁺ cells maintain the CD25 expression and depend on IL-2, which is secreted by co-transmitted CD4⁺ CD25⁻ cells or by Ag-stimulated T cells (Li et al., 2015).

In 2003 several groups identified forkhead box transcription factor (FoxP3), which is said to be the main regulator of CD4 Treg. Its expression is crucial for the suppressive activity of CD4 Treg (Fehervari and Sakaguchi, 2004; Fontenot et al., 2003; Hori et al., 2003). In human studies with immune dysregulation, polyendocrinopathy, enteropathy, X-linked syndrome and in mouse studies, the transcription factor Foxp3 has been identified as an essential player in CD4 Treg has been identified (Brunkow et al., 2001; Ochs et al., 2005; van der Vliet and

Nieuwenhuis, 2007). Based on these findings, the CD4 Treg were defined as FoxP3⁺ CD4 Treg in the present work.

1.4.3 CD8 Treg

Already in the 1970s, CD8⁺ T cells and their suppressive potential were investigated (Gershon and Kondo, 1970). However, the investigation of CD8 Treg was hampered by the lack of specific markers and gene expression regulators (Sakaguchi et al. 1995). In recent years, CD8 Treg have been more investigated with regard to their origin, classification, molecular markers and functional mechanisms. Most of the CD8 Treg subsets can suppress effector T cells, which was measured by the suppression of T cell proliferation or production of IFN- γ (Niederlova et al., 2021).

One of the CD8 Treg subtype is characterized by the surface marker CD122. Dai *et al.* described CD8⁺ CD122⁺ Treg as necessary to maintain T cell homeostasis and to suppress T cell responses. However, CD8⁺ CD122⁺ cells have also been described as memory T cells, making it essential to further characterize these cells (Dai et al., 2010) (Judge et al., 2002; Ku et al., 2000; Zhang et al., 1998). PD-1 (programmed death-1) is a negative co-stimulatory molecule that is critical for suppression of autoimmunity, and local overexpression of its ligand (PD-L1) can induce immune dysfunction (Ansari et al., 2003; Francisco et al., 2009; Nishimura et al., 2001). CD8⁺ CD122⁺ cells contained both PD-1⁺ and PD-1⁻ cells, whereas CD8⁺ CD122⁺ PD-1⁺ Treg suppress the T cell responses in an IL-10 dependent manner *in vitro* and *in vivo* (Dai et al., 2010). The PD-1 expression on CD8⁺ T cells is mainly responsible for their depletion during chronic viral infection, which can be recovered by PD-1 blockade (Barber et al., 2006; Blackburn et al., 2009; Velu et al., 2009). In contrast to CD4 Treg, CD8⁺ CD122⁺ PD-1⁺ Treg do not express FoxP3. Bezie *et al.* reported that Foxp3 is barely expressed in CD8⁺ T cells in mouse, rat and human (Bezie et al., 2017). Furthermore, the surface marker CD127 is absent on CD8 Treg and only recovers in effector and memory T cells (Dai et al., 2010). In the present work, CD8 Treg were defined as CD8⁺ CD122⁺ PD-1⁺ CD127⁻ Treg according to the study by Dai *et al.* (Dai et al., 2010).

1.4.4 Treg in mCMV infection

The study by Jost *et al.* revealed that thymus derived FoxP3⁺ CD4 Treg and FoxP3⁻ CD4 Treg (IL-10 induced Treg) impaired an effective anti-mCMV immune response, while depletion of FoxP3⁺ Treg in mice showed an enhanced T cell activation and reduced viral titers (Jost *et al.*, 2014). The human study by Pastor *et al.* discovered a relation between CD4 Treg and the recovery of virus-specific CD8⁺ T cells after allogeneic stem cell transplantation (SCT) (Pastore *et al.*, 2011). Interestingly, CD4 Treg control the reactivation of latent mCMV infection organ-specific (Almanan *et al.*, 2017). In the spleen, the depletion of CD4 Treg resulted in an enhanced mCMV-specific CD8⁺ T cell response and reduced viral reactivation. In the SG, viral replication was prevented by Treg and their IL-10 production. The CMV reactivation occurs with a simultaneously increase of CD4 Treg and their suppressive capacity (Schwele *et al.*, 2012). Moreover, CD4 Treg impaired mCMV-induced T cell proliferation and activation and induced apoptosis by the PD-1 signaling pathway (Tovar-Salazar and Weinberg, 2020). The latter can be prevented by blocking PD-1.

In comparison to CD4 Treg, the impact of CD8 Treg on immune control after CMV infection has not been investigated yet. There are increasing numbers of studies showing data on the suppressive mechanisms of CD8 Treg (Bezie *et al.*, 2018). The suppressive mechanisms of CD8 Treg have been demonstrated for example in autoimmune encephalomyelitis (Saligrama *et al.*, 2019), multiple sclerosis (Liu *et al.*, 2007), human immunodeficiency virus and Epstein-Barr virus (Boer *et al.*, 2015; Fenoglio *et al.*, 2018; Popescu *et al.*, 2007), or transplantation in mouse, rat, and human (Bezie *et al.*, 2017; Robb *et al.*, 2012, Zheng *et al.*, 2013).

Both CD4 and CD8 Treg use similar suppressive mechanisms (Bezie *et al.*, 2018). However, the different mechanisms are still unknown and it is still unclear how Treg decide which mechanism to apply and whether they switch from one to another mechanism or apply multiple mechanisms simultaneously (Schmidt *et al.*, 2012; Shevach, 2009; Vieyra-Lobato *et al.*, 2018). Therefore, further detailed analyses are needed to define CD8 Treg and to better understand the regulatory mechanisms of both CD4 and CD8 Treg, which could lead to novel cell therapies or prevention of infectious diseases such as CMV (Vieyra-Lobato *et al.*, 2018).

1.5 IL-10 function

IL-10 is a pleiotropic cytokine and modulates both, innate and adaptive immune responses, by anti-inflammatory effects (Moore et al., 2001). First IL-10 was described as a product of T_H2 cells, which are able to inhibit the T_H1 response and cytokine synthesis (Fiorentino et al., 1989). Later it was discovered, that IL-10 is secreted by different immune cells including T cells (Kamanaka et al., 2006; Moore et al., 2001), B cells (Masuda et al., 2002), DC (Iwasaki and Kelsall, 1999; Li et al., 1999) and MΦ (Li et al., 1999) as well as keratinocytes in skin and epithelial cells in the lung (Bonfield et al., 1995; Grewe et al., 1995). IL-10 secretion was detected in the different T cell subsets, such as Treg, T_H1 cells (O'Garra and Vieira, 2007; Trinchieri, 2007), T_H2 cells (Fiorentino et al., 1989; Saraiva and O'Garra, 2010) and T_H17 cells (Awasthi et al., 2007; Fitzgerald et al., 2007; Saraiva and O'Garra, 2010).

Not only is the immunosuppressive cytokine IL-10 produced by the above mentioned cells, but also acts on them. The pathogen activation of DC involves the recognition of pathogen-derived product by PRR (Medzhitov et al., 2007). These PRR triggers the expression of cytokines and other factors. Following their activation, DC can express IL-10 *in vitro* and *in vivo* (Akbari et al., 2001; Boonstra et al., 2006; McGuirk et al., 2002). It has been reported that TLR-2 agonists are specialized in inducing IL-10 expression by APC (Agrawal et al., 2003; Dillon et al., 2004; Hu et al., 2006). IL-10 production is also induced by TLR-4 and TLR-9 ligands (Boonstra et al., 2006). Furthermore, IL-10 can be induced by TLR-independent stimulation such as DC-SIGN or dectin-1 (Geijtenbeek et al., 2003; Rogers et al., 2005). The secretion of IL-10 is important in controlling the balance between inflammation and immune tolerance. IL-10 acting on DC leads to decreased expression of MHC-II and co-stimulatory molecules such as CD80 and CD86 (Clausen and Girard-Madoux, 2013; Corinti et al., 2001). It also inhibits DC maturation and secretion of pro-inflammatory cytokines (Moore et al., 2001; Steinbrink et al., 1997). Moreover, IL-10 produced by CD4⁺ T cells can initiate the development of IL-10 secreting Treg and suppress antigen-specific responses *in vivo* and *in vitro* (Asseman et al., 1999; Groux et al., 1997; Tanchot et al., 1998). For example, it has been shown that Treg exhibit strong adhesiveness to DC which diminishes their ability to interact with other antigen-specific T cells and therefore inhibits T cell priming (Chen et al., 2017; Yan et al., 2017). IL-10 can also act on T cells by inhibiting the development of the T_H1 response and the effector T cell function (Fiorentino et al., 1991; Shouval et al., 2014). IL-10 promotes the stimulation of CD8⁺ T cells, induces their recruitment, cytotoxic activity and proliferation (Groux et al., 1998; Jinquan et al., 1999; Santin et al., 2000).

1.5.1 IL-10 receptor and signaling

The IL-10 receptor (IL-10R) is a member of the interferon receptor (IFNR) family and forms a tetramer which is composed of two IL-10R α , as well as two IL-10R β subunits (Moore et al., 2001) (**Fig. 4**). IL-10R α is the ligand-binding subunit, which is expressed on different hematopoietic cells, including DC and T cells (Ho et al., 1993; Moore et al., 2001; Tan et al., 1993). After activation, IL-10R α expression is downregulated at mRNA and protein levels on T cells (Liu et al., 1994; Tan et al., 1993), while its expression is upregulated on monocytes (Moore et al., 2001). The IL-10R β signaling subunit is expressed on many cells and tissues (Gibbs and Pennica, 1997; Lutfalla et al., 1993) and is shared by several cytokines like IL-22 and IL-26 (Commins et al., 2008; Donnelly et al., 2004). This subunit contributes less to binding affinity of IL-10 and the main function is the recruitment of a Jak kinase into the signaling complex (Kotenko et al., 1997; Spencer et al., 1998).

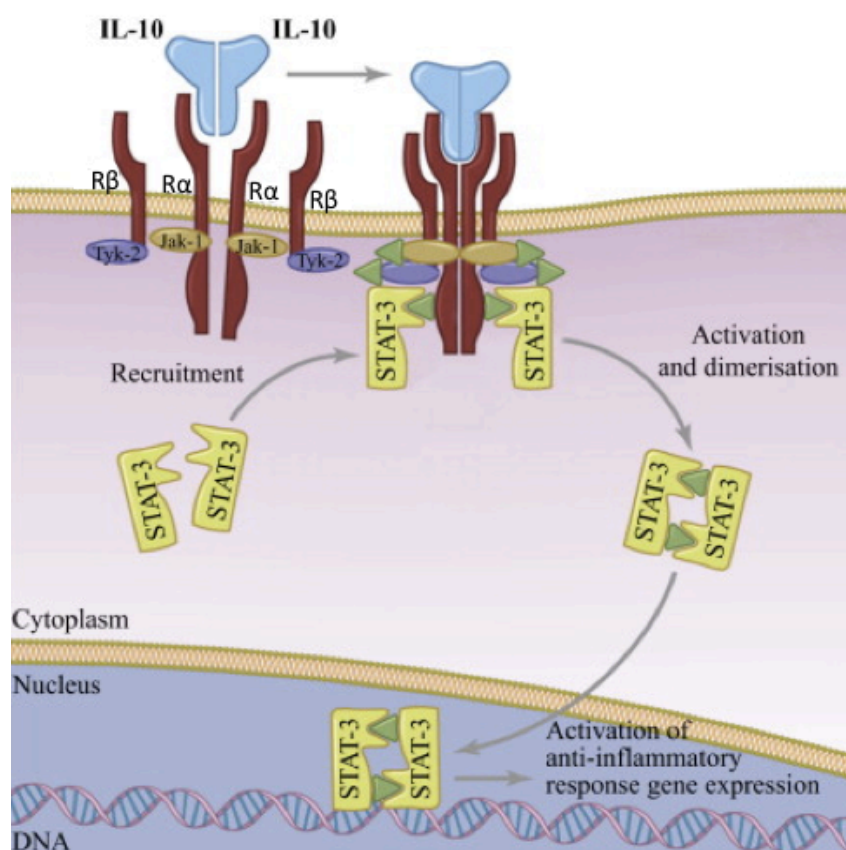


Figure 4: IL-10R signaling.

IL-10 binds to IL-10R which is composed of two IL-10R α and two IL-10R β chains. The intracellular domains of IL-10R α and IL-10R β are associated with the enzymes Jak-1 and Tyk-2. Both enzymes become activated and phosphorylate (green triangle) the IL-10R α chain. STAT3 binds at the receptor and becomes activated by phosphorylation. The phosphorylated STAT3 homodimerizes and translocates into the nucleus where it binds at specific genes to promote their transcription (adapted from Howes et al., 2014).

The assembly of the cell surface IL-10R heterotetramer is the first step in initiating the IL-10 signaling pathway, which activates the Janus tyrosine kinase-1 (JAK-1) coupled with the α subunit and the tyrosine kinase-2 (Tyk-2) associated with the β subunit (Kotenko et al., 1997; Shouval et al., 2014). Subsequently, both kinases phosphorylate the IL-10R α subunit at the intracellular domain, which are recognized by the transcription factor STAT3 (signal transducer and activator of transcription 3). STAT3 is phosphorylated by JAK-1 and forms homodimers, which translocate into the nucleus to bind promoters of IL-10 target genes (Finbloom and Winestock, 1995; Murray, 2007; Shouval et al., 2014).

1.5.2 IL-10 in infectious disease

The cytokine IL-10 can limit the pathogen clearance and enhance the immunopathology. The infection with viruses, bacteria and fungi promotes the T_H1 and CD8⁺ T cell responses that limits the pathology. For example, IL-10 producing T_H1 cells were identified in mice with *Toxoplasma gondii* or *Leishmania major* infections and were suggested to regulate these infections (Anderson et al., 2007; Gazzinelli et al., 1996). In addition, the influenza infection induces the production of IL-10 in the lung, thereby controlling excess inflammation that was associated by a T_H1 response (Sun et al., 2009). IL-10 is also involved in controlling immunopathology during herpes simplex infection, while the deletion of IL-10 caused a severity infection (Sarangi et al., 2008). An excessive IL-10 production can inhibit the pro-inflammatory response and the virus escapes the immune control, resulting in severe immunopathology or a chronic infection. In chronic lymphocytic choriomeningitis virus infection (LCMV), CD8⁻ DC promotes IL-10 production. Therapeutic IL-10R blockade *in vivo*, enhances the anti-viral CD8⁺ T cell responses and results in viral clearance (Brooks et al., 2006; Ejrnaes et al., 2006). Furthermore, mCMV exploits the immune regulation through an IL-10-dependent manner in the SG, which inhibits the mCMV persistence (Humphreys et al., 2007). hCMV harbors a functional and viral IL-10 homologue (vIL-10) to avoid immune surveillance and elimination from the host (Kotenko et al., 2000). *In vitro* experiments demonstrated, that the treatment of immature DC with the supernatant from hCMV-infected cultures inhibit the LPS-induced maturation of immature DC and their pro-inflammatory cytokine production (Chang et al., 2004). During latent hCMV infection, vIL-10 mRNA is expressed and the CD4⁺ T cell response is down-regulated (Cheung et al., 2009; Jenkins et al., 2004). In mCMV infected IL-10 knockout (IL-10^{-/-}) mice, an accumulation of memory CD8⁺ T cells and an increase of anti-viral cytokine production were observed in mCMV

infected IL-10 knockout (IL-10^{-/-}) mice during latent infection. Blocking the IL-10R revealed that IL-10 inhibits memory CD8⁺ T cell responses and a reduction of the viral load. The study of Jones *et al.* demonstrated, that IL-10 has an inhibitory function and restricts the memory cell inflation during mCMV infection (Jones *et al.*, 2010).

1.6 β -catenin/Wnt signaling pathway

β -catenin is a central component of the canonical Wingless-Int (Wnt) signaling pathway. The Wnt pathway plays a critical role in many cellular processes and the organ development (Hoppler and Kavanagh, 2007; Valenta *et al.*, 2012). Without Wnt signaling, cytoplasmic β -catenin is bound to E-cadherin or phosphorylated by the destruction complex, which consists of the Axin, Adenomatous Polyposis Coli (APC), glycogen synthase kinase-3 β (GSK-3 β) and casein kinase 1 α (CK1 α) (Fig. 5).

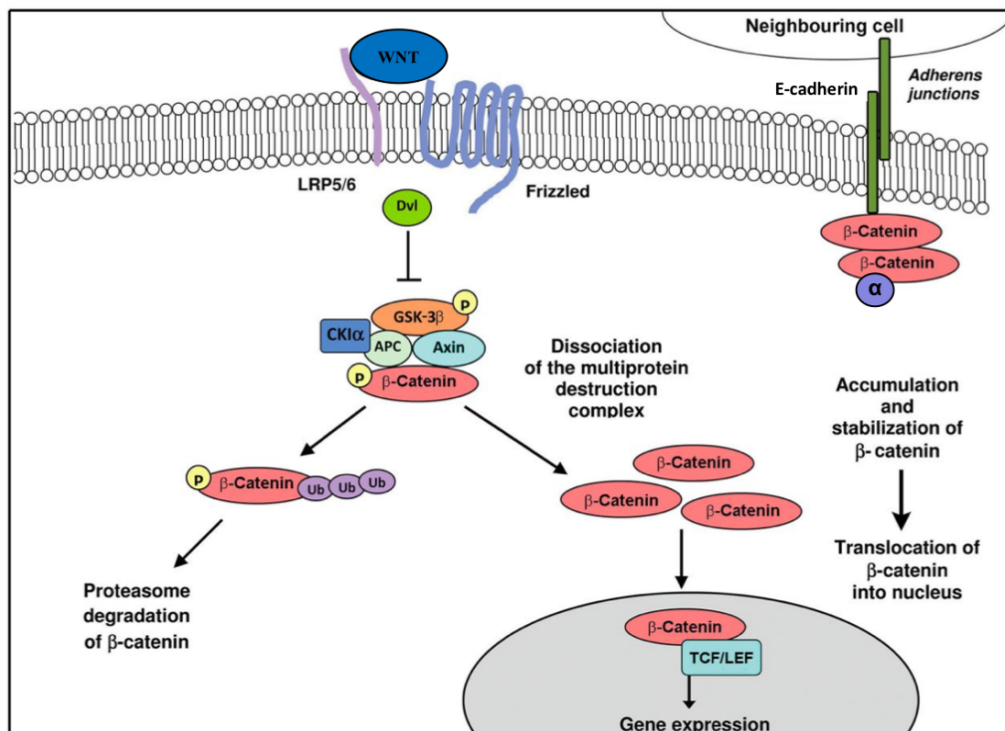


Figure 5: The canonical Wnt/ β -catenin signaling pathway.

Newly synthesized β -catenin is immobilized by E-cadherin for cell-cell adhesion. In the absence of a Wnt signal, free β -catenin is phosphorylated by the destruction complex and polyubiquitinated for the proteasomal degradation. Binding of a Wnt ligand to the Frizzled receptor inhibits the interaction with the destruction complex and β -catenin accumulates in the cytoplasm. Thereupon β -catenin translocates to the nucleus and activates the target gene expression (adapted from Denysenko *et al.*, 2016).

The two kinases of the multi-protein complex phosphorylate β -catenin, which is recognized and degraded by the proteasome. The phosphorylation domain of β -catenin is located in the NH2-terminal region at the 3rd exon (Huber et al., 1997). The binding of a Wnt ligand to its receptor Frizzled inactivates the degradation complex, resulting in the accumulation of β -catenin in the cytoplasm and translocation into the nucleus. The nuclear β -catenin induces the gene expression via its binding to the TCF/LEF transcription factor, which is important for cellular proliferation, differentiation and survival (MacDonald et al., 2009; Ota et al., 2016; Valenta et al., 2012). β -catenin increases either by newly synthesized β -catenin or by release from the cytoskeleton, where β -catenin is involved in the formation of the actin scaffold and cell-cell contacts in a complex with E-cadherin and α -catenin (Nelson, 2008).

1.6.1 β -catenin signaling in DC shape the immune response

β -catenin plays a potential role in the immunity and is associated with a tolerogenic DC function. The activation of β -catenin signaling in bone marrow-derived DC (BMDC) by mechanical cluster disruption results in spontaneous phenotypic DC maturation without the secretion of pro-inflammatory cytokines (Jiang et al., 2007). In addition, cluster disrupted BMDC induce IL-10 producing T cells *in vitro* and protect mice from the induction of experimental autoimmune encephalitis (EAE) *in vivo*. Mice with a specific deletion of β -catenin in CD11c⁺ cells showed a higher susceptibility to dextran-sodium-sulfate (DSS)-induced colitis and resulted in an increased T_H1/T_H17 differentiation, which was accompanied by a blunted response of CD4 Treg (Manicassamy et al., 2010; Suryawanshi et al., 2015). The study by Alves *et al.* showed that the ablation of β -catenin in DC results in a lower frequency of Treg during autoimmune collagen-induced arthritis, whereas the severity of the disease is not aggravated (Alves et al., 2015). Furthermore, β -catenin signaling was shown to inhibit DC cross-priming of CD8⁺ T cells by upregulation of IL-10, resulting in tumor-induced immunosuppression (Fu et al., 2015; Liang et al., 2014). In contrast, stabilized β -catenin expression in CD11c⁺ cells can mediate a pro-inflammatory function and promote the development of an effective CD8⁺ T cell response in the context of viral infection (Cohen et al., 2015). It has been reported that hCMV dysregulates the β -catenin signaling pathway. hCMV infection inhibits the transcriptional activity of β -catenin and the expression of its target genes like cyclin D1, c-myc and Dickkopf- (DKK1) (Angelova et al., 2012). Despite these interesting findings of β -catenin,

whether and to what extent β -catenin signaling in DC affects the Treg differentiation, and controls the acute and latency mCMV infection is so far not known.

1.7 Objectives

Primary CMV infections are largely controlled by CD8⁺ T cells in immunocompetent hosts. After primary infection, CMV is able to establish lifelong latent infection. Reactivation of latent hCMV leads to life-threatening complications, especially in immunocompromised individuals, like bone marrow transplantation (BMT) recipients. Treg are able to suppress the innate and adaptive immune response and thus regulate self-tolerance of the immune system. A major role in the initiation of anti-viral T cell responses are controlled by DC. Yet, they are also important targets of Treg-mediated suppression, which includes the downregulation of co-stimulatory molecules and inhibiting the secretion of pro-inflammatory cytokines. An important mediator of this immune suppression is the secretion of IL-10 by Treg and presumably DC themselves. IL-10 limits CD8⁺ T cell expansion during latent mCMV infection, but to what extent DC are targets or relevant sources of IL-10 during mCMV infection is still unidentified. A second pathway associated with a tolerogenic DC function is the β -catenin signaling pathway. Sudden activation of β -catenin signaling in BMDC induces IL-10-producing T cells *in vitro* and protects mice from EAE induction *in vivo*. In contrast, stabilization of β -catenin in DC promotes a pro-inflammatory function of DC during viral infection. To date, it is unknown whether and to what extent β -catenin signaling in DC impacts Treg differentiation and function of mCMV immunity and latency.

To answer these questions, the role of DC in shaping the virus-specific CD8⁺ T cell response and Treg differentiation in conditional knock-out mice with a specific deletion of IL-10, IL-10 receptor and β -catenin in CD11c⁺ cells or expression of a stabilized form of β -catenin in CD11c⁺ cells (referred to as IL-10^{ACD11c}, IL-10R^{ACD11c}, β -cat^{ACD11c} and β -cat^{ACD11c/EX3}) upon mCMV infection. First, we established an intranasal (i.n.) mCMV infection model which reflects the natural route of infection to offer a profound fundament for future experiments. Therefore, wild-type mice were i.n. infected with mCMV- Δ m157 and the virus-specific CD8⁺ T cell response was analyzed. In the second part, we examined the role of IL-10 production by DC and IL-10 and β -catenin signaling in DC after acute mCMV infection. Therefore, we analyzed DC, virus-specific CD8⁺ T cell response, CD4 and CD8 Treg differentiation in the lung, dLN and spleen. In the blood, the virus-specific CD8⁺ T cell response

during the whole infection period was determined. Viral genomes were assessed in lung by real-time PCR. Third, the role of IL-10 and β -catenin signaling in mCMV latency was studied. For this purpose, the anti-viral CD8⁺ T cell response, DC, CD4 and CD8 Treg differentiation were analyzed in the lung and lymphoid organs. Similarly to acute infection, we followed the kinetic of the virus-specific CD8⁺ T cells and their subpopulations during the whole infection in the blood. Comprehensive characterization of different subpopulations of mCMV-specific CD8⁺ T cells should provide insights into the development and MI of these cells. Finally, latent viral genome load was measured in lung, spleen and liver.

2 Materials and Methods

2.1 Chemicals and buffers

Chemicals were purchased from Sigma (Steinheim), Fluka Chemie (Switzerland), Merck (Darmstadt) or AppliChem (Darmstadt) unless stated otherwise. Solutions were prepared with double distilled water (ddH₂O). Sterility of solutions and chemicals used in cell culture was maintained by working under a sterile hood (Heraeus, Germany).

Table 1. List of used chemicals

Name of Chemical	Supplier
Acetic acid	Roth, Karlsruhe
Agarose, electrophoresis grade	Biozym Scientific GmbH, Hess. Oldendorf
Ammonium chloride	Sigma-Aldrich, Steinheim
Bovine serum albumin (BSA)	Sigma-Aldrich, Steinheim
Calcium chloride	Sigma-Aldrich, Steinheim
Collagenase type IV	Worthington Biochemical, Lakewood, USA
DNase	Promega, Madison, USA
Ethanol, abs.	AppliChem, Darmstadt
Ethylenediamine tetraacetate (EDTA)	Roth, Karlsruhe
Fc-Block	BioXcell, Lebanon, USA
Fetal calf serum (FCS)	Boehringer Ingelheim, Ingelheim am Rhein
Gene Ruler 100bp Plus DNA Ladder	Thermo Fisher Scientific Inc., MA, USA
Histofix 4%	Roth, Karlsruhe
Isoflurane	AbbVie, Ludwigshafen
Isopropanol	AppliChem, Darmstadt
Ketamine	Hameln Pharma GmbH, Hameln
Lysing Solution 10x	BD Bioscience, Heidelberg
Midori Green Advance	NIPPON Genetics EUROPE GmbH, Düren
Phosphate buffered saline (PBS)	Sigma-Aldrich, Steinheim
Potassium hydrogen carbonate	Roth, Karlsruhe
Proteinase K	Roche, Switzerland
REDTaq ReadyMix	Sigma-Aldrich, Steinheim
RPMI-1640 medium	Gibco Life Technologies GmbH, Karlsruhe
Sodium chloride	AppliChem, Darmstadt

Sodium dodecyl sulfate	AppliChem, Darmstadt
Tris/ HCl	AppliChem, Darmstadt
Xylazine	Bayer, Leverkusen
2x M-PCR OPTI Mix	Bioutil, Munich

Used buffers are listed below.

Table 2. List of used buffers.

Buffer	Composition
TENS buffer	50 mM Tris, pH 8.0; 100 mM EDTA; 100 mM NaCl; 0.2% (w/v) SDS; 400 mg/ml proteinase K
FACS buffer	1x PBS, 3% FCS, 2 mM EDTA
Digestion mix	RPMI-1640, 200 U/ml Collagenase IV, 0,5 U/ml DNase
Tris-Acetate-EDTA (TAE) buffer	2 mM Tris, 1 mM acetic acid, 50 mM EDTA
10x ACK lysis buffer	H ₂ O, 150 mM NH ₄ Cl, 100 mM KHCO ₃ , 10 mM EDTA, pH 7.2

2.2 Molecular biology

2.2.1 Isolation of genomic DNA from biopsies

DNA was isolated from toe or tail biopsies, which were lysed over night (o/n) at 56°C in TENS buffer. Subsequently, DNA was precipitated from the solution by the addition of an equal volume of isopropanol. DNA was pelleted by centrifugation, washed in 70% (v/v) EtOH, dried at room temperature (RT) and resuspended in H₂O.

2.2.2 Polymerase Chain Reaction (PCR)

PCR was used to screen mice for the presence of targeted alleles or transgenes and to amplify DNA (primers shown in **Table 3**). Reactions were performed in Triothermocyclers (Biometra, Göttingen, Germany). Genotyping of mice was generally performed in a total volume of 20 µl

or 24 μ l in the following reaction mix: REDTaq ReadyMix™ PCR Reaction Mix or 2x M-PCR OPTI Mix, 100 ng/ μ l of each primer, DNase free water and 1 μ l template DNA. Depending on the mutation, different PCR programs were used (PCR programs shown in Table 4).

Table 3: List of primers used for genotyping.

Gene	Name of primer	Sequence (5'-3')	T _{Ann.} (°C)
β-catenin DEL	C-726	AAG GTA GAG TGA TGA AAG TTG TT	58
	C-727	CAC CAT GTC CTC TGT CTA TCC	58
	C-728	TAC ACT ATT GAA TCA CAG GGA CTT	58
β-catenin EX3	EX3 C-733	GAC ACC GCT GCG TGG ACA ATG	62
	EX3 C-734	GTG CTG ACA GCA GCT TTT CTG	62
CD11c-Cre	CD11c-Cre (boris) s	ACT TGG CAG CTG TCT CCA AG	63
	CD11c-Cre (boris) as	GCG AAC ATC TTC AGG TTC TG	63
IL-10	IL-10floxed (MCO2)	CCA GCA TAG AGA GCT TGC ATT ACA	60
	IL-10floxed (IL-10EX2)	GAG TCG GTT AGC AGT ATG TTG TCC AG	60
IL-10R	IL-10R LoxP-1/ C810	CCA CCA AGA GTC AGG TAG GGA C	56
	IL-10R fLoxP-1	GAG CTT GGG AAC CTC CGC AGG	56

Table 4: PCR programs.

PCR	PCR Mix	hold	Cycles	Cycles			end	hold
				94°C	58°C	75°C	72°C	15°C
β-catenin DEL	2x M-PCR OPTI Mix	94°C 5 min	38 cycles	94°C	58°C	75°C	72°C	15°C
				45 sec	45 sec	45 sec	5 min	∞
β-catenin EX3	2x M-PCR OPTI Mix	95°C 5 min	38 cycles	95°C	62°C	72°C	72°C	15°C
				30 sec	30 sec	45 sec	10 min	∞
CD11c-Cre	RedTaq	95°C 5 min	40 cycles	95°C	63°C	72°C	72°C	15°C
				30 sec	40 sec	45 sec	10 min	∞
IL-10	RedTaq	95°C 5 min	35 cycles	95°C	60°C	72°C	72°C	15°C
				15 sec	1 min	1 min	10 min	∞
IL-10R	2x M-PCR OPTI Mix	95°C 5 min	35 cycles	95°C	56°C	72°C	72°C	15°C
				15 sec	1 min	1 min	10 min	∞

2.2.3 Agarose gel electrophoresis

Separation of DNA fragments from biopsies by size was achieved by electrophoresis in agarose gels (2% (w/v); 1x TAE; 12 µl Midori Green). Agarose gels run at 130 V in 1x TAE buffer and are visualized using a gel documentation system (Bio Rad, Munich). The Gene Ruler DNA Ladder was used as marker to determine the length of DNA fragments.

2.2.4 Isolation of viral DNA

Viral DNA was isolated to determine genome loads from cells. Therefore, cells were lysed for 30 min at 56°C using 400 mg/ml proteinase K. DNA was extracted and prepared with DNeasy Blood & Tissue Kit (QIAGEN GmbH, Hilden) following manufacturer's instructions.

2.2.5 Quantification of DNA

The concentration and quality of nucleic acids from mouse organs could be determined by spectroscopy measuring the absorption of the sample at 260 nm and 280 nm. An OD₂₆₀ of 1 corresponds to approximately 50 µg/ml for double-stranded DNA and 40 µg/ml for single stranded RNA. Purity of nucleic acids was calculated by the ratio OD₂₆₀/OD₂₈₀. The value should be 1.8 and 2.0 for DNA and RNA, respectively.

2.2.6 Quantitative PCR (qPCR)

DNA from cells was extracted and prepared with DNeasy Blood & Tissue Kit (QIAGEN GmbH, Hilden) followed by the quantification of nucleic acids. To determine the mCMV genomes in lung, spleen and liver, qPCR was performed, which allows following amplification of DNA fragments in real time. A sequence-specific probe labeled with a fluorophore binds to double-stranded amplified DNA (e.g. TaqMan) or a fluorescent dye (e.g. SYBR green) intercalates into the amplified DNA. The detected fluorescence intensity is proportional to the number of amplified PCR products. When using SYBR green, a melting curve analysis of the amplicon is required to exclude non-specific amplifications. Intercalated dye is released by gradually increasing the temperature to denature the double-stranded DNA and this loss of fluorescence can be detected. The maximum fluorescence intensity is equal to

the melting temperature of the desired amplified PCR product. Unspecific amplifications differ in melting temperature. The absolute quantification of the template is calculated as follows (N = number of amplified molecules; N_0 = initial amount of molecules; E = PCR efficiency, constant; n = number of cycles):

$$N = N_0 * E^n$$

The plasmid pDrive-gB-PTHrP-BAC was used as standard and contains the partial gene sequences of the *BAC* vector sequence, the viral glycoprotein *gB/M55*, and the cellular housekeeping gene *PTHrP* (Lemmermann et al., 2010). Latter is a single copy gene and therefore allows the normalization of viral and cellular genomes. The viral protein *gB/M55* is transcribed in the late phase of infection. The linearized plasmid was titrated from 0.5×10^1 to 0.5×10^7 copies per μl in Tris buffer and amplified for standard curve. The titration of the standard allows the absolute quantification of the template. The QuantiTect SYBR Green PCR Kit (QIAGEN, Hilden) was used for the absolute quantification of the DNA template and was performed in a total volume of 20 μl in the following reaction mix: 2x QuantiTect SYBR Green PCR master mix, 10 μM of each primer, DNase free water and 2 μl template DNA. Used primers and PCR program are described in **Table 5 and 6**.

Table 5: Primers used for DNA quantification by SYBR Green qPCR.

Name of primer	Sequence (3'-5')
BAC-Taq-for1	GTT CTG TCA TGA TGC CTG CAA
BAC-Taq-rev1	AAT CCG CTC CAC TTC AAC GT
LC-gB-for3	GAA GAT CCG CAT GTC CTT CAG
LC-gB-rev3	AAT CCG TCC AAC ATC TTG TCG
LC-PTHrP-for2	GGT ATC TGC CCT CAT CGT CTG
LC-PTHrP-rev2	CGT TTC TTC CTC CAC CAT CTG

Table 6: SYBR Green PCR program.

hold	Cycles			
95°C 15 min	50 cycles	94°C	62°C	72°C
		15 sec	30 sec	45 sec
	Melting curve temperature increases 1°C per round	95°C	62°C	72°C
		30 sec	30 sec	45 sec

PCR runs were analyzed with the 7500 Fast Real-Time PCR System software and viral genomes were calculated per 10^6 cells (gB = copies of gB; PTHrP = copies of PTHrP):

$$10^6 * \frac{gB}{2 * PTHrP}$$

The determination of the mCMV genome in lung, spleen and liver of i.n. infected mice was kindly performed by the group of Dr. Lemmermann (Institute of Virology, University Medical Center of the Johannes Gutenberg-University Mainz).

2.3 Cell biology

2.3.1 Preparation of single cell suspensions from lung and lymphoid organs

Lung, lung-draining mediastinal lymph node (dLN) and spleen were removed from mice, cut into small pieces and digested with 1 ml digestion mix (**Table 2**) for 30 min at 37°C and 1.200 rpm in a thermoshaker (Buddeberg, Mannheim). Subsequently, 1 ml of digestion mix was added to the lung and digested for further 30 min. To separate cell clusters, EDTA (10 mM) was added to the mix for 5 min at RT. Subsequently, cells were passed through a nylon cell strainer (70 μ m, BD Falcon, Heidelberg) to obtain a single cell suspension and washed with FACS buffer (**Table 2**). Erythrocytes from lung and spleen preparations were lysed with 1 ml of 1x ACK buffer (**Table 2**) for 1-2 min. To stop lysis, cells were immediately washed in 10 ml FACS buffer, centrifuged (5 min, 1.200 rpm, 4°C), resuspended in the appropriate amount of FACS buffer and kept on ice for subsequent processing.

2.3.2 Preparation of blood cells

Blood from tail vein or heart was collected in a tube with heparin (Liquemin, Roche, Mannheim). After extracellular staining, erythrocytes were lysed with 1 ml of 1x Lysing Solution (BD Bioscience, Heidelberg) for 10 min in the dark and immediately diluted in 1 ml FACS buffer (**Table 2**). Cells were centrifuged (10 min, 400 \times g, 4°C) and resuspended in the appropriate amount of FACS buffer and kept on ice for subsequent processing.

2.3.3 Cell counting

Viable cells were assessed using trypan blue dye exclusion test and counted using a Neubauer chamber (Assistant, Sondheim). An aliquot of cell suspension (10 μ l) was diluted with trypan blue solution (Gibco, Long Island, NY, USA). Dead cells are stained blue whereas live cells cannot take up the dye due to their intact membrane. Sixteen single quadrants were counted and the number of live cells was calculated as follows (N = counted cell number; V = dilution factor; 10^4 = chamber factor):

$$N * V * 10^4 = \text{cell number/ml}$$

2.3.4 Flow cytometry

Single cell suspensions were prepared from lung, dLN and spleen and the cell numbers were determined. Cells ($0.5-1 \times 10^6$ per sample) pre-incubated with Fc-Block for 10 min at 4°C, washed with FACS buffer and surface stained with a mix of viability dye (eBioscience, USA) and fluorescence conjugated antibodies in FACS buffer at 4°C in the dark for at least 20 min. Stainings with biotinylated mAbs were followed by a secondary staining step with Streptavidin for 20 min at 4°C. Used Abs are listed below (**Table 7**). To determine mCMV-specific CD8⁺ T cells, the Ab mix additionally contained M38 or M45 Tetramers (kindly provided by Prof. Dr. Ramon Arens, University of Leiden, Netherlands) and were stained at 4°C in the dark for at least 45 min. MHC Tetramers are complexes of four MHC molecules and are associated with a specific peptide and bound to a fluorochrome, which were used to detect antigen-specific T cells by flow cytometry. Peptide-loaded MHC molecules form an MHC-peptide complex that is recognized by specific T cell receptors (Roetzschke et al., 1990). In this study MHC-I Tetramers recognizing CD8⁺ T cells specific for M38₃₁₆₋₃₂₃ (³¹⁶SSPPMFRV³²³) and M45₉₈₅₋₉₉ (⁹⁸⁵HGIRNASFI⁹⁹³) were used. After the cell surface staining, cells were washed with FACS buffer and fixed with 2% Histofix for 15 min at RT, except for Tetramer stainings where stained cells were directly acquired with FACSCanto II (BD Biosciences, Heidelberg). The antibodies FoxP3 and Helios were used for intracellular staining. Therefore, cells were fixed and permeabilized using the Foxp3/Transcription factor kit (eBioscience, USA) according manufacturer's instructions. Stained cells were acquired with FACSCanto II and analyzed with FlowJo software.

Table 7: List of antibodies used for flow cytometry.

Specificity	Clone	Supplier
CD4	RM4-5	BioLegend
CD4	GK1.5	BioLegend
CD8	53-6.7	BioLegend
CD11b	M1/70	BioLegend
CD11c	HL3	BD biosciences
CD11c	N419	BioLegend
CD25 (IL2Ra)	PC61	BioLegend
CD44	IM7	BioLegend
CD45	104	BD biosciences
CD62L (L-Selectin)	MEL-14	BioLegend
CD103	2E7	BioLegend
CD122	5H4	eBioscience
CD127	A734	eBioscience
F4/80	BM8	eBioscience
FoxP3	FJK-16s	eBioscience
Helios	22F6	BioLegend
KLRG-1	2F1	eBioscience
MHCII	M5/114.15.2	eBioscience
PD-1 (CD279)	29F.1A12	BioLegend
SIRPa	P84	eBioscience
TCRb	H57-597	BD biosciences
XCR-1	ZET	BioLegend

2.3.5 mCMV

Mice were infected with the mCMV- Δ m157, which lacks the m157 open reading frame (ORF). mCMV-resistant C57BL/6 mice express the activating NK receptor Ly49H, which interacts with the m157 ligand on the surface of infected cells. To prevent NK cells from controlling mCMV, mice were infected with the mCMV- Δ m157 to prevent stimulation of the Ly49H receptor (Bubic et al., 2004). In this study, all used mouse strains (see 2.4.1) were i.n. infected with this virus (see 2.4.2).

The virus was provided by the group of Prof. Dr. Reddehase (Institute of Virology, University Medical Center of the Johannes Gutenberg-University Mainz) and supplied as virus stocks purified through a Saccharose gradient.

2.4 Mouse experiments

2.4.1 Mice

IL-10^{flox/flox} (Roers et al., 2004) and IL-10R^{flox/flox} (Pils et al., 2010) mice were generated previously and bred to CD11c-Cre mice (Caton et al., 2007) to generate IL-10^{flox/flox}-CD11c-Cre (IL-10^{ΔCD11c}) and IL-10R^{flox/flox}-CD11c-cre (IL-10R^{ΔCD11c}) mice. CD11c-Cre mice were crossed to β -cat^{Exon3/Exon3} (Harada et al., 1999) and β -cat^{Del/Del} (Brault et al., 2001) mice to generate β -cat^{Exon3/Exon3}-CD11c-Cre (β -cat^{CD11c/EX3}) and β -cat^{Del/Del}-CD11c-Cre (β cat^{ΔCD11c}) mice. All mice were backcrossed for at least ten generations to C57BL/6 mice, housed in specific pathogen-free conditions and used in accordance with the guidelines of the Translational Animal Research Center (TARC) of the University Medical Center Mainz. CD11c-Cre^{neg} littermate controls, referred to control mice, were used as controls in all experiments. Both CD11c-Cre⁺ and CD11c-Cre^{neg} mice were co-housed to avoid cage bias.

2.4.2 Infection with mCMV

14- to 18-week- old mice were infected with 2×10^5 PFU of the mCMV- Δ m157 using the i.n. infection route. The virus was diluted in 20 μ l PBS and administered drop by drop with a pipette into one nostril of mice anesthetized with isoflurane (600 ml/min oxygen and 5% isoflurane).

For the latent i.n mCMV infection, mice were anesthetized with 10 μ l ketamine (10 mg ml⁻¹) + xylazine (1 mg ml⁻¹) (g body weight)⁻¹ in 0.9% NaCl, because isoflurane anesthesia resulted in less efficient infection in lung 4 days p.i. (detected by virus titers) (Oduro et al., 2016).

2.4.3 Statistical analysis and software

FACS data were analyzed with FlowJo Version 10. Statistical analysis was performed with Prism Graph Pad Version 9.2 and statistical significance was assessed using two-tailed unpaired Student's *t*-test. Values are typically represented as mean +SEM (standard error of mean). Significance is expressed as *, $p < 0.05$; **, $p < 0.01$; ***, $p < 0.001$.

3 Results

3.1 Establishment of intranasal mCMV infection model

To investigate the role of IL-10 and β -catenin signaling in DC during acute and latency mCMV infection, we first established an i.n. mCMV infection model that reflects the natural route of infection during which mCMV transmits by mucosal routes. Since the CD8⁺ T cell response is necessary to control mCMV infection, we examined the virus-specific CD8⁺ T cell response over time with two different MHC-I Tetramers to identify the highest immune response to mCMV. In 2011, a dominating M45-specific conventional CD8⁺ T cell response was identified during acute infection when C57BL/6 mice were infected with mCMV- Δ m157 (Torti et al., 2011). The M45-specific CD8⁺ T cell response decreased between 7-14 days p.i., while the M38-specific CD8⁺ T cells increased until day 14-28 p.i. and stabilized at higher frequencies. Hence, the used Tetramers and virus in this work were taken from this study. As the primary target organ for mCMV after i.n. infection, we analyzed the virus-specific CD8⁺ T cell response in the lung. The LN of interest after i.n. infection is the lung-draining mediastinal lymph node (dLN). To demonstrate a role of DC migration from lung into the dLN, the virus-specific CD8⁺ T cell response was determined in the dLN. The spleen is a central lymphoid organ and is also an organ site for mCMV latency. The spleen harbors recirculating T cells that have received an antigen signal during patrolling of non-lymphoid tissue sites (Griessler et al., 2021). Therefore, we also studied the virus-specific CD8⁺ T cell response in spleen. Hence, C57BL/6 wild type mice were infected i.n. with 2×10^5 PFU of mCMV- Δ m157 and the CD8⁺ T cell response was determined by MHC-I Tetramer staining. The gating strategy of virus-specific CD8⁺ T cells is given in the supplement (**Fig. S6**).

For the M38 Tetramer, we observed maximum frequencies and absolute cell numbers of mCMV-specific CD8⁺ T cells in lung and spleen about 14 days p.i., whereas the M45 Tetramer response was much weaker and peaked 7 days p.i. (**Fig. 6**). Interestingly, in the dLN the M38-specific CD8⁺ T cell response increases 21 days p.i. and but is present at much lower frequencies (2.5%) than in lung (18.3%) and spleen (6.4%).

Based on these findings, we decided to study the role of DC in β -catenin and IL-10 signaling during acute mCMV infection 14 days p.i. using the M38 Tetramer.

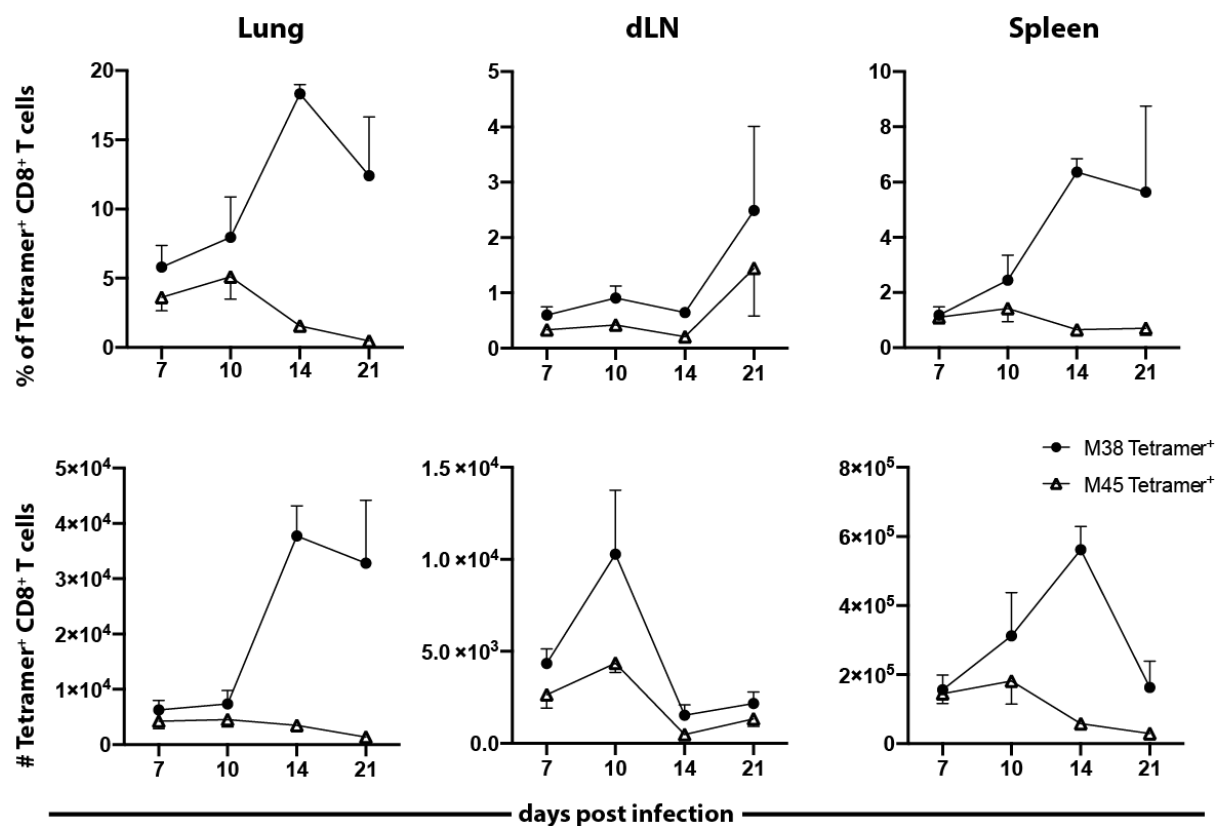


Figure 6: Maximum frequency of M38 -specific CD8⁺ T cells at 14 days p.i.

C57BL/6 wild type mice were infected i.n. with 2×10^5 PFU of mCMV- Δ m157 and the virus-specific CD8⁺ T cell response was monitored 7, 10, 14 and 21 days p.i. in lung, dLN and spleen by FACS staining with M38- and M45-specific Tetramer. Top panel shows frequencies and bottom panel absolute cell numbers of M38 Tetramer⁺ (dots) and M45 Tetramer⁺ (triangle) CD8⁺ T cells (pregated on living CD8⁺ cells). Data are representative of one experiment (n=4). Values are the mean +SEM.

3.2 The influence of IL-10 on DC during mCMV infection

DC are critical regulators of anti-viral immune responses by driving effector T cell activation and Treg induction (Couper et al., 2008; Saraiva and O'Garra, 2010). They are also important targets of Treg-mediated suppression which leads to downregulation of co-stimulatory molecules and pro-inflammatory cytokine production by DC (Clausen and Girard-Madoux, 2013). Another important mechanism of immune suppression is the secretion of the cytokine IL-10 by Treg and presumably also by DC. The immunosuppressive cytokine IL-10 limits CD8⁺ T cell expansion during latent mCMV infection (Cohen et al., 2015; Jones et al., 2010), but to what extent DC are targets or relevant sources of IL-10 during mCMV infection remains elusive.

Our intention was to elucidate the role of IL-10 production by DC and IL-10 signaling in DC during acute mCMV infection. To address these, we used conditional knock-out mice with a CD11c⁺-specific IL-10 or IL-10 receptor deficiency (IL-10^{ACD11c}, IL-10R^{ACD11c}) and infected

the animals i.n. with 2×10^5 PFU of mCMV- Δ m157. As established in **Fig. 6**, we followed the virus-specific CD8⁺ T cell response during the whole infection period in blood. The analysis of the DC compartment, CD4 and CD8 Treg differentiation, and virus-specific CD8⁺ T cell response in lung, dLN and spleen was performed 14 days p.i.. To prove the influence of IL-10 production by DC and IL-10 signaling in DC during i.n. infection, we measured viral load in lung of our mCMV infected conditional knock-out mice compared to control mice.

3.2.1 IL-10 production by DC does not play an essential role during acute mCMV infection

IL-10 is a key immunoregulator and can induce both Treg and Teff cytokine production during viral infections. On the one hand, IL-10 can impede the viral clearance and promote the mCMV replication and persistence. On the other hand, it can ameliorate the immunopathology by inhibiting excessive inflammation (Couper et al., 2008; Saraiva and O'Garra, 2010). During latent mCMV infection, it has been shown that IL-10 restricts the CD8⁺ T cell expansion (Jones et al., 2010). Therefore, we hypothesized that the CD11c⁺-specific deletion of IL-10 will lead to an enhanced mCMV-specific CD8⁺ T cell response and an impaired Treg differentiation during acute mCMV infection. To investigate this, the conditional knock-out mice IL-10^{ACD11c} and control mice were infected i.n. with 2×10^5 PFU of mCMV- Δ m157. Fourteen days p.i., we determined the effect of the IL-10 production on the DC numbers and the DC subsets in lung, dLN and spleen by flow cytometry. In lung and spleen, DC were characterized as CD11c⁺ MHC-II⁺ cells. Additionally, DC in dLN can be discriminated between migratory (CD11c^{int} MHC-II^{hi}) and resident DC (CD11c^{hi} MHC-II^{int}) cells. The complete gating strategy of DC and DC subsets can be found in the supplement (**Fig. S1, S3, S5**), as well as all other gating strategies used in this thesis.

Surprisingly, we did not observe significant differences in DC frequencies (**Fig. 7 A**) or numbers (**Fig. 7 B**) in the lymphoid organs and lung in IL-10^{ACD11c} compared to control mice. In lung, we observed 1.5% of DC among all cells, whereas in spleen most DC with 1.9% were present in IL-10^{ACD11c} after 14 days of infection. Despite the mCMV infection, migratory and resident DC in dLN were not affected in IL-10^{ACD11c} mice (**Fig. 7 A**). A further analysis of DC subsets distribution based on the differential expression of CD103 and CD11b demonstrated no differences between knock-out and control mice (**Fig. 7 C**). These results indicate that IL-10

produced by DC cells does not influence the DC compartment or migration to the dLN during acute mCMV infection.

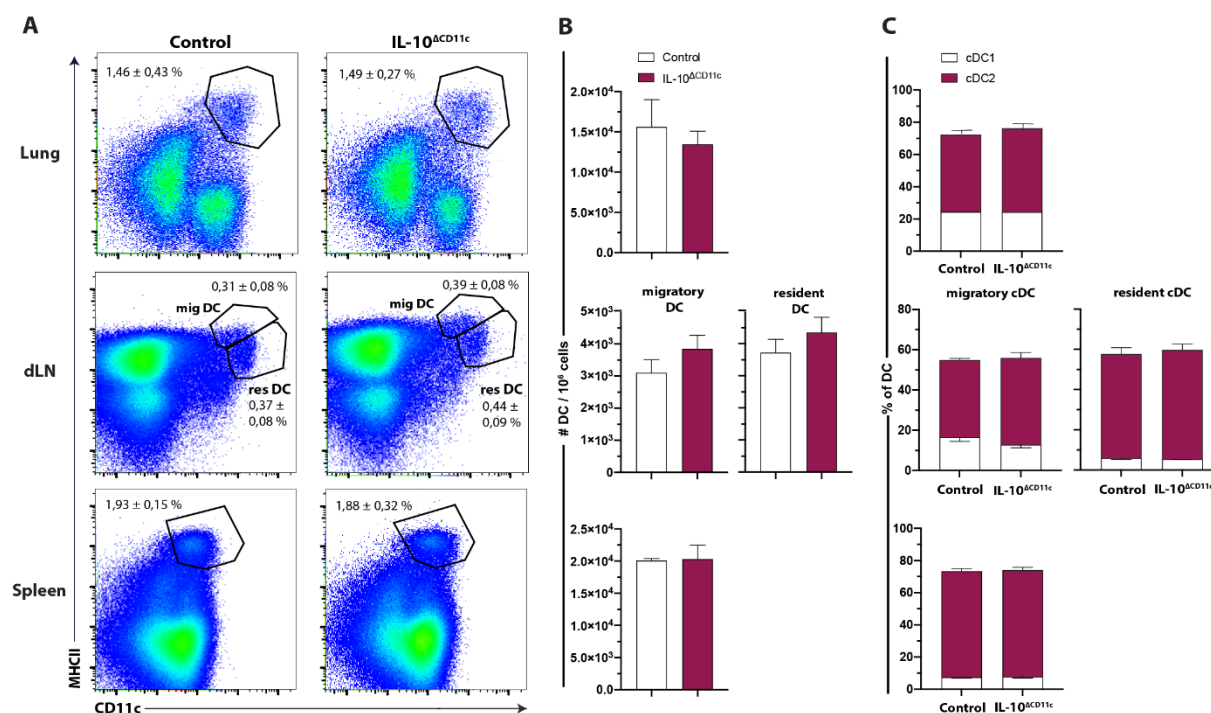


Figure 7: IL-10 production by DC does not affect the DC compartment in lung and lymphoid organs.

Control (white) and IL-10^{ACD11c} (pink) mice were infected i.n. with 2×10^5 PFU of mCMV- Δ m157 for 14 days. (A) Shown are frequencies (flow cytometry plots) of CD45⁺ CD11c⁺ MHC-II⁺ DC in lung, CD45⁺ CD11c^{int} MHC-II^{hi} migratory and CD11c^{hi} MHC-II^{int} resident DC in dLN, and splenic CD11c⁺ MHC-II⁺ DC of control versus IL-10^{ACD11c} mice. (B) Absolute numbers were normalized to 1×10^6 cells of CD45⁺ CD11c⁺ MHC-II⁺ DC in lung, CD45⁺ CD11c^{int} MHC-II^{hi} migratory and CD11c^{hi} MHC-II^{int} resident DC in dLN, and splenic CD11c⁺ MHC-II⁺ DC of control and IL-10^{ACD11c} mice. (C) Frequencies of CD103⁺ cDC1 and CD11b⁺ cDC2 in the lung, dLN (migratory or resident) and spleen in control and IL-10^{ACD11c} mice. Data are representative of two independent experiments (n=4-5). Values are the mean +SEM (unpaired Student's t test).

In the next step, the virus-specific CD8⁺ T cell response in IL-10^{ACD11c} and control mice were investigated in lung, dLN and spleen using the M38 Tetramer. Based on the surface markers CD127, KLRG-1 and CD62L, the M38-specific CD8⁺ T cells were further classified into the subpopulations *early effector cells* – EEC (CD127⁻ KLRG-1⁻ CD62L⁻), *inflationary effector memory T cells* – iTEM (CD127⁻ KLRG-1⁺ CD62L⁻), *double-positive effector T cells* – DPEC (CD127⁺ KLRG-1⁺ CD62L⁻), *conventional effector memory T cells* – cTEM (CD127⁺ KLRG-1⁻ CD62L⁻) and *central memory T cells* – TCM (CD127⁺ KLRG-1⁻ CD62L⁺).

In all organs tested, the M38-specific CD8⁺ T cell response showed no significant differences in frequencies and absolute cell numbers between IL-10^{ACD11c} and control mice (Fig. 8 A, B).

However, a trend towards lower frequencies for virus-specific CD8⁺ T cells in IL-10^{ΔCD11c} mice could be observed for lung and spleen. When comparing the organs, a tissue-specific pattern of mCMV-specific CD8⁺ T cell response is noticeable. In lung of IL-10^{ΔCD11c} mice about 21.8% of CD8⁺ T cells were specific for the M38 Tetramer and were thus twice as high as in spleen with 8.3% (**Fig. 8 A**). Interestingly, in the dLN the M38-specific CD8⁺ T cells did not increase and were present at much lower percentages than in spleen and lung. In addition, the more detailed analysis of the virus-specific CD8⁺ T cell subsets based on the differential expression of CD127, KLRG-1 and CD62L did not reveal any differences between IL-10^{ΔCD11c} and control mice (**Fig. 8 C**). In lung and spleen, the frequencies of DPEC (47.6% - 52.3%) and iTEM (36.3% - 44.2%) dominated over cTEM (5.1% - 7.9%), EEC (2.6% - 3.2%) and TCM (0.1% - 0.6%) in knock-out and control mice. On the contrary, in the dLN mainly DPEC (28.9% - 35.1%) and cTEM (23.8% - 30.9%) were observed, followed by iTEM (17.7% - 22.8%), EEC (11.8% - 13.5%) and finally TCM (6.6% - 8.9%) with the lowest frequency in knock-out and control mice (**Fig. 8 C**). Since neither a difference in DC compartment nor in the virus-specific CD8⁺ T cell response could be seen, the question arose whether the viral replication was impaired by specific deletion of IL-10 in DC. Therefore, viral DNA was isolated from lung tissue and used to determine the viral load. A quantitative *gB*- and *pthrp*-PCR was used to determine the absolute numbers of viral genomes and to normalize *gB* to 1x10⁶ cells using the cellular gene *pthrp*. A comparison of the viral load in IL-10^{ΔCD11c} and control mice 14 days p.i. showed no significant difference in the viral load of the lung (**Fig. 8 D**). Consequently, the IL-10 production by DC alone does not affect the regulation of anti-viral CD8⁺ T cell responses or viral loads after 14 days of mCMV infection.

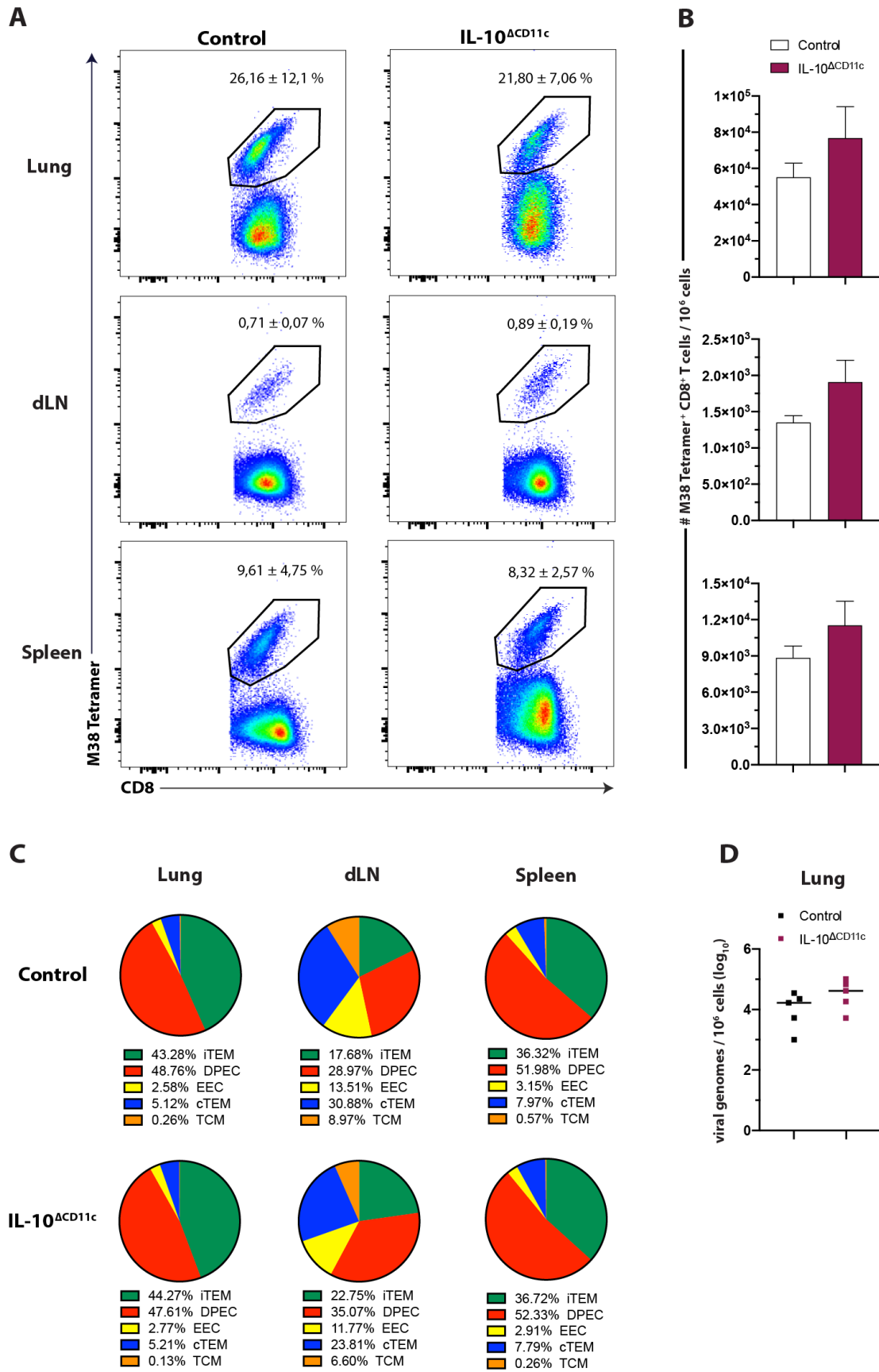


Figure 8: IL-10 production by DC does not play a crucial role in the regulation of anti-viral CD8⁺ T cell responses 14 days after acute mCMV-infection.

Control (white) and IL-10^{ACD11c} (pink) mice were infected i.n. with 2x10⁵ PFU of mCMV-Δm157 for 14 days. (A) Representative flow cytometry plots showing frequencies of M38 Tetramer⁺ CD8⁺ T cells in lung, dLN and spleen (pregated on living CD8⁺ cells) of control versus IL-10^{ACD11c} mice. (B) Bar graphs show absolute cell numbers (normalized to 1x10⁶ cells) in lung, dLN and spleen of control and IL-10^{ACD11c} mice. (C) Frequencies of M38 Tetramer⁺ CD8⁺ T cells further fractionated in CD127⁻ KLRG-1⁺ CD62L⁻ iTEM (green), CD127⁺ KLRG-1⁺ CD62L⁻ DPEC (red), CD127⁻ KLRG-1⁻ CD62L⁻ EEC (yellow), CD127⁺ KLRG-1⁻ CD62L⁻ cTEM (blue) and CD127⁺ KLRG-1⁻ CD62L⁺ TCM (orange) in lung, dLN and spleen in control and IL-10^{ACD11c} mice. (D) DNA was isolated from mice lungs and subjected to quantitative PCR to measure viral genomes. The number of viral genomes was normalized to 1x10⁶ (log₁₀) cells. Each data point represents one individual lung, the black line represents the median. Data are representative of two independent experiments (n=4-5), except D which is representative of one experiment (n=5). Values are the mean +SEM (unpaired Student's t test).

Since IL-10 induces the differentiation of Treg from naïve T cells and this in turn impairs the efficiency of anti-viral immune response, we further investigated the CD4 and CD8 Treg differentiation during acute mCMV infection. Latter can be identified by the surface marker CD122, PD-1 and CD127, while CD4 Treg can be characterized by the expression of the transcription factor FoxP3.

As seen in **Fig. 9 A and B**, we did not find any differences in the FoxP3⁺ CD4 Treg frequencies and absolute numbers in lymphoid organs and lung of mCMV-infected IL-10^{ACD11c} compared to control mice. In IL-10^{ACD11c} mice, the frequency of FoxP3⁺ CD4 Treg was in lung 4.9%, in dLN 7.4% and in spleen 11.4% (**Fig. 9 A**). Similar to the frequency of FoxP3⁺ CD4 Treg, we saw the highest number of FoxP3⁺ CD4 Treg in spleen of IL-10^{ACD11c} mice. In addition, a second type of Treg, the CD8 Treg, has been described. It has been proposed that IL-10 production and the Fas/FasL system mediate suppression by CD8⁺ CD122⁺ cells (Akane et al., 2016; Dai et al., 2014; Liu et al., 2017). We found only about 1% of CD8 Treg in lung and lymphoid tissue 14 days post mCMV infection (**Fig. 9 C**). Both in frequencies (**Fig. 9 C**) and absolute cell numbers (**Fig. 9 D**) an expansion of CD8 Treg could not be detected in IL-10 deficient mCMV infected mice as hypothesized at the beginning.

Taken together, our findings demonstrate that at the peak of the CD8⁺ T cell response following i.n. mCMV-infection, no significant differences in the DC compartment, magnitude of mCMV-specific CD8⁺ T cell responses and Treg differentiation were detected in IL-10^{ACD11c} mice, indicating that IL-10 production by DC does not play an essential role during the acute immune response.

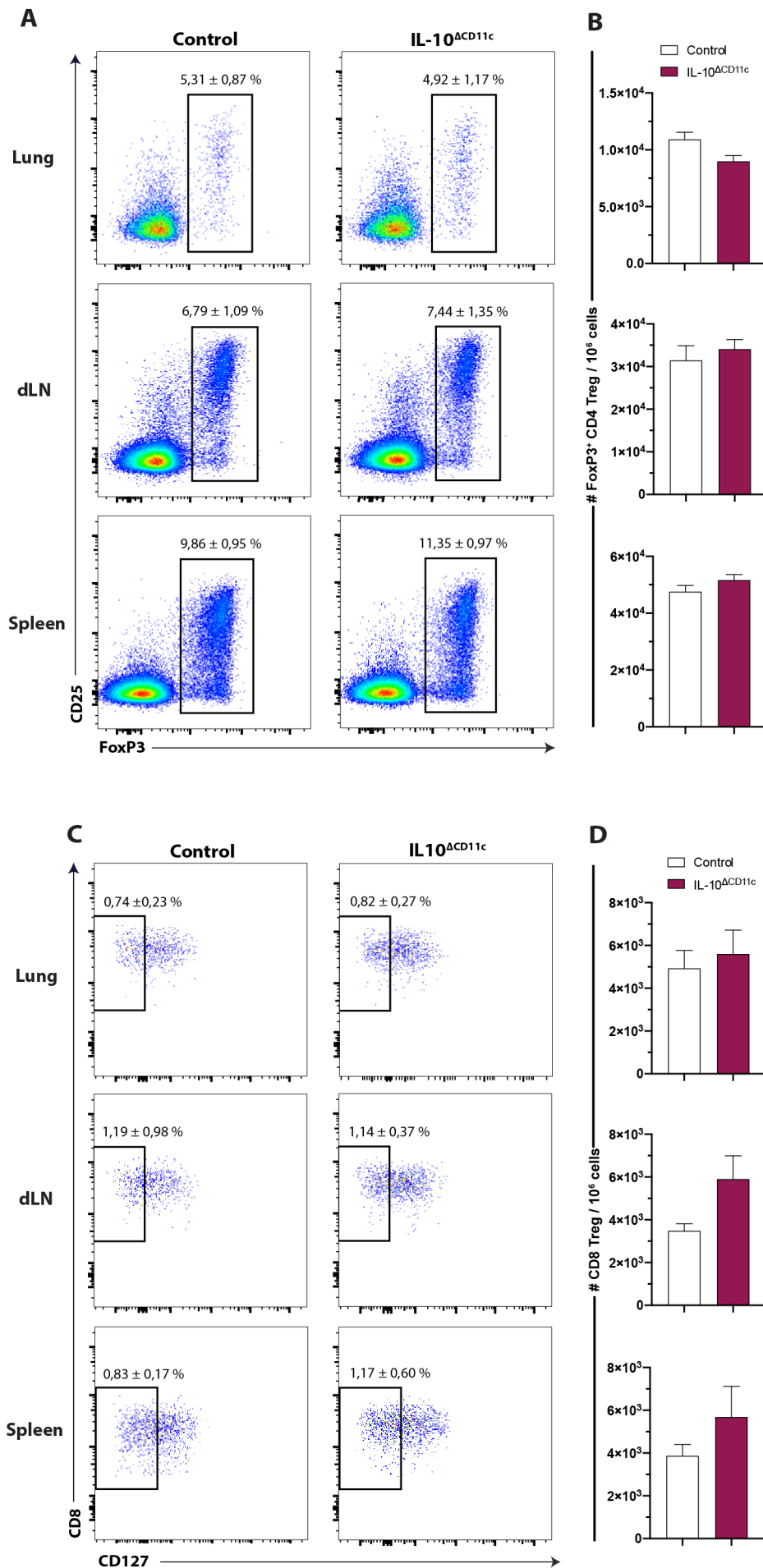


Figure 9: Lack of IL-10 production in DC does not impair the differentiation of CD4 and CD8 Treg during acute mCMV infection.

Control (white) and IL-10^{ACD11c} (pink) mice were infected i.n. with 2x10⁵ PFU of mCMV-Δm157 for 14 days. **(A)** Frequencies (representative dot plots) of FoxP3⁺ CD4 Treg in lung, dLN and spleen in control versus IL-10^{ACD11c} mice. **(B)** Absolute cell numbers were normalized to 1x10⁶ cells (bar graphs) of FoxP3⁺ CD4 Treg in lung, dLN and spleen in control and IL-10^{ACD11c} mice. **(C)** Representative flow cytometry plots with average frequencies of CD122⁺ PD-1⁺ CD127⁻ CD8 Treg in lung, dLN and spleen of control compared to IL-10^{ACD11c} mice (pregated on living TCR-β⁺ CD4⁺ or CD8⁺ cells). **(D)** Bar graphs indicate absolute cell numbers (normalized to 1x10⁶ cells) of CD122⁺ PD-1⁺ CD127⁻ CD8 Treg in lung, dLN and spleen of control and IL-10^{ACD11c} mice. Data are representative of two independent experiments (n=4-5). Values are the mean +SEM (unpaired Student's t test).

3.2.2 IL-10 signaling in DC has no impact on acute mCMV infection

The pleiotropic cytokine IL-10 has potent anti-inflammatory properties that plays an important role by dampening excessive inflammatory responses and limiting the extent of T cell responses (Moore et al., 2001). In both, IL-10 and IL-10 receptor deficient mice an enhanced T_H1/T_H17 response to intestinal bacterial antigens were observed, which resulted in a stronger colitis (Kuhn et al., 1993; Spencer et al., 1998). To investigate the role of IL-10 receptor signaling in DC during acute mCMV infection, IL-10R^{ACD11c} mice were infected i.n. with 2x10⁵ PFU of mCMV-Δm157.

After acute mCMV infection, frequencies (**Fig. 10 A**) and absolute cell numbers (**Fig. 10 B**) of DC were comparable in IL-10R^{ACD11c} and control mice. In lung, we detected 1.6% DC in IL-10R^{ACD11c} and 1.4% DC in control mice (p = 0.257). IL-10 signaling had no influence on the migration of DC to the dLN after mCMV infection. Furthermore, despite the virus infection, we saw no effect on the cDC1 or cDC2 subsets (**Fig. 10 C**). Our results suggest that IL-10 signaling has neither an impact of total DC nor the DC subsets during acute mCMV infection.

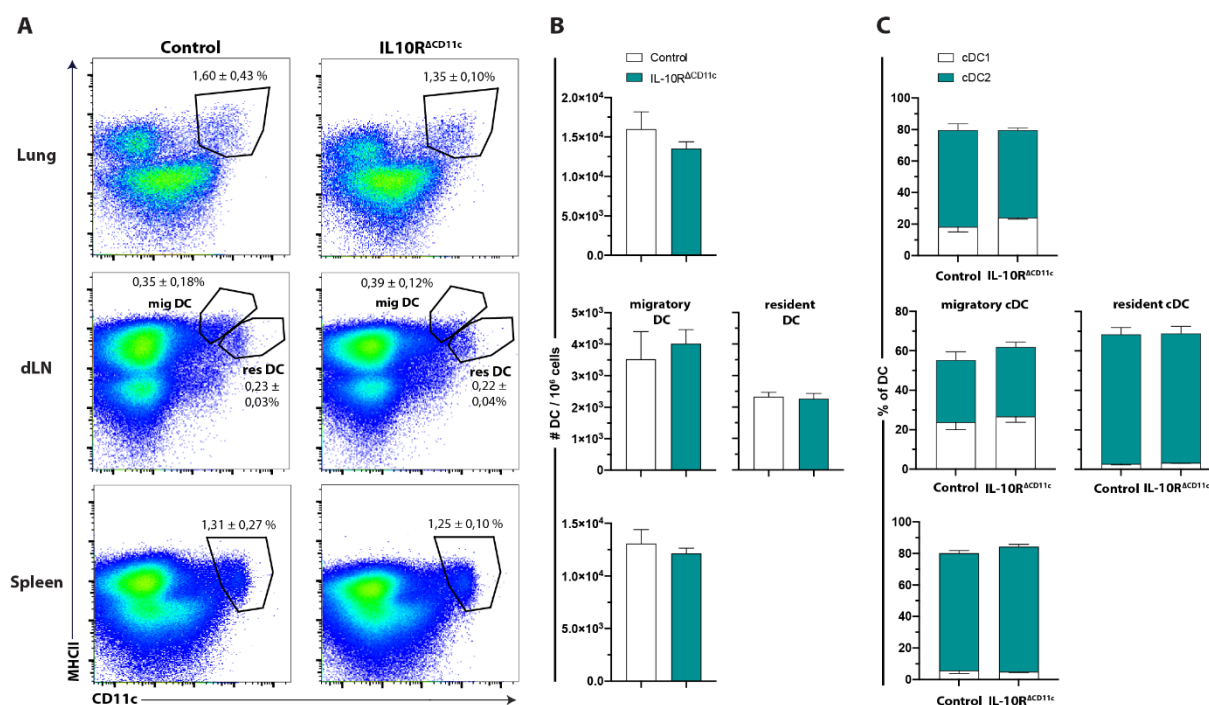


Figure 10: IL-10 signaling has no impact on DC compartment during acute mCMV infection. Control (white) and IL-10R^{ACD11c} (teal) mice were infected i.n. with 2×10^5 PFU of mCMV- Δ m157 for 14 days. (A) Shown are representative flow cytometry dot plots with average frequencies of CD45⁺ CD11c⁺ MHC-II⁺ DC in lung, CD45⁺ CD11^{int} MHC-II^{hi} migratory and CD45⁺ CD11c^{hi} MHC-I^{int} resident DC in dLN, and splenic CD11c⁺ MHC-II⁺ DC of control versus IL-10R^{ACD11c} mice. (B) Bar graphs show absolute cell numbers normalized to 1×10^6 cells of CD45⁺ CD11c⁺ MHC-II⁺ DC in lung, CD45⁺ CD11^{int} MHC-II^{hi} migratory and CD45⁺ CD11c^{hi} MHC-I^{int} resident DC in dLN, and splenic CD11c⁺ MHC-II⁺ DC of control versus IL-10R^{ACD11c} mice. (C) Frequencies of CD103⁺ cDC1 and CD11b⁺ cDC2 in the lung, dLN (migratory or resident) and spleen in control and IL-10R^{ACD11c}. Data are representative of two independent experiments (n=4-5). Values are the mean +SEM (unpaired Student's t test).

To investigate the impact of IL-10R signaling in DC on the protective mCMV-specific CD8⁺ T cells, we determined the kinetic of the virus-specific CD8⁺ T cell response in blood in IL-10R^{ACD11c} compared to control mice during the whole acute infection. Starting from day 10 p.i., we detected M38 Tetramer⁺ CD8⁺ T cells, which showed an increased frequency of 10.3% in IL-10R^{ACD11c} and 13.1% in control mice ($p = 0.461$) 14 days p.i. (Fig. 11 A). Additionally, we observed that M38-specific CD8⁺ T cells in IL-10R^{ACD11c} and control mice showed similar MFI on both time points, indicating similar levels M38 Tetramer binding (Fig. 11 B). For the corresponding M38-specific CD8⁺ T cell subpopulations, we obtained mainly comparable frequencies in IL-10R^{ACD11c} and control mice over the whole infection period in blood (Fig. 11 C). After 10 days of infection, we saw predominantly DPEC (24.9% in IL-10R^{ACD11c} and 40.6% in control mice) and a trend toward less DPEC in IL-10R^{ACD11c} mice, which increased up to 53.1% in IL-10R^{ACD11c} and 54.8% in control mice 14 days p.i. ($p = 0.662$). A second M38

Tetramer⁺ CD8⁺ T cell subset, which was already strongly induced after 10 days of infection, was iTEM (17.3% in IL-10R^{ΔCD11c} and 35.2% in control mice; $p = 0.0731$), which also expanded during the course of infection ($p = 0.799$). In contrast, we detected low frequencies from 1.4 – 13.3% of EEC, cTEM and TCM in IL-10R^{ΔCD11c} and control mice, which further decreased during the course of infection (0.3% - 5.6%) (**Fig. 11 C**). Overall, these results display no effect of the CD11c⁺-specific deletion of IL-10 receptor on the total virus-specific CD8⁺ T cell response and subpopulations in blood during the whole infection period.

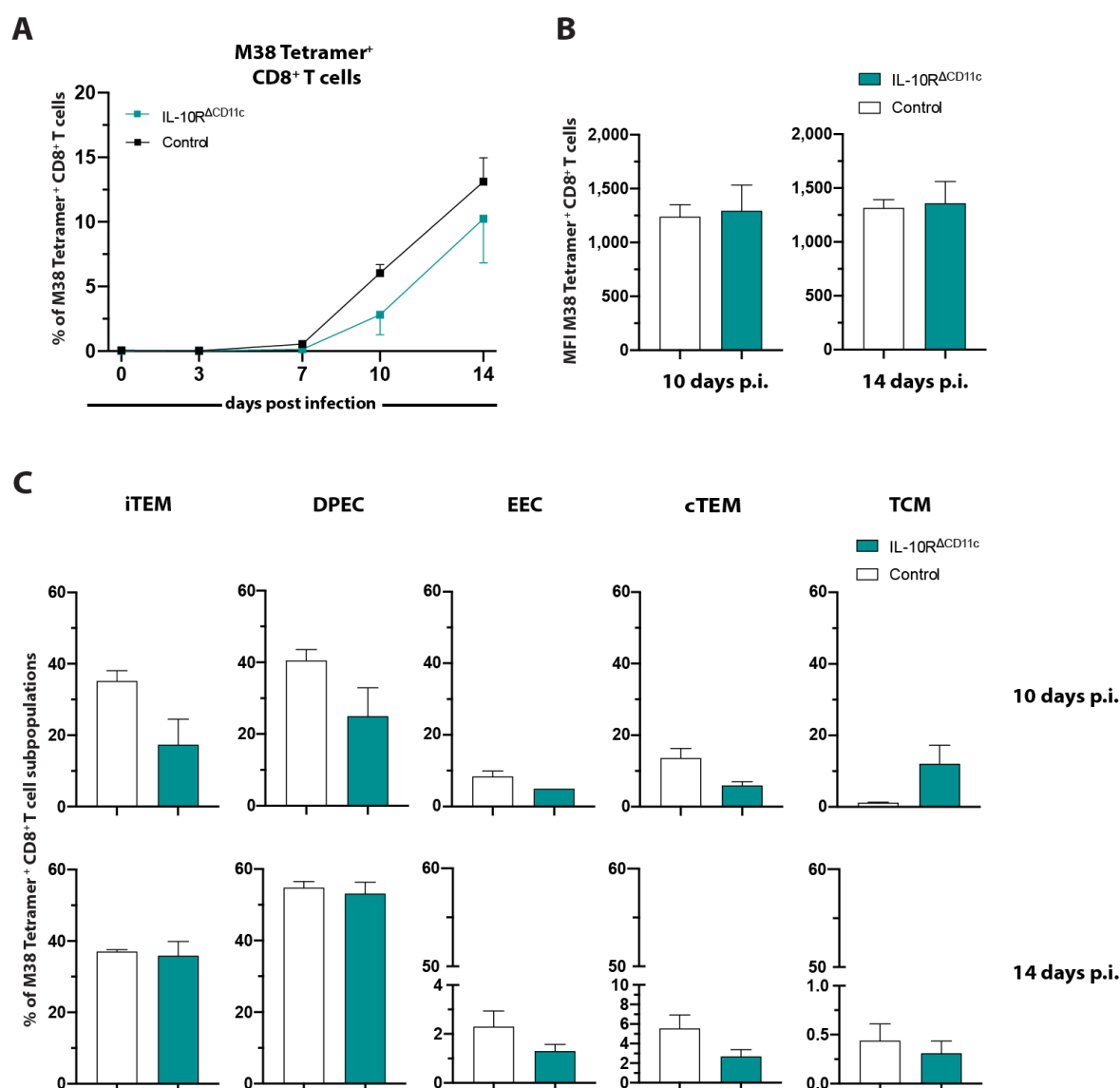


Figure 11: Kinetic of the M38 Tetramer⁺ CD8⁺ T cell response during the acute infection.

At the indicated times after i.n. infection with 2×10^5 PFU of mCMV- Δ m157, blood samples were collected from control (white) and IL-10R^{ACD11c} (teal) mice and cells were stained with the M38 Tetramer to analyze the virus-specific CD8⁺ T cell response. (A) Time course of M38-specific CD8⁺ T cells and (B) M38 Tetramer response was measured by geometric MFI in CD8⁺ T cells of control and IL-10R^{ACD11c} mice. (C) Corresponding frequencies of M38 Tetramer⁺ CD8⁺ T cell subpopulations CD127⁻ KLRG-1⁺ CD62L⁻ iTEM, CD127⁺ KLRG-1⁺ CD62L⁻ DPEC, CD127⁻ KLRG-1⁻ CD62L⁻ EEC, CD127⁺ KLRG-1⁻ CD62L⁻ cTEM and CD127⁺ KLRG-1⁻ CD62L⁺ TCM of control versus IL-10R^{ACD11c} mice 10 and 14 days p.i.. Data are representative of one experiment (n=5). Values are the mean +SEM (unpaired Student's t test).

Systemic characterization of the virus-specific CD8⁺ T cells in blood revealed no impact of the M38 Tetramer⁺ CD8⁺ T cell response and showed a trend toward less DPEC in IL-10R^{ACD11c} mice (10 days p.i.). Therefore, we went one step further and analyzed the organ-specific M38 Tetramer⁺ CD8⁺ T cell response in lung, dLN and spleen 14 days p.i..

Hence by interfering with CD11c⁺-specific IL-10R signaling, we expected a boost of the anti-viral immunity in the IL-10R signaling, but the comparison of knock-out and control mice resulted in comparable M38-specific CD8⁺ T cell responses. At this point, we detected the highest frequencies of M38 Tetramer⁺ CD8⁺ T cells in lung, the major target of the i.n. infection (with 22.3% in IL-10R^{ACD11c} and 21.9% in control mice) (**Fig. 12 A**). In contrast, in dLN about 1,7% CD8⁺ T cells in IL-10R^{ACD11c} and in control mice were specific for the M38 Tetramer, these results were consistent with the absolute cell numbers in both organs (**Fig. 12 B**). The lymphoid organ, i.e. the spleen, showed three times less virus-specific CD8⁺ T cells (7.8% in IL-10R^{ACD11c} and 9.9% in control mice) than in lung, and was equally unaffected by the IL-10 receptor deletion on DC (**Fig. 12 A, B**). Moreover, we further fractionated these virus-specific CD8⁺ T cells based on the differential expression of CD127, KLRG-1 and CD62L in five subpopulations (**Fig. 12 C**). In lung and lymphoid tissue, frequencies of DPEC (33.1% - 46.8%) and iTEM (29.9% - 45.6%) dominated over cTEM (5.0% - 20.5%), EEC (2,73% - 17,20%) and TCM (0.2% - 7.8%) in IL-10R^{ACD11c} and control mice. Compared to lung and spleen, the dominating subpopulations DPEC and iTEM resulted in lower percentages in the dLN. By contrast, the KLRG-1^{neg} subpopulations cTEM, EEC and TCM were higher frequented than in lung and spleen (**Fig. 12 C**). By investigating the viral replication in IL-10R^{ACD11c} and control mice, we detected similar viral genome levels ($p = 0.265$) (**Fig. 12 D**). To sum up, these data indicate that IL-10 signaling in DC cells did not influence the regulation of the anti-viral CD8⁺ T cell response but showed a tissue-specific pattern of this virus-specific CD8⁺ T cell response.

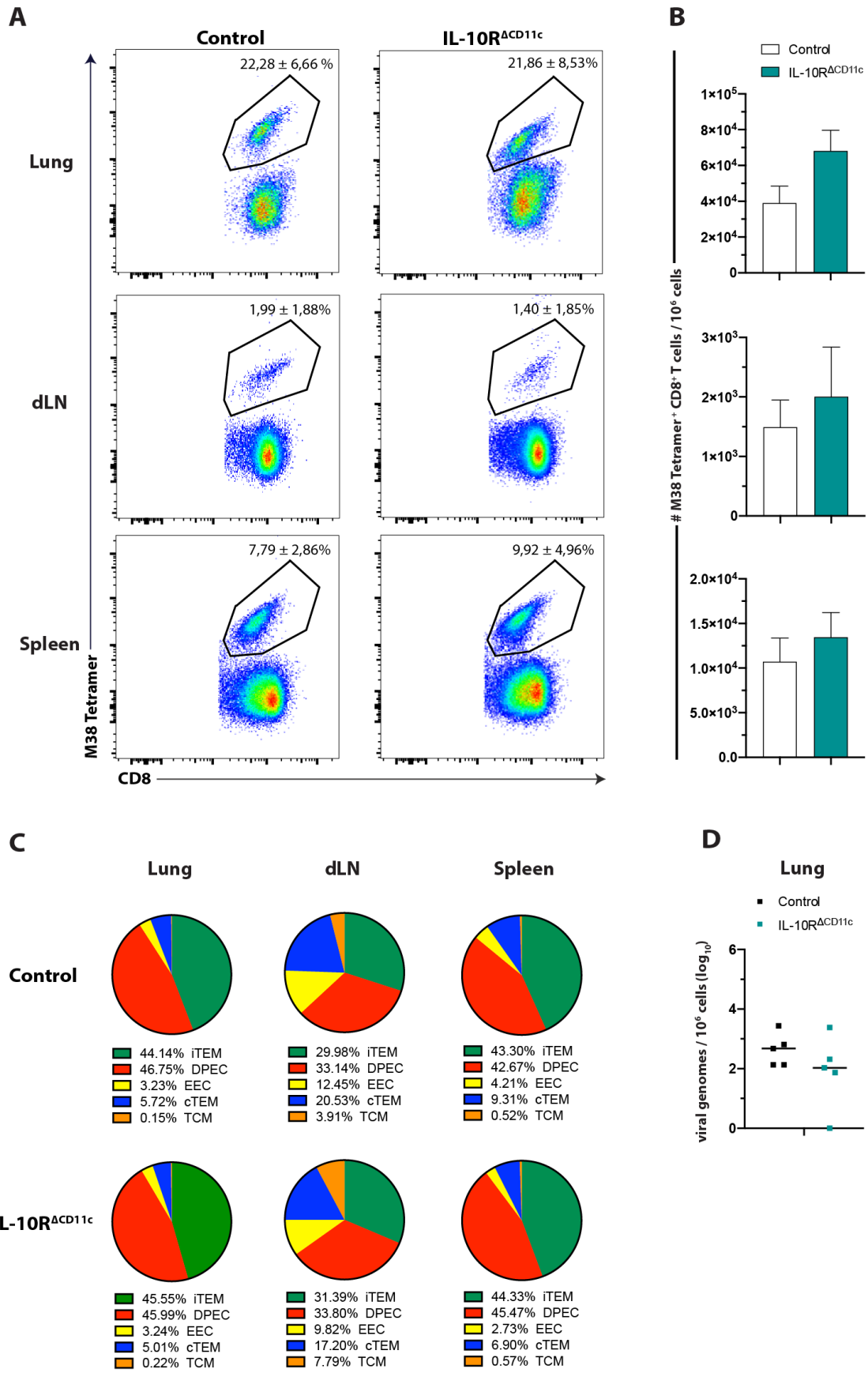


Figure 12: Specific IL-10 receptor-deletion of DC results in similar virus-specific CD8⁺ T cell response compared to control mice.

Both control (white) and IL-10R^{ACD11c} (teal) mice were infected i.n. with 2×10^5 PFU of mCMV- Δ m157 for 14 days. (A) Representative flow cytometry plots showing frequencies of M38 Tetramer⁺ CD8⁺ T cells and (B) absolute cell numbers (normalized to 1×10^6 cells) in lung, dLN and spleen were determined by flow cytometry (pregated on living CD8⁺ cells) of control versus IL-10R^{ACD11c} mice. (C) Frequencies of M38 Tetramer⁺ CD8⁺ T cells further fractionated in CD127⁻ KLRG-1⁺ CD62L⁻ iTTEM (green), CD127⁺ KLRG-1⁺ CD62L⁻ DPEC (red), CD127⁻ KLRG-1⁻ CD62L⁻ EEC (yellow), CD127⁺ KLRG-1⁻ CD62L⁻ cTEM (blue) and CD127⁺ KLRG-1⁻ CD62L⁺ TCM (orange) in lung, dLN and spleen of control and IL-10R^{ACD11c} mice. (D) Lung DNA was isolated and subjected to quantitative PCR to measure viral genomes. The number of viral genomes was normalized to 1×10^6 (\log_{10}) cells and compared from control and IL-10R^{ACD11c} mice. Each point represents the viral genomes of one individual lung, the black line represents the median. Data are representative of two independent experiments (n=4-5), except D which is representative of one experiment (n=5). Values are the mean +SEM (unpaired Student's t test).

The specific deletion of IL-10 receptor resulted in an enhanced T_{H1}/T_{H17} response to intestinal bacterial antigens and induced a stronger colitis. Therefore, we expected in the IL-10R^{ACD11c} mice an enhanced pro-inflammatory response accompanied with a reduced Treg differentiation during acute mCMV infection. To test our hypothesis, we analyzed the CD4 and CD8 Treg in lung, dLN and spleen 14 days p.i..

A comparison in IL-10R^{ACD11c} and control mice showed similar frequencies (**Fig. 13 A**) and absolute cell numbers (**Fig. 13 C**) in the tested organs. In lung and dLN, we discovered frequencies about 6.2% and 6.6% of FoxP3⁺ CD4 Treg in IL-10R^{ACD11c} mice, respectively, in the spleen the frequency was almost doubled with 10.7%. Similarly, absolute cell numbers of FoxP3⁺ CD4 Treg were in the same extent of frequencies (**Fig 13 C**). Additionally, CD4 Treg expressed comparable levels of FoxP3 in knock-out and control mice of all investigated organs (**Fig. 13 B**). Helios is a marker of thymic-derived Treg (tTreg), while Helios⁻ Treg are mentioned as periphery Treg (pTreg). In lung and lymphoid tissue, mainly Helios⁺ tTreg were detected with no significant difference in both populations (**Fig. 13 D**). Moreover, frequencies (**Fig. 13 E**) and absolute cell numbers (**Fig. 13 F**) of CD8 Treg were not affected by a missing IL-10 signaling during acute infection. In all organs, 0,30% - 0,93% of CD8 Treg were detected by flow cytometry in IL-10R^{ACD11c} and control mice (**Fig. 13 E**). Compared to FoxP3⁺ CD4 Treg, CD8 Treg were mainly Helios⁻ pTreg in IL-10R^{ACD11c} and control mice (**Fig. 13 G**).

In conclusion, the missing IL-10 signaling showed neither an effect on the DC compartment nor the virus-specific CD8⁺ T cells during acute mCMV infection. Furthermore, the

CD11c⁺-specific deletion of the IL-10 receptor has no impact and the CD4 and CD8 Treg differentiation in lung and lymphoid organs.

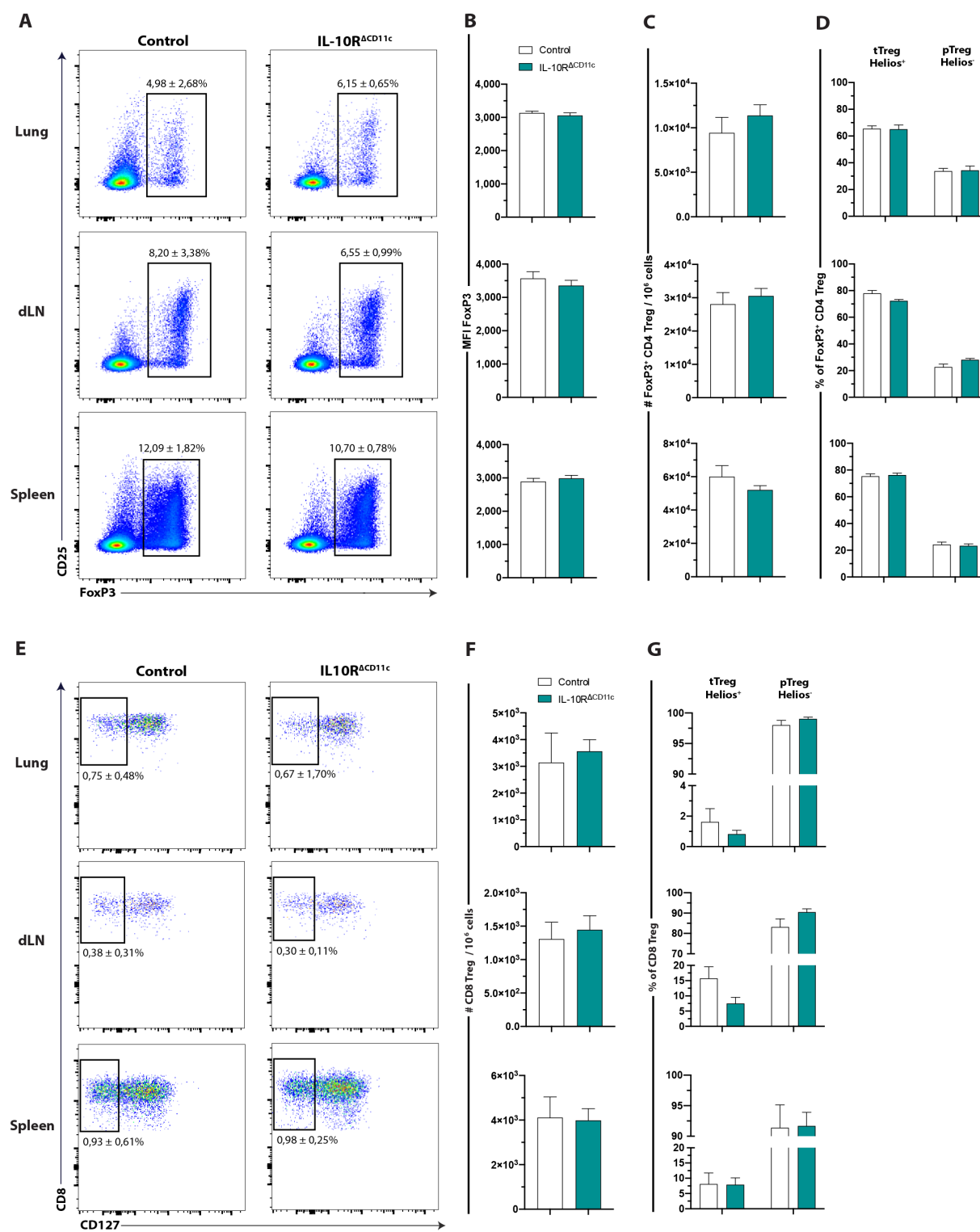


Figure 13: Lack of IL-10R in DC shows similar FoxP3 expression of CD4⁺ T cells during acute mCMV infection.

Control (white) and IL-10R^{ΔCD11c} (teal) mice were infected i.n. with 2x10⁵ PFU of mCMV-Δm157 for 14 days. (A) Frequencies (representative dot plots) of FoxP3⁺ CD4 Treg in lung, dLN and spleen of control compared to IL-10R^{ΔCD11c} mice (pregated on living TCR-β⁺ CD4⁺ cells). (B) FoxP3 expression as measured by geometric mean fluorescence intensity (MFI) in CD4 Treg of lung, dLN and spleen of control versus IL-10R^{ΔCD11c} mice. (C) Absolute cell numbers were normalized to 1x10⁶ cells (bar graphs) of FoxP3⁺ CD4 Treg in lung, dLN and spleen of control and IL-10R^{ΔCD11c} mice. (D) Frequencies of CD4⁺ FoxP3⁺ Helios⁺ tTreg or Helios⁻ pTreg in lung, dLN and spleen of control versus IL-10R^{ΔCD11c} mice. (E) Representative flow cytometry plots showing frequencies of CD122⁺ PD-1⁺ CD127⁻ CD8⁺ Treg in lung, dLN and spleen of control mice versus IL-10R^{ΔCD11c} mice (pregated on living TCR-β⁺ CD8⁺ cells). (F) Absolute cell numbers were normalized to 1x10⁶ cells (bar graphs) of CD8⁺ Treg in lung, dLN and spleen of control and IL-10R^{ΔCD11c} mice. (G) Frequencies of CD8⁺ Helios⁺ tTreg or Helios⁻ pTreg of control compared to IL-10R^{ΔCD11c} mice in lung, dLN and spleen. Data are representative of one experiment (n=5), except E which is two independent experiments (n=4-5). Values are the mean +SEM (unpaired Student's t test).

3.3 The role of β-catenin in DC during mCMV infection

Another pathway associated with a tolerogenic DC function is β-catenin signaling, although controversial data have been published. On the one hand, the activation of β-catenin signaling in bone marrow-derived DC induces IL-10-producing T cells *in vitro* and protects mice from EAE induction *in vivo* (Jiang et al., 2007). Moreover, the specific deletion of β-catenin CD11c⁺ cells resulted in a stronger T_H1/T_H17-mediated colitis, which was associated with reduced CD4 Treg responses (Manicassamy et al., 2010; Suryawanshi et al., 2015). On the other hand, stabilized, constitutively active β-catenin signaling in DC can mediate a pro-inflammatory function and promote the development of an effective CD8⁺ T cell response in the context of viral infection (Cohen et al., 2015).

Since controversial data exist on this pathway, we want to investigate the role of β-catenin signaling in DC during acute mCMV infection. We therefore investigated the mCMV-specific CD8⁺ T cell responses in mCMV-infected mice (2x10⁵ PFU of mCMV-Δm157, i.n.) with a CD11c⁺-specific deletion (β-cat^{ΔCD11c}) or expression of a stabilized form (β-cat^{ΔCD11c/EX3}) of β-catenin. We focused on the DC compartment, virus-specific CD8⁺ T cell response as well as the CD4 and CD8 Treg differentiation in lung, dLN and spleen 14 days p.i.. To determine the viral load of these infected mice, DNA of lung tissue was isolated and quantitated by qPCR.

3.3.1 Deletion of β -catenin in DC does not play a crucial role during acute mCMV infection

β -catenin signaling was suggested to promote a tolerogenic DC phenotype (Jiang et al., 2007), while the specific deletion of β -catenin in CD11c⁺ cells resulted in an enhanced Teff response (Manicassamy et al., 2010). To determine whether β -catenin-deficient DC enhance the mCMV response and interfere the Treg induction during acute mCMV infection, we infected β -cat^{ACD11c} mice with 2×10^5 PFU of mCMV- Δ m157. First, we investigated the DC in lung and lymphoid organs by flow cytometry. In lung and dLN, DC were pregated on living CD45⁺ F4/80⁻ cells and in the dLN the DC were further differentiated between migratory and resident DC (**Fig. S2, S4**).

β -cat^{ACD11c} mice exhibited no differences in total DC frequencies (**Fig. 14 A**) and absolute cell numbers after acute infection (**Fig. 14 B**). We detected in lung 0.3% DC in β -cat^{ACD11c} and 0.4% DC in control mice ($p = 0.169$). Moreover, in β -cat^{ACD11c} and control mice only minor frequencies of migratory and resident DC in dLN were identified despite virus infection. The highest frequency of DC was detected in spleen with 0.9% in β -cat^{ACD11c} and in control mice (**Fig. 14 A**). Further analysis of DC subsets in β -cat^{ACD11c} showed unaffected frequencies until day 14 days p.i. (**Fig. 14 C**). Both, lung and migratory dLN, showed the highest frequencies of cDC1, but they were not impaired by the specific deletion of β -catenin and showed similar frequencies (**Fig. 14 C**). Taken together, these data indicate that the deletion of β -catenin in DC does not have a crucial influence on the DC compartment during acute mCMV infection.

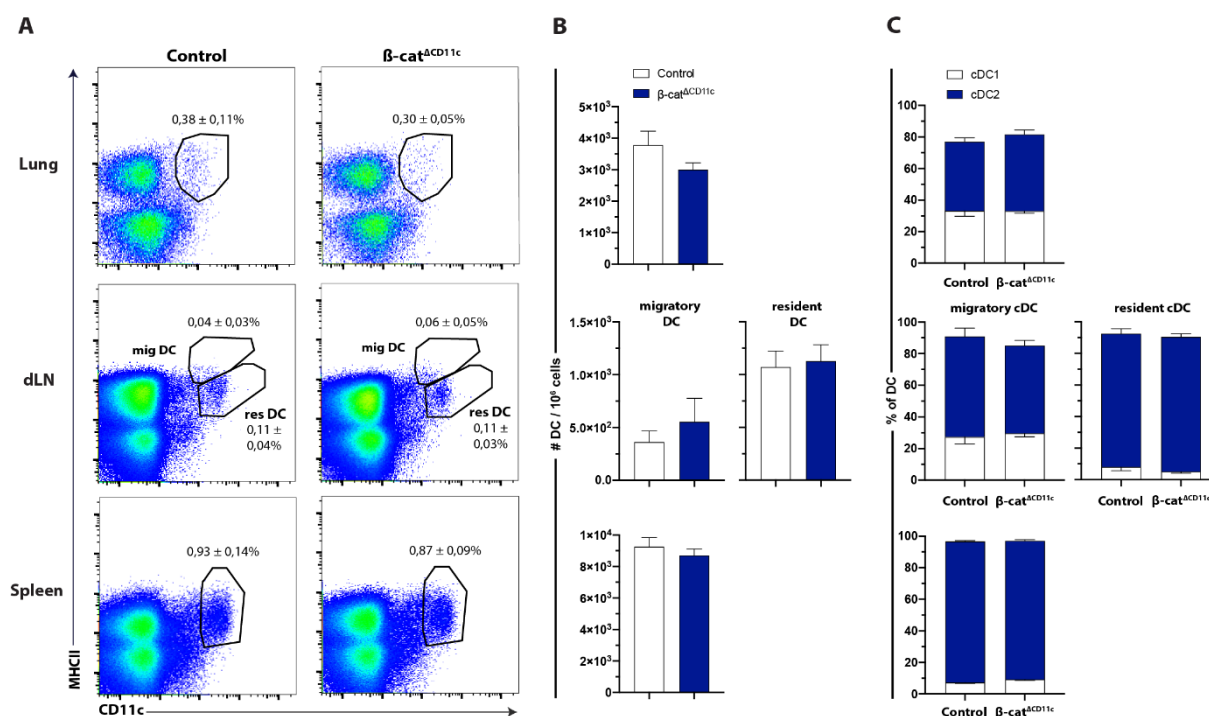


Figure 14: Deletion of β -catenin in DC does not impact the DC numbers during acute mCMV infection.

Control (white) and β -cat^{ACD11c} (blue) mice were infected i.n. with 2×10^5 PFU of mCMV- Δ m157 for 14 days. (A) Shown are frequencies (flow cytometry plots) of CD11c⁺ MHC-II⁺ DC in lung, CD11c^{int} MHC-II^{hi} migratory and CD11c^{hi} MHC-I^{int} resident DC in dLN (pregated on living CD45⁺ F4/80⁻ cells) and splenic CD11c⁺ MHC-II⁺ DC in control and β -cat^{ACD11c} mice. (B) Absolute cell numbers of DC (bar graphs) were normalized to 1×10^6 cells in lung, dLN and spleen of control versus β -cat^{ACD11c} mice. (C) Frequencies of XCR-1⁺ cDC1 and CD172 α ⁺ cDC2 in the lung, dLN and spleen of control compared to β -cat^{ACD11c} mice. Data are representative of two independent experiments (n=5-6). Values are the mean +SEM (unpaired Student's t test).

To assess whether CD11c⁺-specific deletion of β -catenin has an influence of the M38 Tetramer-specific CD8⁺ T cells and their subpopulations, blood was analyzed over the acute infection. The deletion of β -catenin did not affect the virus-specific CD8⁺ T cell response (Fig. 15 A). Ten days p.i. about 2.4% in β -cat^{ACD11c} and 2.8% in control mice of M38 Tetramer⁺ CD8⁺ T cells were measured, which expanded up to 13.9% in β -cat^{ACD11c} and 11.2% in control mice at day 14 p.i.. At the same time, we detected higher M38 Tetramer levels in CD8⁺ T cells during the course of infection, but were unaffected by the β -catenin signaling in DC (Fig. 15 B). Further analysis of virus-specific CD8⁺ T cell subpopulations revealed comparable frequencies of these subpopulations in β -cat^{ACD11c} and control mice (Fig. 15 C). After 10 days of mCMV infection, mainly DPEC (32.5% in β -cat^{ACD11c} and 40.5% in control mice) and iTEM (23.6% in β -cat^{ACD11c} and 30.0% in control mice) were detectable. The DPEC further rose up to 54.3% in β -cat^{ACD11c} and 52.9% in control mice and iTEM to 35.3% in β -cat^{ACD11c} and 37.9% in control

mice. In comparison, EEC, cTEM and TCM were low frequented during the acute infection and continuously decreased with the infection time (**Fig. 15 C**). These data indicate that β -catenin signaling in DC leads to a comparable CD8⁺ T cell response in the blood of both β -cat^{ΔCD11c} and control mice in blood during acute mCMV-infection.

Additionally, we investigated whether the absence of β -catenin in DC facilitated an enhanced CD8⁺ T cell response against mCMV measuring the organ-specific M38 Tetramer⁺ CD8⁺ T cells were measured by flow cytometry. However, we discovered comparable frequencies of virus-specific CD8⁺ T cells in β -cat^{ΔCD11c} and control mice in all tested organs after infection (**Fig. 16 A**). As in the previously tested IL-10^{ΔCD11c} and IL-10R^{ΔCD11c} mice, we detected the highest frequencies (**Fig. 16 A**) and absolute cell numbers (**Fig. 16 B**) of M38-specific CD8⁺ T cells in the lung. In contrast, dLN showed low frequencies of about 0.7% in β -cat^{ΔCD11c} and 0.5% in control mice (**Fig. 16 A**). Furthermore, the absolute cell numbers were also minimal compared to the lung (**Fig. 16 B**). Next, we characterized the M38 Tetramer-specific subpopulations. After 14 days of infection, mainly DPEC and iTEM were observed in lung and spleen (**Fig. 16 C**). While there was no difference between β -cat^{ΔCD11c} and control mice in lung and lymphoid organs, in dLN the dominating subpopulations were DPEC and cTEM. Additionally, TCM and EEC frequencies were higher in dLN than in lung and spleen. Furthermore, the viral genomes remained unaltered by the missing β -catenin signaling ($p = 0.259$) (**Fig. 16 D**). These findings reveal that the β -catenin deletion in DC does not play an essential role in regulation of anti-viral CD8 T cell responses during acute mCMV infection.

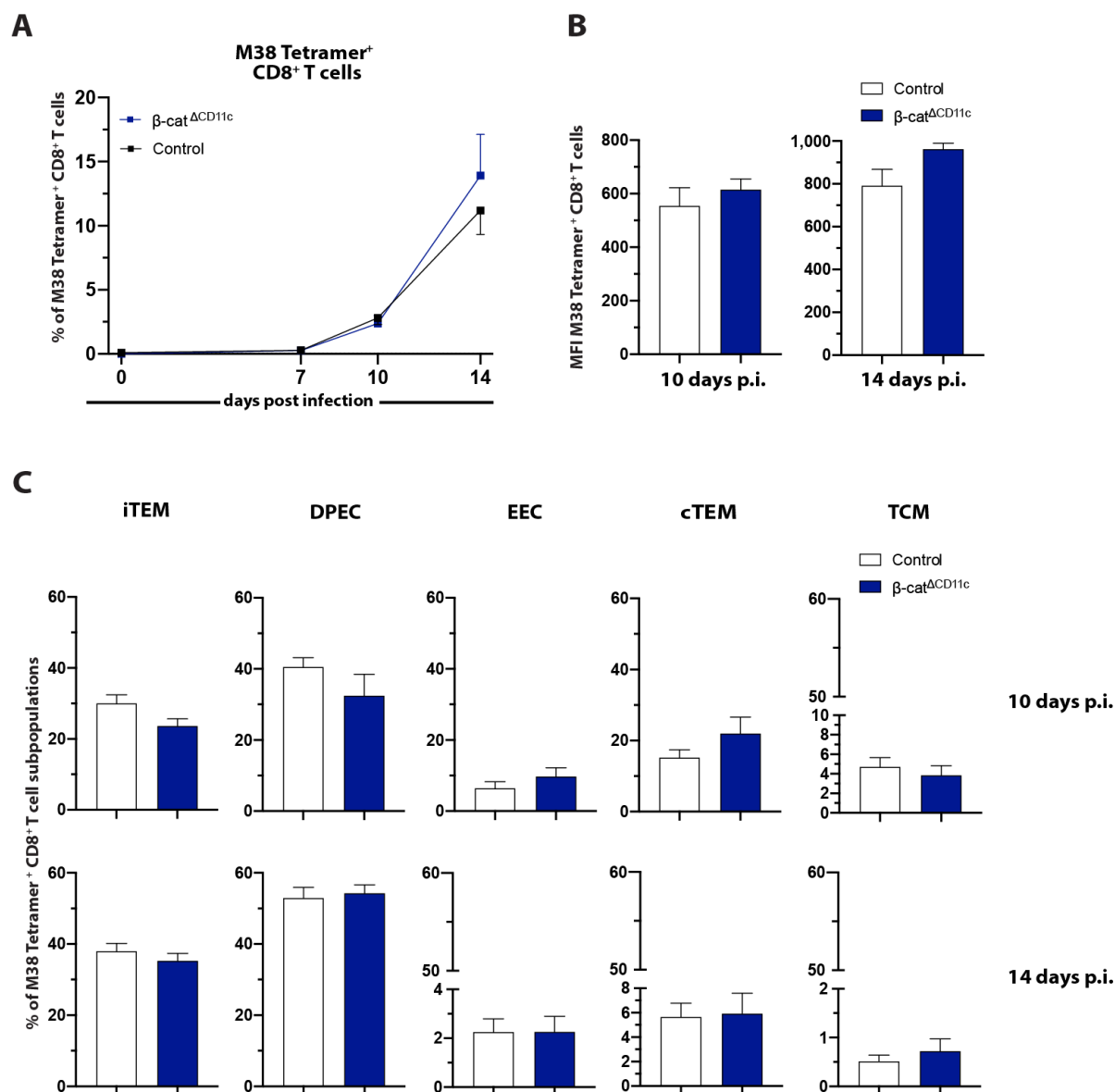


Figure 15: Similar expansion of virus-specific CD8⁺ T cells in β -cat^{ACD11c} mice in blood.

Control (white) and β -cat^{ACD11c} (blue) mice were infected i.n. with 2×10^5 PFU of mCMV- Δ m157 for 14 days. (A) Frequencies of virus-specific CD8⁺ T cell response in blood by flow cytometry with M38 Tetramer (pregated on living CD8⁺ cells). (B) M38 Tetramer expression as measured by geometric MFI in CD8⁺ T cells of control and β -cat^{ACD11c} mice. (C) Corresponding dynamics of M38 Tetramer⁺ CD8⁺ T cell subpopulations of CD127⁻ KLRG-1⁺ CD62L⁻ iTEM, CD127⁺ KLRG-1⁺ CD62L⁻ DPEC, CD127⁻ KLRG-1⁻ CD62L⁻ EEC, CD127⁺ KLRG-1⁻ CD62L⁻ cTEM and CD127⁺ KLRG-1⁻ CD62L⁺ TCM 10 and 14 days p.i.. Data are representative of one experiment (n=5-6). Values are the mean +SEM (unpaired Student's t test).

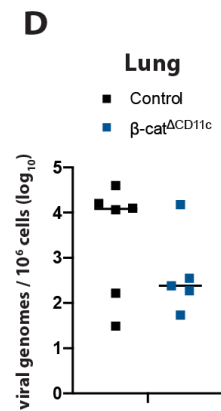
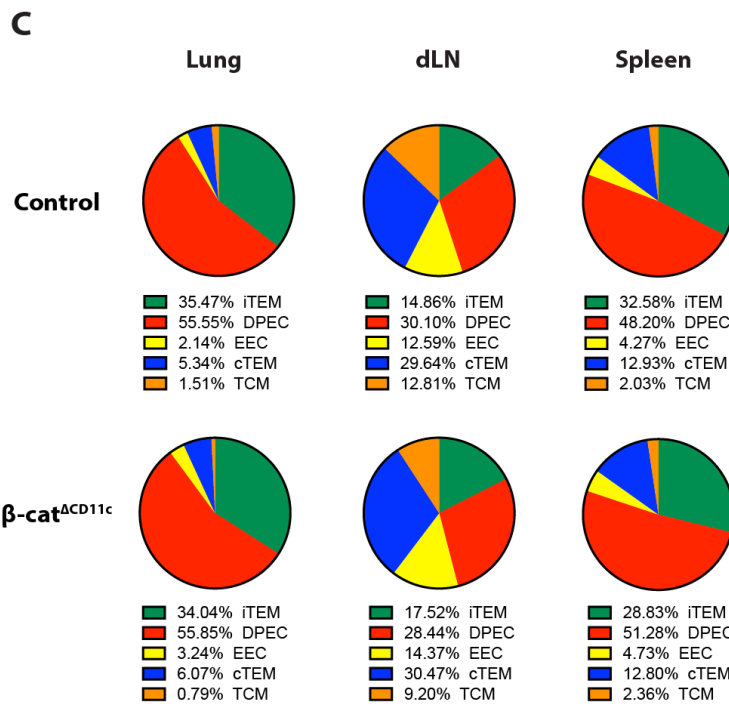
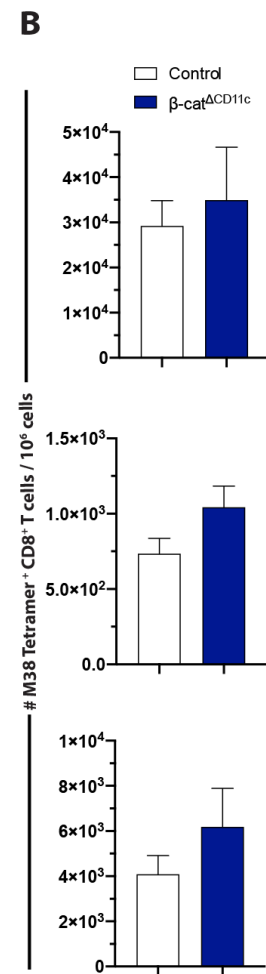
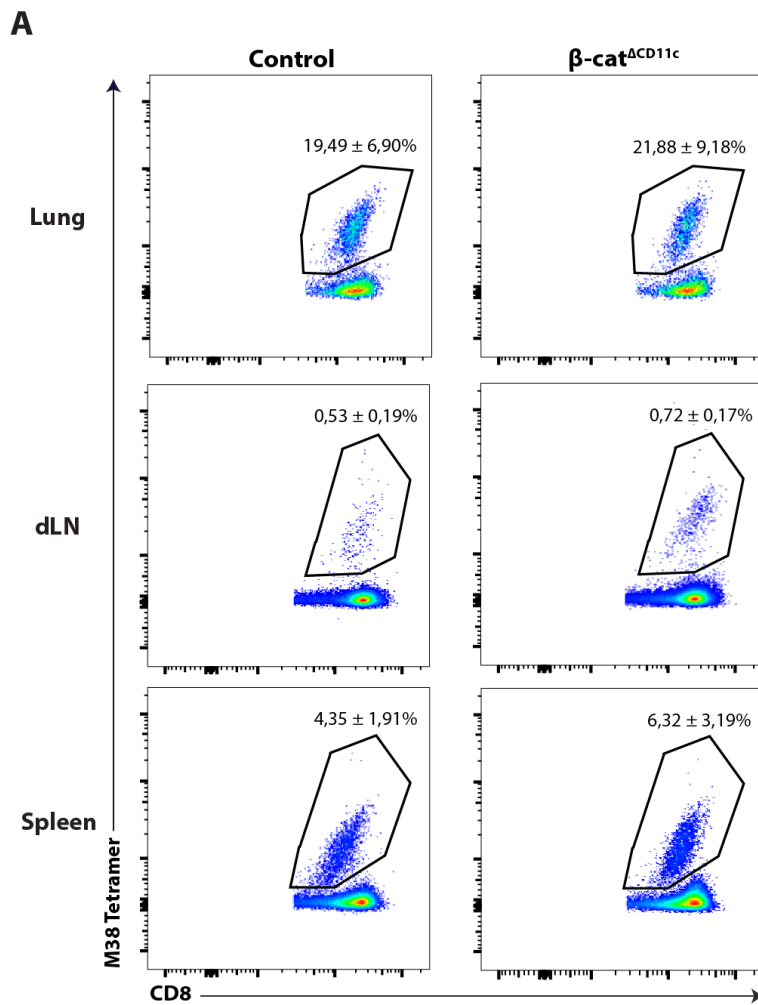


Figure 16: β -catenin signaling in DC does not affect the M38-specific CD8⁺ T cell response during acute mCMV infection.

Control (white) and β -cat^{ACD11c} (blue) mice were infected i.n. with 2×10^5 PFU of mCMV- Δ m157 for 14 days. (A) Representative flow cytometry plots with average frequencies of M38 Tetramer⁺ CD8⁺ T cells in lung, dLN and spleen were determined by flow cytometry (pregated on living CD8⁺ cells). (B) In bar graphs absolute cell numbers (normalized to 1×10^6 cells; bar graphs) in lung, dLN and spleen. (C) Frequencies of M38 Tetramer⁺ CD8⁺ T cells fractionated in CD127⁻ KLRG-1⁺ CD62⁻ iTTEM (green), CD127⁺ KLRG-1⁺ CD62⁻ DPEC (red), CD127⁻ KLRG-1⁻ CD62⁻ EEC (yellow), CD127⁺ KLRG-1⁻ CD62⁻ cTEM (blue) and CD127⁺ KLRG-1⁻ CD62⁺ TCM (orange) in lung, dLN and spleen. (D) From lung DNA were isolated and subjected to quantitative PCR to measure viral genomes. The number of viral genomes was normalized to 1×10^6 (\log_{10}) cells. Each point represents the viral genomes of one individual lung. The black line represents the median. Data are representative of two independent experiments (n=5-6), except D which is representative of one experiment (n=5). Values are the mean +SEM (unpaired Student's t test).

As reported previously, the specific deletion of β -catenin in CD11c⁺ cells resulted in aggravated T_H1/T_H17-mediated colitis accompanied by reduced numbers of Treg (Manicassamy et al., 2010). In accordance with these findings, blunted Treg response were discovered in CD11c⁺-specific deletion of β -catenin during collagen-induced arthritis (Alves et al., 2015). Thus, we investigated whether the lack of β -catenin in DC affects the induction of Treg during acute mCMV infection.

However, the deletion of β -catenin did not reduce FoxP3⁺ CD4 Treg (**Fig. 17 A, C**) and does not alter the FoxP3 expression compared to control mice (**Fig. 17 B**). Fourteen days p.i., we detected 7.3% FoxP3⁺ CD4 Treg in lung and 7.5% in dLN, whereas in spleen the frequency was 11.3% in β -cat^{ACD11c} mice (**Fig. 17 A**). The separation of FoxP3⁺ CD4 Treg in lung, dLN and spleen into tTreg and pTreg did not display any significant difference, but predominantly Helios⁺ tTreg were induced by the infection (**Fig. 17 D**). In addition, the β -catenin signaling resulted in an unaltered CD8 Treg differentiation with observed frequencies of 0.4% and 0.5% in β -cat^{ACD11c} and control mice, respectively (**Fig. 17 E**). **Figure 17 F** rather shows that there is no difference between in β -cat^{ACD11c} and control mice in absolute cell numbers in lung and spleen after acute infection. The separation of tTreg and pTreg based on Helios expression mainly displayed Helios⁻ pTreg. Nevertheless, β -cat^{ACD11c} mice displayed similar amounts of both tTreg and pTreg compared to control mice (**Fig. 17 G**).

Collectively, these data demonstrate that the CD11c⁺-specific deletion of β -catenin does not influence the differentiation of CD4 and CD8 Treg as well as the DC numbers. Furthermore, β -cat^{ACD11c} mice occurred similarly virus-specific CD8⁺ T cells compared to control mice in blood and investigated tissues.

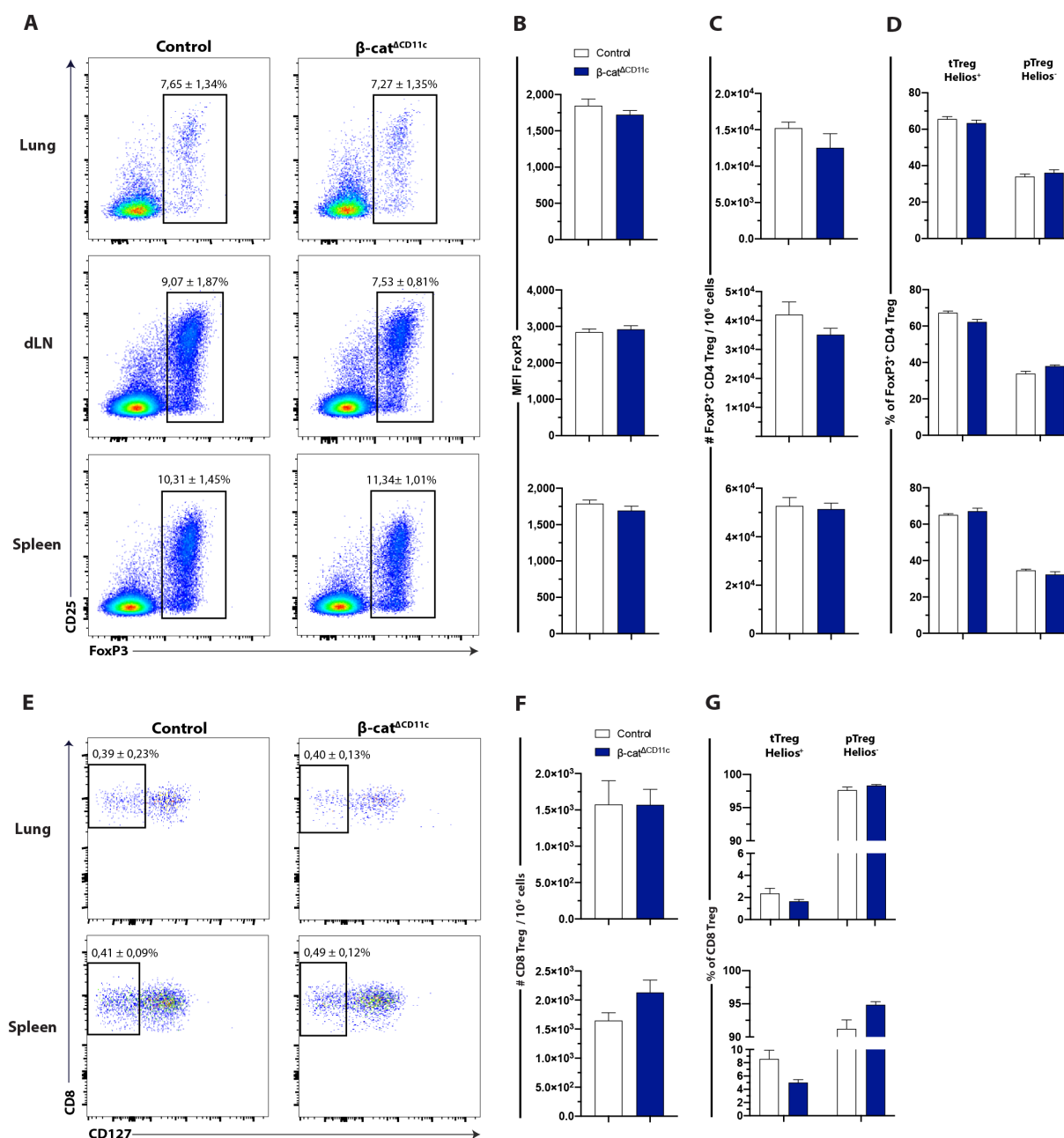


Figure 17: β -cat^{ACD11c} mice shows similar expression of FoxP3⁺ CD4 and CD8 Treg.

Control (white) and β -cat^{ACD11c} (blue) mice were infected i.n. with 2×10^5 PFU of mCMV- Δ m157 for 14 days. (A) Frequencies (representative dot plots) of FoxP3⁺ CD4 Treg in lung, dLN and spleen of control and β -cat^{ACD11c} mice (pregated on living TCR- β^+ CD4⁺ cells). (B) FoxP3 expression as measured by geometric MFI in CD4 Treg of lung, dLN and spleen of control compared to β -cat^{ACD11c} mice. (C) Absolute cell numbers were normalized to 1×10^6 cells (bar graphs) of FoxP3⁺ CD4 Treg in lung, dLN and spleen of control versus IL-10R^{ACD11c} mice. (D) Frequencies of CD4⁺ FoxP3⁺ Helios⁺ tTreg and Helios⁻ pTreg in lung, dLN and spleen of control and β -cat^{ACD11c} mice. (E) Frequencies (flow cytometry plots) and (F) absolute cell numbers (normalized to 1×10^6 cells) of CD122⁺ PD-1⁺ CD127⁻ CD8 Treg in lung and spleen of control compared to β -cat^{ACD11c} mice (pregated on living TCR- β^+ CD8⁺ cells). (G) Frequencies of CD8⁺ Helios⁺ tTreg or Helios⁻ pTreg in lung and spleen of control and β -cat^{ACD11c} mice. Data are representative of two independent experiments (n=5-6) for lung and spleen, whereas dLN is representative of one experiment (n=5-6), except D-G which is one experiment (n=5-6). Values are the mean +SEM (unpaired Student's t test).

3.3.2 Intranasal mCMV infection results in reduced splenic DC numbers in β -cat^{CD11c/EX3} mice accompanied by an expansion of XCR-1⁺ cDC1

Preliminary data of our lab indicate that stabilization of β -catenin in DC exhibit reduced T_H2 responses after the induction of allergic asthma. Therefore, we examined whether the stabilization of β -catenin signaling in DC will enhance the Treg differentiation and affect the mCMV-specific CD8⁺ T cell response during acute mCMV infection.

First, we analyzed the impact of β -catenin signaling on the DC compartment of β -cat^{CD11c/EX3} in comparison to control mice after acute infection. In the β -cat^{CD11c/EX3} mice, the frequencies and absolute cell numbers of DC were similar to control mice in lung and dLN (**Fig. 18 A, B**). Nevertheless, more detailed assessment of dLN demonstrated significantly altered DC distribution towards more XCR-1⁺ cDC1 ($p = 0.018$) and less CD172 α ⁺ cDC2 ($p = 0.018$) resident DC in β -cat^{CD11c/EX3} mice, whereas migratory DC seemed to be unaffected by β -catenin signaling (**Fig. 18 C**). Intriguingly, splenic DC were reduced in β -cat^{CD11c/EX3} mice (**Fig. 18 A, B**). Further analysis of DC subsets in β -cat^{CD11c/EX3} mice revealed a shift toward increased XCR-1⁺ cDC1 ($p = 0.0002$) and diminished CD172 α ⁺ cDC2 ($p = 0.0001$) frequencies (**Fig. 18 C**), by unchanged absolute numbers of cDC (data not shown). Taken together, these data demonstrate that the stabilization of β -catenin affects the splenic DC compartment and resulted in reduced numbers of DC, which was accompanied by an expansion of XCR-1⁺ cDC1. The shift toward elevated XCR-1⁺ cDC1 and reduced CD172 α ⁺ cDC2 were also observed for resident dLN.

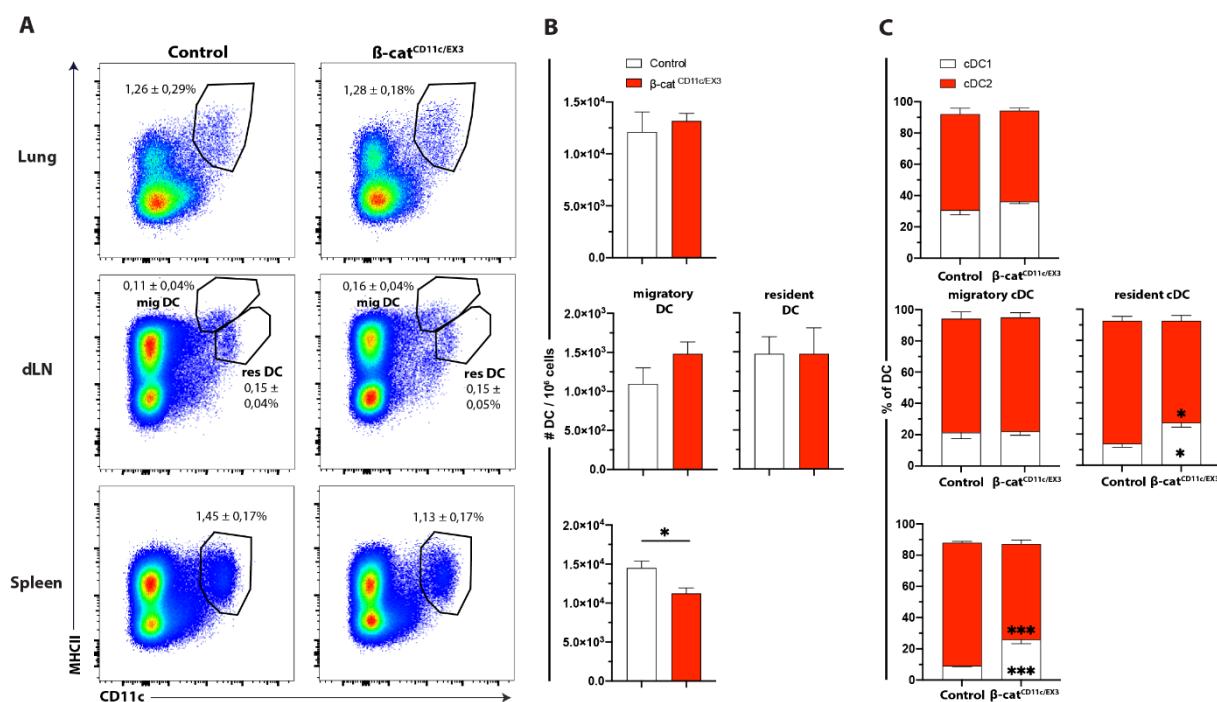


Figure 18: CD11c⁺-specific stabilization of β -catenin results in reduced numbers of splenic DC accompanied by an increase of XCR-1⁺ cDC1.

Control (white) and β -cat^{CD11c/EX3} (red) mice were infected i.n. with 2×10^5 PFU of mCMV- Δ m157 for 14 days. (A) Frequencies (flow cytometry plots) of CD11c⁺ MHC-II⁺ DC in lung, CD11c^{int} MHC-II^{hi} migratory and CD11c^{hi} MHC-I^{int} resident DC in dLN (pregated on living CD45⁺ F4/80⁻ cells) and splenic CD11c⁺ MHC-II⁺ DC in control and β -cat^{CD11c/EX3} mice. (B) Absolute cell numbers of DC (bar graphs) were normalized to 1×10^6 cells in lung, dLN and spleen of control versus β -cat^{CD11c/EX3} mice. (C) Frequencies of XCR-1⁺ cDC1 and CD172 α ⁺ cDC2 in the lung, dLN and spleen of control compared to β -cat^{CD11c/EX3} mice. Data are representative of two independent experiments (n=5-6). Statistical significance (unpaired Student's t test) is indicated as *p < 0.05, **p < 0.01 and ***p < 0.001. Values are the mean +SEM.

Second, we analyzed the mCMV-specific CD8⁺ T cell responses in β -cat^{CD11c/EX3} mice. During acute infection, the kinetic of the virus-specific CD8⁺ T cell response was measured in blood and showed a similar expansion of M38 Tetramer⁺ CD8⁺ T cells (Fig. 19 A). Furthermore, the stabilization of β -catenin did not alter the M38 levels of CD8⁺ T cells (Fig. 19 B). Analysis of the virus-specific CD8 T-cell subpopulation showed no influence of β -catenin signaling. The dominating subsets DPEC and iTEM cells increased in β -cat^{CD11c/EX3} control mice during the course of infection (Fig. 19 C). On the other hand, EEC, cTEM and TCM had low frequencies and decreased in the percentage during infection. These data indicate that β -catenin signaling does neither affect the magnitude nor the quality of the mCMV-specific CD8⁺ T cell response in blood.

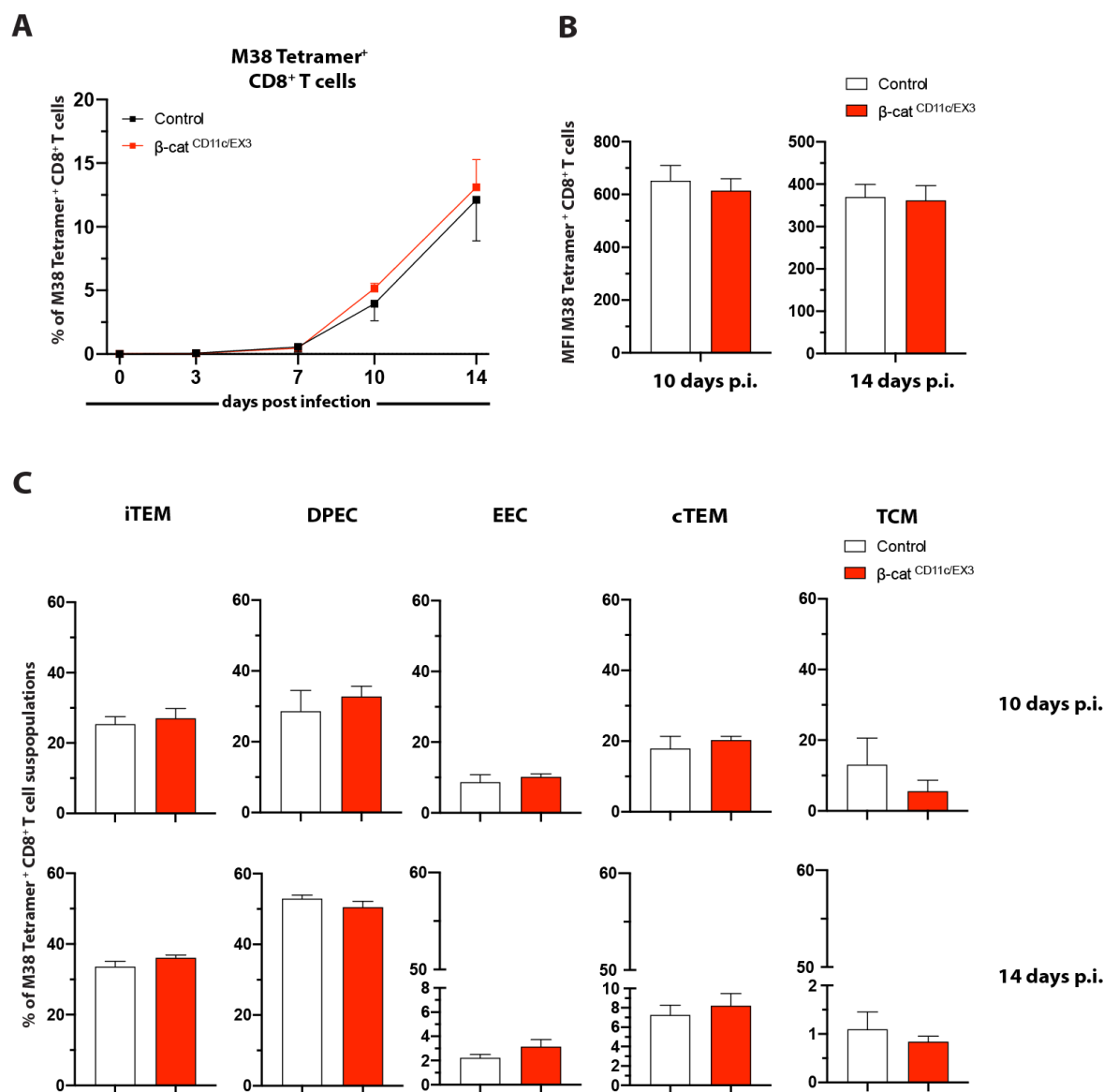


Figure 19: Stabilization of β -catenin does not compromise the CD8⁺ T cell response in blood during acute infection.

At the indicated times after infection i.n. with 2×10^5 PFU of mCMV- Δ m157, blood samples were collected from control (white) and β -cat^{CD11c/EX3} (red) mice and cells were stained with the M38 Tetramer to analyze the virus-specific CD8⁺ T cell response. (A) Time course of the response to M38 Tetramer frequencies and (B) M38 Tetramer expression as measured by geometric MFI in CD8⁺ T cells of control and β -cat^{CD11c/EX3} mice. (C) Shown are related frequencies of M38 Tetramer⁺ CD8⁺ T cell subpopulations CD127⁻ KLRG-1⁺ CD62L⁻ iTEM, CD127⁺ KLRG-1⁺ CD62L⁻ DPEC, CD127⁻ KLRG-1⁻ CD62L⁻ EEC, CD127⁺ KLRG-1⁻ CD62L⁻ cTEM and CD127⁺ KLRG-1⁻ CD62L⁺ TCM of control versus β -cat^{CD11c/EX3} mice 10 and 14 days p.i.. Data are representative of two independent experiments (n=4-6). Values are the mean +SEM (unpaired Student's t test).

Since β -catenin signaling promotes a regulatory DC phenotype inducing CD4 Treg (Jiang et al., 2007), we explored whether the stabilization of β -catenin in DC affects the virus-specific CD8⁺ T cell response in the lung and lymphoid tissue. However, in β -cat^{CD11c/EX3} mice we

observed unaltered virus-specific CD8⁺ T cells in all evaluated organs (**Fig. 20 A, B**). Although there were reduced DC numbers in spleen, this did not appear to alter the CD8⁺ T cell response ($p = 0.672$). The virus-specific response of CD8⁺ T cells in lung was about 21.4% in β -cat^{CD11c/EX3} mice, whereas only 0.7% of these cells were detectable in dLN (**Fig. 20 A**). Additionally, virus-specific CD8⁺ T cells resulted in similar absolute cell numbers of β -cat^{CD11c/EX3} compared to control mice (**Fig. 20 B**). Unexpectedly, further fractionation of M38 Tetramer⁺ CD8⁺ T cells revealed a modification in the distribution of pulmonary CD8⁺ T cell subtypes. First, iTEM with 32.2% in β -cat^{CD11c/EX3} mice ($p = 0.045$) are lower compared to control mice (**Fig. 20 C**). Second, cTEM resulted in a higher frequency with 14.1% in β -cat^{CD11c/EX3} mice ($p = 0.039$) compared to control mice after mCMV infection (**Fig. 20 C**). However, no influence of stabilized β -catenin in DC was detectable on the CD8⁺ T cell populations in the lymphoid organs (**Fig. 20 C**). Because β -catenin signaling had no effect on M38 Tetramer⁺ CD8⁺ T cells, it is not surprising that the number of viral genomes was similar in β -cat^{CD11c/EX3} compared to control mice (**Fig. 20 D**). Taken together, these data reveal a shift in the mCMV-specific CD8⁺ T cell subpopulations toward reduced iTEM and increased cTEM frequencies in β -cat^{CD11c/EX3} mice, which suggest that β -catenin in DC might affect the induction of the effector memory T cell response in lung.

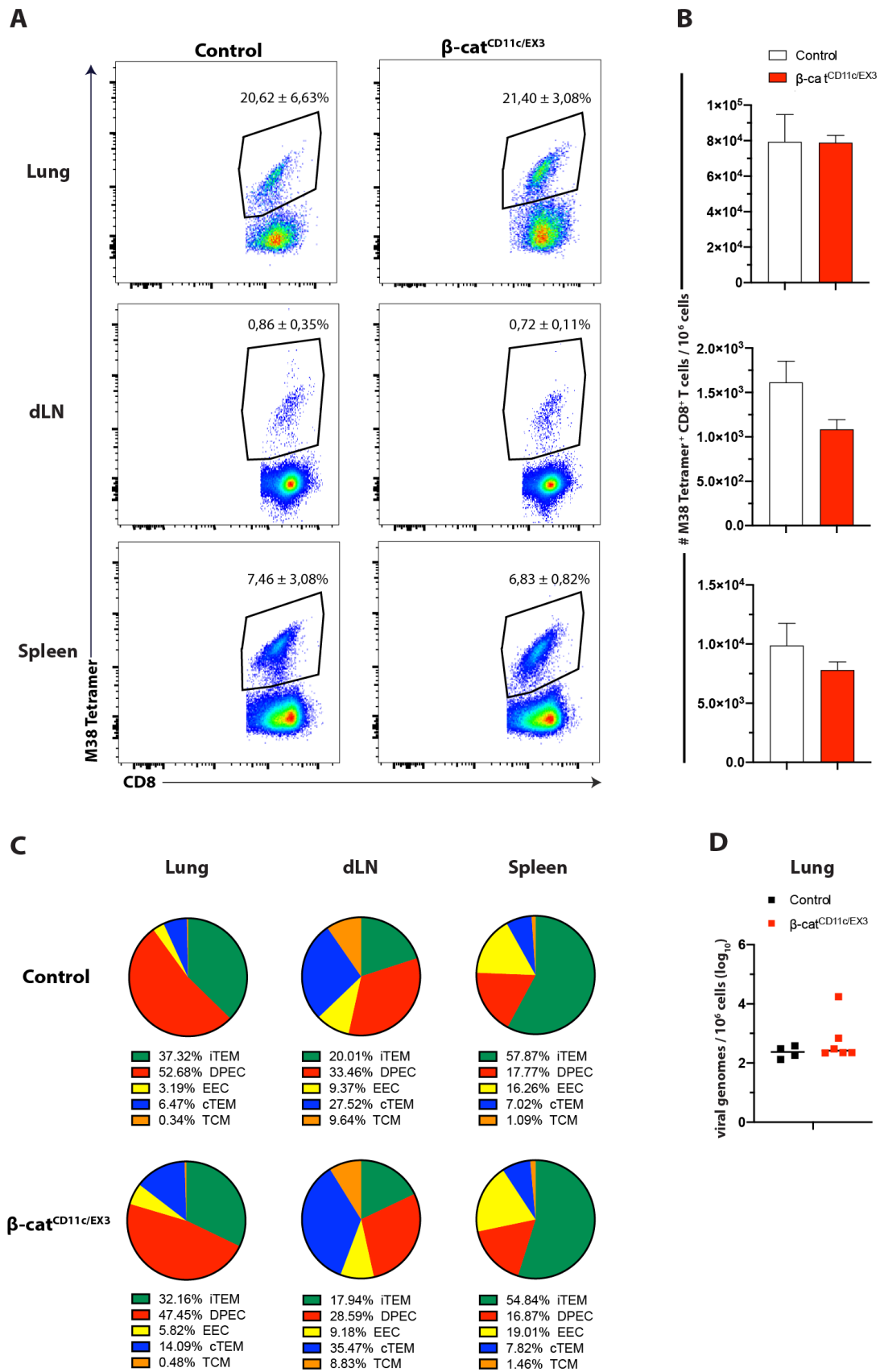


Figure 20: Stabilization of β -catenin induces the effector memory T cells in lung.

Control (white) and β -cat^{CD11c/EX3} (red) mice were infected i.n. with 2×10^5 PFU of mCMV- Δ m157 for 14 days. **(A)** Frequencies (representative FACS plots) and **(B)** absolute cell numbers (normalized to 1×10^6 cells) of M38 Tetramer⁺ CD8⁺ T cells in lung, dLN and spleen of control versus β -cat^{CD11c/EX3} mice (pregated on living CD8⁺ cells). **(C)** Frequencies of M38 Tetramer⁺ CD8⁺ T cells further fractionated in CD127⁻ KLRG-1⁺ CD62L⁻ iTEM (green) CD127⁺ KLRG-1⁺ CD62L⁻ DPEC (red), CD127⁻ KLRG-1⁻ CD62L⁻ EEC (yellow), CD127⁺ KLRG-1⁻ CD62L⁻ cTEM (blue) and CD127⁺ KLRG-1⁻ CD62L⁺ TCM (orange) in lung, dLN and spleen of control and β -cat^{CD11c/EX3} mice. **(D)** DNA of lung were isolated and subjected to real-time PCR to measure viral genomes. The number of viral genomes was normalized to 1×10^6 (log10) cells and compared from control and β -cat^{CD11c/EX3} mice. Each point represents the viral genomes of one individual lung. The black line represents the median. Data are representative of two independent experiments (n=4-6). Statistical significance (unpaired Student's t test) is indicated as *p < 0.05, **p < 0.01 and ***p < 0.001. Values are the mean \pm SEM.

Moreover, we also investigated the differentiation of FoxP3⁺ CD4 in β -cat^{CD11c/EX3} mice after mCMV infection. Here, we observed increased absolute numbers of FoxP3⁺ CD4 Treg in all examined organs and a significant increase of cell frequencies in spleen and dLN (**Fig. 21 A, C**). These expansion of FoxP3⁺ CD4 Treg was already seen in steady state (**Fig. S9**). After 14 days of infection, we measured higher frequencies of FoxP3⁺ CD4 Treg in β -cat^{CD11c/EX3} mice of in dLN (p = 0.0062) and spleen (p = 0.0012), whereas the expression levels of FoxP3 stayed comparable to control mice (**Fig. 21 B**). Moreover, the elevated FoxP3⁺ CD4 Treg numbers were due to higher numbers of Helios⁺ CD4 tTreg, which we also observed in non-infected β -cat^{CD11c/EX3} mice (**Fig S9**). Lung and lymphoid organs exhibited frequencies of Helios⁺ tTreg about 76.7% - 83.6% in β -cat^{CD11c/EX3} and 63.8% - 75.3% in control mice (**Fig. 21 D**). Interestingly, the stabilization of β -catenin did not affect the CD8 Treg differentiation (**Fig. 21 E, F**). In all organs, only 0.2% - 0.5% of CD8 Treg were detected by flow cytometry in β -cat^{CD11c/EX3} and control mice (**Fig. 21 E**). Additionally, the differentiation of tTreg and pTreg were unaltered in β -cat^{CD11c/EX3} mice during acute mCMV infection (**Fig. 21 G**).

Collectively, these data suggest that the CD11c⁺-specific stabilization of β -catenin results in a significant expansion of FoxP3⁺ CD4 Treg. In addition, splenic DC numbers were significantly reduced accompanied by an expansion of XCR-1⁺ cDC1. The shift toward elevated XCR-1⁺ cDC1 and reduced CD172 α ⁺ cDC2 were also observed for resident dLN. In lung, the mCMV-specific CD8⁺ T cell response exhibits a modification in the distribution of mCMV-specific CD8⁺ T cell subpopulations to diminished iTEM and increased cTEM in

β -cat^{CD11c/EX3} mice. These results suggest a crucial role of β -catenin in DC for the induction of FoxP3⁺ CD4⁺ Treg and probably CD8⁺ memory T cells during mCMV infection.

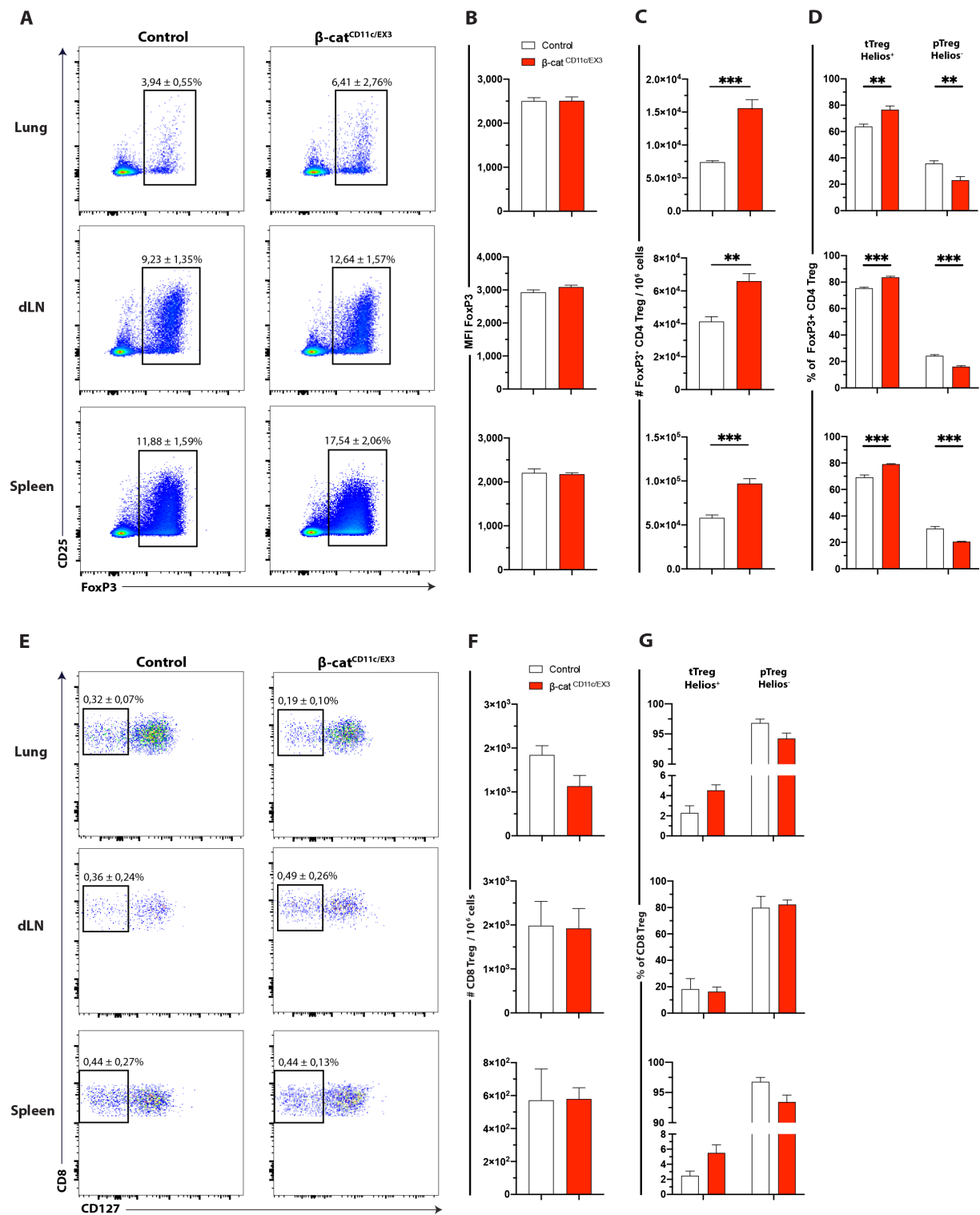


Figure 21: Acute mCMV infection results in a strong CD4 Treg expansion in β -cat^{ΔCD11c/EX3} mice. Control (white) and β -cat^{ΔCD11c/EX3} (red) mice were infected i.n. with 2×10^5 PFU of mCMV-Δm157 for 14 days. (A) Frequencies (representative dot plots) of FoxP3⁺ CD4 Treg in lung, dLN and spleen of control versus β -cat^{ΔCD11c/EX3} mice (pregated on living TCR- β^+ CD4⁺ cells). (B) FoxP3 expression as measured by MFI in CD4 Treg of lung, dLN and spleen of control and β -cat^{ΔCD11c/EX3} mice. (C) Absolute cell numbers were normalized to 1×10^6 cells of FoxP3⁺ CD4 Treg in lung, dLN and spleen of control versus β -cat^{ΔCD11c/EX3} mice. (D) Frequencies of CD4⁺ FoxP3⁺ Helios⁺ tTreg and Helios⁻ pTreg in lung, dLN and spleen of control compared to β -cat^{ΔCD11c/EX3} mice. (E) Frequencies and (F) absolute cell numbers of CD122⁺ PD-1⁺ CD127⁻ CD8 Treg in lung, dLN and spleen of control compared to β -cat^{ΔCD11c/EX3} mice. (G) Frequencies of CD8⁺ Helios⁺ tTreg or Helios⁻ pTreg in lung, dLN and spleen of control versus β -cat^{ΔCD11c} mice. Data are representative of two independent experiments (n=5-6), except E-G which are representative of one experiment (n=5-6). Statistical significance (unpaired Student's t test) is indicated as *p < 0.05, **p < 0.01 and ***p < 0.001. Values are the mean +SEM.

3.4 mCMV latency

During mCMV latency, viral genomes were maintained in the absence of infectious virus in infected cells. The continuous accumulation of virus-specific CD8⁺ T cells in latent mCMV infection is a phenomenon which is known as memory inflation (MI) (Holtappels et al., 2020; Holtappels et al., 2002; Karrer et al., 2003). This MI was firstly monitored as an age depend increase of hCMV-specific T cell response (Northfield et al., 2005). These cells have an effector memory phenotype and show no features of T cell exhaustion (Klenerman and Oxenius, 2016). It has been described that the IL-10R blockade in latently infected wild-type mice led to an increase of mCMV-specific CD8⁺ T cells and reduced viral DNA load in spleen and lung (Jones et al., 2010). Moreover, in β -cat^{CD11c/EX3} mice, we observed an expansion of FoxP3⁺ CD4 Treg, which was accompanied by a shift in the virus-specific CD8⁺ T cell subpopulations during acute mCMV infection.

Based on these findings, we aimed to investigate whether IL-10 or β -catenin signaling in DC affects anti-viral immune responses, including mCMV-specific CD8⁺ T cells and Treg, during mCMV latency and reactivation.

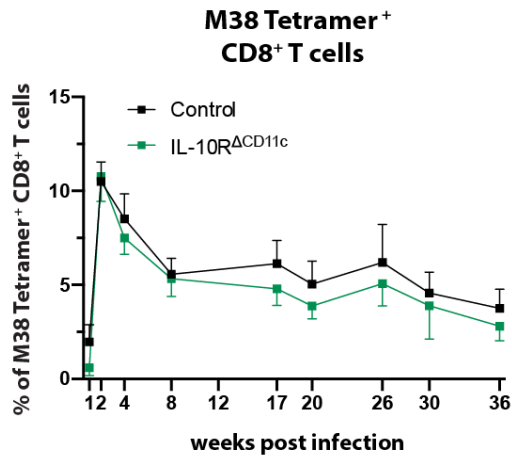
3.4.1 IL-10 signaling in DC reveals unaltered memory CD8⁺ T cell inflation during latent mCMV infection

Our previous results in IL-10R^{ΔCD11c} mice during acute mCMV infection indicate that IL-10 signaling in DC might not play an essential role neither in DC nor T cell compartment and function (see 3.2.2). The recent work by Jones and colleagues (Jones et al., 2010) has shown

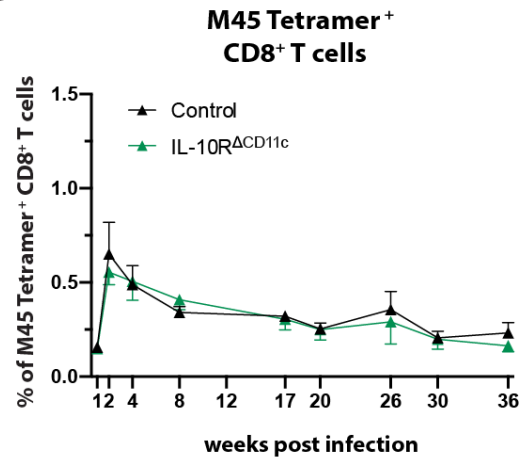
that the MI is dramatically amplified after latent mCMV infection of IL-10 knockout (IL-10^{-/-}) mice, which was accompanied by reduced latent viral loads in IL-10^{-/-} mice. Moreover, these results were confirmed by IL-10R blockade during latency in wild type mice. Based on both findings, we asked for the role of IL-10 signaling in DC of IL-10R^{ACD11c} mice during latent mCMV infection. Therefore, IL-10R^{ACD11c} and control mice were infected i.n. with 2x10⁵ PFU of mCMV-Δm157 and the kinetics of the virus-specific CD8⁺ T cell response and their subpopulations during the whole infection period in blood were examined. However, the M38 Tetramer⁺ subpopulations were not shown after 1 week of infection, because the total M38 Tetramer⁺ CD8⁺ T cell response revealed low frequencies and a further fraction of these cells is not precise enough.

In **Fig. 22 A** frequencies of total M38 Tetramer⁺ CD8⁺ T cells were quantified up to 36 weeks of IL-10R^{ACD11c} compared to control mice. Surprisingly, we observed no MI in IL-10R^{ACD11c} and control mice. We saw a maximum frequency (10.8% in IL-10R^{ACD11c} and 10.5 % in control mice) of M38 Tetramer⁺ CD8⁺ T cells 2 weeks p.i., i.e. during acute infection, which decreased in the latent infection up to 2.8% in IL-10R^{ACD11c} and 3.8% control mice after 36 weeks of infection. On the other hand, the CD8⁺ T cell response for the M45 Tetramer was much weaker for mCMV (**Fig. 22 B**), consistent with our previous observations in the establishment of intranasal infection (**Fig. 6**). This Tetramer is generally used for the analysis of acute mCMV infections and was therefore used as a control for non-MI (**Fig. 22 B**). For the corresponding frequencies of M38 Tetramer⁺ subpopulation, we detected comparable frequencies in IL-10R^{ACD11c} and control mice over the whole infection course (**Fig. 22 C**). Predominantly DPEC and iTEM with minimal contributions of EEC, cTEM and TCM were identified. No significant change was observed in iTEM during infection, and the percentage remained stable about 40% in IL-10R^{ACD11c} and control mice. On the other hand, for the DPEC population a minimal reduction was detectable in latency phase, whereas TCM slightly increased with the course of infection. (**Fig. 22 C**). These results show neither a MI nor an increase of mCMV-specific CD8⁺ T cells in latently infected IL-10R^{ACD11c} mice.

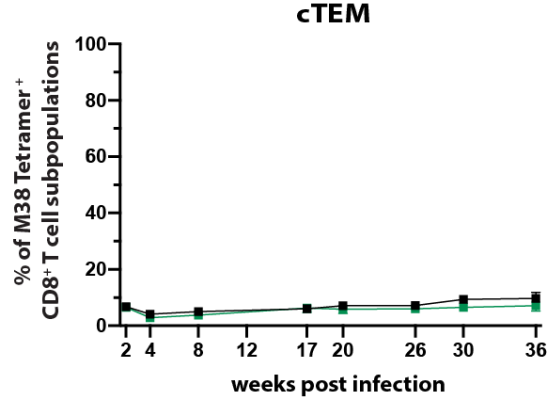
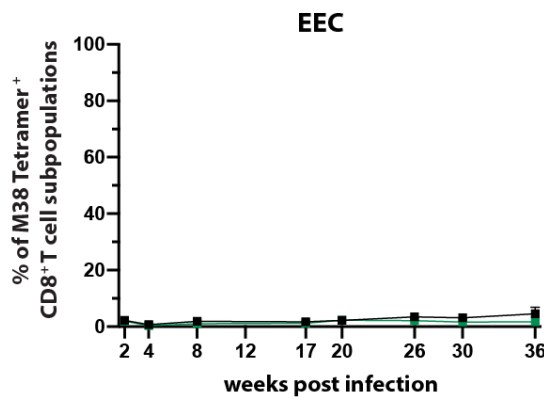
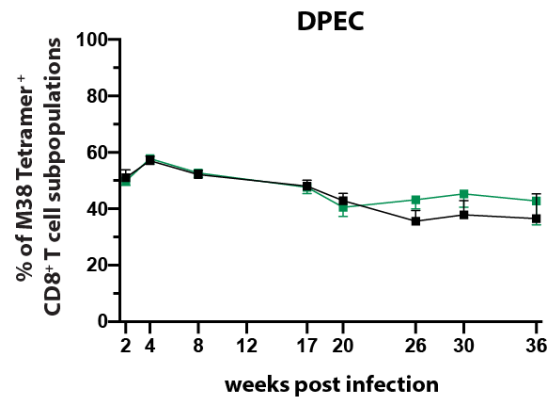
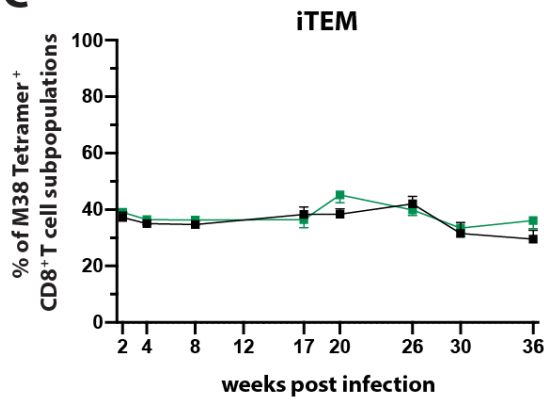
A



B



C



TCM

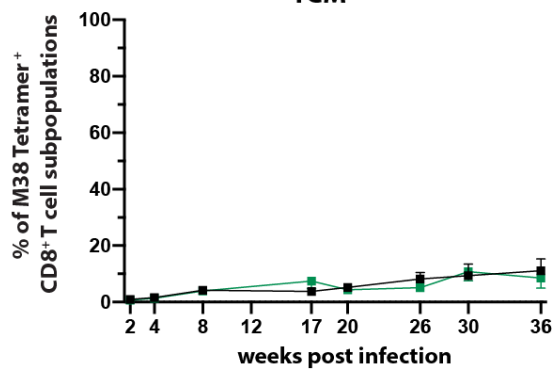


Figure 22: Latent mCMV infection consists predominantly of DPEC and iTEM in blood.

At the indicated times after i.n. infection with 2×10^5 PFU of mCMV- Δ m157, blood samples were collected from control (white) and IL-10R^{ACD11c} (teal) mice. (A) Frequencies of M38 Tetramer⁺ and (B) M45 Tetramer⁺ CD8⁺ T cells in control and IL-10R^{ACD11c} mice. (C) Related frequencies of M38 Tetramer⁺ CD8⁺ T cell subpopulations CD127⁻ KLRG-1⁺ CD62L⁻ iTEM), CD127⁺ KLRG-1⁺ CD62L⁻ DPEC, CD127⁻ KLRG-1⁻ CD62L⁻ EEC, CD127⁺ KLRG-1⁻ CD62L⁻ cTEM and CD127⁺ KLRG-1⁻ CD62L⁺ TCM of control versus IL-10R^{ACD11c} mice of the whole infection course. Data are representative of two independent experiments (n=5). Values are the mean +SEM (unpaired Student's t test).

Since we observed no effect on the virus-specific CD8⁺ T cell response systemically, we analyzed this response tissue-specific, in lung and lymphoid organs. A first cohort of animals was analyzed after 26 weeks and a second cohort after 36 weeks of infection. The latent CD8⁺ T cell response in lung, measured 26 and 36 weeks p.i., showed similar results of M38 Tetramer⁺ CD8⁺ T cells in IL-10R^{ACD11c} compared to control mice (**Fig. 23 A, B**), whereas the study by Jones and colleagues (Jones et al., 2010) showed that IL-10 limited the memory CD8⁺ T cell inflation in lung and spleen during latent infection. In addition, our analysis revealed that no MI and the frequencies of M38-specific CD8⁺ T cells decreased during latency (**Fig. 23 A**), which is also reflected in the absolute cell numbers (**Fig. 23 B**). The M38-specific CD8⁺ T cells consists predominantly of DPEC and iTEM, followed by TCM and cTEM subpopulations (**Fig. 23 C**). The characterization of CD8⁺ T cell subpopulations in latently infected lungs showed no appreciable differences in the course of infection and achieved similar frequencies in IL-10R^{ACD11c} versus control mice, yet revealed a slight increase of TCM in IL-10R^{ACD11c} mice (**Fig. 23 C**). The non-inflationary M45 Tetramer was used as a control for the latent infection and only a percentage of 0.3% - 0.4% of CD8⁺ T cells defined as background were Tetramer positive (**Fig. 23 D**).

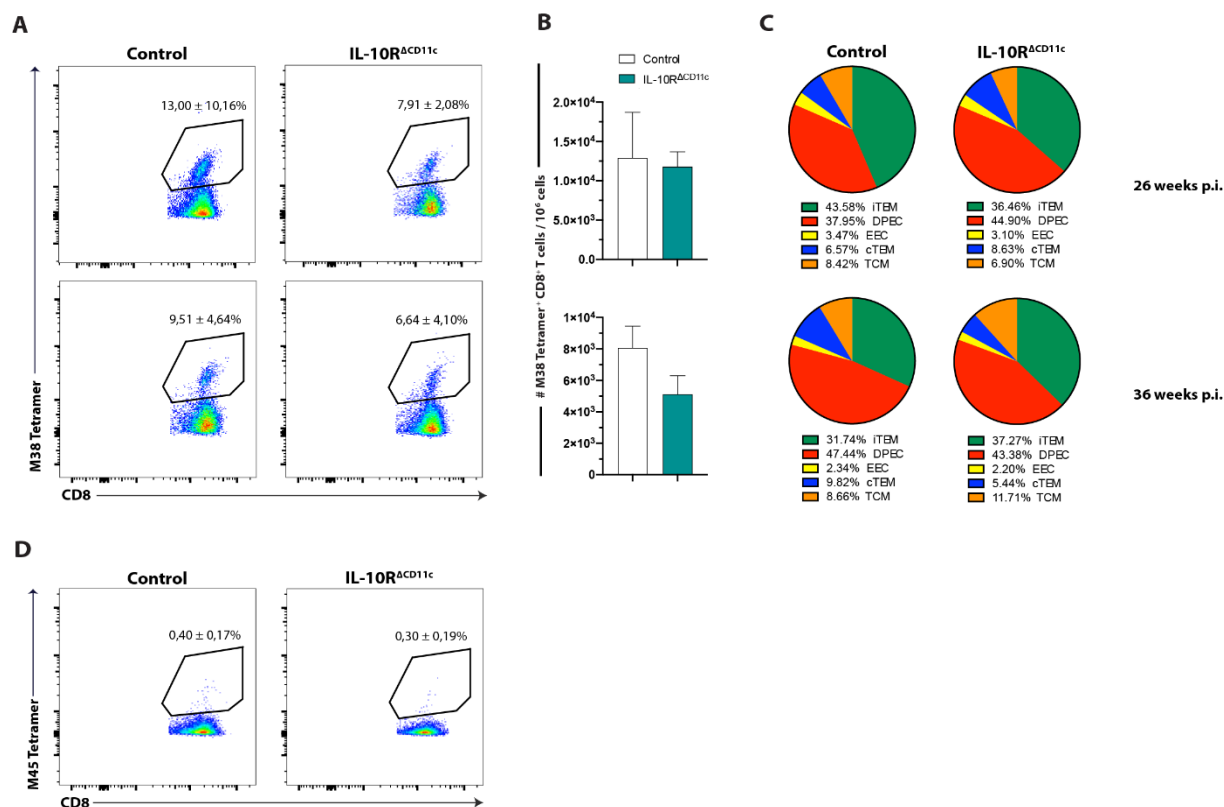


Figure 23: IL-10 signaling does not affect the virus-specific CD8⁺ T cell response in lung during latent mCMV infection.

Both control (white) and IL-10R^{ΔCD11c} (teal) mice were infected with 2×10^5 PFU of mCMV- $\Delta m157$ for 26 and 36 weeks. (A) Representative flow cytometry plots showing frequencies of M38 Tetramer⁺ CD8⁺ T cells and (B) absolute cell numbers (normalized to 1×10^6 cells) in lung (pregated on living CD8⁺ cells) of control versus IL-10R^{ΔCD11c} mice. (C) Frequencies of M38 Tetramer⁺ CD8⁺ T cells further fractionated in CD127⁻ KLRG-1⁺ CD62L⁻ iTEM (green), CD127⁺ KLRG-1⁺ CD62L⁻ DPEC (red), CD127⁻ KLRG-1⁻ CD62L⁻ EEC (yellow), CD127⁺ KLRG-1⁻ CD62L⁻ cTEM (blue) and CD127⁺ KLRG-1⁻ CD62L⁺ TCM (orange) in lung of control compared to IL-10R^{ΔCD11c} mice. (D) Frequencies of M45 Tetramer⁺ CD8⁺ T cells as negative control for latent infection in control and IL-10R^{ΔCD11c} mice. Data are representative of one experiment (n=5). Values are the mean +SEM (unpaired Student's t test).

In addition to the lung, virus-specific CD8⁺ T cells and subpopulations were analyzed in the lymphoid organs after 26 and 36 weeks of infection. Here, we found only low frequencies between 0.5% - 1.3% (Fig. 24 A) and absolute cell numbers (Fig. 24 B) of M38 Tetramer⁺ CD8⁺ T cells in the dLN. A comparison of IL-10R^{ΔCD11c} and control mice revealed in a similar M38-specific CD8⁺ T cell response during latent infection. As described in the review by Torti and Oxenius, TCM are localized in secondary lymphoid organs, whereas TEM are excluded from LN because they cannot upregulate the cell-surface receptors CD62L and CCR7 and are therefore restricted to peripheral tissues (Torti and Oxenius, 2012). The analysis of the M38-specific CD8⁺ T cells showed that TCM between 35.6% - 45.9% were the dominating subpopulations in IL-10R^{ΔCD11c} and control mice (Fig. 24 C). Unexpectedly, we detected also

high frequencies of cTEM between 27.1% - 35.8% in IL-10R^{ACD11c} and control mice, whereas DPEC and iTEM frequencies were reduced in dLN of latently infected mice. These data show an exactly opposite distribution of the virus-specific CD8⁺ T cell subpopulations compared to the lung. However, they should be interpreted with caution because the characterization of subpopulations in dLN is based on very low frequencies of total M38 Tetramer⁺ CD8⁺ T cell response. Additionally, we analyzed as a control the response of the M45 Tetramer⁺ CD8⁺ T cells and detected frequencies between 0.2% - 0,4% in latent infected IL-10R^{ACD11c} and control mice (**Fig. 24 D**). The spleen, the second investigated lymphoid organ, displayed lower frequencies of M38 Tetramer⁺ cells (1.9% - 3.7% in IL-10R^{ACD11c} and control mice) (**Fig. 25 A**) than in lung (6.6% - 13.0% in IL-10R^{ACD11c} and control mice; see **Fig 23 A**). Furthermore, the M38-specific CD8⁺ T cells decreased from 3.7% to 2.4% between 26 and 36 weeks of IL-10R^{ACD11c} mice and thus no MI was observed during latent infection. This decrease of virus-specific CD8⁺ T cells was also seen in absolute cell numbers during this period (**Fig. 25 B**). The further fractionation of CD8⁺ T cells into subpopulations resulted in comparable distribution in IL-10R^{ACD11c} and control mice (**Fig. 25 C**). As in lung, the DPEC and iTEM were the main populations in spleen. Surprisingly, in spleen more cTEM were detected with frequencies of 13.4% - 22.3% (**Fig. 25 C**) compared to lung with 5.4% - 9.8% (**Fig. 23 C**) in latent IL-10R^{ACD11c} and control infected mice. As control for the latent infection, the virus-specific CD8⁺ T cell response of the M45 Tetramer was determined and only 0.2% of CD8⁺ T cells were detected in spleen, which can be defined as background (**Fig. 25 D**). Taken together, in lung and lymphoid tissue the specific deletion of IL-10 receptor in DC showed neither a MI nor an impact on the virus-specific CD8⁺ T cells response during mCMV latency.

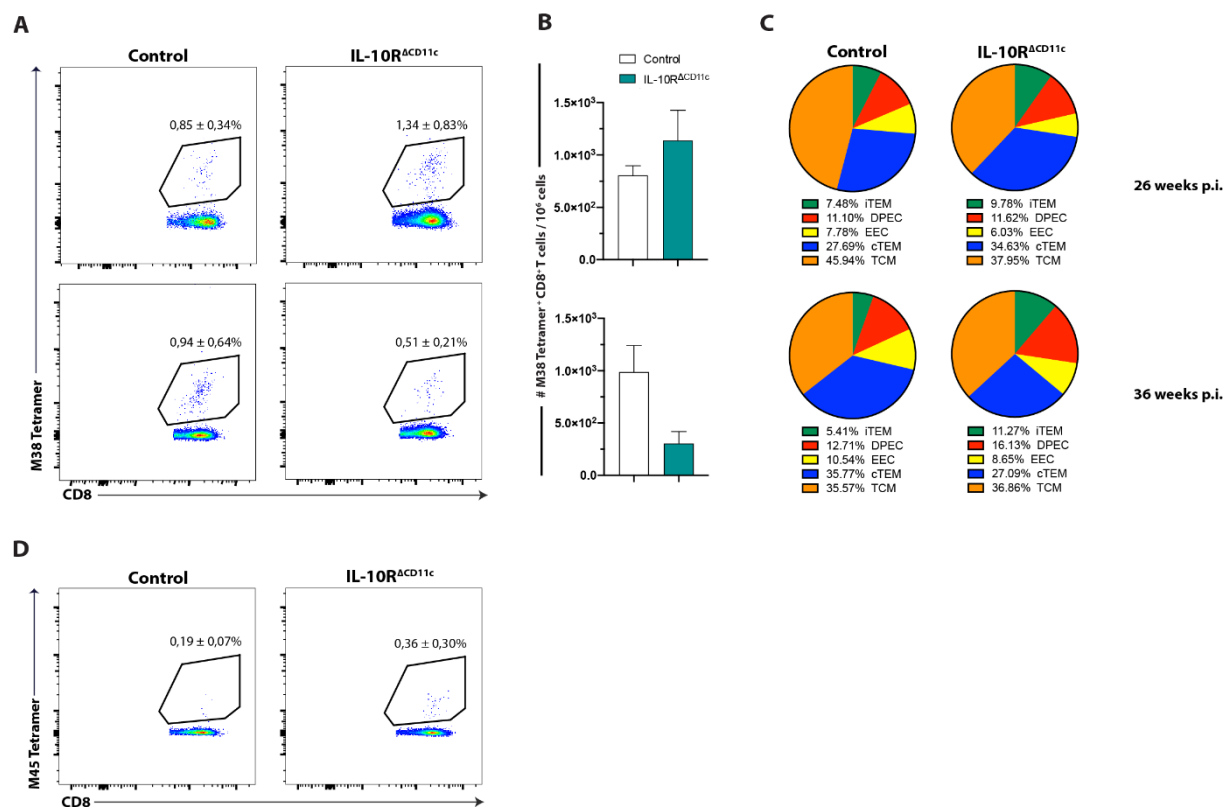


Figure 24: IL-10 receptor signaling has no impact of the virus-specific CD8⁺ T cell response in dLN during latent mCMV infection.

Control (white) and IL-10R^{ΔCD11c} (teal) mice were infected i.n. with 2×10^5 PFU of mCMV-Δm157 for 26 and 36 weeks. **(A)** Representative flow cytometry plots showing frequencies of M38 Tetramer⁺ CD8⁺ T cells and **(B)** absolute cell numbers (normalized to 1×10^6 cells) in dLN (pregated on living CD8⁺ cells) of control versus IL-10R^{ΔCD11c} mice. **(C)** Frequencies of M38 Tetramer⁺ CD8⁺ T cells further fractionated in CD127⁻ KLRG-1⁺ CD62L⁻ iTEM (green), CD127⁺ KLRG-1⁺ CD62L⁻ DPEC (red), CD127⁻ KLRG-1⁻ CD62L⁻ EEC (yellow), CD127⁺ KLRG-1⁻ CD62L⁻ cTEM (blue) and CD127⁺ KLRG-1⁻ CD62L⁺ TCM (orange) in dLN in control versus IL-10R^{ΔCD11c} mice. **(D)** Shown are frequencies of M45 Tetramer⁺ CD8⁺ T cells as negative control of latent infection in control and IL-10R^{ΔCD11c} mice. Data are representative of one experiment (n=2-3). Values are the mean +SEM (unpaired Student's t test).

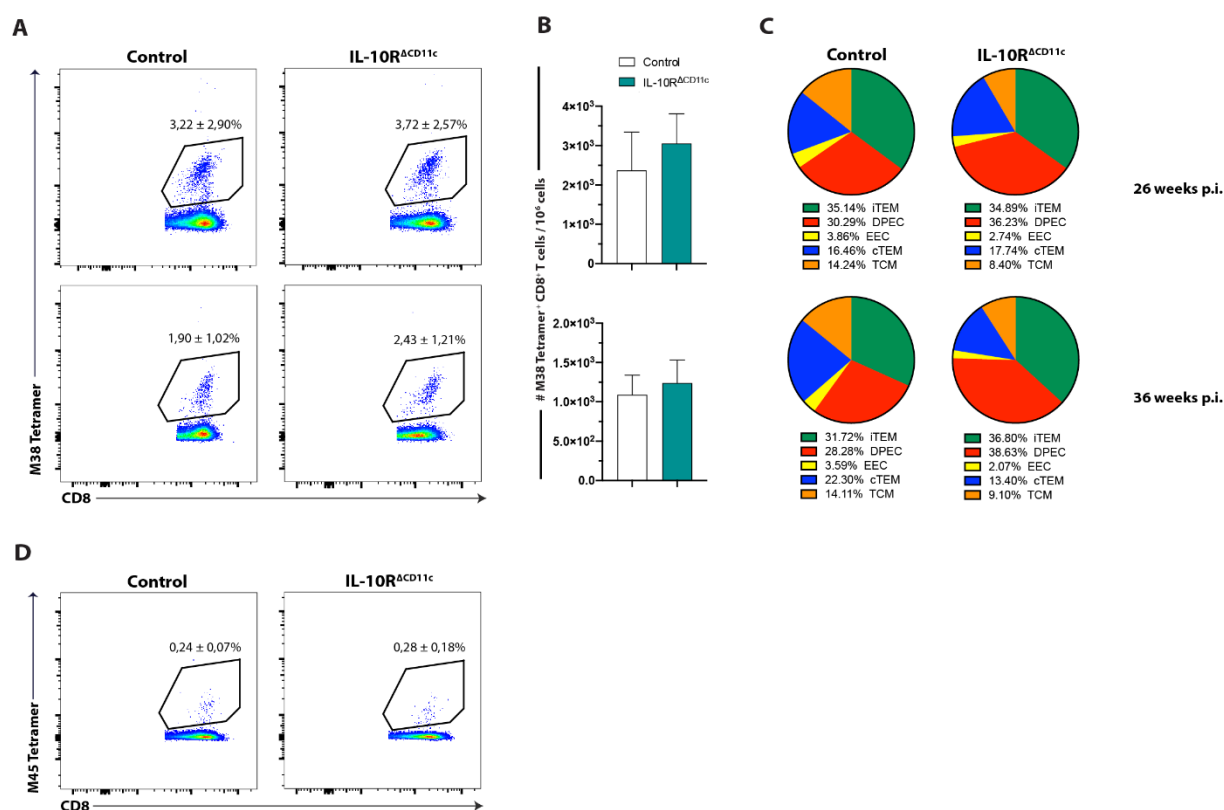


Figure 25: Similar expansion of virus-specific CD8⁺ T cells in IL-10R^{ΔCD11c} and control mice. Control (white) and IL-10R^{ΔCD11c} (teal) mice were intranasal infected with 2×10^5 PFU of mCMV- Δ m157 for 26 and 36 weeks. **(A)** Representative flow cytometry plots with average frequencies of M38 Tetramer⁺ CD8⁺ T cells and **(B)** absolute cell numbers (normalized to 1×10^6 cells) in spleen were determined by flow cytometry (pregated on living CD8⁺ cells). **(C)** Frequencies of M38 Tetramer⁺ CD8⁺ T cells fractionated in CD127⁻ KLRG-1⁺ CD62⁻ iTEM (green), CD127⁺ KLRG-1⁺ CD62L⁻ DPEC (red), CD127⁻ KLRG-1⁻ CD62L⁻ EEC (yellow), CD127⁺ KLRG-1⁻ CD62L⁻ cTEM (blue) and CD127⁺ KLRG-1⁻ CD62L⁺ TCM (orange) in spleen of control versus IL-10R^{ΔCD11c} mice. **(D)** Shown are frequencies of M45 Tetramer⁺ CD8⁺ T cells as negative control of latent infection in control and IL-10R^{ΔCD11c} mice. Data are representative of one experiment (n=5). Values are the mean +SEM (unpaired Student's t test).

The mCMV latency is defined by a lifelong maintenance of viral genomes, but in the absence of infectious virus. In a well-established HCT model by Griessl *et al.*, viral genomes remained present in lung over 8 months p.i. with a significant decrease in organ load between 4 and 6 months (Griessl *et al.*, 2021). Hence, we investigated the viral genomes in the lung, spleen and liver from i.n. infected mice (2×10^5 PFU of mCMV- Δ m157), which are all known by a long-term maintenance of viral genomes during latent mCMV infection. We observed low viral genomes after 26 weeks of infection, which were down to the limit of detection. Further, there was a decrease between 26 and 36 weeks p.i and more or less no viral genomes were detectable in all evaluated organs (**Fig. 26**). These results display that IL-10 signaling does not affect latent

mCMV genomes, which are also less detectable in latently infected mice by the i.n. infection model.

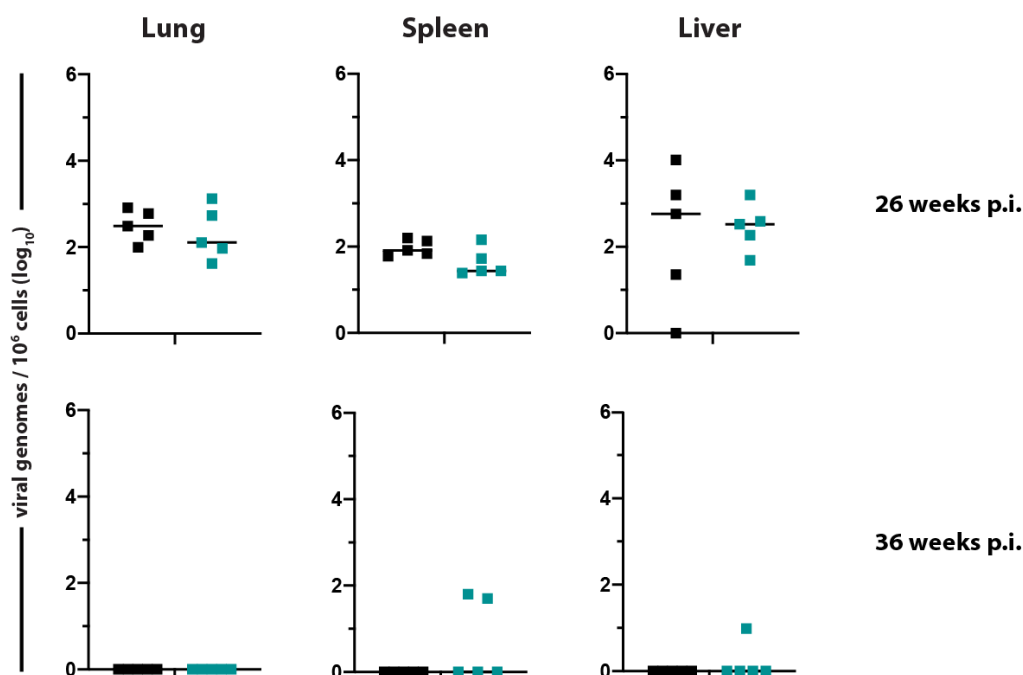


Figure 26: Viral genomes in latent infected IL-10R^{ACD11c} mice.

Latent viral DNA load determined for lung, spleen and liver pieces of control (white) and IL-10R^{ACD11c} (teal) mice after 26 and 36 weeks of infection. The number of viral genomes was normalized to 1×10^6 (log₁₀) cells. Each point represents the viral genomes of one individual mice. The black line represents the median. Data are representative of one experiment (n=5).

Furthermore, we investigated whether FoxP3⁺ CD4 Treg differentiation is influenced in IL-10R^{ACD11c} mice after 26 and 36 weeks of infection. As seen in **Fig. 27 A and C**, no significant differences in FoxP3⁺ CD4 Treg frequencies and absolute cell numbers in lung of IL-10R^{ACD11c} in comparison to control mice can be found. After 26 weeks of infection, the frequency of FoxP3⁺ CD4 Treg was about 10.9% in IL-10R^{ACD11c} mice and increased up to 13.1% after 36 weeks of infection, whereas the frequency in control mice was stable about 12.8% (**Fig. 27 A**). However, absolute cell numbers revealed a trend of an increase in FoxP3⁺ CD4 Treg in IL-10R^{ACD11c} mice after 26 weeks of infection, but they did not reach statistical significance ($p = 0.099$) (**Fig. 27 C**). In addition, the CD11c⁺-specific deletion of IL-10 receptor demonstrated similar expression levels of FoxP3 compared to control mice, but total the expression seemed to be elevated after 36 weeks of infection in both mice (**Fig. 27 B**). The separation of FoxP3⁺ CD4 Treg into tTreg and pTreg showed predominately Helios⁺ tTreg during latent infection (**Fig. 27 D**). As in the lung, no effect of IL-10 signaling on CD4 Treg

differentiation was detected in the spleen and resulted in similar frequencies (**Fig. 27 E**) and absolute cell numbers (**Fig. 27 G**) in knock-out and control mice. However, we observed a 2.5 times higher frequency of FoxP3⁺ CD4 Treg (~27%) in spleen than in the lung. In accordance with the lung, expression levels of FoxP3 were higher after 36 weeks than 26 weeks of infection (**Fig. 27 F**). Moreover, mainly Helios⁺ tTreg were induced during latent infection, but there was difference for IL-10R^{ΔCD11c} compared to control mice (**Fig. 27 H**). Our results showed a trend for

higher pulmonary FoxP3⁺ CD4 Treg numbers in IL-10R^{ΔCD11c} mice after 26 weeks of infection.

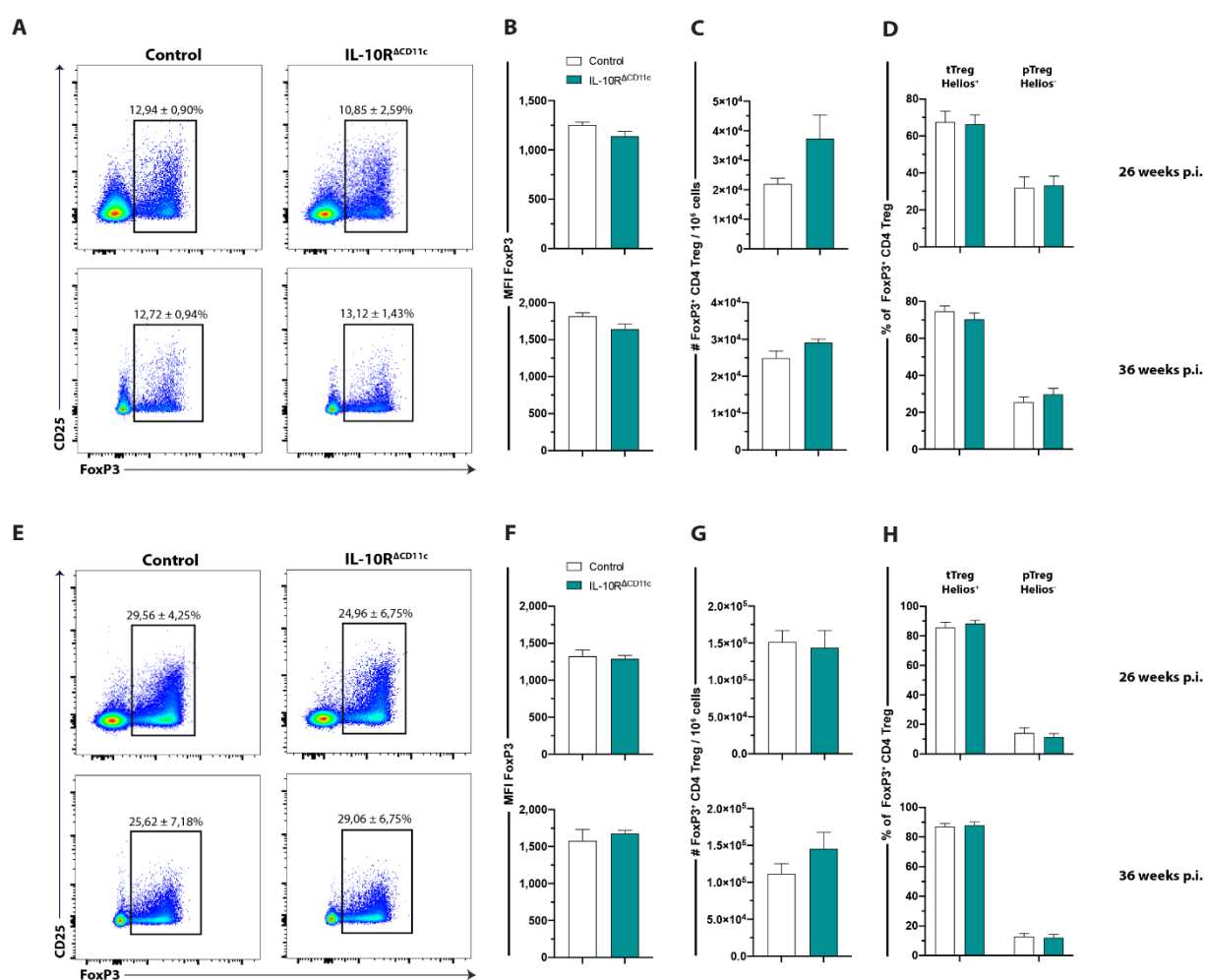


Figure 27: IL-10R^{ACD11c} mice show no significant impact on FoxP3⁺ CD4 Treg differentiation. Control (white) and IL-10R^{ACD11c} (teal) mice were infected i.n. with 2×10^5 PFU of mCMV- Δ m157 CMV for 26 and 36 weeks. **(A)** Frequencies (representative dot plots) of FoxP3⁺ CD4 Treg in lung of control compared to IL-10R^{ACD11c} mice (pregated on living TCR- β ⁺ CD4⁺ cells). **(B)** Shown are FoxP3 expression measured by geometric intensity MFI in CD4 Treg of lung of control versus IL-10R^{ACD11c} mice. **(C)** Bar graphs show absolute cell numbers (normalized to 1×10^6 cells) of FoxP3⁺ CD4 Treg in lung of control and IL-10R^{ACD11c} mice. **(D)** Frequencies of CD4⁺ FoxP3⁺ Helios⁺ tTreg or Helios⁻ pTreg in lung of control versus IL-10R^{ACD11c} mice. **(E)** Representative flow cytometry plots showing frequencies of FoxP3⁺ CD4 Treg in spleen of control versus IL-10R^{ACD11c} mice. **(F)** FoxP3 expression as measured by geometric MFI in CD4 Treg of spleen of control and IL-10R^{ACD11c} mice. **(G)** Absolute cell numbers of FoxP3⁺ CD4 Treg in spleen of control compared to IL-10R^{ACD11c} mice. **(H)** Frequencies of CD4⁺ FoxP3⁺ Helios⁺ tTreg and Helios⁻ pTreg in spleen of control and IL-10R^{ACD11c} mice. Data are representative of two independent experiments (n=5) after 26 weeks of infection, whereas data are representative of one experiment (n=5) after 36 weeks of infection. Values are the mean +SEM (unpaired Student's t test).

In addition to the well-known CD4 Treg, we also investigated the impact of IL-10 signaling in DC for the CD8 Treg differentiation during mCMV latency and reactivation. The CD11c⁺-specific deletion of IL-10 receptor resulted in unaltered CD8 Treg frequencies (**Fig. 28 A**) and absolute cell numbers (**Fig. 28 B**) in lung compared to control mice. At both, 26 and 36 weeks after infection low frequencies between 0.7% and 1.3% of CD8 Treg in IL-10R^{ACD11c} and control mice were detected, but a small increase could be observed after 36 weeks of infection (**Fig. 28 A**). Nevertheless, IL-10R^{ACD11c} mice displayed comparable amounts of Helios⁺ tTreg and Helios⁻ pTreg as compared to control mice (**Fig. 28 C**). In contrast to CD4 Treg (**Fig. 27 D**), predominantly Helios⁻ pTreg were fluorometrically analyzed in lung. Similarly, the IL-10 signaling did not affect the CD8 Treg differentiation in spleen and resulted in low percentages about 0.8% - 2.2% of IL-10R^{ACD11c} and control mice (**Fig. 28 D**). As in the lung, elevated CD8 Treg were seen after 36 weeks of infection (**Fig 28 D, E**). During latent infection, both tTreg and pTreg revealed unaltered frequencies in IL-10R^{ACD11c} compared to control mice, and mainly pTreg (74.3% - 89.6% in IL-10R^{ACD11c} and control mice) were observed (**Fig. 28 F**). These results display that the deletion of IL-10 receptor in DC has no significant impact on the CD8 Treg differentiation in lung and spleen during latent mCMV infection.

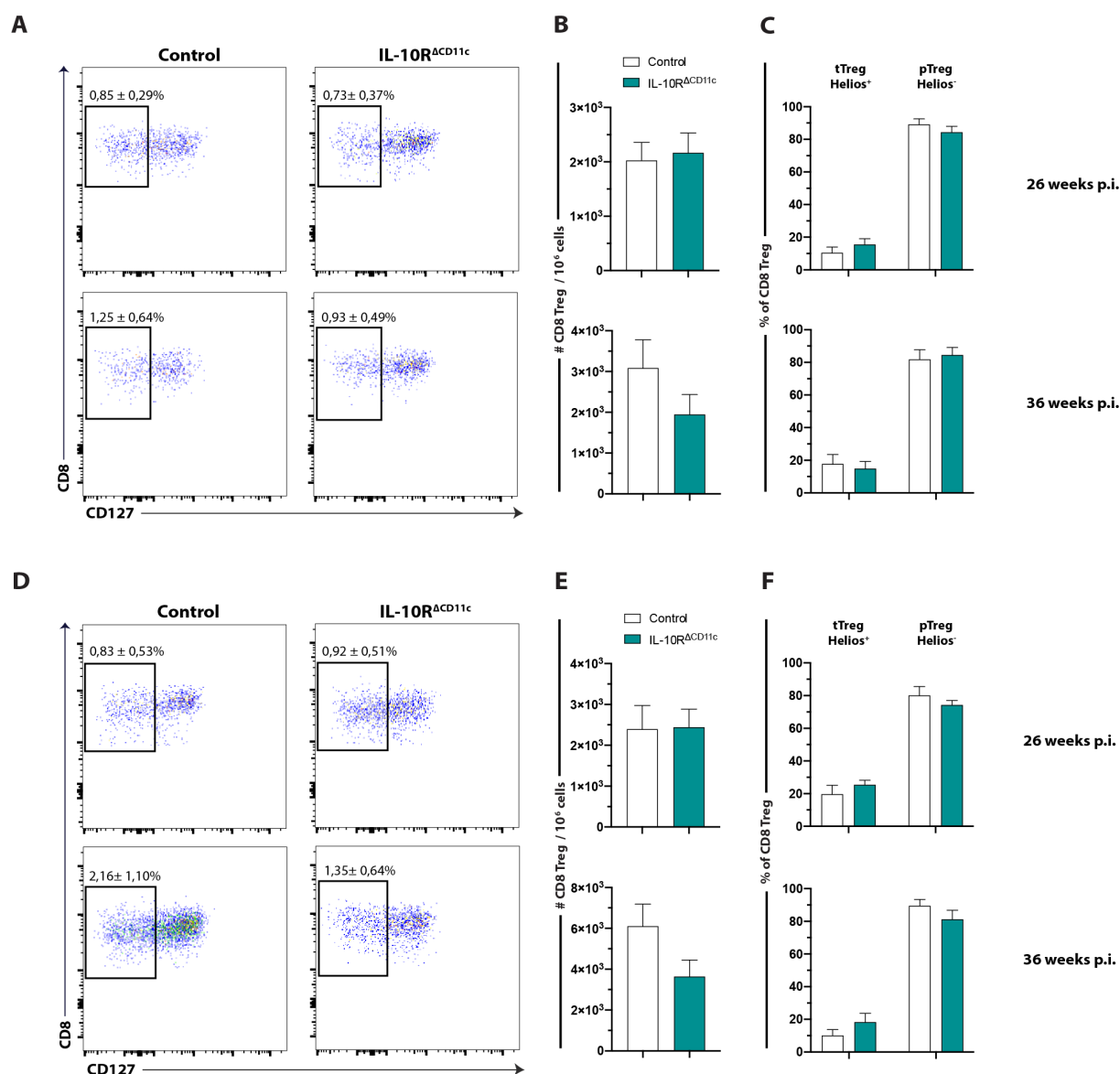


Figure 28: Deletion of IL-10 receptor in DC has no effect on CD8 Treg differentiation in latently infected mice.

Control (white) and IL-10R^{ΔCD11c} (teal) mice were infected i.n. with 2×10^5 PFU of mCMV- Δ m157 for 26 and 36 weeks. (A) Frequencies (flow cytometry plots) and (B) absolute cell numbers (normalized to 1×10^6 cells) of CD122⁺ PD-1⁺ CD127⁻ CD8 Treg in lung of control compared to IL-10R^{ΔCD11c} mice (pregated on living TCR- β ⁺ CD8⁺ cells). (C) Frequencies of CD8⁺ Helios⁺ tTreg or Helios⁻ pTreg in lung of control and IL-10R^{ΔCD11c} mice. (D) Representative flow cytometry plots showing frequencies and (E) absolute cell numbers of CD8 Treg in spleen of control and IL-10R^{ΔCD11c} mice. (F) Frequencies of CD8⁺ Helios⁺ tTreg or Helios⁻ pTreg in lung of control versus IL-10R^{ΔCD11c} mice. Data are representative of one experiment (n=5). Values are the mean +SEM (unpaired Student's t test).

Finally, we examined a possible role of IL-10 signaling in DC of IL-10R^{ΔCD11c} mice during latent infection. In lung, frequencies (Fig. 29 A) and absolute cell numbers (Fig. 29 B) of total DC remain unaltered by the specific deletion of IL-10 receptor at 26 (p = 0.121) and 36 weeks (p = 0.194) p.i.. Moreover, no significant difference was observed in the mice even during the

course of infection. **Figure 29 C** shows the XCR-1⁺ cDC1 and CD172α⁺ cDC2 subsets in lung, which were also not impaired by the lost IL-10 signaling. After 26 weeks of infection, frequencies of XCR-1⁺ cDC1 were 37.2% in IL-10R^{ΔCD11c} and 40.7% in control mice, and decreased to 34.7% in IL-10R^{ΔCD11c} and 30.5% in control mice after 36 weeks of infection. Since spleen is an organ where the mCMV latency establishes, we additionally studied the DC in this organ after 26 and 36 weeks of infection. As in the previous experiments (**Fig. 10**), we did not see an effect of the IL-10 signaling in terms of DC frequencies (**Fig. 29 D**) or absolute cell numbers (**Fig. 29 E**) in spleen during viral latency. The DC populations were stable during the infection period and their frequencies were about 2% in IL-10R^{ΔCD11c} and control mice (**Fig. 29 D**). In contrast to the lung, only 3.9% - 5.9% of XCR-1⁺ cDC1 were observed in spleen in IL-10R^{ΔCD11c} and control mice during latent infection (**Fig. 29 F**).

In conclusion, the CD11c⁺-specific deletion of IL-10 receptor does not influence DC in lung and spleen during latent mCMV infection. Furthermore, IL-10 signaling in the tested organs showed neither an influence nor an expansion of M38-specific CD8⁺ T cells (MI), which was accompanied by an unaffected CD4 and CD8 Treg differentiation. These results indicate that IL-10 signaling in DC do not play an essential role during latent immune response.

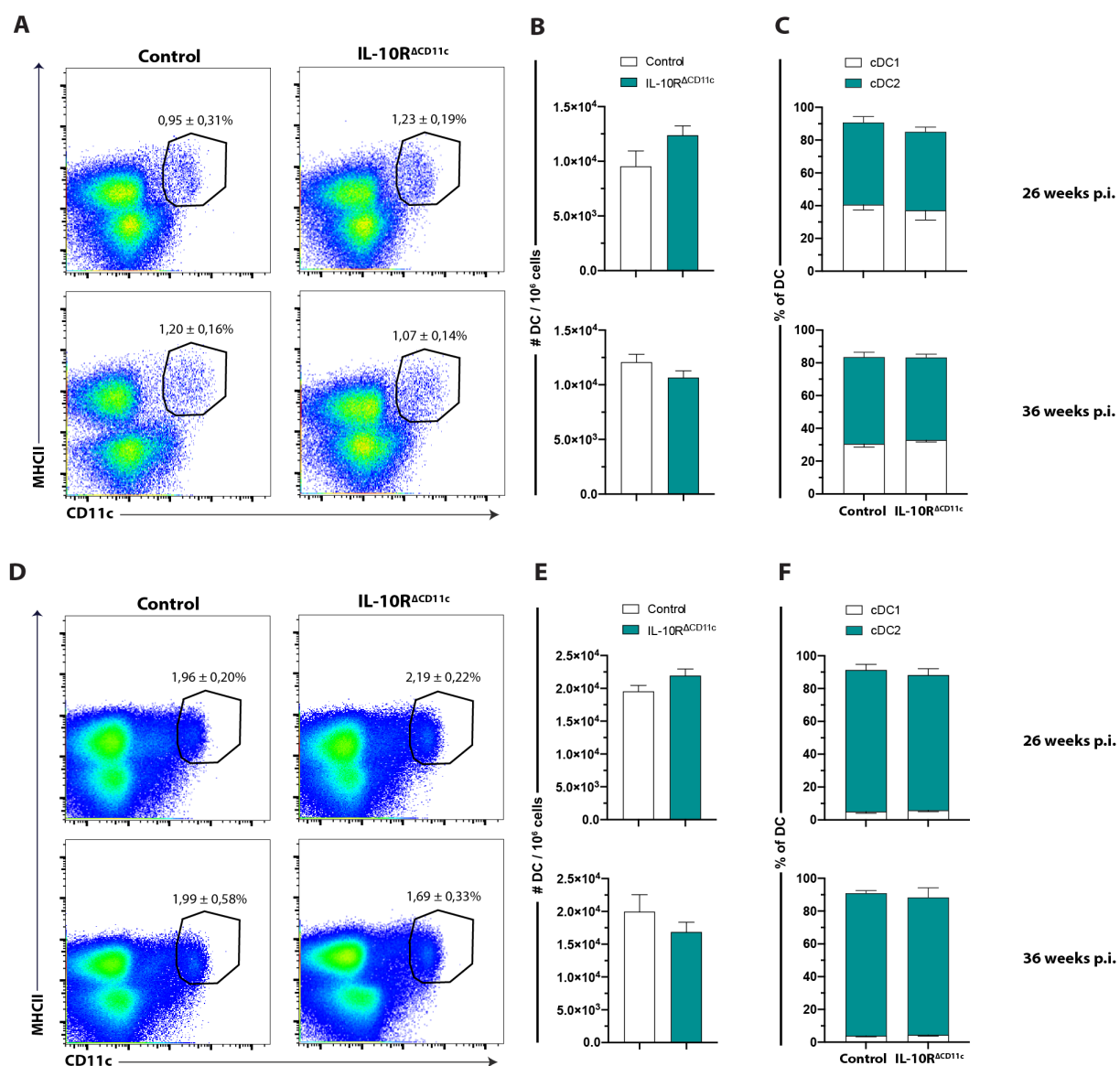


Figure 29: IL-10 signaling does not impair DC numbers during latent infection.

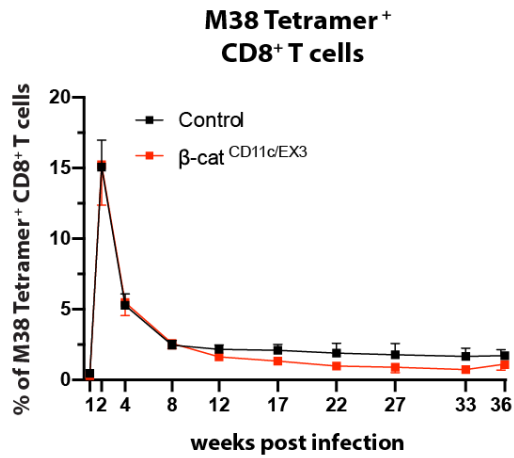
Control (white) and IL-10R^{ΔCD11c} (teal) mice were infected i.n. with 2×10^5 PFU of mCMV- Δ m157 for 26 and 36 weeks. (A) Shown are frequencies (flow cytometry plots) of CD11c⁺ MHC-II⁺ DC in lung (pregated on living CD45⁺ F4/80⁻ cells) in control and IL-10R^{ΔCD11c} mice. (B) Absolute cell numbers of DC (bar graphs) were normalized to 1×10^6 cells in lung of control versus IL-10R^{ΔCD11c} mice. (C) Frequencies of XCR-1⁺ cDC1 and CD172 α ⁺ cDC2 in the lung of control compared to IL-10R^{ΔCD11c} mice. (D) Frequencies (flow cytometry plots) of CD11c⁺ MHC-II⁺ DC in spleen of control versus IL-10R^{ΔCD11c} mice. (E) Absolute cell numbers of DC in spleen of control compared to IL-10R^{ΔCD11c} mice. (F) Frequencies of XCR-1⁺ cDC1 and CD172 α ⁺ cDC2 in the spleen of control compared to IL-10R^{ΔCD11c} mice. Data are representative of two independent experiments (n=5) after 26 weeks of infection, whereas data are representative of one experiment (n=5) after 36 weeks of infection. Values are the mean +SEM (unpaired Student's t test).

3.4.2 β -catenin signaling impacts the virus-specific memory CD8⁺ T cell response accompanied by an expansion of Treg during latent infection

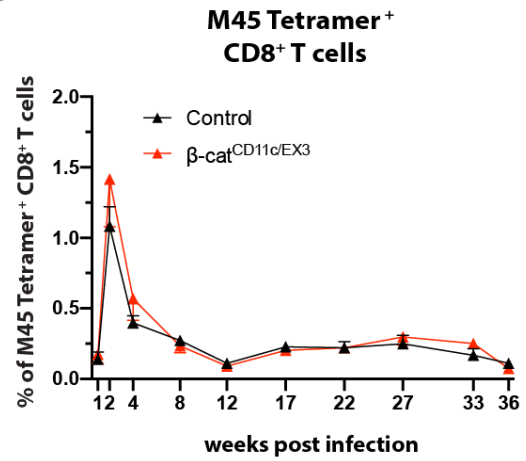
During acute mCMV infection, our findings showed that the stabilization of β -catenin in DC resulted in a reduction of DC and a shift toward increased XCR-1⁺ cDC1 in spleen (**Fig. 18**). Furthermore, in the β -cat^{CD11c/EX3} mice we detected a significant expansion of FoxP3⁺ CD4 Treg in total numbers, which was accompanied by a higher Helios⁺ tTreg proportion (**Fig. 21**). For the mCMV-specific CD8 T cell response, we observed similar expansion of M38 Tetramer⁺ cells after 14 days p.i. in lung and lymphoid tissue, but in lung we detected changes in the virus-specific CD8⁺ T cell subpopulations (**Fig. 20**). Based on these results, we decided to investigate the role of β -catenin signaling in mCMV latency and reactivation and expected an influence on the formation of effector memory T cells in latently infected β -cat^{CD11c/EX3} mice. For this purpose, β -cat^{CD11c/EX3} and control mice were infected i.n. with 2×10^5 PFU of mCMV- Δ m157.

First, the anti-viral CD8⁺ T cell response was determined during the course of infection in blood. As with the IL-10R^{ΔCD11c} mice, the M38 Tetramer⁺ subpopulations were not shown after 1 week of infection in β -cat^{CD11c/EX3} mice because the total M38 Tetramer⁺ CD8⁺ T cell response revealed low frequencies and a further fraction of these cells were not precise enough. In the latently infected mice we observed no expansion of the M38-specific CD8⁺ T cells (MI) and a comparable response in β -cat^{CD11c/EX3} compared to control mice (**Fig. 30 A**). After 2 weeks of infection, we observed the maximum frequency of 15% of M38-specific CD8⁺ T cells, which decreased to 1.5% after 36 weeks of infection. In **Fig. 30 B** the response of M45 Tetramer resulted in a low CD8⁺ T cell response with 1.4% in β -cat^{CD11c/EX3} mice and the non-inflatory Tetramer was used as control for the latent infection. Further analysis of the M38 Tetramer⁺ CD8⁺ T cells revealed comparable frequencies in β -cat^{CD11c/EX3} in comparison to control mice. Mainly DPEC and iTTEM were observed during the latent infection (**Fig. 30 C**). Whereas the iTTEM proportion remained stable about 25% of M38-specific CD8⁺ T cells in β -cat^{CD11c/EX3} and control mice, the DPEC fraction decreased from 57% to 30% during the course of infection. On the other hand, the cTEM, TCM and EEC possessed low frequencies and were unaltered during infection, with only TCM increasing slightly up to 25% towards the end of infection (**Fig. 30 C**). These data display that the M38-specific CD8⁺ T cells undergo no MI and predominantly DPEC and iTTEM are detected in latently infected β -cat^{CD11c/EX3} mice, suggesting that β -catenin signaling in DC does not play a crucial role.

A



B



C

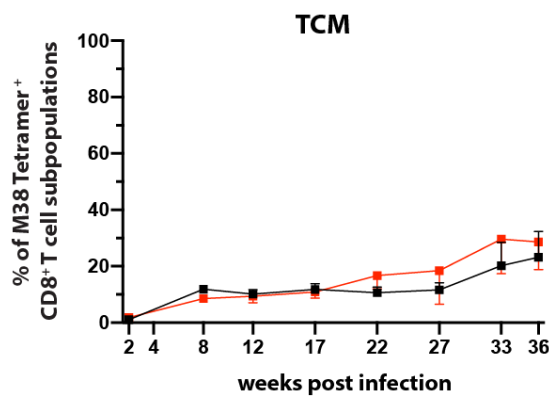
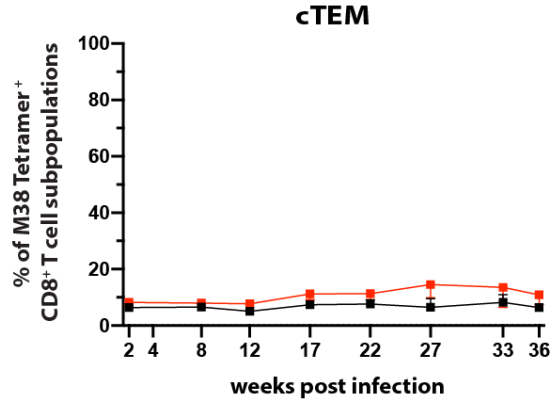
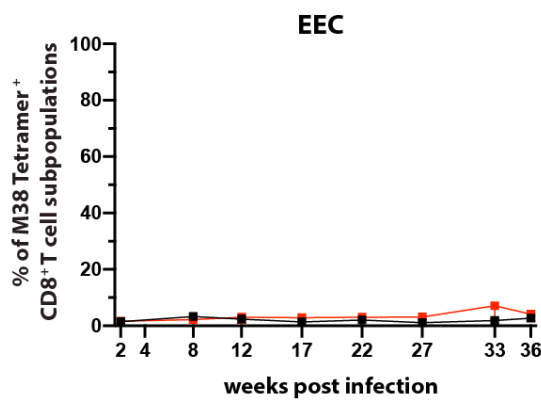
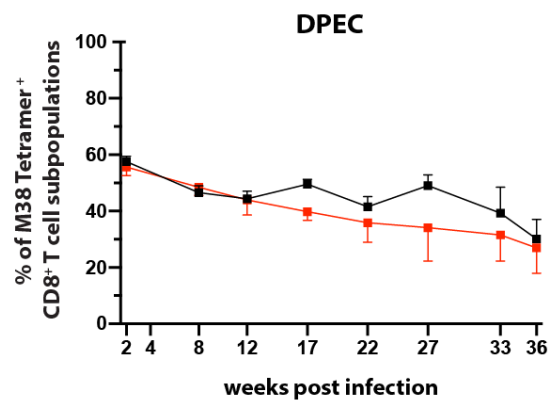
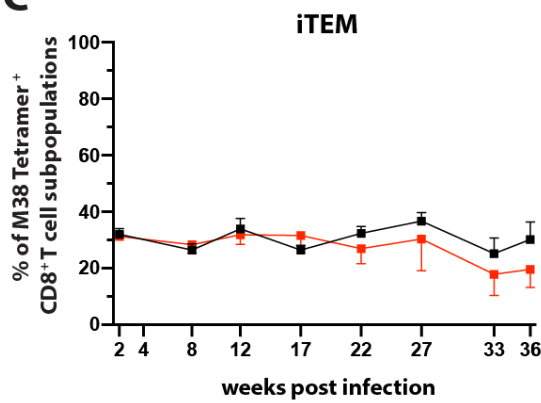


Figure 30: Similar expansion of virus-specific CD8⁺ T cells in β -cat^{CD11c/EX3} and control mice during latent infection.

Control (white) and β -cat^{CD11c/EX3} (red) mice were infection i.n. with 2×10^5 PFU of mCMV- Δ m157 and blood samples were collected at indicated time points. (A) Shown are frequencies of M38 Tetramer⁺ and (B) M45 Tetramer⁺ CD8⁺ T cells of control compared to β -cat^{CD11c/EX3} mice. (C) Related frequencies of M38 Tetramer⁺ CD8⁺ T cell subpopulations CD127⁻ KLRG-1⁺ CD62L⁻ iTEM, CD127⁺ KLRG-1⁺ CD62L⁻ DPEC, CD127⁻ KLRG-1⁻ CD62L⁻ EEC, CD127⁺ KLRG-1⁻ CD62L⁻ cTEM and CD127⁺ KLRG-1⁻ CD62L⁺ TCM of control versus β -cat^{CD11c/EX3} mice of the whole infection course. Data are representative of one experiment (n=3-11). Values are the mean +SEM (unpaired Student's t test).

In the next step, we explored the influence of β -catenin signaling of the virus-specific CD8⁺ T cell response in lung and lymphoid organs after 17, 26 and 36 weeks of infection. We observed no MI, but a trend for a lower M38-specific CD8⁺ T cell response in lung of β -cat^{CD11c/EX3} mice (**Fig. 31 A, B**). After 17 weeks of infection the CD8⁺ T cell response reached the highest frequencies about 6.8% and absolute cell numbers in β -cat^{CD11c/EX3}, which decreased to 2.7% after 36 weeks of infection. In addition, we found a comparable reduction in absolute cell numbers during latency (**Fig. 31 B**). Moreover, the characterization of these virus-specific CD8⁺ T cells revealed that the DPEC subset, followed by iTEM, TCM, cTEM, and finally EEC dominates in latently infected mice (**Fig. 31 C**). Only after 17 weeks of infection, we observed significant differences in the CD8⁺ T cell composition in lung. First, the cTEM ($p = 0.00015$) and EEC ($p = 0.001$) subpopulations were increased in β -cat^{CD11c/EX3} mice. Second, the DPEC ($p = 0.006$) showed decreased percentage. Third, for iTEM and TCM no impact on β -catenin signaling was observed. As in blood, the TCM increased in the lung of β -cat^{CD11c/EX3} mice after 26 and 36 weeks of infection, but these frequencies were not significantly higher than in control mice. Additionally, we used the non-inflamatory M45 Tetramer as control for the latent infection and detected less frequency about 0.1% of M45-specific CD8⁺ T cells, which can be defined as background (**Fig. 31 D**).

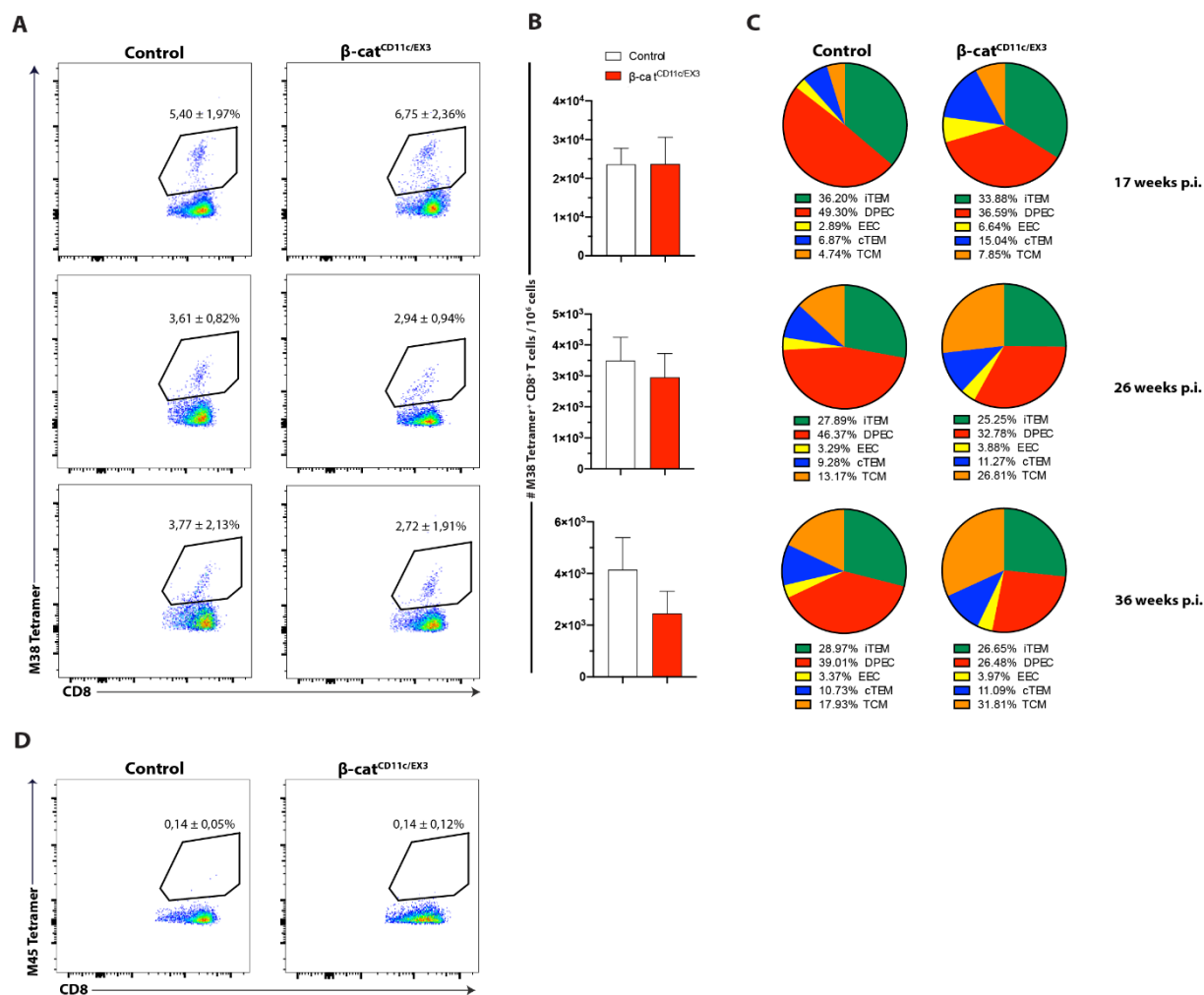


Figure 31: No memory inflation of M38-specific CD8⁺ T cells in lung upon i.n. mCMV infection. Control (white) and β -cat^{CD11c/EX3} (red) mice were infected i.n. with 2×10^5 PFU of mCMV- Δ m157 for 17, 26 and 36 weeks. **(A)** Representative flow cytometry plots showing frequencies of M38 Tetramer⁺ CD8⁺ T cells and **(B)** absolute cell numbers (normalized to 1×10^6 cells) in lung (pregated on living CD8⁺ cells) of control and β -cat^{CD11c/EX3} mice. **(C)** Frequencies of M38 Tetramer⁺ CD8⁺ T cells further fractionated in CD127⁻ KLRG-1⁺ CD62L⁻ iTEM (green), CD127⁺ KLRG-1⁺ CD62L⁻ DPEC (red), CD127⁻ KLRG-1⁻ CD62L⁻ EEC (yellow), CD127⁺ KLRG-1⁻ CD62L⁻ cTEM (blue) and CD127⁺ KLRG-1⁻ CD62L⁺ TCM (orange) in lung of control versus β -cat^{CD11c/EX3} mice. **(D)** Frequencies of M45 Tetramer⁺ CD8⁺ T cells as negative control for latent infection in control and β -cat^{CD11c/EX3} mice. Statistical significance (unpaired Student's t test) is indicated as * $p < 0.05$, ** $p < 0.01$ and *** $p < 0.001$. Data are representative of one experiment ($n=3-11$ after 17 weeks of infection; $n=3-5$ after 26 and 36 weeks of infection).

In parallel to the lung, we also analyzed the M38-specific CD8⁺ T cell response in lymphoid tissue, the dLN. In both β -cat^{CD11c/EX3} and control mice, we found only low responses between 0.4% - 0.5% to M38 Tetramer⁺ CD8⁺ T cells during latent infection, which were also not affected by β -catenin signaling (**Fig. 32 A**). Similarly, to frequencies, the absolute cell numbers were comparable low in β -cat^{CD11c/EX3} and control mice (**Fig. 32 B**). Comparable to the lung, the latent T cell pool is predominantly composed by TCM between 45.5% - 54.7% and cTEM

between 24.2% - 33.7% with low contributions of DPEC between 5.2% - 13.2%, EEC between 4.7% - 7.8% and iTEM between 4.7% - 6.8% of CD8⁺ T cells in β -cat^{CD11c/EX3} and control mice (**Fig. 32 C**). As opposed to the lung, in dLN no significant differences in CD8⁺ T cell subpopulations during latency were detected. However, they should be interpreted with caution because the characterization of subpopulations in dLN is based on very low frequencies of total M38 Tetramer⁺ CD8⁺ T cell response. **Figure 32 D** shows that the M45-specific CD8⁺ T cells have a frequency of 0.1% in latently infected mice. In addition, we analyzed the anti-viral immune response in the spleen. Contrary to our expectations, we did not observe an impaired M38-specific CD8⁺ T cell response in the spleen (**Fig. 33 A, B**) despite significantly reduced DC numbers (**Fig. 37 E**). In comparison to lung, the frequency of M38-specific CD8⁺ T cells was much lower with 1.2% in β -cat^{CD11c/EX3} mice after 17 weeks of infection and dropped to 0.7% after 26 weeks of infection (**Fig. 33 A**). Interestingly, with increasing infection time, the response of CD8⁺ T cells seemed to increase again up to 1.0% in β -cat^{CD11c/EX3} mice. However, the M38-specific CD8⁺ T cells underwent no MI. Absolute cell numbers showed a similar range in β -cat^{CD11c/EX3} and control mice (**Fig. 33 B**). Furthermore, we fractionated these virus-specific CD8⁺ T cells into the different subpopulations and observed an effect of the T cell formation again only after 17 weeks of infection (**Fig. 33 C**). In β -cat^{CD11c/EX3} mice the cTEM were significantly elevated ($p = 0.0016$) at 38.7%, whereas DPEC decreased to 23.0% ($p = 0.0031$) (**Fig. 33 C**), similar to the lung (**Fig. 21 C**). In contrast, all other subpopulations showed no significant differences in β -cat^{CD11c/EX3} compared to control mice. In contrast to lung, iTEM and DPEC further increased in spleen of latently infected β -cat^{CD11c/EX3} mice. As seen in **Figure 33 D**, the virus-specific CD8⁺ T cell response of the M45 Tetramer was about 0.1%. Taken together, these data show a trend of a lower M38-specific CD8⁺ T cell response in lung of β -cat^{CD11c/EX3} mice. Moreover, an increase of mCMV-specific cTEM in lung and spleen occurs only after 17 weeks of infection, whereas DPEC significantly diminishes.

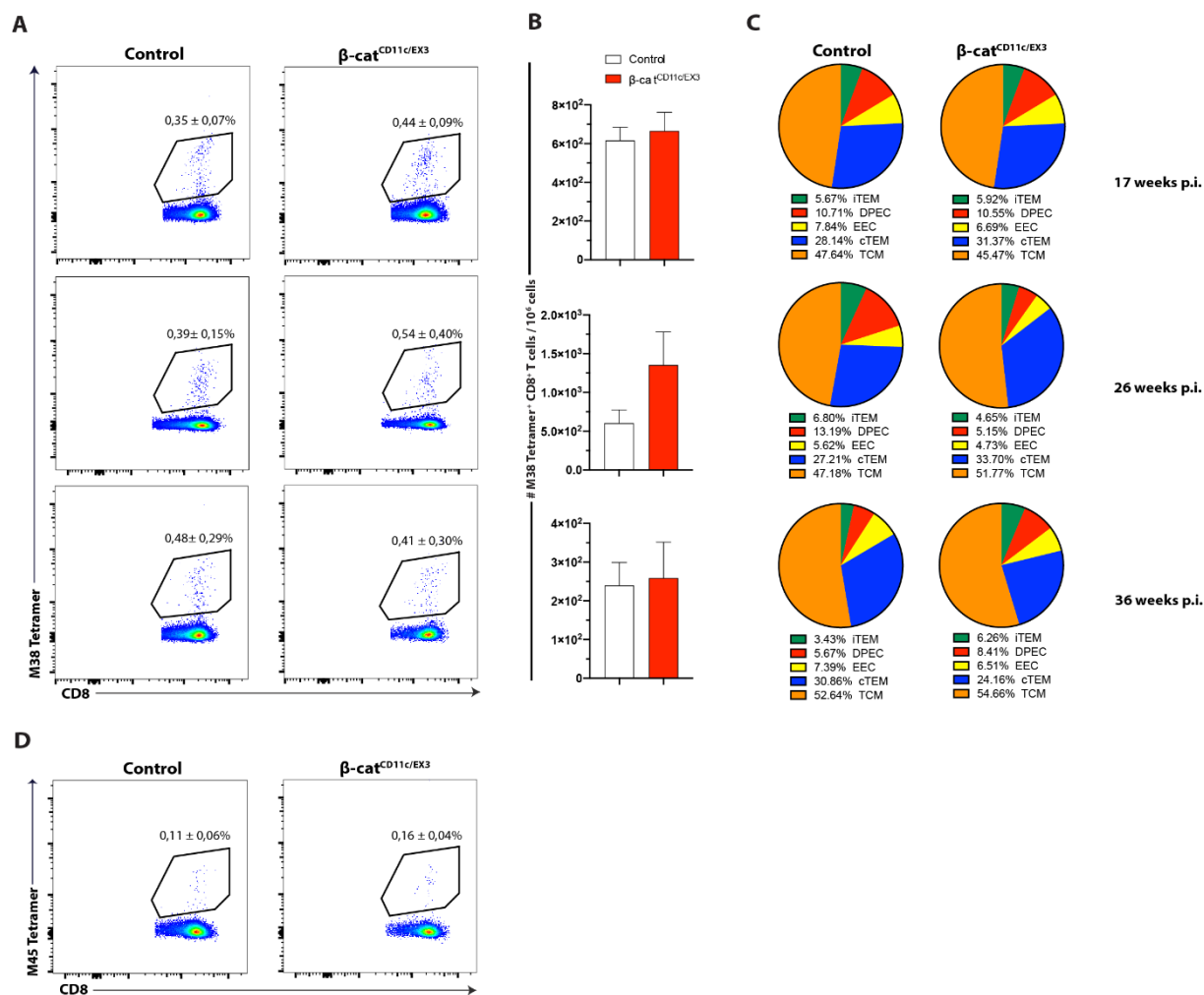


Figure 32: Latent infection results in low virus-specific CD8⁺ T cell response in dLN.

Control (white) and β -cat^{ACD11c/EX3} (red) mice were infected with 2×10^5 PFU of mCMV- Δ m157 for 17, 26 and 36 weeks. **(A)** Shown are representative flow cytometry plots with average frequencies of M38 Tetramer⁺ CD8⁺ T cells and **(B)** bar graphs of absolute cell numbers (normalized to 1×10^6 cells) in dLN (pregated on living CD8⁺ cells) of control compared to β -cat^{ACD11c/EX3} mice. **(C)** Frequencies of M38 Tetramer⁺ CD8⁺ T cells further separated in CD127⁻ KLRG-1⁺ CD62L⁻ iTEM (green), CD127⁺ KLRG-1⁺ CD62L⁻ DPEC (red), CD127⁻ KLRG-1⁻ CD62L⁻ EEC (yellow), CD127⁺ KLRG-1⁻ CD62L⁻ cTEM (blue) and CD127⁺ KLRG-1⁻ CD62L⁺ TCM (orange) in dLN of control versus β -cat^{ACD11c/EX3} mice. **(D)** Shown are frequencies of M45 Tetramer⁺ CD8⁺ T cells as negative control of latent infection in control and β -cat^{ACD11c/EX3} mice. Data are representative of one experiment (n=3-11 after 17 weeks of infection; n=3-5 after 26 and 36 weeks of infection). Values are the mean +SEM (unpaired Student's t test).

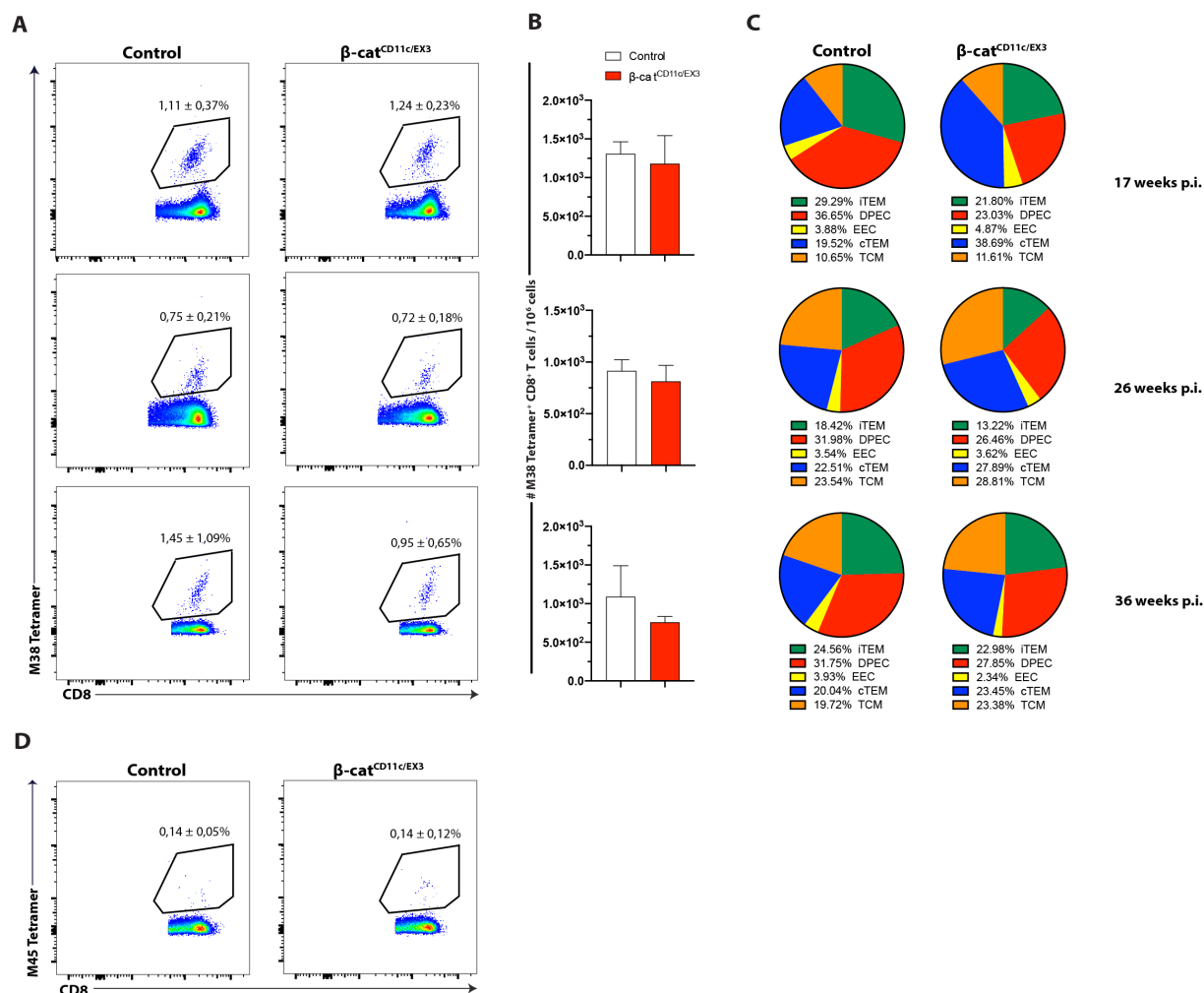


Figure 33: M38-specific CD8⁺ T cells undergo no MI in spleen in latently infected β -cat^{ACD11c/EX3} mice.

Both, control (white) and β -cat^{ACD11c/EX3} (red) mice were infected i.n. with 2×10^5 PFU of mCMV- Δ m157 for 17, 26 and 36 weeks. (A) Frequencies (flow cytometry plots) of M38 Tetramer⁺ CD8⁺ T cells and (B) absolute cell numbers (bar graphs) were normalized to 1×10^6 cells in spleen (pregated on living CD8⁺ cells) of control compared β -cat^{ACD11c/EX3} mice. (C) Frequencies of M38 Tetramer⁺ CD8⁺ T cells further fractionated in CD127⁻ KLRG-1⁺ CD62L⁻ iTEM (green), CD127⁺ KLRG-1⁺ CD62L⁻ DPEC (red), CD127⁻ KLRG-1⁻ CD62L⁻ EEC (yellow), CD127⁺ KLRG-1⁻ CD62L⁻ cTEM (blue) and CD127⁺ KLRG-1⁻ CD62L⁺ TCM (orange) in lung of control versus β -cat^{ACD11c/EX3} mice. (D) Frequencies of M45 Tetramer⁺ CD8⁺ T cells as negative control for latent infection in control and β -cat^{ACD11c/EX3} mice. Statistical significance (unpaired Student's t test) is indicated as * $p < 0.05$, ** $p < 0.01$ and *** $p < 0.001$. Data are representative of one experiment (n=3-11 after 17 weeks of infection; n=3-5 after 26 and 36 weeks of infection).

Because we did not observe any influence of the virus-specific CD8⁺ T cell response in latency in either the lung or lymphoid organs, we expected equal viral genomes in the β -cat^{ACD11c/EX3} and control mice. As can be seen in **Figure 34**, the viral genomes were near the detection limit or were not measurable. The significant difference after 26 weeks of infection in the lung was due to the fact that minimal amounts of viral DNA load could be detected in only one of four

control mice. In conclusion, the viral DNA loads were rarely measurable in latent infected mice, making a statement about the influence of the β -catenin signaling pathway not possible.

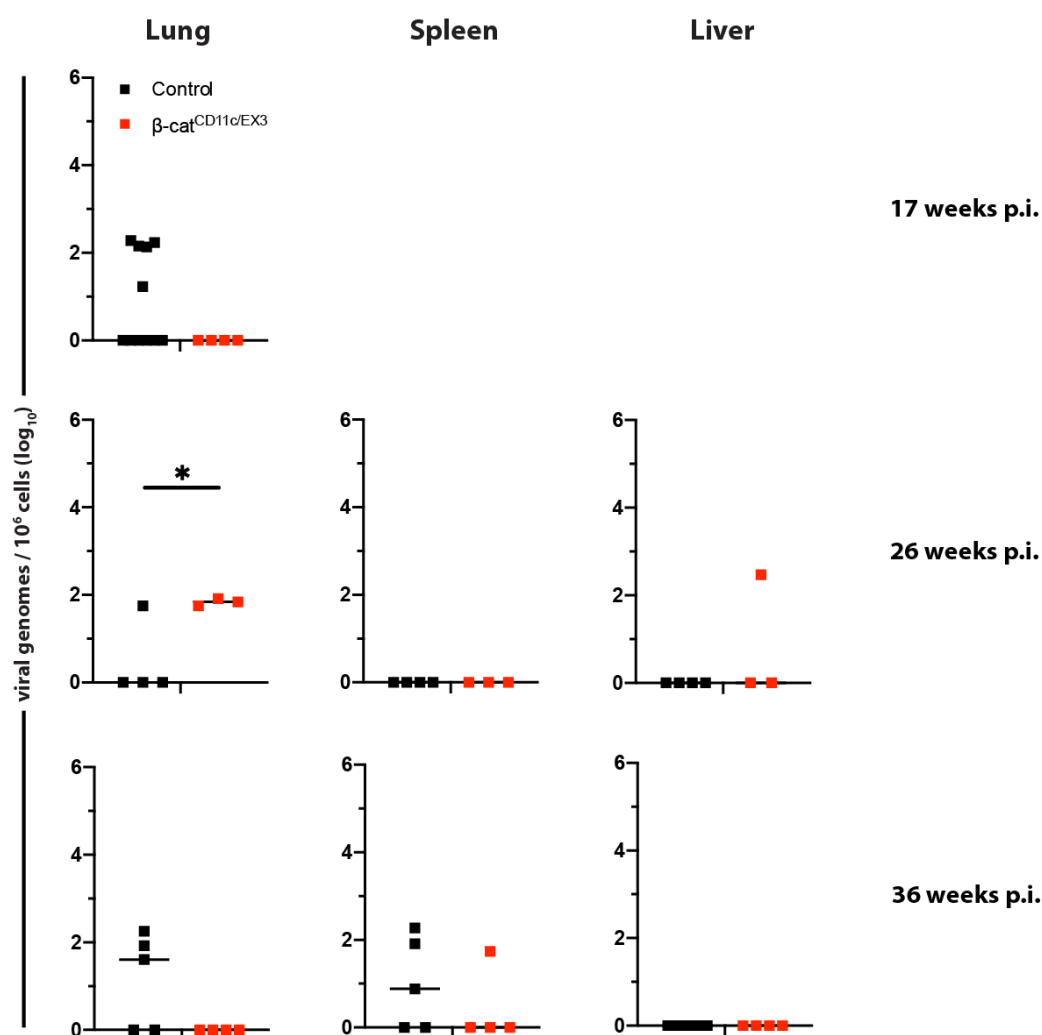


Figure 34: Viral genomes of latent mCMV infected β -cat $^{\Delta CD11c/EX3}$ mice.

From control (white) and β -cat $^{\Delta CD11c/EX3}$ (red) mice latent viral DNA load were determined for lung after 17, 26 and 36 weeks of infection. After 26 and 36 weeks of infection, viral loads were also determined in spleen and liver. The number of viral genomes was normalized to 1×10^6 (\log_{10}) cells. Each point represents the viral genomes of one individual mice. The black line represents the median. Data are representative of one experiment (n=3-11 after 17 weeks of infection; n=3-5 after 26 and 36 weeks of infection). Statistical significance is indicated as *p < 0.05, **p < 0.01 and ***p < 0.001.

In addition to the analysis of the virus-specific CD8⁺ T cell response, we studied the differentiation of CD4 and CD8 Treg in β -cat $^{\Delta CD11c/EX3}$ during latent infection. In lung, FoxP3⁺ CD4 Treg frequencies (**Fig. 35 A**) and absolute cell numbers (**Fig. 35 C**) were significantly increased during acute mCMV infection (**Fig. 21 A, B**) and also in non-infected (**Fig. S9**) β -cat $^{\Delta CD11c/EX3}$ mice.

After 17 weeks of infection, the frequency of FoxP3⁺ CD4 Treg was 12.1% ($p = 0.0002$) in β -cat^{CD11c/EX3} mice ($p = 0.0002$) and decreased to 10.2% after 26 weeks ($p = 0.0011$). Interestingly, they increased again to 12.7% ($p = 0.0438$) in the further infection time (**Fig. 35 A**). The absolute cell numbers of FoxP3⁺ CD4 Treg were comparable to the corresponding frequencies in β -cat^{CD11c/EX3} and control mice at the different infection time points, but after 36 weeks, the numbers were slightly lower in the β -cat^{CD11c/EX3} mice (**Fig. 35 C**). In addition, the CD11c⁺-specific stabilization of β -catenin demonstrated similar FoxP3 expression of CD4 Treg as compared to control mice and showed consistent levels during infection (**Fig. 35 B**). The discrimination of FoxP3⁺ CD4 Treg into tTreg and pTreg showed predominately Helios⁺ tTreg, but a comparison of β -cat^{CD11c/EX3} and control mice exhibited similar tTreg and pTreg (**Fig. 35 D**). Furthermore, it is noticeable that tTreg elevated from 68.8% to 79.3% in β -cat^{CD11c/EX3} mice during the course of infection, whereas pTreg decreased from 30.1% to 20.7%. Additionally, we explored the differentiation of FoxP3⁺ CD4 Treg in β -cat^{CD11c/EX3} mice in spleen and observed a substantial expansion after 17 and 26 weeks of infection (**Fig. 35**). After 17 weeks of infection, in β -cat^{CD11c/EX3} we measured 22.0% FoxP3⁺ CD4 Treg ($p = 0.0013$) and decreased minimal to 20.3% ($p = 0.0358$) after 26 weeks. In comparison to lung, these Treg did not expand after further infection time and were not increased in β -cat^{CD11c/EX3} mice ($p = 0.4919$) (**Fig. 35 E**). Furthermore, absolute cell numbers were similar in β -cat^{CD11c/EX3} and control mice at the different infection time points, except after 36 weeks, the numbers were slightly elevated in the control mice and therefore not significantly different could be detected (**Fig. 35 G**). As previously in the lung, comparable FoxP3 expression of CD4 Treg was detected in β -cat^{CD11c/EX3} and control mice (**Fig. 35 F**). In contrast to acute mCMV infection, we did not detect more tTreg in latent infected β -cat^{CD11c/EX3} mice despite significant increase in FoxP3⁺ CD4 Treg. During the infection time, tTreg increased from 75.4% to 81.2% in β -cat^{CD11c/EX3} mice, while pTreg fall down from 16.1% to 13.6% (**Fig. 33 H**), which we had already observed in lung (**Fig. 33 D**). In conclusion, the specific stabilization of β -catenin in DC leads to a strong expansion of FoxP3⁺ CD4 Treg in lung and spleen during latent mCMV infection.

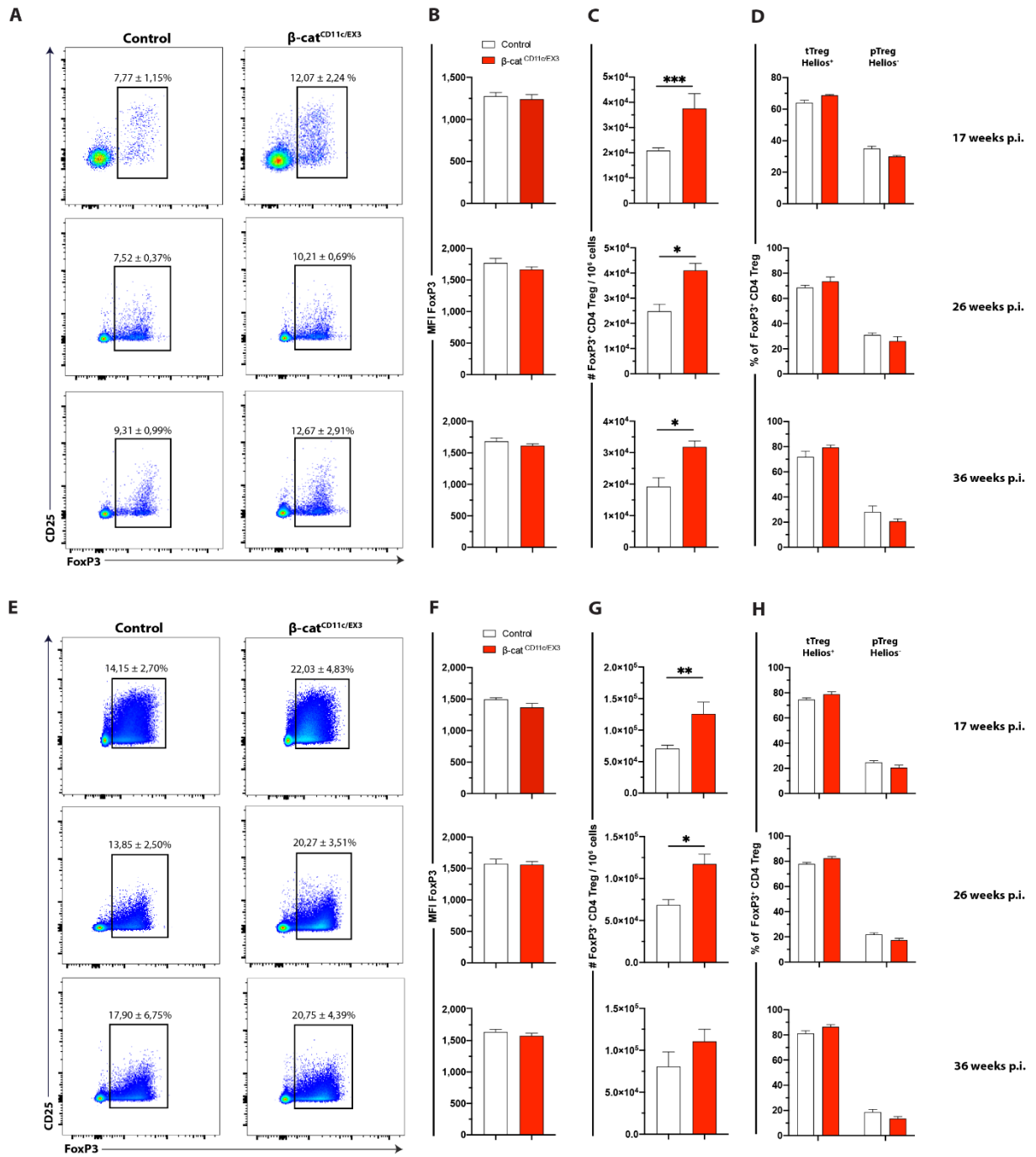


Figure 35: β -catenin signaling induces expansion of FoxP3⁺ CD4 Treg.

Control (white) and β -cat^{ΔCD11c/EX3} (red) mice were infected i.n. with 2×10^5 PFU of mCMV-Δm157 for 17, 26 and 36 weeks. **(A)** Frequencies (representative dot plots) of FoxP3⁺ CD4 Treg in lung of control versus β -cat^{ΔCD11c/EX3} mice (pregated on living TCR- β^+ CD4⁺ cells). **(B)** FoxP3 expression as measured by geometric MFI in CD4 Treg in lung of control and β -cat^{ΔCD11c/EX3} mice. **(C)** Absolute cell numbers (bar graphs) were normalized to 1×10^6 cells of FoxP3⁺ CD4 Treg in lung of control compared to β -cat^{ΔCD11c/EX3} mice. **(D)** Frequencies of CD4⁺ FoxP3⁺ Helios⁺ tTreg and Helios⁻ pTreg in lung of control and β -cat^{ΔCD11c/EX3} mice. **(E)** Representative flow cytometry plots showing frequencies of FoxP3⁺ CD4 Treg in spleen of control compared to β -cat^{ΔCD11c/EX3} mice. **(F)** FoxP3 expression in CD4 Treg of spleen of control and β -cat^{ΔCD11c/EX3} mice. **(G)** Absolute cell numbers of FoxP3⁺ CD4 Treg in spleen of control versus β -cat^{ΔCD11c/EX3} mice. **(H)** Frequencies of CD4⁺ FoxP3⁺ Helios⁺ tTreg and Helios⁻ pTreg in spleen of control and β -cat^{ΔCD11c/EX3} mice. Data are representative of one experiment (n=3-11). Statistical significance (unpaired Student's t test) is indicated as *p < 0.05, **p < 0.01 and ***p < 0.001. Values are the mean +SEM.

Next, we analyzed the CD8 Treg differentiation in β -cat^{CD11c/EX3} mice and observed that the stabilization of β -catenin neither affected CD8 Treg frequencies nor absolute cell numbers in lung. Throughout the course of infection, the frequencies of these CD8 Treg were less than 1% and slightly increased after 26 weeks of infection (**Fig. 36 A**). Consistent with the frequencies, we recognized low absolute cell numbers (**Fig. 36 B**). Both, 26 and 36 weeks of infection revealed only a trend for higher CD8 Treg numbers in β -cat^{CD11c/EX3} mice, but this was not significant. Furthermore, β -cat^{CD11c/EX3} mice displayed comparable amounts of Helios⁺ tTreg and Helios⁻ pTreg as compared to control mice. In comparison to CD4 Treg, we saw mainly Helios⁻ pTreg in lung (**Fig. 36 C**). Comparable to lung, the stabilization of β -catenin in spleen resulted in an unaltered CD8 Treg differentiation and only low percentages between 0.4% - 0.7% were measured in β -cat^{CD11c/EX3} and control mice (**Fig. 36 D**). At 36 weeks of infection, CD8 Treg appeared to increase slightly. In addition, the absolute cell numbers might be elevated in β -cat^{CD11c/EX3} mice, but a significant increase were not detectable (**Fig. 36 E**). As seen in **Figure 36 F**, predominantly pTreg (75.4% - 88.3%) were observed in latent infected β -cat^{CD11c/EX3} and control mice. Taken together, these results demonstrate that the CD11c⁺-specific stabilization of β -catenin might affect the CD8 Treg differentiation in β -cat^{CD11c/EX3} mice during latent mCMV infection.

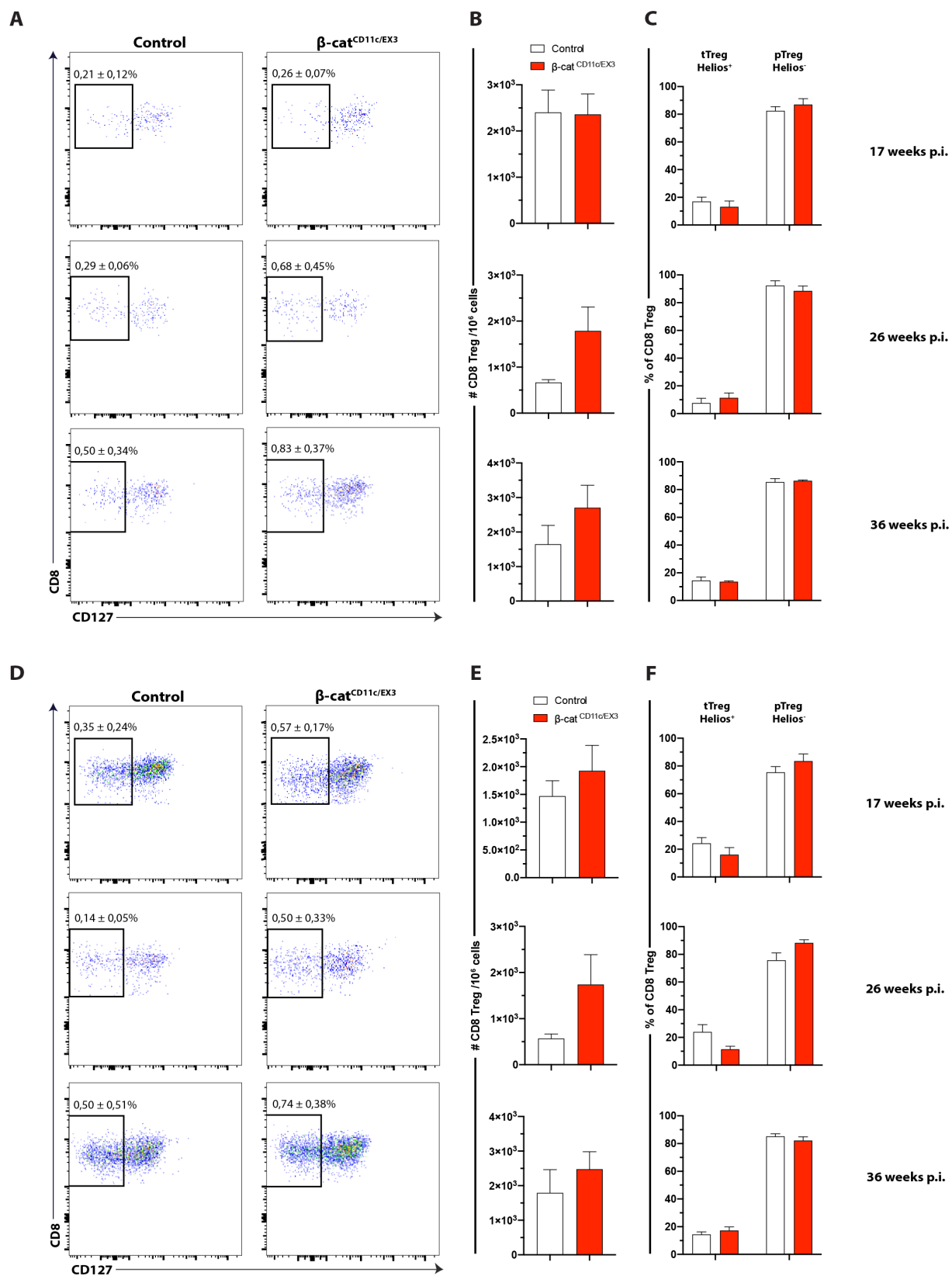


Figure 36: Latent mCMV infection shows no significant impact on CD8 Treg differentiation. Control (white) β -cat^{ΔCD11c/EX3} (red) mice were intranasal infected with 2×10^5 PFU of mCMV-Δm157 for 17, 26 and 36 weeks. (A) Frequencies (flow cytometry plots) and (B) absolute cell numbers (normalized to 1×10^6 cells) of CD122⁺ PD-1⁺ CD127⁻ CD8 Treg in lung of control and β -cat^{ΔCD11c/EX3} mice (pregated on living TCR- β ⁺ CD8⁺ cells). (C) Frequencies of CD8⁺ Helios⁺ tTreg or Helios⁻ pTreg in lung of control compared to β -cat^{ΔCD11c/EX3} mice. (D) Representative flow cytometry plots showing frequencies of CD122⁺ PD-1⁺ CD127⁻ CD8 Treg in spleen of control mice versus β -cat^{ΔCD11c/EX3} mice. (E) Absolute cell numbers of CD122⁺ PD-1⁺ CD127⁻ CD8 Treg in spleen of control versus β -cat^{ΔCD11c/EX3} mice. (F) Frequencies of CD8⁺ Helios⁺ tTreg or Helios⁻ pTreg of control compared to β -cat^{ΔCD11c/EX3} mice spleen. Data are representative of one experiment (n=3-11). Values are the mean \pm SEM (unpaired Student's t test).

Furthermore, we explored the role of β -catenin signaling on the DC compartment in latently infected mice and therefore analyzed the total and DC subsets after 17, 26 and 36 weeks of infection. The lung as main target organ of the i.n. infection remained unaffected by the stabilization of β -catenin and showed similar DC frequencies about 1% (**Fig. 37 A**) and absolute cell numbers (**Fig. 37 B**) during the different time points after infection. Further analysis of DC subsets revealed no significant difference between β -cat^{CD11c/EX3} and control mice after 17 and 26 weeks of infection (**Fig. 37 C**). However, we detected significantly lower frequencies of CD172 α ⁺ cDC2 in the lung after 36 weeks of infection ($p = 0.008$), but not for absolute cell numbers (data not shown). In addition to the lung, we analyzed the DC compartment of β -cat^{CD11c/EX3} in spleen during latency infection. In β -cat^{CD11c/EX3} mice, splenic DC frequencies (**Fig. 37 D**) and absolute cell numbers (**Fig. 37 E**) were significantly reduced in the same ratio during the latent infection. Already after 17 weeks of infection, only 1.0% DC ($p = 0.0052$) are still present in β -cat^{CD11c/EX3} mice and achieved percentages similar to those in lung (**Fig. 37 D**). Further discrimination of DC into XCR-1⁺ cDC1 and CD172 α ⁺ cDC2 revealed a shift toward increased XCR-1⁺ cDC1 and diminished CD172 α ⁺ cDC2 frequencies (**Fig. 37 F**) in β -cat^{CD11c/EX3} after 17 and 36 weeks of infection, which we had observed previously during acute mCMV infection (**Fig. 18**). In contrast, the infection after 26 weeks resulted in similar XCR-1⁺ cDC1 ($p = 0.630$) and CD172 α ⁺ cDC2 ($p = 0.255$) percentages (**Fig. 37 F**). However, it should be considered that the experiment was only performed once.

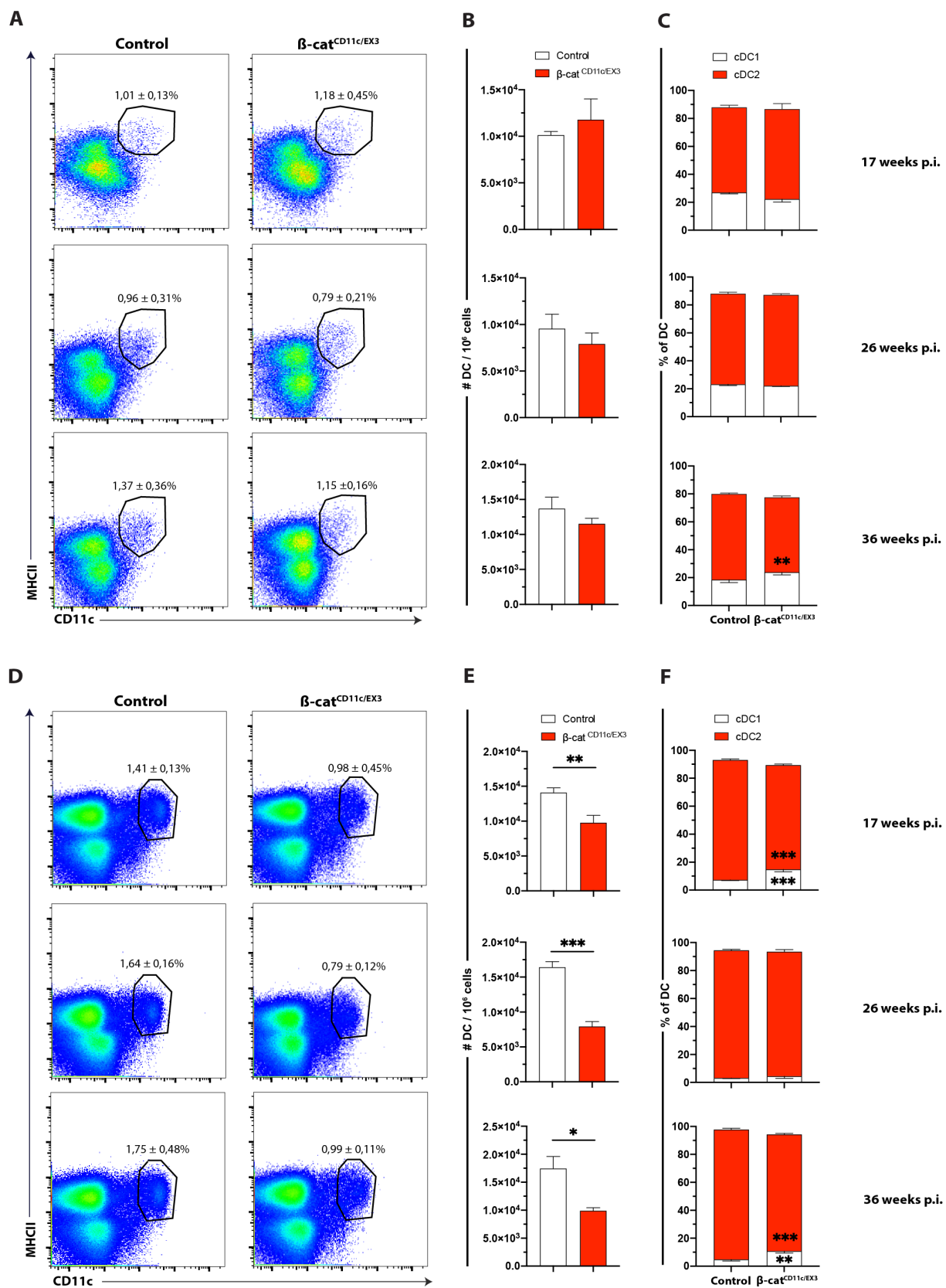


Figure 37: Latent infected β -cat ^{Δ CD11c/EX3} mice shows reduced DC accompanied by an increase of XCR-1⁺ cDC1 in spleen.

Control (white) and β -cat ^{Δ CD11c/EX3} (red) mice were infected i.n. with 2×10^5 PFU of mCMV- Δ m157 for 17, 26 and 36 weeks. (A) Representative flow cytometry plots with average frequencies of CD11c⁺ MHC-II⁺ DC in lung (pregated on living CD45⁺ F4/80⁻ cells) in control versus β -cat ^{Δ CD11c/EX3} mice. (B) Absolute cell numbers of DC (bar graphs) were normalized to 1×10^6 cells in lung of control compared to β -cat ^{Δ CD11c/EX3} mice. (C) Frequencies of XCR-1⁺ cDC1 and CD172 α ⁺ cDC2 in the lung of control versus β -cat ^{Δ CD11c/EX3} mice. (D) Frequencies of CD11c⁺ MHC-II⁺ DC in spleen of control and β -cat ^{Δ CD11c/EX3} mice. (E) Absolute cell numbers of DC in spleen of control compared to β -cat ^{Δ CD11c/EX3} mice. (F) Shown are frequencies of XCR-1⁺ cDC1 and CD172 α ⁺ cDC2 in the spleen of control versus to β -cat ^{Δ CD11c/EX3} mice. Data are representative of one experiment (n=3-11). Statistical significance (unpaired Student's t test) is indicated as *p < 0.05, **p < 0.01 and ***p < 0.001. Values are the mean +SEM.

Collectively, these results demonstrate that β -catenin signaling in spleen induces a reduction of DC and a shift toward elevated XCR-1⁺ cDC1 and reduced CD172 α ⁺ cDC2 in β -cat ^{Δ CD11c/EX3} mice after 17 and 36 weeks of mCMV infection, while the lung, as the main target organ of i.n. infection, appears mainly to be unaffected. Furthermore, the mCMV infections displays an increase of virus-specific memory cTEM and lower DPEC in lung and spleen after 17 weeks of infection, which is associated by elevated FoxP3⁺ CD4 Treg numbers. These data suggest an important role of β -catenin in DC for the induction of FoxP3⁺ CD4 Treg and possibly the CD8⁺ memory T cell response during mCMV infection.

4 Discussion and Outlook

During the early phase of CMV infection, DC are critical regulators of the anti-viral immune response by initiating the effector T cells and the induction of Treg. After primary infection, CMV establishes lifelong latency in specific cells of its natural host. However, the reactivation of latent CMV can lead to life-threatening complications in immunocompromised patients such as HCT recipients. The CD8⁺ T cells provide the main contribution to immune control of CMV infections and were initiated by DC. Moreover, DC play an important role in shaping the Teff response by affecting the differentiation of naïve T cells into Treg. Simultaneously, DC are also important targets for Treg-mediated suppression of immune responses, leading to downregulation of co-stimulatory molecules and pro-inflammatory cytokine production. Both IL-10 and β -catenin signaling in DC have been reported to play an important role in severe disease models. Hence, the aim of this work was to establish an i.n. infection model to analyze the impact of IL-10 and β -catenin signaling in DC on the virus-specific CD8⁺ T cell response and the Treg differentiation in blood, lung and lymphoid organs during acute and latent mCMV infection using IL-10^{ACD11c}, IL-10R^{ACD11c}, β -cat^{ACD11c} mice and β -cat^{CD11c/EX3} mice.

4.1 Intranasal infection route

At the beginning of this work we established an i.n. infection model to investigate the impact of IL-10 and β -catenin signaling in DC during acute and latent mCMV infection. The pathogenesis of mCMV infection is studied using different inoculation routes such as systemic infection by the intraperitoneal (i.p.) (Katzenstein et al., 1983; Munks et al., 2006) and intravenous (i.v.) route (Handke et al., 2013; Karrer et al., 2003), the i.n. route (Oduro et al., 2016; Zhang et al., 2019) or the infection via intraplantar (footpad) (Reddehase et al., 1984; Saederup et al., 2001; Sinickas et al., 1985) in adult mice. The i.n. route of entry has been suggested as a natural route of infection (Oduro et al., 2016). It is assumed that the infection after birth likely occurs via mucosal surfaces which are exposed to infectious secretions. The i.n. inoculation allows mCMV infection and dissemination throughout the body (Jordan, 1978; Oduro et al., 2016; Shanley and Pesanti, 1985). mCMV targets the olfactory epithelium in the nasal mucosa but not the respiratory epithelium (Farrell et al., 2016; Zhang et al., 2015). This might be explained by the presence of heparan sulfate, which is expressed apical and basolateral on the olfactory epithelium (Gillet et al., 2015). Both hCMV and mCMV infect cells by binding to heparan and thus allow the virus to enter the host (Price et al., 1995). The infection of the

olfactory epithelium through binding of heparan sulfate has been identified for murid herpesvirus-4 (MuHV-4) or herpes simplex virus 1 (HSV-1) (Milho et al., 2012; Shivkumar et al., 2013). The i.n. mCMV infection resulted in a sufficient infection of the nasal mucosa (Zhang et al., 2019). Lungs were reported as a primary target organ of i.n. infection and mCMV was detected after 48 h of inoculation (Jordan, 1978). Subsequently, mCMV disseminated via bloodstream to other organs such as spleen and SG. A study used reporter mutants of mCMV and identified transgenic virus in lungs of neonates (laryngopharyngeal infection) and adult mice (i.n. infection), which implies that the respiratory mucosa may serve as a major site of virus entry to the host (Stahl et al., 2013). Analysis of neonates and adult mice revealed delayed control of viral replication in neonatal lung characterized by a delayed expansion of neonatal CD8⁺ T cell clones. A subsequent study by this group showed that the viral protein Mck-2 determines viral pathogenicity in the lungs of laryngopharyngeal infected newborn mice (Stahl et al., 2015). The i.n. infection of adult BALB/c mice revealed a robust and long-termed viral replication in the lung during primary infection, with secondary dissemination to the SG (Oduro et al., 2016). Additionally, the infection induces a strong mCMV-specific CD8⁺ T cell response and underwent MI with similar kinetics after i.p. infection. In C57BL/6J mice T cells were primed in the mandibular, deep-cervical and mediastinal LN within 3 day of i.n. infection and also induced a MI (Zhang et al., 2019). Interestingly, only the i.n. infection, but not i.p. and footpad infection, displayed a prolonged viral replication in the lung. Collectively, these data imply that the i.n. infection reflects the natural entry of mCMV into the host and provides a robust model to study the short- and long-termed biology of mCMV infection.

In this work, we established the i.n. infection route in C57BL/6J wild type mice and determined the mCMV specific CD8⁺ T cell responses over 3 weeks. After 14 days of infection, we detected maximal M38-specific CD8⁺ T cell response in lung and spleen, whereas the M38-specific CD8⁺ T response in dLN increased until 21 days post infection (**Fig. 6**). On the other hand, the M45-specific CD8⁺ T cells showed a much weaker response and peaked after 7 days of infection in lung and spleen. Previous study showed comparable frequencies of M38-specific CD8⁺ T cells in lung and spleen to our results (Torti et al., 2011). However, the maximal M38-specific CD8⁺ T cell response peaked at 28 days, which may be due to of i.v. infection route. In accordance with our results, the M45-specific CD8⁺ T cell response peaked 7 days of infection and contracted thereafter in lung and spleen. In LN both M45-and M38-specific CD8⁺ T cells were present at much lower frequencies than in lung and spleen, as also shown by our data. Based on these results, we decided to investigate the influence of DC on the

M38-specific CD8⁺ T cell response in the context of the IL-10 and β -catenin signaling after 14 days of i.n. mCMV infection.

4.2 The role of IL-10 in DC during mCMV infection

4.2.1 IL-10 production during acute mCMV infection

During the early phase of viral infections, DC play a crucial role as they initiate the adaptive immune response through antigen-specific activation of naïve T cells (Steinman, 1991). After i.n. mCMV infection, lung DC migrate to the mediastinal lymph nodes (mLN), then entered the blood and reached the SG (Farrell et al., 2019). In the study by Farrell *et al.*, they demonstrated a virus-driven DC recirculation. Both, pDC and cDC subsets are activated through MyD88-dependent TLR-9 signaling after mCMV infection and produce IL-12 (Alexandre et al., 2014; Dalod et al., 2013). While pDC are not infected by mCMV *in vivo*, both cDC1 and cDC2 can be infected by mCMV (Dalod et al., 2013). In the literature the mCMV interactions with DC have been mainly focused on pDC. pDC are known as the main producers of IFN- α/β which limits mCMV replication during early stages of infection (Dalod et al., 2002). IFN- α/β regulates various DC responses, e.g. limiting the viral replication in all DC subsets or inhibiting IL-12 production especially in cDC2, which enhance their maturation (Dalod et al., 2003). In other systems, cDC2 have been reported to be efficient in CD4⁺ T cell priming (Pooley et al., 2001). Therefore, the IFN- α/β -mediated regulation of cDC2 could influence the CD4⁺ T cell responses during viral infections. Simultaneous, IFN- α/β promotes pDC accumulation and is required for the maturation of cDC1 *in vivo* (Dalod et al., 2003). This subset is preferentially infected by mCMV after 36-48 h of infection. However, after 18 h of infection, splenic cDC1 do not produce infectious virus in contrast to cDC2 (Busche et al., 2013). The expression of mCMV antigens is mainly restricted to cDC1 *in vivo* (Dalod et al., 2003). This subset of DC cross-presents exogenous antigens via MHC-I (Alexandre et al., 2014). Hence, cDC1 are most sufficient in the activation of mCMV-specific CD8⁺ T cells. In an asthma model with intratracheal mCMV infection, cDC1 and cDC2 were already activated in the airway mucosa one day post infection, which have been associated with a T_H2-driven response and antigen cross-presentation (Reuter et al., 2019). The activated cDC migrated into the draining LN and induces strong anti-viral CD8⁺ T cell response.

In the here presented work, we investigated DC and cDC subsets in the intermediate stage of mCMV infection around 14 days p.i.. Mice were i.n. infected with mCMV- Δ m157 preventing

the activation of NK cells by the Ly49H. Thus, the mCMV immune control was primarily mediated by CD8⁺ T cells and not by broad activation of NK cells (Bubic et al., 2004). After 14 days of infection, the CD11c⁺-specific deletion of IL-10^{ΔCD11c} and IL-10R^{ΔCD11c} mice did not impact the DC compartment in lung and lymphoid organs (**Fig. 7, 10**), although it has been proposed that IL-10 inhibits T cell responses by suppressing the function of APC and the expression of MHC-II and co-stimulatory molecules by APC (Moore et al., 1993; O'Garra et al., 2008). However, some reports showed contradictory functions for IL-10 upon viral infections. On the one hand, IL-10 limits the immunopathology during acute influenza and herpes simplex infection (Sarangi et al., 2008; Sun et al., 2009). On the other hand, excessive IL-10 production inhibits the pro-inflammatory response and results in prolonged viral replication during LCMV infection (Brooks et al., 2006). To explore the role of IL-10 production by DC and IL-10 signaling in DC after i.n. mCMV infection, DC should be investigated 1-2 days post infection in IL-10^{ΔCD11c} and the IL-10R^{ΔCD11c} mice. It will also be interesting to study whether IL-10 differentially affects the maturation status of cDC during mCMV infection. Previous *in vivo* studies showed the upregulation of MHC-I and co-stimulatory molecules such as CD40, CD80 and CD86 in DC during mCMV infections (Alexandre et al., 2014). To evaluate the potential role of DC and IL-10 for activation of mCMV-specific CD8⁺ T cells, their accessibility to viral antigens for MHC-I presentation should be investigated.

Additionally, we tested whether CD11c⁺-specific IL-10 production and IL-10R signaling influence the anti-viral CD8⁺ T cell response. For IL-10^{ΔCD11c} and IL-10R^{ΔCD11c} mice we hypothesized an enhanced mCMV-specific CD8⁺ T cells response. However, in both mouse lines the acute mCMV infection resulted in comparable M38-specific CD8⁺ T cell responses and did also not affect the M38-specific CD8⁺ T cell subpopulations (**Fig. 8, 12**). The lymphoid organs seemed to be poorly infected by mCMV after i.n. infection because the M38-specific CD8⁺ T cells responses were present at much lower frequencies compared to the lung. Similar to our result, the weak mCMV-specific CD8⁺ T cell response in dLN were also observed in i.n. infected BALB/c mice (Oduro et al., 2016). This tissue-specific pattern of the mCMV-specific CD8⁺ T cell response was also reported in C57BL/6 mice after i.p. infection (Torti et al., 2011). The second lymphoid organ, the spleen, showed three times less mCMV-specific CD8⁺ T cells than in the lung. The reduced mCMV-specific CD8⁺ T cell response in spleen were also detected in BALB/c mice (Oduro et al., 2016). As expected, the lung, as the main target organ of the i.n. infection route, revealed the highest M38-specific CD8⁺ T cell response 14 days p.i. (**Fig. 8 A, 12 A**). Despite the strong mCMV-specific CD8⁺ T cell response in lung, we detected

only low viral genome load (**Fig. 8 D, 12 D**). In Oduro *et al.* they detected already one day post infection virus in the lung of i.n. infected mice, which increased with the infection time (Oduro *et al.*, 2016). Fourteen days post infection, the viral loads in lung were significantly elevated compared with our genome load after i.n. infection. One possibility for the differences in viral genomes could be the use of different viruses. While, we used the mCMV- Δ m157 to avoid the influence of the NK cell response, the study by Oduro *et al.* infected their mice with bacterial-artificial chromosome (BAC)-derived mCMV-BAC^{WT} (Oduro *et al.*, 2016). Moreover, they investigated the i.n. infection in BALB/c mice, which might also be a reason for a different virus replication. Interestingly, it has been reported that the anesthesia affected the viral loads in lung (Oduro *et al.*, 2016). While the ketamine anesthesia resulted in high viral loads, the anesthesia with isoflurane were inefficient in the i.n. infection and viral loads were mainly under the detection limit 4 days post infection. Since our mice were anaesthetized with isoflurane, this could explain the lower levels of viral genomes present. Moreover, an efficient immune control of acute infection results in low latent viral load, while an inefficient immune control of acute infection reveals a high latent load (Jones *et al.*, 2010; Redeker *et al.*, 2014). The effective immune control in IL-10^{ACD11c} and IL-10R^{ACD11c} mice could be a plausible explanation for our low viral genomes during the acute phase of infection.

To clarify whether the lack of IL-10 and IL-10R expressing DC impairs the Treg differentiation, we analyzed CD4 and CD8 Treg in lung and lymphoid organs. Since we already observed no effect on the anti-viral CD8⁺ T cell responses, it was not surprising that Treg were also unaffected (**Fig. 9, 13**). On the other hand, FoxP3⁺ CD4 natural occurring Treg (tTreg) and FoxP3⁻ CD4 IL-10-induced Treg (pTreg) impaired the immune response to mCMV (Jost *et al.*, 2014). The depletion of FoxP3⁺ Treg from mCMV-infected mice displayed an enhanced T cell activation in lung and spleen at day 7 p.i., which was accompanied by reduced viral loads in SG. IL-10 has an important role during mCMV infection (Redpath *et al.*, 1999), but the cellular source of IL-10 has not been identified. Although Treg impair an effective immune response by secretion of IL-10 in various disease models (Betts *et al.*, 2012; Cabrera *et al.*, 2004; Punkosdy *et al.*, 2011), the Treg-specific IL-10 deletion in mice did not enhance the CD8⁺ T cell response to mCMV (Jost *et al.*, 2014).

Taken together, our results reveal that the deletion of IL-10 and IL-10R in DC does induce a stronger anti-viral immune response to mCMV because we observed neither an enhanced mCMV-specific CD8⁺ T cell response nor an impaired Treg induction. As IL-10 is also produced by other innate and adaptive immune cells such as macrophages, B cells and T cells, it is likely that the loss of IL-10 in DC is compensated by other cells in mCMV infected mice.

4.2.2 IL-10R signaling during latent mCMV infection

IL-10 is a potent inhibitor of the memory T cell inflation during mCMV infection (Jones et al., 2010). Ninety days post mCMV infection, the MI was dramatically amplified in IL-10^{-/-} mice and the mCMV-specific CD8⁺ T cells expressed higher levels of the anti-viral cytokines IFN- γ and TNF- α , which was associated with reduced latent viral genome load. Moreover, the blockade of IL-10R signaling using mAb resulted also in an increased memory CD8⁺ T cell expansion and reduced viral genome loads in IL-10^{-/-} mice. Surprisingly, our i.n. infected IL-10R^{ACD11c} mice showed no MI of M38-specific CD8⁺ T cells in blood, lung and lymphoid organs after 26 weeks and 36 weeks of infection (**Fig. 22 – 25**). However, it has been reported that the i.n. infection initiated a robust mCMV-specific CD8⁺ T cell response and underwent a MI (Oduro et al., 2016; Zhang et al., 2019). The MI of virus-specific CD8⁺ T cells was accompanied by an induction of a robust and long-termed viral replication in lung and SG upon i.n. infection. By contrast, both IL-10R^{ACD11c} and control mice revealed low viral genomes in lung, spleen and liver after 26 weeks of infection (**Fig. 26**). Over the course of infection, viral genomes decreased down to the detection limit in all tested organs. Compared to the literature, the i.n. infection led to high latent viral genomes in lung and spleen after 26 weeks of infection (Oduro et al., 2016). It has been shown that a low-dose mCMV infection resulted in a low viral genome load and severely impaired inflation of memory CD8⁺ T cells (Redeker et al., 2014), so the amount of the applicated virus appears to be an influence factor for the MI. Furthermore, the acute infection defines the load of latent viral genomes and risk to reactivate from latency (Reddehase et al., 1994). A robust virus replication in the acute infection promotes high latent viral load in the same organ (Bohm et al., 2009; Oduro et al., 2016). This was also shown by Redeker *et al.* where a large dose of mCMV infection resulted in higher latent viral load (Redeker et al., 2014). These results indicate that the dose of infection can modulates the viral load and has impact on the MI during viral latency. It is likely that the i.n. infection diminishes the antigen burden, resulting in reduced T cell priming and expansion. One reason for this could be that the infection does not break through the barrier tissue in the lungs and the administered virus is not inhaled deeply enough. Thus, the virus is partially washed away by nasal secretions or swallowed into the stomach. Collectively, the CD11c⁺-specific deletion of IL-10R displays no impact on the mCMV-specific CD8⁺ T cell response and does not undergo a MI, which is associated with low latent viral loads. However, it should be considered that the experiment was only performed once and a repetition of the experiment should be performed with a higher infectious dose. Moreover, it could be interesting to investigate the SG during latent infection

because it has been reports that the blockade of the IL-10R enabled a better control of mCMV in the SG (Humphreys et al., 2007).

4.3 The role of β -catenin in DC during mCMV infection

4.3.1 β -catenin signaling during acute mCMV infection

β -catenin signaling is involved in the DC maturation and promotes a tolerogenic DC phenotype (Jiang et al., 2007). The activation of β -catenin signaling in BMDC by cluster disruption of E-cadherin induced their phenotypic maturation. Matured DC upregulated MHC-II, co-stimulatory molecules and chemokine receptors. *In vitro*, these cluster disrupted BMDC induced IL-10 producing T cells and protected mice from EAE. Consistent with these findings, specific deletion of β -catenin in DC revealed a higher susceptibility to DSS-induced colitis and resulted in an increased T_H1/T_H17 differentiation accompanied by a reduced CD4 Treg response (Manicassamy et al., 2010; Suryawanshi et al., 2015). This led us to the hypothesis that the deletion in β -catenin in DC might enhance the CD8⁺ T cell response by interfering with Treg induction during acute mCMV infection. However, the i.n. infection in β -cat^{ACD11c} mice displayed comparable DC, mCMV-specific CD8⁺ T cells and Treg frequencies und numbers (**Fig. 14 - 17**) in all evaluated organs. Since we did not examine co-stimulatory molecules or chemokine receptors of DC, we cannot draw conclusions about a phenotypic maturation of DC in the mCMV infection model, which could be done in future studies in earlier stages of mCMV infection. The mCMV-specific CD8⁺ T cell response in β -cat^{ACD11c} mice appeared to be slightly higher than in control mice. It is likely that this response can be enhanced by a higher infection dose, as discussed previously (4.2.2). Therefore, it is possible that the infection dose also affects the CD8⁺ T cell response during acute infection, which could explain the low viral genomes in β -cat^{ACD11c} and control mice. Although the i.n. infection with 2×10^5 PFU of mCMV- Δ m157 induced a virus-specific CD8⁺ T cell response, the immune control of acute infection appeared to be effective and resulted in low viral loads (**Fig. 16 D**) compared to the literature (Oduro et al., 2016). By contrast, the deletion of β -catenin in DC had no impact on the severity of the collagen-induced arthritis (CIA) (Alves et al., 2015). However, in the absence of β -catenin the Treg frequencies were reduced in the CIA model, while we observed no reduction of Treg in β -cat^{ACD11c} mice during mCMV infection (**Fig. 17**). Furthermore, in mice with a CD11c⁺-specific deletion of β -catenin, stimulation of FoxP3⁺ CD4 Treg was observed only in

the intestine, whereas Treg and their cytokine production in spleen were not affected by the deletion of β -catenin (Manicassamy et al., 2010). Taken together, our data show no improved mCMV-specific CD8⁺ T cell response in β -cat^{ΔCD11c} mice after 14 days of infection. The reduction of Treg during inflammation as reported by Manicassamy *et al.* and Alves *et al.* could not be observed during acute mCMV infection. These results suggest that the deletion of β -catenin signaling in DC does not have an impact on the anti-viral immunity and thus does not enhance the immunopathology during mCMV infection.

Moreover, we examined whether and to what extent an enhanced β -catenin signaling in DC impairs the control of mCMV infection. Hence, we i.n. infected β -cat^{CD11c/EX3} mice that exhibit a stabilization of β -catenin in DC and analyzed them in comparison to control mice. After 14 days of mCMV infection, splenic DC were reduced in β -cat^{CD11c/EX3} compared to control mice associated with a shift toward increased XCR-1⁺ cDC1 and diminished CD172 α ⁺ cDC2 frequencies (**Fig. 18**). This finding is consistent with several studies that indicate a role for cDC1 in Ag cross-presentation and activation of virus-specific CD8⁺ T cells (Alexandre et al., 2014; Ohata et al., 2016). Since we observed elevated cDC1 in spleen but no enhanced CD8⁺ T cell response during acute mCMV infection, the Ag presentation by DC, in particular cross-presenting cDC1, should be investigated by measuring MHC-I and co-stimulatory molecules such as CD40 and CD86. It is likely that the unaltered virus-specific CD8⁺ T cell response is due to the lack of cross-presentation by cDC1 in mice with altered β -catenin signaling. This consideration is supported by previous studies where the genetic activation of β -catenin in DC or induced by tumors suppresses the CD8⁺ T cell response by inhibiting the cross-priming of cDC1 (Liang et al., 2014). The DC subsets, their maturation status and the cytokines appear to affect their capacity of cross-priming (Melief, 2008; Joffre et al., 2012; Wagner et al., 2012). Preliminary data of our lab showed that the stabilization of β -catenin in DC resulted in a spontaneous maturation of pulmonary DC during steady state, whereas splenic DC and BMDC were not affected by altered β -catenin signaling (unpublished data). The enhanced β -catenin signaling in DC attenuated the allergic asthma response by modulating DC maturation and lower levels of T_H2 cytokines. Based on these results, it could be useful to study the DC maturation at early stages of mCMV infection (1-2 days p.i.) characterized by co-stimulatory molecules such as CD40, CD80 and CD86, as well as chemokine receptor CCR7, to determine whether stabilized β -catenin affects DC maturation. As mentioned before, β -catenin in DC plays an important role in the regulation of the cytokine induction (Jiang et al.,

2007; Manicassamy et al., 2010). Future studies might therefore examine the DC cytokine profile of β -cat^{CD11c/EX3} mice in context of mCMV infection.

Interestingly, previous data of our group showed that alveolar macrophages (AM) were reduced in β -cat^{CD11c/EX3} mice in steady state (unpublished data). AM are known to play an important role for the protection against respiratory viral infections by the production of anti-viral cytokines, phagocytosis of virus and infected cells, and their wound-healing function in lung (Kumagai et al., 2007; Newton et al., 2016; Schneider et al., 2014). The activation of β -catenin inhibited AM proliferation but promoted their inflammatory activity (Zhu et al., 2021). During influenza A virus infection (IAV), AM inflammatory activity mediated by β -catenin promoted host morbidity. Already 1 day after i.n. mCMV infection, AM were infected by mCMV and they reduced the acute viral replication in the lung (Farrell et al., 2016). As a result, the impact of AM in β -cat^{CD11c/EX3} mice should be evaluated during mCMV infection.

As mentioned above, the mCMV-specific CD8⁺ T cell response resulted in similar frequencies and numbers in β -cat^{CD11c/EX3} and control mice in blood, lung, and lymphoid organs (**Fig. 19, 20**). In line with our findings, *Toxoplasma gondii* infection resulted in equivalent parasite-specific CD8⁺ T cell response in β -cat^{CD11c/EX3} compared to control mice, while the stabilization of β -catenin affected CD4 and NK cell IFN- γ response (Cohen et al., 2015). By contrast, vaccinia virus infection (VACV) revealed an increase of virus-specific CD8⁺ T cells in β -cat^{CD11c/EX3} mice. A re-stimulation of splenocytes with viral peptides displayed elevated IFN- γ CD8⁺ T cells. These results displayed that CD11c⁺-specific stabilization of β -catenin impact the development of virus-specific CD8⁺ T cells. However, the altered β -catenin signaling in DC did not affect the CD8⁺ T cell response in β -cat^{CD11c/EX3} mice and was accompanied by low viral genome loads during acute mCMV infection (**Fig. 19, 20**). The further fractionation of mCMV-specific CD8⁺ T cells showed mainly iTEM and DPEC cells in blood, lung and spleen, whereas in dLN DPEC and cTEM were the dominating subpopulations. A comparison of mCMV-specific CD8⁺ T cells in intraplantar infected BALB/c mice revealed similar distribution of the subpopulations after one week of mCMV infection (Holtappels et al., 2020). In both spleen and lung, iTEM and DPEC dominated over cTEM, TCM and EEC subpopulations. In addition, this distribution of subpopulations was also observed in i.n. infected mice in blood (Oduro et al., 2016; Zhang et al., 2019) and spleen (Oduro et al., 2016) after 2 weeks of infection. In contrast to our data, the non-draining LN and dLN revealed a TCM phenotype (Oduro et al., 2016). However, our data should be interpreted with caution because the characterization of subpopulations in dLN is based on very low frequencies of total M38 Tetramer⁺ CD8⁺ T cell response. To investigate these subpopulations in dLN, in future

analyses mice numbers should be enhanced and isolated cells should be pooled to increase cell numbers. Interestingly, comparison of β -cat^{CD11c/EX3} with control mice of the virus-specific CD8⁺ T cell subpopulations displayed a modified distribution of pulmonary CD8⁺ T cell subpopulations. While iT_{EM} decreased in β -cat^{CD11c/EX3} mice, cT_{EM} were elevated after 14 days of infection. These data suggest that altered β -catenin signaling in DC might affect the induction of CD8⁺ memory T cells.

Next, we analyzed the differentiation of CD4 and CD8 Treg in β -cat^{CD11c/EX3} mice after acute mCMV infection because previous studies indicated that Treg impair the mCMV immunity (Li et al., 2014; Lindenberg et al., 2014; Mayer et al., 2012; Pomie et al., 2008). *In vitro*, Treg suppress the function of mCMV-specific CD8⁺ T cells through the secretion of TGF- β (Li et al., 2010). During acute mCMV infection, Treg depletion displayed an enhanced mCMV-specific CD8⁺ T cell response and reduced viral loads *in vivo* (Jost et al., 2014). Based on these findings, we hypothesized that the stabilization of β -catenin might promote Treg induction and thus suppresses virus-specific CD8⁺ T cell response in mCMV infection. After the acute infection, we discovered an increase of FoxP3⁺ CD4 Treg in lung and lymphoid organs of β -cat^{CD11c/EX3} mice (**Fig. 21 A - D**). The expansion of FoxP3⁺ CD4 Treg was due to higher Helios⁺ CD4 tTreg. However, this FoxP3⁺ CD4 Treg expansion in β -cat^{CD11c/EX3} mice were not only elevated after mCMV infection but already visible in steady state (**Fig. S9**). In lung and lymphoid organs, β -cat^{CD11c/EX3} mice revealed elevated FoxP3⁺ CD4 Treg frequencies, which was also caused by a strong expansion of tTreg. A study by Ding *et al.* already reported that β -catenin prolongs the survival of Treg and induced anergy in non-regulatory CD4⁺ T cells (Ding et al., 2008). These findings might explain in part that FoxP3⁺ CD4 Treg were elevated in our β -cat^{CD11c/EX3} mice but did not impair the mCMV-specific CD8⁺ T cell response. In contrast to CD4 Treg, the function and phenotype of CD8 Treg is still controversial and there are few data available about their suppressive function. The secretion of IL-10 by CD8 Treg is described as the main suppressive mechanism (Dai et al., 2010; Endharti et al., 2005; Li et al., 2014; Rifa'i et al., 2008). CD8 Treg showed the ability to suppress the IFN- γ production by CD8⁺ T cells through the production of IL-10 *in vitro* (Endharti et al., 2005). However, in β -cat^{CD11c/EX3} and control mice CD8 Treg resulted in low frequencies of less than 1% in all analyzed organs (**Fig. 21 E - G**). These findings indicate that CD8 Treg do not appear to impair the mCMV immune response and show no suppressive function of the mCMV-specific CD8⁺ T cell response. Both CD4 and CD8 Treg do not use a single suppressive mechanism, but rather an arsenal of different mechanisms (Schmidt et al., 2012; Shevach 2009; Vieyra-Lobato et al., 2018). Up to now, it is unclear when Treg use the different mechanisms and

whether Treg switch from one to another mechanism or use multiple mechanisms simultaneously (Schmidt et al., 2012). In addition, different CD8 Treg subgroups exist and further research is needed to clarify the subgroup and function of the CD8 Treg and which mechanisms are responsible for Treg-mediated suppression. To examine whether the stabilization of β -catenin in DC and/or the mCMV infection influences the function of FoxP3⁺ CD4 and CD8 Treg, future studies should examine their suppressive potential *in vitro* using a Treg suppression assay in β -cat^{CD11c/EX3} compared to control mice and during steady state compared to mCMV infection. To clarify which mechanisms are responsible for the suppressive effect of Treg, cytokine secretion from supernatants of suppression assay cultures should be determine in future experiments.

In conclusion, our data demonstrate that CD11c⁺-specific stabilization of β -catenin results in unaltered immune control of mCMV infection, but exhibits a shift in mCMV-specific CD8⁺ T cell subpopulations toward reduced iT_H17 and elevated cT_H17. It might be possible that β -catenin signaling elicits an earlier memory T cell induction and contributes to viral latency and reactivation. Although cross-presenting XCR-1⁺ cDC1 are reduced in spleen of β -cat^{CD11c/EX3} mice, the unaffected CD8⁺ T cell response against mCMV may be due to the fact that β -catenin in DC inhibits the cross-priming of cDC1 (Liang et al., 2014). On one side, enhanced β -catenin signaling in DC are useful to control inflammatory and autoimmune disease (Jiang et al., 2007; Manicassamy et al., 2010). On the other side, the stabilization of β -catenin in DC resulted in an increased pro-inflammatory response in context of viral infections (Cohen et al., 2015). It is therefore appropriate to examine the cytokine profile to identify the T helper cell response and their activation status during mCMV infection. The expansion of FoxP3⁺ CD4 Treg numbers is observed after mCMV infection and during steady state. Future studies would be useful to study their suppressive capacity in context of mCMV infection.

4.3.2 β -catenin signaling during latent mCMV infection

The acute mCMV infection in β -cat^{CD11c/EX3} mice displayed a shift in pulmonary mCMV-specific memory T cell formation and increased FoxP3⁺ CD4 Treg. Hence, we investigated the impact of β -catenin signaling in DC during mCMV latency in β -cat^{CD11c/EX3} mice. Surprisingly, the M38-specific CD8⁺ T cells did not show MI after i.n. infection (**Fig. 30 - 33**). As previously described in detail (4.2.2), several studies showed that mCMV-specific CD8⁺ T cells underwent MI after i.n. infection and resulted in an induction of

a robust and long-termed viral replication in lung and SG (Oduro et al., 2016; Zhang et al., 2019), while only low levels of viral genomes were detectable or not measurable in the investigated organs of β -cat^{CD11c/EX3} and control mice (**Fig. 34**). Markedly more viral genomes were detected in the lung of latent infected mice after intraplantar infection, suggesting that the mCMV genomes may be dependent on the route of infection (Griessl et al., 2021). Moreover, the TCR avidity is a factor that influences the CD8⁺ T cell inflation during mCMV infection (Baumann et al., 2019). High avidity interactions play an important role by the recognition of mCMV-infected cells as the virus expresses immune evasion molecules, also known as vRAP (Bohm et al., 2009; Reddehase, 2002). These molecules affect the MHC-I surface expression, resulting in reduced numbers of MHC-I molecules available for recognition by T cells (Holtappels et al., 2006). CD8⁺ T cells with a high avidity are more likely to become activated and produce IFN- γ even if low numbers of MHC-I complexes are present. Specifically, the amount of cTEM and TCM were a determining factor for the overall magnitude of the inflationary T cell pool (Baumann et al., 2019; Holtappels et al., 20220; Sydner at al., 2008; Welten et al., 2020). The avidity maturation is not only addressed to the pool of iTEM, but also to the pools of cTEM and TCM (Holtappels et al., 2020). The fractionation of the M38-specific CD8⁺ T cells in β -cat^{CD11c/EX3} mice revealed that the CD8⁺ T cell pool is predominantly composed by iTEM and DPEC in lung (**Fig. 31 C**). These two subpopulations and also the cTEM continuously decreased during viral latency, whereas the central memory pool expanded. Intraplantar infection also resulted in a reduction of iTEM and expansion of TCM in lung (Holtappels et al., 2020). The cTEM showed a similar kinetic like TCM and expanded during latency. In parallel, the virus-specific CD8⁺ T cell subpopulations were also examined in spleen (**Fig. 33**). In β -cat^{CD11c/EX3} and control mice, iTEM decreased upon 26 weeks post infection and then expanded again. The TCM and cTEM subpopulation showed an opposite effect to iTEM and increased after 26 weeks of infection followed by a decrease. In contrast to control mice, the cTEM in β -cat^{CD11c/EX3} mice did not increase during the course of infection and showed a continuously decrease. Other analysis of mCMV-specific CD8⁺ T cells showed an EM phenotype in blood (Oduro et al., 2016; Zhang et al., 2019) and spleen upon i.n. infection (Oduro et al., 2016). These results are in line with our data and we mainly observed iTEM and cTEM (**Fig. 30, 32**). An intraplantar infection revealed the same trend of decreased iTEM and increasing frequencies of cTEM and TCM in spleen, which was associated with a avidity maturation in lung and spleen (Holtappels et al., 2020). The MI based primarily on the expansion of high avidity memory T cells, and unexpectedly a loss of high avidity cells could be detected after 70 weeks of infection. Moreover, the comparison of β -cat^{CD11c/EX3} and control

mice showed a significant increase of cTEM and a reduction of DPEC in lung and spleen of mice with stabilized β -catenin (**Fig. 31, 33**). It might be possible that the stabilization of β -catenin resulted in multiple rounds of re-stimulation of TCM to generate cTEM and then iTEM. Based on these findings, the latent i.n. infection in β -cat^{CD11c/EX3} mice should be repeated with a higher infection dose to induce a MI of virus-specific CD8⁺ T cells and investigate the avidity of the CD8⁺ T cell pool by determining the IFN- γ secretion after stimulation with peptides.

Furthermore, we examined the FoxP3⁺ CD4 Treg in i.n. infected in β -cat^{CD11c/EX3} to determine the impact of the stabilization of β -catenin in DC during latent mCMV infection. In lung and spleen, FoxP3⁺ CD4 Treg were increased in mice with enhanced β -catenin signaling, which was due to higher Helios⁺ CD4 tTreg (**Fig. 35**). FoxP3⁺ CD4 Treg in β -cat^{CD11c/EX3} mice were also elevated after acute mCMV infection (**Fig. 21 A, C**) and already during steady state (**Fig. S9**). Comparison of FoxP3⁺ CD4 Treg in acute and latency infection revealed increased Treg frequencies during the course of infection. A study by Almanan *et al.* confirmed that FoxP3⁺ CD4 Treg increased during mCMV latency (Almanan *et al.*, 2017). The depletion of Treg induced an increase of functional mCMV-specific CD8⁺ T cells and reduced the viral reactivation in spleen, which was accompanied by elevated levels of TNF- α and IFN- γ . Therefore, Treg promote viral persistence and suppressed mCMV-specific CD8⁺ T cell response in spleen, while in the SG the Treg prevent the IL-10 production and limit viral replication and reactivation. However, the ablation of FoxP3⁺ CD4 Treg does not influence numbers of mCMV-specific CD8⁺ T cell in SG, whereas the mCMV-specific CD4⁺ T cell response were increased. These data show that Treg suppress CD4⁺ but not CD8⁺ T cells in SG during latent mCMV infection. It might be possible that the elevated FoxP3⁺ CD4 Treg do not suppress the CD8⁺ T cell response in β -cat^{CD11c/EX3} mice or they do not have a suppressive function during latent infection. Based on these findings, further studies should investigate the mCMV-specific CD4⁺ T cell response and the suppressive capacity of FoxP3⁺ CD4 Treg as well as cytokine levels in β -cat^{CD11c/EX3} mice. However, it should be considered that the study by Almanan *et al.* used the i.p. infection with 5-fold higher higher dose of mCMV K181 strain. The i.p. inoculation introduces virus systemically and the inflammatory populations were increased in comparison to i.n. infection (Oduro *et al.*, 2016). Hence, the infection route of mCMV appears to be an important factor and could affect the mCMV-specific CD8⁺ T cell response or Treg.

Surprisingly, we observed reduced DC numbers in spleen of β -cat^{CD11c/EX3} mice after 17 and 36 weeks of infection (**Fig. 37**). As in the acute infection (**Fig. 18 C**), the latently infected mice

revealed a shift toward increased XCR-1⁺ cDC1 and diminished CD172α⁺ cDC2 frequencies. The acute phase of infection is driven by the priming of mCMV-specific CD8⁺ T cells response which relies on the cross-presentation of DC (Snyder et al., 2010; Torti et al., 2011), whereas the accumulation of CD8⁺ T cells during latency is DC-independent and occurs even in the absence of cross-presenting DC (Torti et al., 2011). These results indicate that the MI requires different antigen presentation. During latency MI is dependent of the antigen presentation by non-hematopoietic cells (Seckert et al., 2011; Torti et al., 2011). A minimal cross-presentation of DC could partially explain the observation (**Fig. 37**), but is a disagreement with previous results. However, it should be considered that the experiment was only performed once. More biological replicates might shed light on the remaining questions.

Taken together, these data demonstrate that the stabilization of β-catenin in DC enhances the FoxP3⁺ CD4⁺ Treg in latently infected β-cat^{CD11c/EX3} mice but does not affect the mCMV-specific CD8⁺ T cell response or viral genome load, and hence not the viral immune response. In addition, the mCMV-specific CD8⁺ T cells showed no MI after i.n. infection. For a better understanding of β-catenin signaling in DC, the i.n. infection should be tested with a higher infection dose or a different infection route, in particular i.p. infection, to induce a MI of mCMV-specific CD8⁺ T cells. Moreover, it would be necessary to investigate the suppressive capacity of FoxP3⁺ CD4⁺ Treg and analyze their cytokine levels. Although we observed an increase of cTEM and a reduction of DPEC in lung and spleen of β-cat^{CD11c/EX3} mice, we cannot draw a conclusion about their function since various factors such as infection dose, the suppressive function of Treg, or the inhibitory function of β-catenin on the cross-presentation of cDC1 are still not clear.

5 Supplement

The following figures show the flow cytometric gating strategies used in this thesis with cells isolated from i.n. mCMV infected mice.

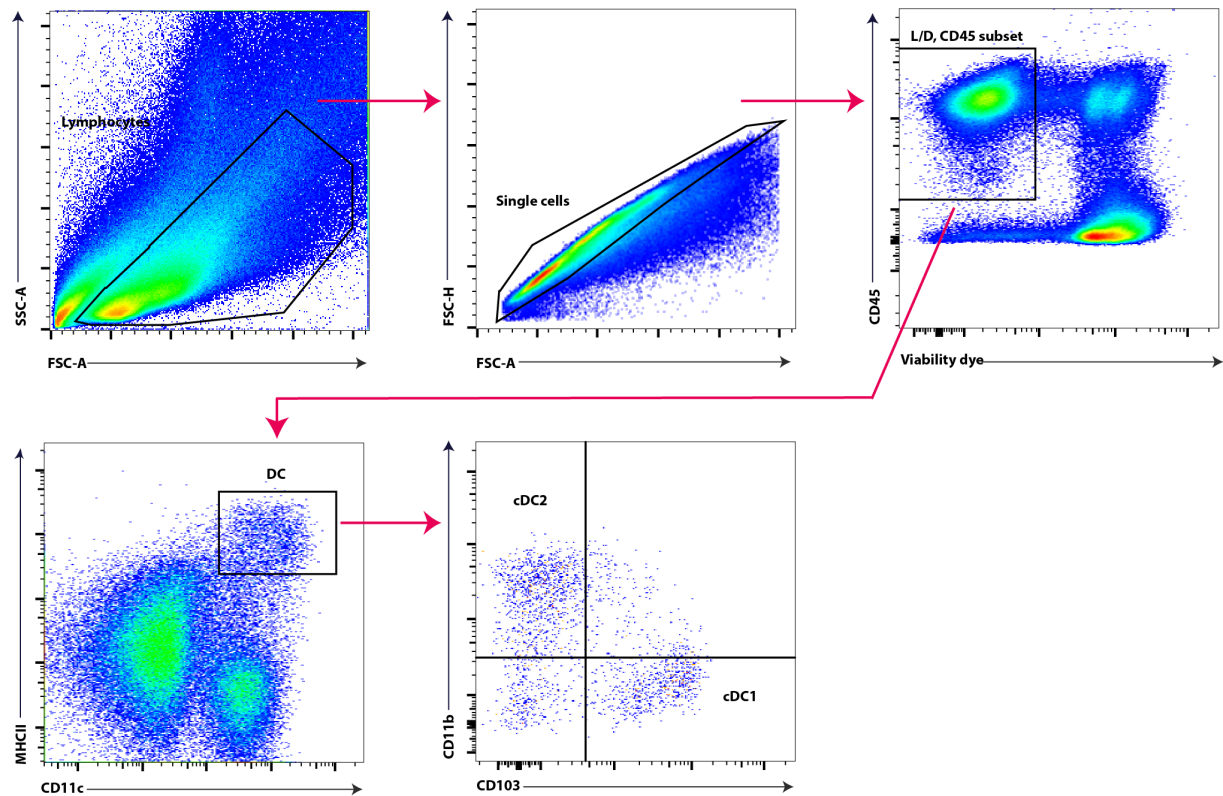


Figure S1: First flow cytometric gating strategy of DC in the lung.

Lung cells analyzed with specific DC markers. All cells were gated by forward (FSC-A) against sideward scatter (SSC-A). Single cells were gated with FSC-A against FSC-H. Living leukocytes were identified with viability dye and CD45 marker. DC were characterized with high expression of CD11c and MHC-II. cDC in lung were identified by the expression of CD103 and CD11b.

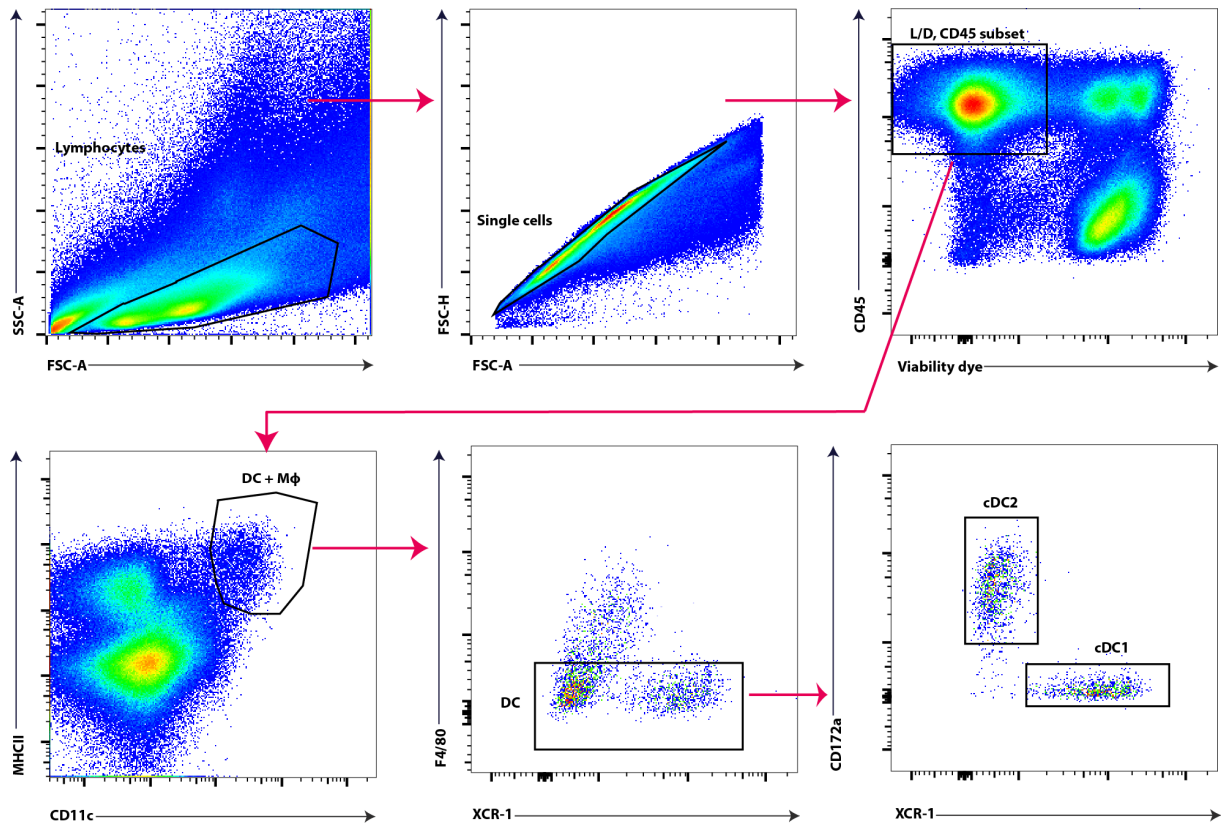


Figure S2: Second flow cytometric gating strategy of DC in the lung.

Lung cells were isolated and analyzed with specific DC markers. All cells were gated by forward (FSC-A) against sideward scatter (SSC-A). Single cells were gated with FSC-A against FSC-H. Living leukocytes were identified with viability dye and CD45 marker. DC were identified with high expression of CD11c and MHC-II, and were F4/80^{low} cells. cDC in lung were further characterized by the expression of XCR-1 and CD172 α .

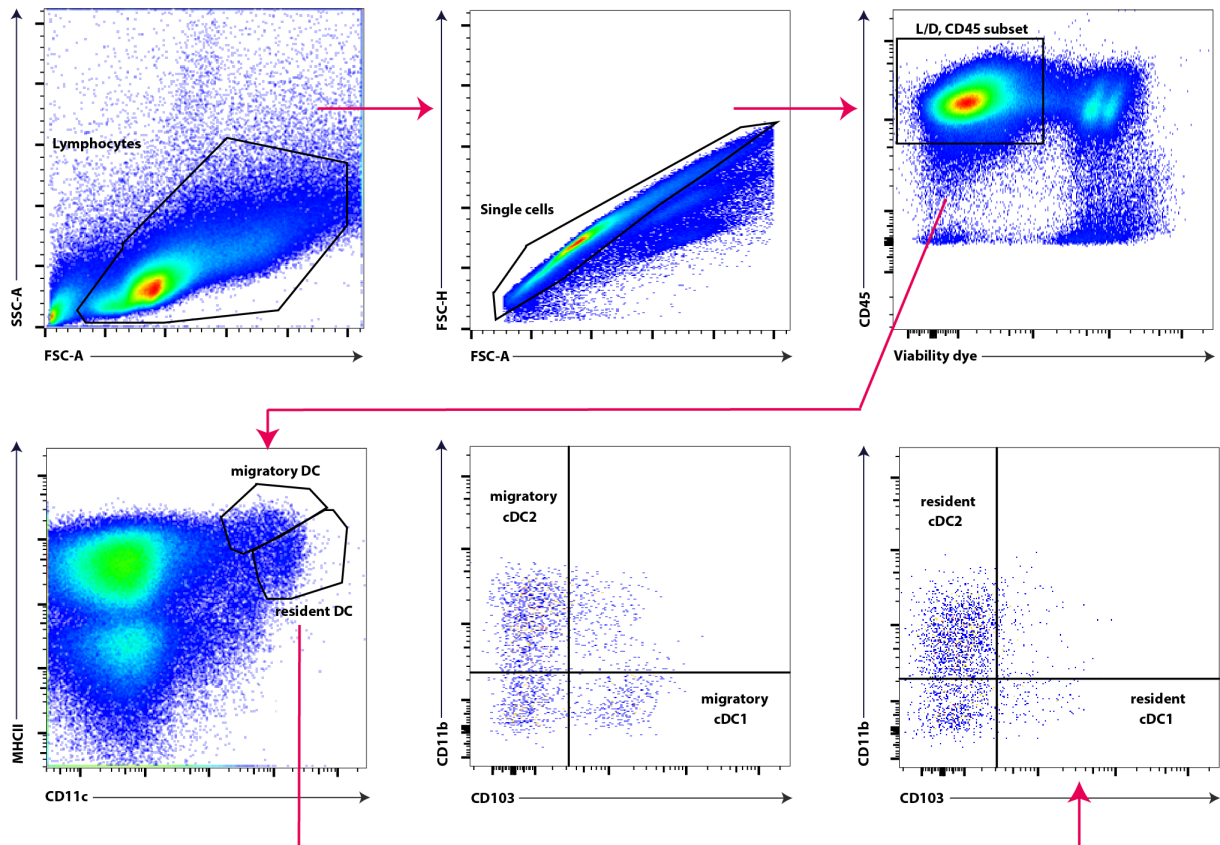


Figure S3: First flow cytometric gating strategy of DC in the dLN.

dLN were analyzed by specific DC markers. All cells were gated by forward (FSC-A) against sideward scatter (SSC-A). Single cells were gated with FSC-A against FSC-H. Living leukocytes were identified with viability dye and CD45 marker. DC were characterized with high expression of CD11c and MHC-II. cDC in dLN were further characterized by the expression of CD103 and CD11b.

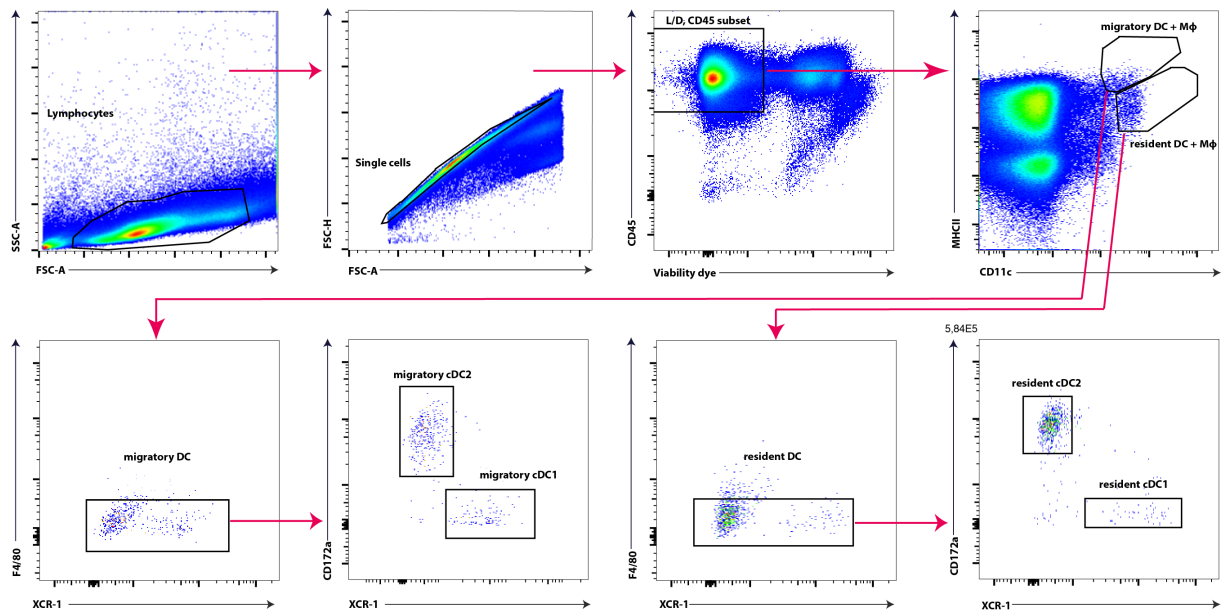


Figure S4: Second flow cytometric gating strategy of DC in the dLN.

dLN were analyzed by specific DC markers. All cells were gated by forward (FSC-A) against sideward scatter (SSC-A). Single cells were gated with FSC-A against FSC-H. Living leukocytes were identified with viability dye and CD45 marker. DC and M Φ were characterized with high expression of CD11c and MHC-II. Then macrophages were excluded by F4/80. cDC in dLN were further characterized by the expression of XCR-1 and CD172 α .

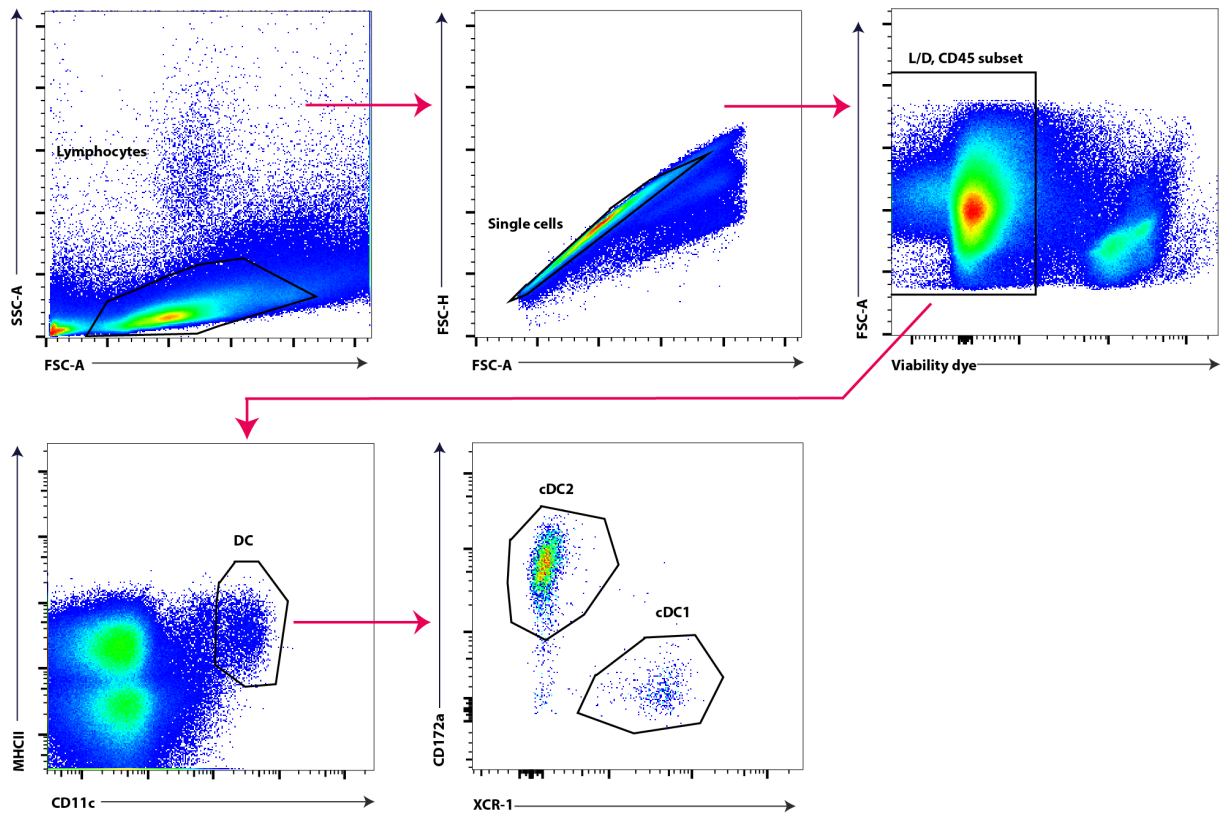


Figure S5: Flow cytometric gating strategy of DC in the spleen.

Spleen were analyzed by specific DC markers. All cells were gated by forward (FSC-A) against sideward scatter (SSC-A). Single cells were gated with FSC-A against FSC-H. Living leukocytes were identified with viability dye. DC were characterized with high expression of CD11c and MHC-II. cDC were identified by the expression of XCR-1 and CD172 α .

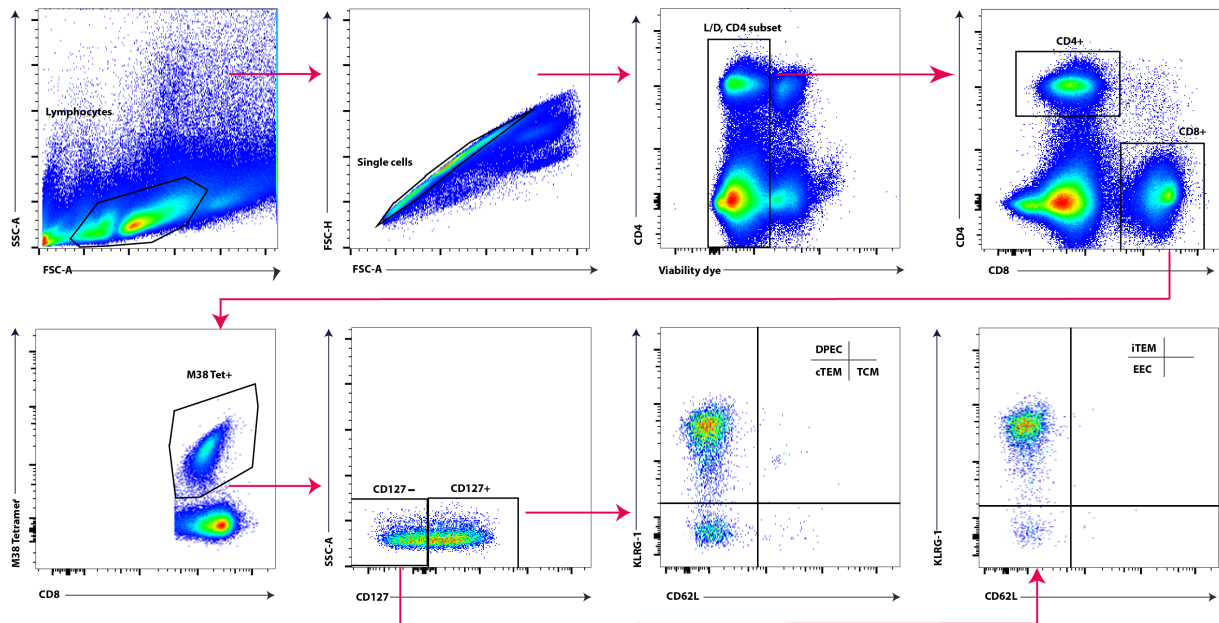


Figure S6: Flow cytometric gating strategy of M38 Tetramer⁺ CD8⁺ T cells and subsets in the lung, spleen, dLN and blood.

Organs and blood were analyzed by specific T cell markers. All cells were gated by forward (FSC-A) against sideward scatter (SSC-A). Single cells were gated with FSC-A against FSC-H. Living leukocytes were identified with viability dye and then CD4⁺ and CD8⁺ cells were distinguished. Next, virus-specific CD8⁺ T cells were identified by the M38 Tetramer and further differentiated in CD127⁻ KLRG-1⁺ CD62L⁻ iTEM, CD127⁺ KLRG-1⁺ CD62L⁻ DPEC, CD127⁻ KLRG-1⁻ CD62L⁻ EEC, CD127⁺ KLRG-1⁻ CD62L⁻ cTEM and CD127⁺ KLRG-1⁻ CD62L⁺ TCM.

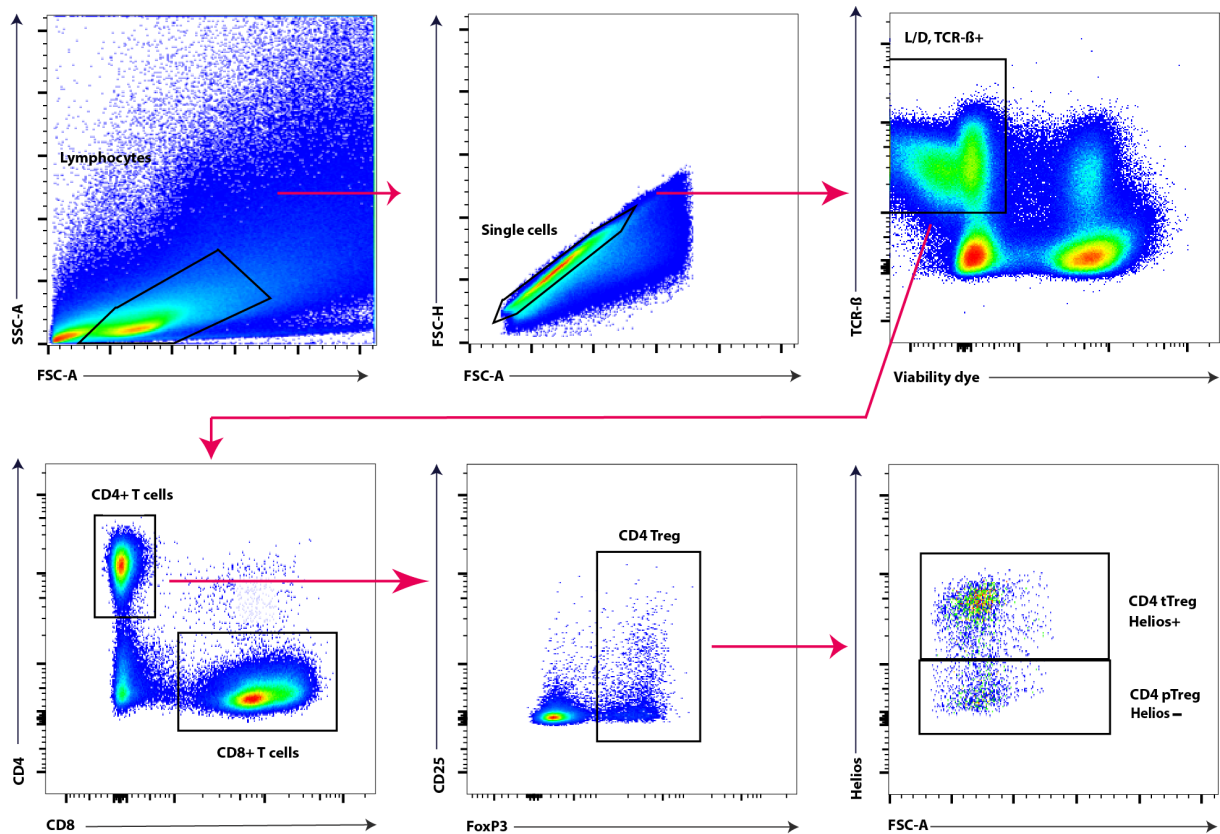


Figure S7: Flow cytometric gating strategy of CD4 Treg in the lung, spleen and dLN.

Organs were analyzed by specific T cell markers. All cells were gated by forward (FSC-A) against sideward scatter (SSC-A). Single cells were gated with FSC-A against FSC-H. Living leukocytes were identified with viability dye against TCR- β and distinguished between CD4⁺ and CD8⁺ T cells. With the use of FoxP3, CD4 Treg can be identified and further characterized by Helios in tTreg and pTreg.

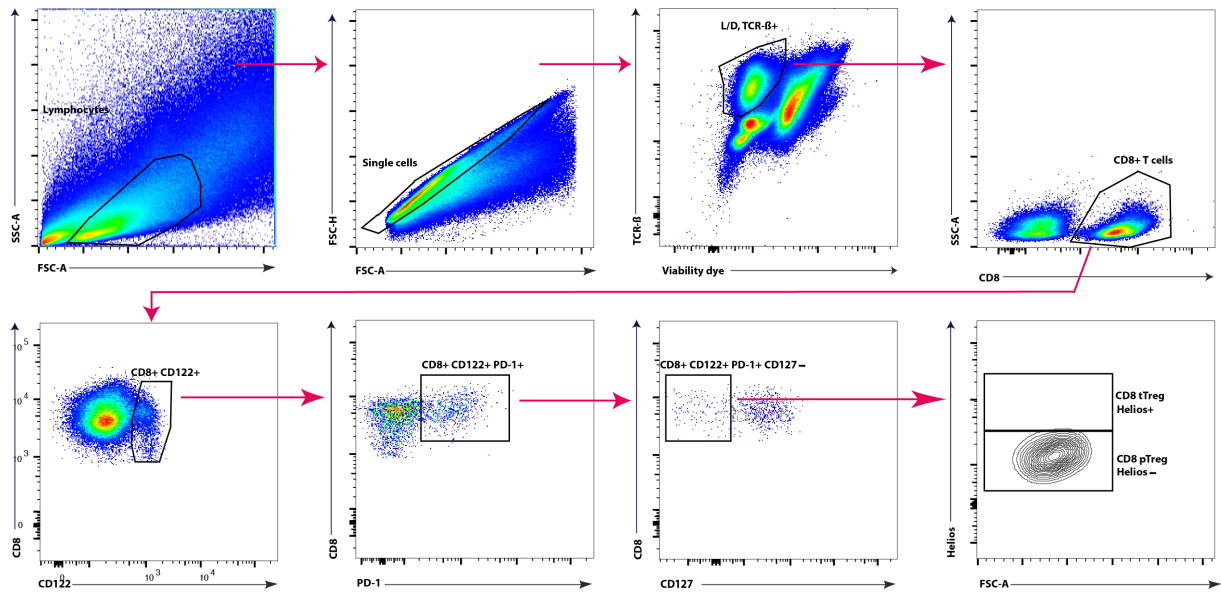


Figure S8: Flow cytometric gating strategy of CD8 Treg in the lung, spleen and dLN.

Organs were analyzed by specific T cell markers. All cells were gated by forward (FSC-A) against sideward scatter (SSC-A). Single cells were gated with FSC-A against FSC-H. Living leukocytes were identified with viability dye against TCR- β and distinguished between CD4⁺ and CD8⁺ T cells. The CD8 Treg were characterized by CD122⁺ PD-1⁺ and CD127 markers. Next, CD8 Treg were further characterized by Helios in tTreg and pTreg.

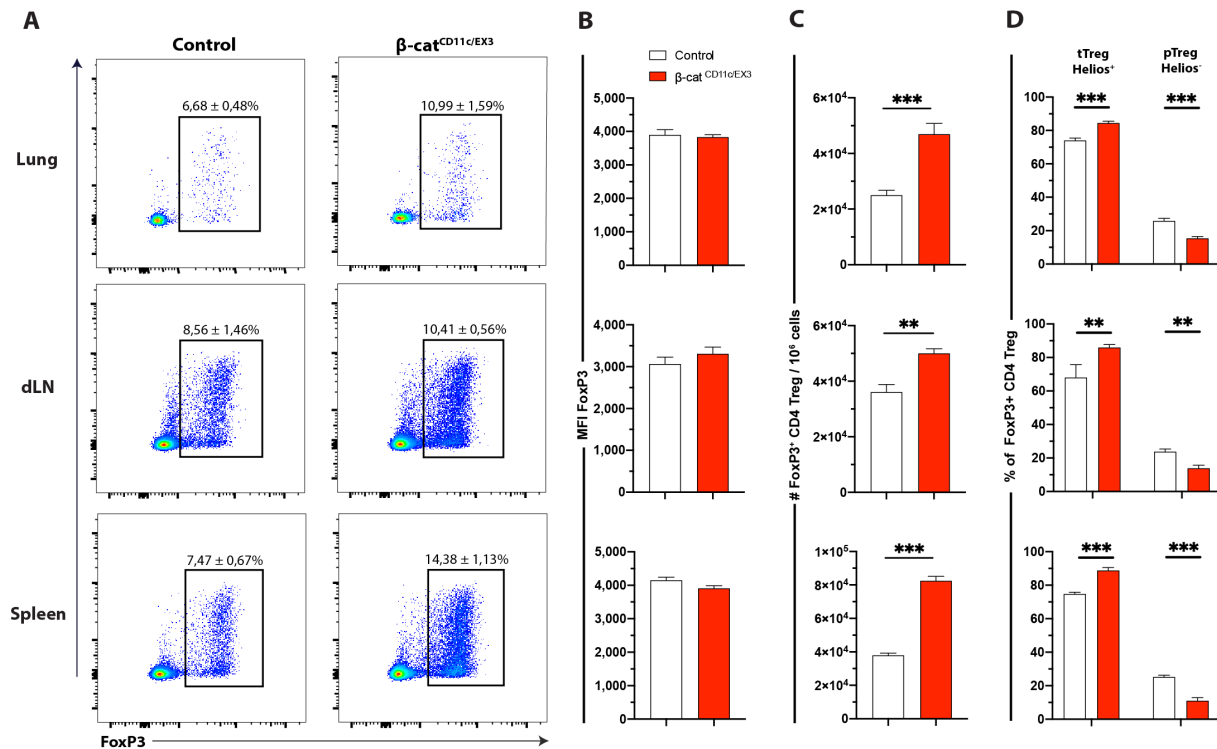


Figure S9: Elevated CD4 Treg numbers in non-infected mice.

(A) Frequencies (representative dot plots) of FoxP3⁺ CD4 Treg in lung, dLN and spleen of non-infected control (white) and β -cat^{ΔCD11c/EX3} mice (red) (pregated on living TCR-β⁺ CD4⁺ cells). (B) FoxP3 expression as measured by MFI in CD4 Treg of lung, dLN and spleen of control versus β -cat^{ΔCD11c/EX3} mice. (C) Absolute cell numbers were normalized to 1x10⁶ cells of FoxP3⁺ CD4 Treg in lung, dLN and spleen of control and β -cat^{ΔCD11c/EX3} mice. (D) Frequencies of CD4⁺ FoxP3⁺ Helios⁺ tTreg and Helios⁻ pTreg in lung, dLN and spleen of control compared to β -cat^{ΔCD11c/EX3} mice. Data are representative of two independent experiments (n=5-6). Statistical significance (unpaired Student's t test) is indicated as *p < 0.05, **p < 0.01 and ***p < 0.001. Values are the mean +SEM.

6 References

- Agrawal, S., Agrawal, A., Doughty, B., Gerwitz, A., Blenis, J., van Dyke, T., and Pulendran, B. (2003). Cutting edge: different Toll-like receptor agonists instruct dendritic cells to induce distinct Th responses via differential modulation of extracellular signal-regulated kinase-mitogen-activated protein kinase and c-Fos. *J Immunol* *171*, 4984–4989.
- Akane, K., Kojima, S., Mak, T.W., Shiku, H., and Suzuki, H. (2016). CD8+CD122+CD49d^{low} regulatory T cells maintain T-cell homeostasis by killing activated T cells via Fas/FasL-mediated cytotoxicity. *Proc Natl Acad Sci U S A* *113*, 2460-2465.
- Akbari, O., DeKruyff, R. H., and Umetsu, D. T. (2001). Pulmonary dendritic cells producing IL-10 mediate tolerance induced by respiratory exposure to antigen. *Nat Immunol* *2*, 725–731.
- Alexandre, Y.O., Cocita, C.D., Ghilas, S., and Dalod, M. (2014). Deciphering the role of DC subsets in MCMV infection to better understand immune protection against viral infections. *Front Microbiol* *5*, 378.
- Allan, R.S., Waithman, J., Bedoui, S., Jones, C.M., Villadangos, J.A., Zhan, Y., Lew, A.M., Shortman, K., Heath, W.R., and Carbone, F.R. (2006). Migratory dendritic cells transfer antigen to a lymph node-resident dendritic cell population for efficient CTL priming. *Immunity* *25*, 153-162.
- Almanan, M., Raynor, J., Sholl, A., Wang, M., Chougnet, C., Cardin, R.D., and Hildeman, D.A. (2017). Tissue-specific control of latent CMV reactivation by regulatory T cells. *PLoS Pathog* *13*, e1006507.
- Alves, C.H., Ober-Blobaum, J.L., Brouwers-Haspels, I., Asmawidjaja, P.S., Mus, A.M., Razawy, W., Molendijk, M., Clausen, B.E., and Lubberts, E. (2015). Dendritic Cell-Specific Deletion of beta-Catenin Results in Fewer Regulatory T-Cells without Exacerbating Autoimmune Collagen-Induced Arthritis. *PLoS One* *10*, e0142972
- Alexandre, Y.O., Cocita, C.D., Ghilas, S., and Dalod, M. (2014). Deciphering the role of DC subsets in MCMV infection to better understand immune protection against viral infections. *Front Microbiol* *5*, 378.

- Allan, R.S., Waithman, J., Bedoui, S., Jones, C.M., Villadangos, J.A., Zhan, Y., Lew, A.M., Shortman, K., Heath, W.R., and Carbone, F.R. (2006). Migratory dendritic cells transfer antigen to a lymph node-resident dendritic cell population for efficient CTL priming. *Immunity* 25, 153-162.
- Almanan, M., Raynor, J., Sholl, A., Wang, M., Chougnet, C., Cardin, R.D., and Hildeman, D.A. (2017). Tissue-specific control of latent CMV reactivation by regulatory T cells. *PLoS Pathog* 13, e1006507.
- Almeida, A. R. M., Legrand, N., Papiernik, M., and Freitas A. A. (2002). Homeostasis of peripheral CD4⁺ T cells: IL-2R alpha and IL-2 shape a population of regulatory cells that controls CD4⁺ T cell numbers. *J Immunol* 169, 4850– 4860.
- Alves, C.H., Ober-Blobaum, J.L., Brouwers-Haspels, I., Asmawidjaja, P.S., Mus, A.M., Razawy, W., Molendijk, M., Clausen, B.E., and Lubberts, E. (2015). Dendritic Cell-Specific Deletion of beta-Catenin Results in Fewer Regulatory T-Cells without Exacerbating Autoimmune Collagen-Induced Arthritis. *PLoS One* 10, e0142972.
- Anderson, C.F., Oukka, M., Kuchroo, V.J., and Sacks, D. (2007). CD4(+)CD25(-)Foxp3(-) Th1 cells are the source of IL-10-mediated immune suppression in chronic cutaneous leishmaniasis. *J Exp Med* 204, 285-297.
- Andrews, D.M., Andoniou, C.E., Granucci, F., Ricciardi-Castagnoli, P., and Degli-Esposti, M.A. (2001). Infection of dendritic cells by murine cytomegalovirus induces functional paralysis. *Nat Immunol* 2, 1077-1084.
- Angelova, M., Zwezdaryk, K., Ferris, M., Shan, B., Morris, C.A., and Sullivan, D.E. (2012). Human cytomegalovirus infection dysregulates the canonical Wnt/beta-catenin signaling pathway. *PLoS Pathog* 8, e1002959.
- Annacker, O., Pimenta-Araujo, R., Burlen-Defranoux, O., Barbosa, T.C., Cumano, A., and Bandeira, A. (2001). CD25⁺ CD4⁺ T cells regulate the expansion of peripheral CD4 T cells through the production of IL-10. *J Immunol* 166, 3008-3018.
- Ansari, M. J. I., Salama, A. D., Chitins, T., Smith, R. N., Yagita, H., Akiba, H., Yamazaki, T., Azuma, M., Iwai, H., Khoury, S. J., Auchincloss, H., and Sayegh M. H. (2003). The programmed death-1 (PD-1) pathway regulates autoimmune diabetes in nonobese diabetic (NOD) mice. *J Exp Med* 198, 63–69.

- Arase, H., Mocarski, E.S., Campbell, A.E., Hill, A.B., and Lanier, L.L. (2002). Direct recognition of cytomegalovirus by activating and inhibitory NK cell receptors. *Science* *296*, 1323-1326.
- Asseman, C., Mauze, S., Leach, M.W., Coffman, R.L., and Powrie, F. (1999). An essential role for interleukin 10 in the function of regulatory T cells that inhibit intestinal inflammation. *J Exp Med* *190*, 995-1004.
- Awasthi, A., Carrier, Y., Peron, J.P., Bettelli, E., Kamanaka, M., Flavell, R.A., Kuchroo, V.K., Oukka, M., and Weiner, H.L. (2007). A dominant function for interleukin 27 in generating interleukin 10-producing anti-inflammatory T cells. *Nat Immunol* *8*, 1380-1389.
- Bachmann, M.F., Wolint, P., Schwarz, K., Jager, P., and Oxenius, A. (2005). Functional properties and lineage relationship of CD8⁺ T cell subsets identified by expression of IL-7 receptor alpha and CD62L. *J Immunol* *175*, 4686-4696.
- Bain, M., Reeves, and J. Sinclair (2006). Regulation of human cytomegalovirus gene expression by chromatin remodeling. In *Cytomegaloviruses: molecular biology and immunology*, M.J. Reddehase, ed. (Wyomondham, Caister Academic Press), pp. 167-183.
- Bajana, S., Turner, S., Paul, J., Ainsua-Enrich, E., and Kovats, S. (2016). IRF4 and IRF8 Act in CD11c⁺ Cells To Regulate Terminal Differentiation of Lung Tissue Dendritic Cells. *J Immunol* *196*, 1666-1677.
- Balthesen, M., Dreher, L., Lucin, P., and Reddehase, M.J. (1994). The establishment of cytomegalovirus latency in organs is not linked to local virus production during primary infection. *J Gen Virol* *75 (Pt 9)*, 2329-2336.
- Balthesen, M., Messerle, M., and Reddehase, M.J. (1993). Lungs are a major organ site of cytomegalovirus latency and recurrence. *J Virol* *67*, 5360-5366.
- Banchereau, J., Briere, F., Caux, C., Davoust, J., Lebecque, S., Liu, Y.J., Pulendran, B., and Palucka, K. (2000). Immunobiology of dendritic cells. *Annu Rev Immunol* *18*, 767-811.
- Banchereau, J., and Steinman, R. M. (1998). Dendritic cells and the control of immunity. *Nature* *392*, 245-252.
- Banh, C., Fugere, C., and Brossay, L. (2009). Immunoregulatory functions of KLRG1 cadherin interactions are dependent on forward and reverse signaling. *Blood* *114*, 5299-5306.

- Basta, S., and Alatery, A. (2007). The cross-priming pathway: a portrait of an intricate immune system. *Scand J Immunol* *65*, 311-319.
- Baumann, N.S., Torti, N., Welten, S.P.M., Barnstorf, I., Borsa, M., Pallmer, K., Oduro, J.D., Cicin-Sain, L., Ikuta, K., Ludewig, B., and Oxenius, A. (2018). Tissue maintenance of CMV-specific inflationary memory T cells by IL-15. *PLoS Pathog* *14*, e1006993.
- Baumann, N.S., Welten, S.P.M., Torti, N., Pallmer, K., Borsa, M., Barnstorf, I., Oduro, J.D., Cicin-Sain, L., and Oxenius, A. (2019). Early primed KLRG1- CMV-specific T cells determine the size of the inflationary T cell pool. *PLoS Pathoh* *15*, e1007785.
- Barber, D. L., Wherry, E. J., Masopust, D., Zhu, B., Allison, J. P., Sharpe, A. H., Freeman, G. J., and Ahmed, R. (2006). Restoring function in exhausted CD8 T cells during chronic viral infection. *Nature* *439*, 682–687.
- Belkaid, Y., and Rouse, B.T. (2005). Natural Regulatory T Cells in Infectious Disease. *Nat Immunol* *6*, 353-360.
- Berod, L., Puttur, F., Huehn, J., and Sparwasser, T. (2012). Tregs in infection and vaccinology: heroes or traitors? *Microb Biotechnol* *5*, 260–269.
- Betts RJ, Prabhu N, Ho AW, Lew FC, Hutchinson PE, Rotzschke O et al. Influenza A virus infection results in a robust, antigen-responsive, and widely disseminated Foxp3+ regulatory T cell response. *J Virol* 2012; 86: 2817–2825.
- Bevan, I.S., Sammons, C.C., and Sweet, C. (1996). Investigation of murine cytomegalovirus latency and reactivation in mice using viral mutants and the polymerase chain reaction. *J Med Virol* *48*, 308-320.
- Bezie, S., Anegon, I., and Guillonneau, C. (2018). Advances on CD8+ Treg Cells and Their Potential in Transplantation. *Transplantation* *102*, 1467–1478.
- Bezie, S., Meistermann, D., Boucault, L., Kilens, S., Zoppi, J., Autrusseau, E., Donnart, A., Nerriere-Daguin, V., Bellier-Waast, F., Charpentier, E., Duteille, F., David, L., Anegon, I., and Guillonneau, C. (2017). Ex Vivo Expanded Human Non-Cytotoxic CD8+CD45RC^{low}/- Tregs Efficiently Delay Skin Graft Rejection and GVHD in Humanized Mice. *Front Immunol* *8*, 2014.

- Blackburn, S. D., Shin, H., Haining, W. N., Zou, T., Workman, C. J., Polley, A., Betts, M. R., Freeman, G. J., Vignali, D. A. A., and Wherry, E. J. (2009). Coregulation of CD8⁺ T cell exhaustion by multiple inhibitory receptors during chronic viral infection. *Nat Immunol* *10*, 29–37.
- Blattman, J.N., Antia, R., Sourdive, D.J., Wang, X., Kaech, S.M., Murali-Krishna, K., Altman, J.D., and Ahmed, R. (2002). Estimating the precursor frequency of naive antigen-specific CD8 T cells. *J Exp Med* *195*, 657-664.
- Boeckh, M., Nichols, W., Papanicolaou, G., Rubin, R., Wingard, J. R., and Zaia, J. (2003). Cytomegalovirus in hematopoietic stem cell transplant recipients: current status, known challenges, and future strategies. *Biol Blood Marrow Transplant* *9*, 543–558.
- Boer, M.C., Prins, C., van Meijgaarden, K.E., van Dissel, J.T., Ottenhoff, T.H., and Joosten, S.A. (2015). Mycobacterium bovis BCG Vaccination Induces Divergent Proinflammatory or Regulatory T Cell Responses in Adults. *Clin Vaccine Immunol* *22*, 778-788.
- Boer, M.C., van Meijgaarden, K.E., Joosten, S.A., and Ottenhoff, T.H. (2014). CD8⁺ regulatory T cells, and not CD4⁺ T cells, dominate suppressive phenotype and function after in vitro live Mycobacterium bovis-BCG activation of human cells. *PLoS One* *9*, e94192.
- Bogunovic, M., Ginhoux, F., Helft, J., Shang, L., Hashimoto, D., Greter, M., Liu, K., Jakubzick, C., Ingersoll, M.A., Leboeuf, M., *et al.* (2009). Origin of the lamina propria dendritic cell network. *Immunity* *31*, 513-525.
- Bohm, V., Podlech, J., Thomas, D., Deegen, P., Pahl-Seibert, M.F., Lemmermann, N.A., Grzimek, N.K., Oehrlein-Karpi, S.A., Reddehase, M.J., and Holtappels, R. (2008). Epitope-specific in vivo protection against cytomegalovirus disease by CD8 T cells in the murine model of preemptive immunotherapy. *Med Microbiol Immunol* *197*, 135-144.
- Bohm, V., Seckert, C.K., Simon, C.O., Thomas, D., Renzaho, A., Gendig, D., Holtappels, R., Reddehase, M.J. (2009). Immune evasion proteins enhance cytomegalovirus latency in the lungs. *J Virol* *83*, 10293–10298.
- Bonfield, T.L., Konstan, M.W., Burfeind, P., Panuska, J.R., Hilliard, J.B., and Berger, M. (1995). Normal bronchial epithelial cells constitutively produce the anti-inflammatory cytokine interleukin-10, which is downregulated in cystic fibrosis. *Am J Respir Cell Mol Biol* *13*, 257-261.

- Boonstra, A., Rajsbaum, R., Holman, M., Marques, R., Asselin-Paturel, C., Pereira, J.P., Bates, E.E., Akira, S., Vieira, P., Liu, Y.J., *et al.* (2006). Macrophages and myeloid dendritic cells, but not plasmacytoid dendritic cells, produce IL-10 in response to MyD88- and TRIF-dependent TLR signals, and TLR-independent signals. *J Immunol* *177*, 7551-7558.
- Boyle, K.A., and Compton, T. (1998). Receptor-binding properties of a soluble form of human cytomegalovirus glycoprotein B. *J Virol* *72*, 1826-1833.
- Brault, V., Moore, R., Kutsch, S., Ishibashi, M., Rowitch, D. H., McMahon, A. P., Sommer, L., Boussadia, O., Kemler, R. (2001). Inactivation of the β -catenin gene by Wnt1-Cre-mediated deletion results in dramatic brain malformation and failure of craniofacial development. *Development* *128*, 1253–1264.
- Brinkmann, M.M., Dag, F., Hengel, H., Messerle, M., Kalinke, U., and Cicin-Sain, L. (2015). Cytomegalovirus immune evasion of myeloid lineage cells. *Med Microbiol Immunol* *204*, 367–82.
- Brooks, D.G., Trifilo, M.J., Edelmann, K.H., Teyton, L., McGavern, D.B., and Oldstone, M.B. (2006). Interleukin-10 determines viral clearance or persistence in vivo. *Nat Med* *12*, 1301-1309.
- Brunkow, M.E., Jeffery, E.W., Hjerrild, K.A., Paepers, B., Clark, L.B., Yasayko, S.A., Wilkinson, J.E., Galas, D., Ziegler, S.F., and Ramsdell, F. (2001). Disruption of a new forkhead/winged-helix protein, scurfy, results in the fatal lymphoproliferative disorder of the scurfy mouse. *Nat Genet* *27*, 68-73.
- Bubic, I., Wagner, M., Krmpotic, A., Saulig, T., Kim, S., Yokoyama, W. M., Jonjic, S., and Koszinowski, U. H. (2004). Gain of virulence caused by loss of a gene in murine cytomegalovirus. *J Virol* *78*, 7536–7544.
- Bukowski, J.F., and Welsh, R.M. (1985). Inability of interferon to protect virus-infected cells against lysis by natural killer (NK) cells correlates with NK cell-mediated antiviral effects in vivo. *J Immunol* *135*, 3537-3541.
- Busch, D.H., Pilip, I.M., Vijn, S., and Pamer, E.G. (1998). Coordinate regulation of complex T cell populations responding to bacterial infection. *Immunity* *8*, 353-362.

- Busche, A., Jirmo, A.C., Welten, S.P., Zischke, J., Noack, J., Constabel, H., Gatzke, A.K., Keyser, K.A., Arens, R., Behrens, G.M., and Messerle, M. (2013). Priming of CD8⁺ T cells against cytomegalovirus-encoded antigens is dominated by cross-presentation. *J Immunol* *190*, 2767-2777.
- Buser, C., Walther, P., Mertens, T., and Michel, D. (2007). Cytomegalovirus primary envelopment occurs at large infoldings of the inner nuclear membrane. *J Virol* *81*, 3042-3048.
- Butcher, S.J., Aitken, J., Mitchell, J., Gowen, B., and Dargan, D.J. (1998). Structure of the human cytomegalovirus B capsid by electron cryomicroscopy and image reconstruction. *J Struct Biol* *124*, 70-76.
- Butz, E.A., and Bevan, M.J. (1998). Massive expansion of antigen-specific CD8⁺ T cells during an acute virus infection. *Immunity* *8*, 167-175.
- Cabrera, R., Tu, Z., Xu, Y., Firpi, R.J., Rosen, H.R., Liu, C. (2004). An immunomodulatory role for CD4(+)CD25(+) regulatory T lymphocytes in hepatitis C virus infection. *Hepatology* *40*, 1062–1071.
- Calabro, S., Liu, D., Gallman, A., Nascimento, M.S., Yu, Z., Zhang, T.T., Chen, P., Zhang, B., Xu, L., Gowthaman, U., *et al.* (2016). Differential Intrasplenic Migration of Dendritic Cell Subsets Tailors Adaptive Immunity. *Cell Rep* *16*, 2472-2485.
- Caton, M. L., Smith-Raska, M. R., and Reizis, B. (2007). Notch-RBP-J signaling controls the homeostasis of CD8⁻ dendritic cells in the spleen. *J Exp Med* *204*, 1653-1664.
- Chang, W.L., Baumgarth, N., Yu, D., and Barry, P.A. (2004). Human cytomegalovirus-encoded interleukin-10 homolog inhibits maturation of dendritic cells and alters their functionality. *J Virol* *78*, 8720-8731.
- Chee, M.S., Bankier, A.T., Beck, S., Bohni, R., Brown, C.M., Cerny, R., Horsnell, T., Hutchison, C.A., 3rd, Kouzarides, T., Martignetti, J.A., and *et al.* (1990). Analysis of the protein-coding content of the sequence of human cytomegalovirus strain AD169. *Curr Top Microbiol Immunol* *154*, 125-169.
- Chen, B., Dodge, M.E., Tang, W., Lu, J., Ma, Z., Fan, C.W., Wei, S., Hao, W., Kilgore, J., Williams, N.S., Roth, M.G., Amatruda, J.F., Chen, C., Lum, L. (2009). Small molecule-

mediated disruption of Wnt-dependent signaling in tissue regeneration and cancer. *Nat Chem Biol* 5, 100–107.

Chen, D.H., Jiang, H., Lee, M., Liu, F., and Zhou, Z.H. (1999). Three-dimensional visualization of tegument/capsid interactions in the intact human cytomegalovirus. *Virology* 260, 10-16.

Chen, J., Ganguly, A., Mucsi, A.D., Meng, J., Yan, J., Detampel, P., Munro, F., Zhang, Z., Wu, M., Hari, A., *et al.* (2017). Strong adhesion by regulatory T cells induces dendritic cell cytoskeletal polarization and contact-dependent lethargy. *J Exp Med* 214, 327-338.

Chen, P., Liu, X., Sun, Y., Zhou, P., Wang, Y., and Zhang, Y. (2016). Dendritic cell targeted vaccines: Recent progresses and challenges. *Hum Vaccin Immunother* 12, 612-622.

Cheng, T.P., Valentine, M.C., Gao, J., Pingel, J.T., and Yokoyama, W.M. (2010). Stability of murine cytomegalovirus genome after in vitro and in vivo passage. *J Virol* 84, 2623-2628.

Cheung, A.K., Gottlieb, D.J., Plachter, B., Pepperl-Klindworth, S., Avdic, S., Cunningham, A.L., Abendroth, A., and Slobedman, B. (2009). The role of the human cytomegalovirus UL111A gene in down-regulating CD4⁺ T-cell recognition of latently infected cells: implications for virus elimination during latency. *Blood* 114, 4128-4137.

Clausen, B.E., and Girard-Madoux, M.J. (2013). IL-10 control of dendritic cells in the skin. *Oncoimmunology* 2, e23186.

Clevers H. (2006). Wnt/beta-catenin signaling in development and disease. *Cell* 127, 469–480.

Cohen, S.B., Smith, N.L., McDougal, C., Pepper, M., Shah, S., Yap, G.S., Acha-Orbea, H., Jiang, A., Clausen, B.E., Rudd, B.D., and Denkers, E.Y. (2015). Beta-catenin signaling drives differentiation and proinflammatory function of IRF8-dependent dendritic cells. *J Immunol* 194, 210-222.

Collins, T., Pomeroy, C., and Jordan, M.C. (1993). Detection of latent cytomegalovirus DNA in diverse organs of mice. *J Infect Dis* 168, 725-729.

Commins, S., Steinke, J.W., and Borish, L. (2008). The extended IL-10 superfamily: IL-10, IL-19, IL-20, IL-22, IL-24, IL-26, IL-28, and IL-29. *J Allergy Clin Immunol* 121, 1108-1111.

Compton, T. and Feira A.L. (2007). Early events in human cytomegalovirus infection. In *Human Herpesviruses: Biology, Therapy, and Immunoprophylaxis*, A. Arvin, G. Campadelli-

- Fiume, E.S. Mocarski, P.S. Moore, B. Roizman, R. Whitley, K. Yamanishi, eds. (Cambridge: Cambridge University Press).
- Compton, T., Nepomuceno, R.R., and Nowlin, D.M. (1992). Human cytomegalovirus penetrates host cells by pH-independent fusion at the cell surface. *Virology* *191*, 387-395.
- Compton, T., Nowlin, D.M., and Cooper, N.R. (1993). Initiation of human cytomegalovirus infection requires initial interaction with cell surface heparan sulfate. *Virology* *193*, 834-841.
- Connolly, S.A., Jardetzky, T.S., and Longnecker, R. (2021). The structural basis of herpesvirus entry. *Nat Rev Microbiol* *19*, 110-121.
- Cook, C.H., Trgovcich, J., Zimmerman, P.D., Zhang, Y., and Sedmak, D.D. (2006). Lipopolysaccharide, tumor necrosis factor alpha, or interleukin-1beta triggers reactivation of latent cytomegalovirus in immunocompetent mice. *J Virol* *80*, 9151-9158.
- Corinti, S., Albanesi, C., la Sala, A., Pastore, S., and Girolomoni, G. (2001). Regulatory activity of autocrine IL-10 on dendritic cell functions. *J Immunol* *166*, 4312-4318.
- Couper, K.N., Blount, D.G., and Riley, E.M. (2008). IL-10: the master regulator of immunity to infection. *J Immunol* *180*, 5771-5777.
- Dai, H., Wan, N., Zhang, S., Moore, Y., Wan, F., and Dai, Z. (2010). Cutting edge: programmed death-1 defines CD8⁺CD122⁺ T cells as regulatory versus memory T cells. *J Immunol* *185*, 803-807.
- Daley-Bauer, L.P., Roback, L.J., Wynn, G.M., and Mocarski, E.S. (2014). Cytomegalovirus hijacks CX3CR1(hi) patrolling monocytes as immune-privileged vehicles for dissemination in mice. *Cell Host Microbe* *15*, 351-362.
- Dalod, M., and Biron, C.A. (2013). Immunoregulatory cytokine networks discovered and characterized during murine cytomegalovirus infections. In *Cytomegaloviruses: From molecular pathogenesis to intervention*, J.M. Reddehase, ed. (Wymondham, Norfolk, United Kingdom: Caister Academic Press), pp. 232–58.
- Dalod, M., Hamilton, T., Salomon, R., Salazar-Mather, T.P., Henry, S.C., Hamilton, J.D., and Biron, C.A. (2003). Dendritic cell responses to early murine cytomegalovirus infection: subset functional specialization and differential regulation by interferon alpha/beta. *J Exp Med* *197*, 885-898.

- Dalod, M., Salazar-Mather, T.P., Malmgaard, L., Lewis, C., Asselin-Paturel, C., Briere, C.F., Trinchieri, G., and Biron C.A. (2002). Interferon alpha/beta and interleukin 12 responses to viral infections: pathways regulating dendritic cell cytokine expression in vivo. *J Exp Med* *195*, 517–528.
- Davison, A.J., Dolan, A., Akter, P., Addison, C., Dargan, D.J., Alcendor, D.J., McGeoch, D.J., and Hayward, G.S. (2003). The human cytomegalovirus genome revisited: comparison with the chimpanzee cytomegalovirus genome. *J Gen Virol* *84*, 17-28.
- De Smedt, T., Pajak, B., Muraille, E., Lespagnard, L., Heinen, E., De Baetselier, P., Urbain, J., Leo, O., and Moser, M. (1996). Regulation of dendritic cell numbers and maturation by lipopolysaccharide in vivo. *J Exp Med* *184*, 1413-1424.
- den Haan, J.M., and Bevan, M.J. (2001). Antigen presentation to CD8+ T cells: cross-priming in infectious diseases. *Curr Opin Immunol* *13*, 437-441.
- Denysenko, T., Annovazzi, L., Cassoni, P., Melcarne, A., Mellai, M., and Schiffer, D. (2016). WNT/beta-catenin Signaling Pathway and Downstream Modulators in Low- and High-grade Glioma. *Cancer Genomics Proteomics* *13*, 31-45.
- Diao, J., Winter, E., Cantin, C., Chen, W., Xu, L., Kelvin, D., Phillips, J., and Catral, M.S. (2006). In situ replication of immediate dendritic cell (DC) precursors contributes to conventional DC homeostasis in lymphoid tissue. *J Immunol* *176*, 7196-7206.
- Dillon, S., Agrwal, A., van Dyke, T., Landreth, G., McCauley, L., Koh, A., Maliszewski, C., Akira, S., and Pulendran, B. (2004). A Toll-like receptor 2 ligand stimulates Th2 responses *in vivo*, via induction of extracellular signal-regulated kinase mitogen-activated protein kinase and c-Fos in dendritic cells. *J Immunol* *172*, 4733–4743.
- Ding, Y., Shen, S., Lino, A.C., Curotto de Lafaille, M.A., and Lafaille, J.J. (2008). Beta-catenin stabilization extends regulatory T cell survival and induces anergy in nonregulatory T cells. *Nat Med* *14*, 162-169.
- Dioverti, M.V., and Razonable, R.R. (2016). Cytomegalovirus. *Microbiol Spectr* *4*.
- Docke, W.D., Prosch, S., Fietze, E., Kimel, V., Zuckermann, H., Klug, C., Syrbe, U., Kruger, D.H., von Baehr, R., and Volk, H.D. (1994). Cytomegalovirus reactivation and tumour necrosis factor. *Lancet* *343*, 268-269.

- Doherty, P. C (1993). Cell-mediated cytotoxicity. *Cell* 75, 607-12.
- Donnelly, R.P., Sheikh, F., Kolenko, S.V., and Dickensheets, H. (2004). The expanded family of class II cytokines that share the IL-10 receptor-2 (IL-10R2) chain. *J Leukoc Biol* 76, 314-321.
- Doom, C.M., and Hill, A.B. (2008). MHC class I immune evasion in MCMV infection. *Med Microbiol Immunol* 197, 191-204.
- Durai, V., and Murphy, K.M. (2016). Functions of Murine Dendritic Cells. *Immunity* 45, 719-736.
- Ebert, S., Podlech, J., Gillert-Marien, D., Gergely, K.M., Buttner, J.K., Fink, A., Freitag, K., Thomas, D., Reddehase, M.J., and Holtappels, R. (2012). Parameters determining the efficacy of adoptive CD8 T-cell therapy of cytomegalovirus infection. *Med Microbiol Immunol* 201, 527-539.
- Ejrnaes, M., Filippi, C.M., Martinic, M.M., Ling, E.M., Togher, L.M., Crotty, S., and von Herrath, M.G. (2006). Resolution of a chronic viral infection after interleukin-10 receptor blockade. *J Exp Med* 203, 2461-2472.
- Endharti, A. T., Rifa'i, M., Shi, Z., Fukuoka, Y., Nakahara, Y., Kawamoto, Y., Takeda, K., K.-Isobe, I., and Suzuki, H. (2005). Cutting edge: CD8+CD122+ regulatory T cells produce IL-10 to suppress IFN-gamma production and proliferation of CD8+ T cells. *J Immunol* 175, 7093–7097.
- Ersland, K., Wuthrich, M., and Klein, B.S. (2010). Dynamic interplay among monocyte-derived, dermal, and resident lymph node dendritic cells during the generation of vaccine immunity to fungi. *Cell Host Microbe* 7, 474-487.
- Farrell, H.E., Bruce, K., Lawler, C., Oliveira, M., Cardin, R., Davis-Poynter, N., and Stevenson, P.G. (2017). Murine Cytomegalovirus Spreads by Dendritic Cell Recirculation. *mBio* 8.
- Farrell, E.H., Lawler, C., Tan, C.S.E., MacDonald, K., Bruce, K., Mach, M., Davis-Poynter, N., and Stevenson, P.G. (2016). Murine Cytomegalovirus Exploits Olfaction To Enter New Hosts. *mBio* 7.
- Fehervari, Z., and Sakaguchi, S. (2004). CD4+ Tregs and immune control. *J Clin Invest* 114, 1209-1217.

- Feire, A.L., and Compton T. (2013). Virus entry and activation of innate defence. In *Cytomegaloviruses: From Molecular Pathogenesis to Intervention*, MJ Reddehase, ed. (Wyomondham, Norfolk, United Kingdom: Caister Academic Press), pp. 125–140.
- Feire, A.L., Koss, H., and Compton T. (2004). Cellular integrins function as entry receptors for human cytomegalovirus via a highly conserved disintegrin-like domain. *Proc Natl Acad Sci USA* *101* 15470-15475.
- Fenoglio, D., Dentone, C., Signori, A., Di Biagio, A., Parodi, A., Kalli, F., Nasi, G., Curto, M., Cenderello, G., de Leo, P., Bartolacci, V., Orofino, G., Nicolini, L. A., Taramasso, L., Fiorillo, E., Orru, V., Traverso, P., Bruzzone, B., Ivaldi, F., Mantia, E., Guerra, M., S. NEGRINI, Giacomini, M., Bhagani, S., and Filaci, G. (2018). CD8+CD28-CD127loCD39+ regulatory T-cell expansion: A new possible pathogenic mechanism for HIV infection? *J Allergy Clin Immunol* *141*: 2220-2233.e4.
- Feuerer, M., Hill, J.A., Mathis, D., and Benoist, C. (2009). Foxp3+ regulatory T cells: differentiation, specification, subphenotypes. *Nat Immunol* *10*, 689-695.
- Finbloom, D.S., and Winestock, K.D. (1995). IL-10 induces the tyrosine phosphorylation of tyk2 and Jak1 and the differential assembly of STAT1 alpha and STAT3 complexes in human T cells and monocytes. *J Immunol* *155*, 1079-1090.
- Fink, A., Lemmermann, N.A.W., Gillert-Marien, D., Thomas, D., Freitag, K., Boehm, V., Wilhelmi, V., Reifenberg, K., Reddehase, M.J., and Holtappels, R. (2012). Antigen presentation under the influence of 'immune evasion' proteins and its modulation by interferon-gamma: Implications for immunotherapy of cytomegalovirus infection with antiviral CD8 T cells. *Med Microbiol Immunol* *201*, 513–525.
- Fiorentino, D.F., Bond, M.W., and Mosmann, T.R. (1989). Two types of mouse T helper cell. IV. Th2 clones secrete a factor that inhibits cytokine production by Th1 clones. *J Exp Med* *170*, 2081-2095.
- Fiorentino, D.F., Zlotnik, A., Vieira, P., Mosmann, T.R., Howard, M., Moore, K.W., and O'Garra, A. (1991). IL-10 acts on the antigen-presenting cell to inhibit cytokine production by Th1 cells. *J Immunol* *146*, 3444-3451.

- Fitzgerald, D.C., Zhang, G.X., El-Behi, M., Fonseca-Kelly, Z., Li, H., Yu, S., Saris, C.J., Gran, B., Ciric, B., and Rostami, A. (2007). Suppression of autoimmune inflammation of the central nervous system by interleukin 10 secreted by interleukin 27-stimulated T cells. *Nat Immunol* 8, 1372-1379.
- Fontenot, J.D., Gavin, M.A., and Rudensky, A.Y. (2003). Foxp3 programs the development and function of CD4⁺CD25⁺ regulatory T cells. *Nat Immunol* 4, 330-336.
- Francisco, L. M., Salinas, V. H., Brown, K. E., Vanguri, V. K., Freeman, G. J., Kuchroo, V. K., and Sharpe, A. H. (2009). PD-L1 regulates the development, maintenance, and function of induced regulatory T cells. *J Exp Med* 206, 3015–3029.
- Fu, C., Liang, X., Cui, W., Ober-Blobaum, J.L., Vazzana, J., Shrikant, P.A., Lee, K.P., Clausen, B.E., Mellman, I., and Jiang, A. (2015). beta-Catenin in dendritic cells exerts opposite functions in cross-priming and maintenance of CD8⁺ T cells through regulation of IL-10. *Proc Natl Acad Sci U S A* 112, 2823-2828.
- Furtado, G.C., Curotto de Lafaille, M.A., Kutchukhidze, N., and Lafaille, J.J. (2002). Interleukin 2 signaling is required for CD4⁽⁺⁾ regulatory T cell function. *J Exp Med* 196, 851-857.
- Gavin, M.A., Clarke, S.R., Negrou, E., Gallegos, A., and Rudensky, A. (2002). Homeostasis and anergy of CD4⁽⁺⁾CD25⁽⁺⁾ suppressor T cells in vivo. *Nat Immunol* 3, 33-41.
- Gazzinelli, R.T., Wysocka, M., Hieny, S., Scharon-Kersten, T., Cheever, A., Kuhn, R., Muller, W., Trinchieri, G., and Sher, A. (1996). In the absence of endogenous IL-10, mice acutely infected with *Toxoplasma gondii* succumb to a lethal immune response dependent on CD4⁺ T cells and accompanied by overproduction of IL-12, IFN-gamma and TNF-alpha. *J Immunol* 157, 798-805.
- Geijtenbeek, T. B., van Vliet, S.J., Koppel, E.A., Sanchez-Hernandez, M., Vandenbroucke-Grauls, C.M.J.E., Appelmelk, B., and van Kooyk, Y. (2003). Mycobacteria target DC-SIGN to suppress dendritic cell function. *J Exp Med* 197, 7–17.
- Gibbs, V.C., and Pennica, D. (1997). CRF2-4: isolation of cDNA clones encoding the human and mouse proteins. *Gene* 186, 97-101.

- Gillet, L., Frederico, B., and Stevenson, P.G. (2015). Host entry by gamma-herpesviruses-lessons from viral animal viruses?. *Curr Opin Virol* 15, 34-40.
- Ginhoux, F., Liu, K., Helft, J., Bogunovic, M., Greter, M., Hashimoto, D., Price, J., Yin, N., Bromberg, J., Lira, S.A., *et al.* (2009). The origin and development of nonlymphoid tissue CD103+ DCs. *J Exp Med* 206, 3115-3130.
- Giugni, T.D., Soderberg, C., Ham, D.J., Bautista, R.M., Hedlund, K.O., Moller, E., and Zaia, J.A. (1996). Neutralization of human cytomegalovirus by human CD13-specific antibodies. *J Infect Dis* 173, 1062-1071.
- Goodbourn, S., Didcock, L., and Randall, R.E. (2000). Interferons: cell signalling, immune modulation, antiviral response and virus countermeasures. *J Gen Virol* 81, 2341-2364.
- Grandvaux, N., tenOever, B.R., Servant, M.J., and Hiscott, J. (2002). The interferon antiviral response: from viral invasion to evasion. *Curr Opin Infect Dis* 15, 259-267.
- Greter, M., Helft, J., Chow, A., Hashimoto, D., Mortha, A., Agudo-Cantero, J., Bogunovic, M., Gautier, E.L., Miller, J., Leboeuf, M., *et al.* (2012). GM-CSF controls nonlymphoid tissue dendritic cell homeostasis but is dispensable for the differentiation of inflammatory dendritic cells. *Immunity* 36, 1031-1046.
- Grewe, M., Gyufko, K., and Krutmann, J. (1995). Interleukin-10 production by cultured human keratinocytes: regulation by ultraviolet B and ultraviolet A1 radiation. *J Invest Dermatol* 104, 3-6.
- Griessler, M., Renzaho, A., Freitag, K., Seckert, C.K., Reddehase, M.J., and Lemmermann, N.A.W. (2021). Stochastic Episodes of Latent Cytomegalovirus Transcription Drive CD8 T-Cell "Memory Inflation" and Avoid Immune Evasion. *Front Immunol* 12, 668885.
- Groux, H., Bigler, M., de Vries, J.E., and Roncarolo, M.G. (1998). Inhibitory and stimulatory effects of IL-10 on human CD8+ T cells. *J Immunol* 160, 3188-3193.
- Groux, H., O'Garra, A., Bigler, M., Rouleau, M., Antonenko, S., de Vries, J.E., and Roncarolo, M.G. (1997). A CD4+ T-cell subset inhibits antigen-specific T-cell responses and prevents colitis. *Nature* 389, 737-742.
- Guermonez, P., Valladeau, J., Zitvogel, L., Théry, C., and Amigorena, S. (2002). Antigen presentation and T cell stimulation by dendritic cells. *Annu Rev Immunol* 20, 621-667.

- Guilliams, M., Ginhoux, F., Jakubzick, C., Naik, S.H., Onai, N., Schraml, B.U., Segura, E., Tussiwand, R., and Yona, S. (2014). Dendritic cells, monocytes and macrophages: a unified nomenclature based on ontogeny. *Nat Rev Immunol* *14*, 571-578.
- Guilliams, M., Lambrecht, B.N., and Hammad, H. (2013). Division of labor between lung dendritic cells and macrophages in the defense against pulmonary infections. *Mucosal Immunol* *6*, 464-473.
- Gunn, M.D., Tangemann, K., Tam, C., Cyster, J.G., Rosen, S.D., and Williams, L.T. (1998). A chemokine expressed in lymphoid high endothelial venules promotes the adhesion and chemotaxis of naive T lymphocytes. *Proc Natl Acad Sci USA* *95*, 258-263.
- Gurevich, I., Feferman, T., Milo, I., Tal, O., Golani, O., Drexler, I., and Shakhar, G. (2017). Active dissemination of cellular antigens by DCs facilitates CD8(+) T-cell priming in lymph nodes. *Eur J Immunol* *47*, 1802-1818.
- Hahn, G., Jores, R., and Mocarski, E.S. (1998). Cytomegalovirus remains latent in a common precursor of dendritic and myeloid cells. *Proc Natl Acad Sci U S A* *95*, 3937-3942.
- Hamann, D., Baars, P.A., Rep, M.H., Hooibrink, B., Kerkhof-Garde, S.R., Klein, M.R., and van Lier, R.A. (1997). Phenotypic and functional separation of memory and effector human CD8+ T cells. *J Exp Med* *186*, 1407-1418.
- Harada, N., Tamai, Y., Ishikawa, T., Sauer, B., Takaku, K., Oshima, M., Taketo, M. M. (1999). Intestinal polyposis in mice with a dominant stable mutation of the β -catenin gene. *EMBO J* *18*, 5931-5942.
- Hartmann, G., Weiner, G.J., and Krieg, A.M. (1999). CpG DNA: a potent signal for growth, activation, and maturation of human dendritic cells. *Proc Natl Acad Sci USA* *96*, 9305-9310.
- Harty, J.T., and Badovinac, V.P. (2008). Shaping and reshaping CD8+ T-cell memory. *Nat Rev Immunol* *8*, 107-119.
- Harty, J.T., Tvinnereim, A.R., and White, D.W. (2000). CD8+ T cell effector mechanisms in resistance to infection. *Annu Rev Immunol* *18*, 275-308.

- Hasan, M., Krmpotic, A., Ruzsics, Z., Bubic, I., Lenac, T., Halenius, A., Loewendorf, A., Messerle, M., Hengel, H., Jonjic, S., and Koszinowski, U.H. (2005). Selective down-regulation of the NKG2D ligand H60 by mouse cytomegalovirus m155 glycoprotein. *J Virol* *79*, 2920-2930.
- Heath, W.R., Belz, G.T., Behrens, G.M., Smith, C.M., Forehan, S.P., Parish, I.A., Davey, G.M., Wilson, N.S., Carbone, F.R., and Villadangos, J.A. (2004). Cross-presentation, dendritic cell subsets, and the generation of immunity to cellular antigens. *Immunol Rev* *199*, 9-26.
- Hengel, H., Lucin, P., Jonjic, S., Ruppert, T., and Koszinowski, U.H. (1994). Restoration of cytomegalovirus antigen presentation by gamma interferon combats viral escape. *J Virol* *68*, 289-297.
- Hengel, H., Reusch, U., Gutermann, A., Ziegler, H., Jonjic, S., Lucin, P., and Koszinowski, U.H. (1999). Cytomegaloviral control of MHC class I function in the mouse. *Immunol Rev* *168*, 167-176.
- Henson, S.M., Franzese, O., Macaulay, R., Libri, V., Azevedo, R.I., Kiani-Alikhan, S., Plunkett, F.J., Masters, J.E., Jackson, S., Griffiths, S.J., *et al.* (2009). KLRG1 signaling induces defective Akt (ser473) phosphorylation and proliferative dysfunction of highly differentiated CD8+ T cells. *Blood* *113*, 6619-6628.
- Hertel, L., Lacaille, V.G., Strobl, H., Mellins, E.D., and Mocarski, E.S. (2003). Susceptibility of immature and mature Langerhans cell-type dendritic cells to infection and immunomodulation by human cytomegalovirus. *J Virol* *77*, 7563-7574.
- Hettinger, J., Richards, D.M., Hansson, J., Barra, M.M., Joschko, A.C., Krijgsveld, J., and Feuerer, M. (2013). Origin of monocytes and macrophages in a committed progenitor. *Nat Immunol* *14*, 821-830.
- Ho, A.S., Liu, Y., Khan, T.A., Hsu, D.H., Bazan, J.F., and Moore, K.W. (1993). A receptor for interleukin 10 is related to interferon receptors. *Proc Natl Acad Sci U S A* *90*, 11267-11271.
- Ho, M. (2008). The history of cytomegalovirus and its diseases. *Med Microbiol Immunol* *197*, 65-73.
- Hochrein, H., Shortman, K., Vremec, D., Scott, B., Hertzog, P., and O'Keeffe, M. (2001). Differential production of IL-12, IFN-alpha, and IFN-gamma by mouse dendritic cell subsets. *J Immunol* *166*, 5448-5455.

- Holtappels, R., Freitag, K., Renzaho, A., Becker, S., Lemmermann, N.A.W., and Reddehase, M.J. (2020). Revisiting CD8 T-cell 'Memory Inflation': New Insights with Implications for Cytomegaloviruses as Vaccine Vectors. *Vaccines (Basel)* 8.
- Holtappels, R., Gillert-Marien, D., Thomas, D., Podlech, J., Deegen, P., Herter, S., Oehrlein-Karpi, S.A., Strand, D., Wagner, M., and Reddehase, M.J. (2006). Cytomegalovirus encodes a positive regulator of antigen presentation. *J Virol* 80, 7613-7624.
- Holtappels, R., Pahl-Seibert, M.F., Thomas, D., and Reddehase, M.J. (2000). Enrichment of immediate-early 1 (m123/pp89) peptide-specific CD8 T cells in a pulmonary CD62L(lo) memory-effector cell pool during latent murine cytomegalovirus infection of the lungs. *J Virol* 74, 11495-11503.
- Holtappels, R., Thomas, D., Podlech, J., and Reddehase, M.J. (2002). Two antigenic peptides from genes m123 and m164 of murine cytomegalovirus quantitatively dominate CD8 T-cell memory in the H-2d haplotype. *J Virol* 76, 151-164.
- Hoppler, S., and Kavanagh, C.L. (2007). Wnt signalling: variety at the core. *J Cell Sci* 120, 385-393.
- Hori, S., Nomura, T., and Sakaguchi, S. (2003). Control of regulatory T cell development by the transcription factor Foxp3. *Science* 299, 1057-1061.
- Howes, A., Gabrysova, L. and O'Garra, A. (2014). Role of IL-10 and the IL-10 receptor in immune response. Elsevier, Reference Module in Biomedical Sciences, 3rd edition.
- Hu, X., Piak, P.K., Chen, J., Yamilina, A., Kockeritz, L., Lu, T.T., Woodgett, J.R., and Ivashkiv, L.B. (2006). IFN- γ suppresses IL-10 production and synergizes with TLR2 by regulating GSK3 and CREB/AP-1 proteins. *Immunity* 24, 563-574.
- Huber, A.H., Nelson, W.J., and Weis, W.I. (1997): Three-Dimensional Structure of the Armadillo Repeat Region of β -Catenin. *Cell* 90, 871-882.
- Humphreys, I.R., de Trez, C., Kinkade, A., Benedict, C.A., Croft, M., and Ware, C.F. (2007). Cytomegalovirus exploits IL-10-mediated immune regulation in the salivary glands. *J Exp Med* 204, 1217-1225.

- Idoyaga, J., Suda, N., Suda, K., Park, C.G., and Steinman, R.M. (2009). Antibody to Langerin/CD207 localizes large numbers of CD8alpha+ dendritic cells to the marginal zone of mouse spleen. *Proc Natl Acad Sci U S A* *106*, 1524-1529.
- Isomura, H., Stinski, M.F., Murata, T., Yamashita, Y., Kanda, T., Toyokuni, S., and Tsurumi, T. (2011). The human cytomegalovirus gene products essential for late viral gene expression assemble into prereplication complexes before viral DNA replication. *J Virol* *85*, 6629-6644.
- Iwasaki, A., and Kelsall, B.L. (1999). Freshly isolated Peyer's patch, but not spleen, dendritic cells produce interleukin 10 and induce the differentiation of T helper type 2 cells. *J Exp Med* *190*, 229-239.
- Janeway, C. A., Jr., & Medzhitov, R. (2002). Innate immune recognition. *Annu Rev Immunol*, *20*, 197- 216.
- Jeitziner, S.M., Walton, S.M., Torti, N., Oxenius, A. (2013). Adoptive transfer of cytomegalovirus- specific effector CD4+ T cells provides antiviral protection from murine CMV infection. *J Immunol* *43*, 2886–2895.
- Jenkins, C., Abendroth, A., and Slobedman, B. (2004). A novel viral transcript with homology to human interleukin-10 is expressed during latent human cytomegalovirus infection. *J Virol* *78*, 1440-1447.
- Jiang, A., Bloom, O., Ono, S., Cui, W., Unternaehrer, J., Jiang, S., Whitney, J.A., Connolly, J., Banchereau, J., and Mellman, I. (2007). Disruption of E-cadherin-mediated adhesion induces a functionally distinct pathway of dendritic cell maturation. *Immunity* *27*, 610-624.
- Jinquan, T., Quan, S., Feili, G., Larsen, C.G., and Thestrup-Pedersen, K. (1999). Eotaxin activates T cells to chemotaxis and adhesion only if induced to express CCR3 by IL-2 together with IL-4. *J Immunol* *162*, 4285-4292.
- Joffre, O. P., Segura, E., Savina, A., and Amigorena, S. (2012). Cross-presentation by dendritic cells. *Nat Rev Immunol* *12*, 557-569.
- Jones, M., Ladell, K., Wynn, K.K., Stacey, M.A., Quigley, M.F., Gostick, E., Price, D.A., and Humphreys, I.R. (2010). IL-10 restricts memory T cell inflation during cytomegalovirus infection. *J Immunol* *185*, 3583-3592.

- Jonjic, S., Bubic, I., and Krmpotic, A. (2006). Innate immunity to cytomegalovirus. In *Cytomegaloviruses: molecular biology and immunology*, M.J. Reddehase, ed. (Wymondham, Norfolk, United Kingdom: Caister Academic Press), pp. 285-320.
- Jonjic, S., Pavic, I., Lucin, P., Rukavina, D., Koszinowski, U.H. (1990). Efficacious control of cytomegalovirus infection after long-term depletion of CD8+ T lymphocytes. *J Virol* 64, 5457–5464.
- Joshi, N.S., Cui, W., Chandele, A., Lee, H.K., Urso, D.R., Hagman, J., Gapin, L., and Kaech, S.M. (2007). Inflammation directs memory precursor and short-lived effector CD8(+) T cell fates via the graded expression of T-bet transcription factor. *Immunity* 27, 281-295.
- Jost, N.H., Abel, S., Hutzler, M., Sparwasser, T., Zimmermann, A., Roers, A., Muller, W., Klopffleisch, R., Hengel, H., Westendorf, A.M., *et al.* (2014). Regulatory T cells and T-cell-derived IL-10 interfere with effective anti-cytomegalovirus immune response. *Immunol Cell Biol* 92, 860-871.
- Judge, A. D., Zhang, X., Fujii, H., Surh, C. D., and Sprent, J. (2002). Interleukin 15 controls both proliferation and survival of a subset of memory-phenotype CD8(+) T cells. *J Exp Med* 196, 935–946.
- Kaech, S.M., Tan, J.T., Wherry, E.J., Konieczny, B.T., Surh, C.D., and Ahmed, R. (2003). Selective expression of the interleukin 7 receptor identifies effector CD8 T cells that give rise to long-lived memory cells. *Nat Immunol* 4, 1191-1198.
- Kaech, S.M., Wherry, E.J., and Ahmed, R. (2002). Effector and memory T-cell differentiation: implications for vaccine development. *Nat Rev Immunol* 2, 251-262.
- Kamanaka, M., Kim, S.T., Wan, Y.Y., Sutterwala, F.S., Lara-Tejero, M., Galan, J.E., Harhaj, E., and Flavell, R.A. (2006). Expression of interleukin-10 in intestinal lymphocytes detected by an interleukin-10 reporter knockin tiger mouse. *Immunity* 25, 941-952.
- Karrer, U., Sierro, S., Wagner, M., Oxenius, A., Hengel, H., Koszinowski, U.H., Phillips, R.E., and Klenerman, P. (2003). Memory inflation: continuous accumulation of antiviral CD8+ T cells over time. *J Immunol* 170, 2022-2029.

- Kashiwada, M., Pham, N.L., Pewe, L.L., Harty, J.T., and Rothman, P.B. (2011). NFIL3/E4BP4 is a key transcription factor for CD8alpha(+) dendritic cell development. *Blood* *117*, 6193-6197.
- Keil, G.M., Ebeling-Keil, A., and Koszinowski, U.H. (1984). Temporal regulation of murine cytomegalovirus transcription and mapping of viral RNA synthesized at immediate early times after infection. *J Virol* *50*, 784-795.
- Kim, J., Kim, A.R., and Shin, E.C. (2015). Cytomegalovirus Infection and Memory T Cell Inflation. *Immune Netw* *15*, 186-190.
- Kim, R., and Sejnowski, T.J. (2021). Strong inhibitory signaling underlies stable temporal dynamics and working memory in spiking neural networks. *Nat Neurosci* *24*, 129-139.
- King, I.L., Kroenke, M.A., and Segal, B.M. (2010). GM-CSF-dependent, CD103+ dermal dendritic cells play a critical role in Th effector cell differentiation after subcutaneous immunization. *J Exp Med* *207*, 953-961.
- Kleijmeer, M.J., Escola, J.M., UytdeHaag, F.G., Jakobson, E., Griffith, J.M., Osterhaus, A.D., Stoorvogel, W., Melief, C.J., Rabouille, C., and Geuze, H.J. (2001). Antigen loading of MHC class I molecules in the endocytic tract. *Traffic* *2*, 124-137.
- Klenerman, P., and Oxenius, A. (2016). T cell responses to cytomegalovirus. *Nat Rev Immunol* *16*, 367-377.
- Klenovsek, K., Weisel, F., Schneider, A., Appelt, U., Jonjic, S., Messerle, M., Bradel-Tretheway, B., Winkler, T.H., and Mach, M. (2007). Protection from CMV infection in immunodeficient hosts by adoptive transfer of memory B cells. *Blood* *110*, 3472-3479.
- Kloetzel, P.M. (2001). Antigen processing by the proteasome. *Nat Rev Mol Cell Biol* *2*, 179-187.
- Koffron, A.J., Hummel, M., Patterson, B.K., Yan, S., Kaufman, D.B., Fryer, J.P., Stuart, F.P., and Abecassis, M.I. (1998). Cellular localization of latent murine cytomegalovirus. *J Virol* *72*, 95-103.
- Koffron, A.J., Patterson, B.K., Yan, S., Kaufman, D.B., Fryer, J.P., Stuart, F.P., and Abecassis, M.I. (1997). Latent human cytomegalovirus: a functional study. *Transplant Proc* *29*, 793-795.

- Kondo, K., Kaneshima, H., and Mocarski, E.S. (1994). Human cytomegalovirus latent infection of granulocyte-macrophage progenitors. *Proc Natl Acad Sci U S A* *91*, 11879-11883.
- Kotenko, S.V., Krause, C.D., Izotova, L.S., Pollack, B.P., Wu, W., and Pestka, S. (1997). Identification and functional characterization of a second chain of the interleukin-10 receptor complex. *EMBO J* *16*, 5894-5903.
- Kotenko, S.V., Saccani, S., Izotova, L.S., Mirochnitchenko, O.V., and Pestka, S. (2000). Human cytomegalovirus harbors its own unique IL-10 homolog (cmvIL-10). *Proc Natl Acad Sci U S A* *97*, 1695-1700.
- Krmpotic, A., Bubic, I., Polic, B., Lucin, P., and Jonjic, S. (2003). Pathogenesis of murine cytomegalovirus infection. *Microbes Infect* *5*, 1263-1277.
- Krmpotic, A., Hasan, M., Loewendorf, A., Saulig, T., Halenius, A., Lenac, T., Polic, B., Bubic, I., Kriegeskorte, A., Pernjak-Pugel, E., *et al.* (2005). NK cell activation through the NKG2D ligand MULT-1 is selectively prevented by the glycoprotein encoded by mouse cytomegalovirus gene m145. *J Exp Med* *201*, 211-220.
- Ku, C. C., Murakami, M., Sakamoto, A., Kappler, J., and Marrack P. (2000). Control of homeostasis of CD8⁺ memory T cells by opposing cytokines. *Science* *288*, 675–678.
- Kuhn, R., Lohler, J., Rennick, D., Rajewsky, K., and Muller, W. (1993). Interleukin-10-deficient mice develop chronic enterocolitis. *Cell* *75*, 263-274.
- Kumagai, Y., Takeuchi, O., Kato, H., Kumar, H., Matsui, K., Morii, E., Aozasa, K., Kawai, T., and Akira, S. (2007). Alveolar macrophages are the primary interferon-alpha producer in pulmonary infection with RNA viruses. *Immunity* *27*, 240–252.
- Kurz, S.K., and Reddehase, M.J. (1999). Patchwork pattern of transcriptional reactivation in the lungs indicates sequential checkpoints in the transition from murine cytomegalovirus latency to recurrence. *J Virol* *73*, 8612-8622.
- La Rosa, C., and Diamond, D. J. (2012). The immune response to human CMV. *Future Virol* *7*, 279–293.

- Laidlaw, B. J., Cui, W., Amezcua, R. A., Gray, S. M., Guan, T., Lu, Y., Kobayashi, Y., Flavell, R. A., Kleinstein, S. H., Craft, J., and Kaech S. M. (2015). Production of IL-10 by CD4(+) regulatory T cells during the resolution of infection promotes the maturation of memory CD8(+) T cells. *Nat Immunol* *16*, 871–879.
- Lambrecht, B.N., and Hammad, H. (2012). Lung dendritic cells in respiratory viral infection and asthma: from protection to immunopathology. *Annu Rev Immunol* *30*, 243-270.
- Lancini, D., Faddy, H.M., Flower, R., and Hogan, C. (2014). Cytomegalovirus disease in immunocompetent adults. *Med J Aust* *201*, 578-580.
- Lanteri, M. C., O'Brien, K. M., Purtha, W. E., Cameron, M. J., Lund, J. M., Owen, R. E., Heitman, J. W., Custer, B., Hirschhorn, D. F., Tobler, L. H., Kiely, N., Prince, H. E., Ndhlovu, L. C., Nixon, D. F., Kamel, H. T., Kelvin, D. J., Busch, M. P., Rudensky, A. Y., Diamond, M. S., and Norris P. J. (2009). Tregs control the development of symptomatic West Nile virus infection in humans and mice. *J Clin Invest* *119*, 3266–3277.
- Lemmermann, N.A., Podlech, J., Seckert, C.K., Kropp, K.A., Grzimek, N.K.A., Reddehase, M.J., Holtappels, R. (2010). CD8 T cell immunotherapy of cytomegalovirus disease in the murine model. In *Methods in Microbiology*, D. Kabelitz, S.H.E. Kaufmann, eds. (London: Academic Press), pp. 369–420.
- Lenac, T., Budt, M., Arapovic, J., Hasan, M., Zimmermann, A., Simic, H., Krmpotic, A., Messerle, M., Ruzsics, Z., Koszinowski, U.H., *et al.* (2006). The herpesviral Fc receptor fcr-1 down-regulates the NKG2D ligands MULT-1 and H60. *J Exp Med* *203*, 1843-1850.
- Li, C., Corraliza, I., and Langhorne, J. (1999). A defect in interleukin-10 leads to enhanced malarial disease in *Plasmodium chabaudi chabaudi* infection in mice. *Infect Immun* *67*, 4435-4442.
- Li, Z., Li, D., Tsun, A., and Li, B. (2015). FOXP3+ regulatory T cells and their functional regulation. *Cell Mol Immunol* *12*, 558-565.
- Li, Y.N., Liu, X.L., Huang, F., Zhou, H., Huang, Y.J., Fang, F. (2010). CD4+CD25+ regulatory T cells suppress the immune responses of mouse embryo fibroblasts to murine cytomegalovirus infection. *Immunol Lett* *131*, 131–8.

- Li, S., Xie, Q., Zeng, Y., Zou, C., Liu, X., Wu, S., Deng, H., Xu, Y., Li, X.C., and Dai, Z. (2014). A naturally occurring CD8(+)CD122(+) T-cell subset as a memory-like Treg family. *Cell Mol Immunol* *11*, 326–331.
- Liang, X., Fu, C., Cui, W., Ober-Blobaum, J.L., Zahner, S.P., Shrikant, P.A., Clausen, B.E., Flavell, R.A., Mellman, I., and Jiang, A. (2014). beta-catenin mediates tumor-induced immunosuppression by inhibiting cross-priming of CD8(+) T cells. *J Leukoc Biol* *95*, 179-190.
- Liao, Y., Liu, X., Huang, Y., Huang, H., Lu, Y., Zhang, Y., Shu, S., and Fang, F. (2017). Expression pattern of CD11c on lung immune cells after disseminated murine cytomegalovirus infection. *Virol J* *14*, 132.
- Lindenberg, M., Solmaz, G., Puttur, F., and Sparwasser, T. (2014). Mouse cytomegalovirus infection overrules T regulatory cell suppression on natural killer cells. *Virol J* *11*, 145.
- Liu, G.-Z., Fang, L.-B., Helmstroem, P., and Gao, X.-G. (2007). Increased CD8+ central memory T cells in patients with multiple sclerosis. *Mult Scler* *13*, 149–155.
- Liu, K., and Nussenzweig, M.C. (2010). Origin and development of dendritic cells. *Immunol Rev* *234*, 45-54.
- Liu, H., Wang, Y., Zeng, Q., Zeng, Y.Q., Liang, C.L., Qiu, F., Nie, H., and Dai, Z. (2017). Suppression of allograft rejection by CD8+CD122+PD-1+ Tregs is dictated by their Fas ligand-initiated killing of effector T cells versus Fas-mediated own apoptosis. *Oncotarget* *8*, 24187-24195.
- Liu, K., Waskow, C., Liu, X., Yao, K., Hoh, J., and Nussenzweig, M. (2007). Origin of dendritic cells in peripheral lymphoid organs of mice. *Nat Immunol* *8*, 578-583.
- Liu, Y., Wei, S.H., Ho, A.S., de Waal Malefyt, R., and Moore, K.W. (1994). Expression cloning and characterization of a human IL-10 receptor. *J Immunol* *152*, 1821-1829.
- Lodoen, M., Ogasawara, K., Hamerman, J.A., Arase, H., Houchins, J.P., Mocarski, E.S., and Lanier, L.L. (2003). NKG2D-mediated natural killer cell protection against cytomegalovirus is impaired by viral gp40 modulation of retinoic acid early inducible 1 gene molecules. *J Exp Med* *197*, 1245-1253.

- Loewendorf, A., Kruger, C., Borst, E.M., Wagner, M., Just, U., and Messerle, M. (2004). Identification of a mouse cytomegalovirus gene selectively targeting CD86 expression on antigen-presenting cells. *J Virol* *78*, 13062-13071.
- Lucin, P., Jonjic, S., Messerle, M., Polic, B., Hengel, H., and Koszinowski, U.H. (1994). Late phase inhibition of murine cytomegalovirus replication by synergistic action of interferon-gamma and tumour necrosis factor. *J Gen Virol* *75*, 101–110.
- Lutfalla, G., Gardiner, K., and Uze, G. (1993). A new member of the cytokine receptor gene family maps on chromosome 21 at less than 35 kb from IFNAR. *Genomics* *16*, 366-373.
- MacDonald, B.T., Tamai, K., and He, X. (2009). Wnt/beta-catenin signaling: components, mechanisms, and diseases. *Dev Cell* *17*, 9-26.
- MacDonald, K.P., Rowe, V., Bofinger, H.M., Thomas, R., Sasmono, T., Hume, D.A., and Hill, G.R. (2005). The colony-stimulating factor 1 receptor is expressed on dendritic cells during differentiation and regulates their expansion. *J Immunol* *175*, 1399-1405.
- Malek, T. R., Yu, A., Vineck, V., Scibelli, P., and Kong, L. (2002). CD4 Regulatory T Cells Prevent Lethal Autoimmunity in IL-2R β -Deficient Mice. *Immunity* *17*, 167–178.
- Manicassamy, S., Reizis, B., Ravindran, R., Nakaya, H., Salazar-Gonzalez, R.M., Wang, Y.C., and Pulendran, B. (2010). Activation of beta-catenin in dendritic cells regulates immunity versus tolerance in the intestine. *Science* *329*, 849-853.
- Manz, M.G., Traver, D., Miyamoto, T., Weissman, I.L., and Akashi, K. (2001). Dendritic cell potentials of early lymphoid and myeloid progenitors. *Blood* *97*, 3333-3341.
- Maraskovsky, E., Brasel, K., Teepe, M., Roux, E.R., Lyman, S.D., Shortman, K., and McKenna, H.J. (1996). Dramatic increase in the numbers of functionally mature dendritic cells in Flt3 ligand-treated mice: multiple dendritic cell subpopulations identified. *J Exp Med* *184*, 1953-1962.
- Masopust, D., Vezys, V., Marzo, A.L., and Lefrancois, L. (2001). Preferential localization of effector memory cells in nonlymphoid tissue. *Science* *291*, 2413-2417.
- Masuda, A., Yoshikai, Y., Aiba, K., and Matsuguchi, T. (2002). Th2 cytokine production from mast cells is directly induced by lipopolysaccharide and distinctly regulated by c-Jun N-terminal kinase and p38 pathways. *J Immunol* *169*, 3801-3810.

- Mayer, C. T., Berod, L. and Sparwasser, T. (2012). Layers of dendritic cell-mediated T cell tolerance, their regulation and the prevention of autoimmunity. *Front Immunol* 3: 183.
- McGuirk, P., McCann, C., and Mills, K. H. (2002). Pathogen- specific T regulatory 1 cells induced in the respiratory tract by a bacterial molecule that stimulates interleukin 10 production by dendritic cells: a novel strategy for evasion of protective T helper type 1 responses by *Bordetella pertussis*. *J. Exp. Med.* 195, 221–231.
- McWilliam, A.S., Napoli, S., Marsh, A.M., Pemper, F.L., Nelson, D.J., Pimm, C.L., Stumbles, P.A., Wells, T.N., and Holt, P.G. (1996). Dendritic cells are recruited into the airway epithelium during the inflammatory response to a broad spectrum of stimuli. *J Exp Med.* 184, 2429-2432.
- Medzhitov, R. (2007). Recognition of microorganisms and activation of the immune response. *Nature* 449, 819–826.
- Meier, J.L. and Stinski, M.F. (2013). Major immediate-early enhancer and its gene products. In *Cytomegalovirus: From Molecular Pathogenesis to Intervention*, M.J. Reddehase, ed. (Wymondham, Norfolk, United Kingdom: Caister Academic Press), pp. 152-173.
- Melief, C.J.M. (2008). Cancer immunotherapy by dendritic cells. *Immunity* 29, 372-83.
- Mellman, I., and Steinman, R.M. (2001). Dendritic cells: specialized and regulated antigen processing machines. *Cell* 106, 255-258.
- Merad, M., Sathe, P., Helft, J., Miller, J., and Mortha, A. The dendritic cell lineage: ontogeny and function of dendritic cells and their subsets in the steady state and the inflamed setting. *Annu Rev Immunol* 31, 563–604 (2013).
- Mescher, M.F., Curtsinger, J.M., Agarwal, P., Casey, K.A., Gerner, M., Hammerbeck, C.D., Popescu, F., and Xiao, Z. (2006). Signals required for programming effector and memory development by CD8+ T cells. *Immunol Rev* 211, 81-92.
- Meylan, E., Tschopp, J., and Karin, M. (2006). Intracellular pattern recognition receptors in the host response. *Nature* 442, 39-44.
- Mildner, A., and Jung, S. (2014). Development and function of dendritic cell subsets. *Immunity* 40, 642-656.

- Milho, R., Frederico, B., Efstathiou, S., and Stevenson, G. (2012). A Heparan-Dependent Herpesvirus Targets the Olfactory Neuroepithelium for Host Entry. *PLoS Pathog* 8, e1002986.
- Miller, W. J., Mccullough, J., Balfour, H. H., Haake, R. J., Ramsay, N. K., Goldman, A., Bowman, R., and Kersey, J. (1991). Prevention of cytomegalovirus infection following bone marrow transplantation: a randomized trial of blood product screening. *Bone marrow transplantation* 7, 227–234.
- Mocarski, E. (1996). Cytomegalovirus and their Replication. In: *Virology* (B.N.Fields, D.M.Knipe, and P.M. Howley, eds.), Lippincott-Raven Publishers, Philadelphia, pp. 2447-2492.
- Mocarski, E.S., Jr. (2002). Immunomodulation by cytomegaloviruses: manipulative strategies beyond evasion. *Trends Microbiol* 10, 332-339.
- Mocarski, E.S., and C.T. Courcelle. 2001. Cytomegaloviruses and their replication. In: *Virology* (D.M. Knipe, and P.M. Howley, eds.). Lippincott-Raven, Philadelphia, pp. 2629-2673.
- Mocarski, E. S., T. Shenk, and R. F. Pass (2007). Cytomegaloviruses. In: *Virology* (D.M. Knipe, and P.M. Howley, eds.), Lippincott-Raven, Philadelphia, pp. 2701-22772.
- Moore, K. W., O'Garra, A., de Waal Malefyt, R., Vieira, P., and Mosmann, T.R (1993). Interleukin-10. *Annu Rev Immunol* 11, 165–190.
- Moore, K.W., de Waal Malefyt, R., Coffman, R.L., and O'Garra, A. (2001). Interleukin-10 and the interleukin-10 receptor. *Annu Rev Immunol* 19, 683-765.
- Munks, M.W., Cho, K.S., Pinto, A.K., Siero, S., Klenerman, P., and Hill, A.B. (2006). Four distinct patterns of memory CD8 T cell responses to chronic murine cytomegalovirus infection. *J Immunol* 177, 450-458.
- Murali-Krishna, K., Altman, J.D., Suresh, M., Sourdive, D., Zajac, A., and Ahmed, R. (1998). In vivo dynamics of anti-viral CD8 T cell responses to different epitopes. An evaluation of bystander activation in primary and secondary responses to viral infection. *Adv Exp Med Biol* 452, 123-142.
- Murphy, E., Rigoutsos, I., Shibuya, T., and Shenk, T.E. (2003). Reevaluation of human cytomegalovirus coding potential. *Proc Natl Acad Sci U S A* 100, 13585-13590.

- Murphy, K.M. (2013). Transcriptional control of dendritic cell development. *Adv Immunol* 120, 239-267.
- Murray, P.J. (2007). The JAK-STAT signaling pathway: input and output integration. *J Immunol* 178, 2623-2629.
- Naik, S.H., Metcalf, D., van Nieuwenhuijze, A., Wicks, I., Wu, L., O'Keeffe, M., and Shortman, K. (2006). Intrasplenic steady-state dendritic cell precursors that are distinct from monocytes. *Nat Immunol* 7, 663-671.
- Naik, S.H., Sathe, P., Park, H.Y., Metcalf, D., Proietto, A.I., Dakic, A., Carotta, S., O'Keeffe, M., Bahlo, M., Papenfuss, A., *et al.* (2007). Development of plasmacytoid and conventional dendritic cell subtypes from single precursor cells derived in vitro and in vivo. *Nat Immunol* 8, 1217-1226.
- Nakano, H., Yanagita, M., and Gunn, M.D. (2001). CD11c(+)B220(+)Gr-1(+) cells in mouse lymph nodes and spleen display characteristics of plasmacytoid dendritic cells. *J Exp Med* 194, 1171-1178.
- Nauerth, M., Weißbrich, B., Knall, R., Franz, T., Dössinger, G., Bet, J., Paszkiewicz, P.J., Pfeifer, L., Bunse, M., and Uckert, W. (2013). TCR-ligand ko rate correlates with the protective capacity of antigen-specific CD8+ T cells for adoptive transfer. *Sci Transl Me.* 2013, 5, 192ra87.
- Neinamn, P. E., Reeves, W., Ray, G., Flournoy, N., Lerner, K. G., Sale, G. E., and Thomas, E. D. (1977). A prospective analysis interstitial pneumonia and opportunistic viral infection among recipients of allogeneic bone marrow grafts. *J Infect Dis* 136, 754– 767.
- Nelson, W.J. (2008). Regulation of cell-cell adhesion by the cadherin-catenin complex. *Biochem Soc Trans* 36, 149-155.
- Newton, A.H., Cardani, A., and Braciale, T.J. (2016). The host immune response in respiratory virus infection: balancing virus clearance and immuno- pathology. *Semin Immunopathol* 38, 471–482.
- Neyt, K., and Lambrecht, B.N. (2013). The role of lung dendritic cell subsets in immunity to respiratory viruses. *Immunol Rev* 255, 57-67.

- Niederlova, V., Tsyklauri, O., Chadimova, T., and Stepanek O. (2021). CD8⁺ Tregs revisited: A heterogeneous population with different phenotypes and properties. *J Immunol* 191, 512–530.
- Nigam, P., Velu, V., Kannanganat, S., Chennareddi, L., Kwa, S., Siddiqui, M., and Amara, R.R. (2010). Expansion of FOXP3⁺ CD8 T cells with suppressive potential in colorectal mucosa following a pathogenic simian immunodeficiency virus infection correlates with diminished antiviral T cell response and viral control. *J Immunol* 184, 1690-1701.
- Nishimura, H., Okazaki, T., Tanaka, Y., Nakatani, K., Hara, M., Matsumori, A., Sasayama, S., Mizoguchi, A., Hiai, H., Minato, N., and Honjo T. (2001). Autoimmune dilated cardiomyopathy in PD-1 receptor-deficient mice. *Science* 291, 319–322.
- Northfield, J., Lucas, M., Jones, H., Young, N.T., and Klenerman, P. (2005). Does memory improve with age? CD85j (ILT-2/LIR-1) expression on CD8 T cells correlates with 'memory inflation' in human cytomegalovirus infection. *Immunol Cell Biol* 83, 182-188.
- O'Garra, A., and Vieira, P. (2007). T(H)1 cells control themselves by producing interleukin-10. *Nat Rev Immunol* 7, 425-428.
- Obar, J.J., Jellison, E.R., Sheridan, B.S., Blair, D.A., Pham, Q.M., Zickovich, J.M., and Lefrancois, L. (2011). Pathogen-induced inflammatory environment controls effector and memory CD8⁺ T cell differentiation. *J Immunol* 187, 4967-4978.
- Obar, J.J., and Lefrancois, L. (2010a). Early events governing memory CD8⁺ T-cell differentiation. *Int Immunol* 22, 619-625.
- Obar, J.J., and Lefrancois, L. (2010b). Memory CD8⁺ T cell differentiation. *Ann N Y Acad Sci* 1183, 251-266.
- Ochs, H.D., Ziegler, S.F., and Torgerson, T.R. (2005). FOXP3 acts as a rheostat of the immune response. *Immunol Rev* 203, 156-164.
- O'Garra, A., Barrat, F.J., Castro, A.G., Vicari, A., and Hawrylowicz, C. (2008). Strategies for use of IL-10 or its antagonists in human disease. *Immunol Rev* 223, 114–131.
- Ogawa-Goto, K., Tanaka, K., Gibson, W., Moriishi, E., Miura, Y., Kurata, T., Irie, S., and Sata, T. (2003). Microtubule network facilitates nuclear targeting of human cytomegalovirus capsid. *J Virol* 77, 8541-8547.

- Ohl, L., Mohaupt, M., Czeloth, N., Hintzen, G., Kiafard, Z., Zwirner, J., Blankenstein, T., Henning, G., and Forster, R. (2004). CCR7 governs skin dendritic cell migration under inflammatory and steady-state conditions. *Immunity* 21, 279-288.
- Ohta, T., Sugiyama, M., Hemmi, H., Yamazaki, C., Okura, S., Sasaki, I., Fukuda, Y., Orimo, T., Ishii, K.J., Hoshino, K., Ginhoux, F., and Kaisho, T. (2016). Crucial roles of XCR1-expressing dendritic cells and the XCR1-XCL1 chemokine axis in intestinal immune homeostasis. *Sci Rep* 6, 23505.
- Ojala, P.M., Sodeik, B., Ebersold, M.W., Kutay, U., and Helenius, A. (2000). Herpes simplex virus type 1 entry into host cells: reconstitution of capsid binding and uncoating at the nuclear pore complex in vitro. *Mol Cell Biol* 20, 4922-4931.
- Onai, N., Kurabayashi, K., Hosoi-Amaiike, M., Toyama-Sorimachi, N., Matsushima, K., Inaba, K., and Ohteki, T. (2013). A clonogenic progenitor with prominent plasmacytoid dendritic cell developmental potential. *Immunity* 38, 943-957.
- Onai, N., Obata-Onai, A., Tussiwand, R., Lanzavecchia, A., and Manz, M.G. (2006). Activation of the Flt3 signal transduction cascade rescues and enhances type I interferon-producing and dendritic cell development. *J Exp Med* 203, 227-238.
- Ota, C., Baarsma, H.A., Wagner, D.E., Hilgendorff, A., and Konigshoff, M. (2016). Linking bronchopulmonary dysplasia to adult chronic lung diseases: role of WNT signaling. *Mol Cell Pediatr* 3, 34.
- Pahl-Seibert, M.F., Juelch, M., Podlech, J., Thomas, D., Deegen, P., Reddehase, M.J., and Holtappels, R. (2005). Highly protective in vivo function of cytomegalovirus IE1 epitope-specific memory CD8 T cells purified by T-cell receptor-based cell sorting. *J Virol* 79, 5400-5413.
- Pandiyani, P., Conti, H. R., Zheng, L., Peterson, A. C., Mathern, D. R., Hernandez-Santos, N., Edgerton, M., Gaffen, S. L., and Lenardo, M. J. (2011). CD4(+)CD25(+)Foxp3(+) regulatory T cells promote Th17 cells in vitro and enhance host resistance in mouse *Candida albicans* Th17 cell infection model. *Immunity* 34, 422-434.
- Pastore, D., Delia, M., Mestice, A., Perrone, T., Carluccio, P., Gaudio, F., Giordano, A., Rossi, A.R., Ricco, A., Leo, M., *et al.* (2011). Recovery of CMV-specific CD8+ T cells and Tregs

after allogeneic peripheral blood stem cell transplantation. *Biol Blood Marrow Transplant* 17, 550-557.

Persson, E.K., Uronen-Hansson, H., Semmrich, M., Rivollier, A., Hagerbrand, K., Marsal, J., Gudjonsson, S., Hakansson, U., Reizis, B., Kotarsky, K., and Agace, W.W. (2013). IRF4 transcription-factor-dependent CD103(+)CD11b(+) dendritic cells drive mucosal T helper 17 cell differentiation. *Immunity* 38, 958-969.

Pils, M. C., Pisano, F., Fasnacht, N., Heinrich, J.M., Groebe, L., Schippers, A., Rozell, B., Jack, R.S., and Mueller, W. (2010). Monocytes/macrophages and/or neutrophils are the target of IL-10 in the LPS endotoxemia model. *Eur J Immunol* 40, 443–448.

Plummer, G. (1967). Comparative virology of the herpes group. *Prog Med Virol* 9, 302-340.

Pober, J.S., Merola, J., Liu, R., and Manes, T.D. (2017). Antigen Presentation by Vascular Cells. *Front Immunol* 8, 1907.

Polansky, J. K., and Huehn J. (2007). To be or not to be a Treg: Epigenetische Regulation der Foxp3-Expression in regulatorischen T-Zellen. *Zeitschrift für Rheumatologie* 66, 417–420.

Polic, B., Hengel, H., Krmpotic, A., Trgovcich, J., Pavic, I., Luccaronin, P., Jonjic, S., and Koszinowski, U.H. (1998). Hierarchical and redundant lymphocyte subset control precludes cytomegalovirus replication during latent infection. *J Exp Med* 188, 1047-1054.

Pomie, C., Menager-Marcq, I., and van Meerwijk, J. P. M. V (2008). Murine CD8⁺ regulatory T lymphocytes: the new era. *Hum Immunol* 69, 708–714.

Pooley, J.L., Heath, W.R., and Shortman, K. (2001). Cutting edge: intravenous soluble antigen is presented to CD4 T cells by CD8-dendritic cells, but cross-presented to CD8 T cells by CD8⁺ dendritic cells. *J Immunol* 166, 5327-30.

Popescu, I., Macedo, C., Abu-Elmagd, K., Shapiro, R., Hua, Y., Thomson, A.W., Morelli, A.E., Storkus, W.J., and Metes, D. (2007). EBV-specific CD8⁺ T cell reactivation in transplant patients results in expansion of CD8⁺ type-1 regulatory T cells. *Am J Transplant* 7, 1215-1223.

Potena, L., and Valantine, H.A. (2007). Cytomegalovirus-associated allograft rejection in heart transplant patients. *Curr Opin Infect Dis* 20, 425-431.

- Powers, C. DeFilippis, V., Malouli, D., and Früh, K. (2008). Cytomegalovirus immune evasion. *Curr Top Microbiol Immunol* 325, 333–359.
- Price, P., Allcock, R.J., Coombe, D.R., Sgellam, G.R., and McCluskey, J. (1995). MHC proteins and heparan sulphate proteoglycans regulate murine cytomegalovirus infection. *Immunol Cell Biol* 73, 308-15.
- Prosch, S., Wuttke, R., Kruger, D.H., and Volk, H.D. (2002). NF-kappaB--a potential therapeutic target for inhibition of human cytomegalovirus (re)activation? *Biol Chem* 383, 1601-1609.
- Punkosdy, G.A., Blain, M., Glass, D.D., Lozano, M.M., O'Mara, L., and Dudley, J.P. (2011). Regulatory T-cell expansion during chronic viral infection is dependent on endogenous retroviral superantigens. *Proc Natl Acad Sci USA* 108, 3677–3682.
- Puttur, F., Francozo, M., Solmaz, G., Bueno, C., Lindenberg, M., Gohmert, M., Swallow, M., Tufa, D., Jacobs, R., and Lienenklaus, S. (2016). Conventional dendritic cells confer protection against mouse cytomegalovirus infection via TLR9 and MyD88 signaling. *Cell Rep* 17, 1113–27.
- Quinnan, G. V., Manischewitz, J.E., and Ennis, F. A. (1978). Cytotoxic T lymphocyte response to murine cytomegalovirus infection. *Nature* 273, 541-3.
- Quirici, N., Soligo, D., Caneva, L., Servida, F., Bossolasco, P., and Deliliers, G.L. (2001). Differentiation and expansion of endothelial cells from human bone marrow CD133(+) cells. *Br J Haematol* 115, 186-194.
- Rammensee, H. G., Falk, K., and Roetzschke, O (1993). Peptides naturally presented by MHC class I molecules. *Annu Rev Immunol* 11, 213–244.
- Randolph, G. J., Angeli, V., and Swartz, M.A. (2005). Dendritic-cell trafficking to lymph nodes through lymphatic vessels. *Nat Rev Immunol* 5, 617–628.
- Rawlinson, W.D., Farrell, H.E., and Barrell, B.G. (1996). Analysis of the complete DNA sequence of murine cytomegalovirus. *J Virol* 70, 8833-8849.

- Redpath, S., Angulo, A., Gascoigne, N.R., Ghazal, P. (1999). Murine cytomegalovirus infection down-regulates MHC class II expression on macrophages by induction of IL-10. *J Immunol* *162*, 6701–6707.
- Reddehase, M.J. (2002). Antigen and immunoevasin: opponents in cytomegalovirus immune surveillance. *Nat Rev Immunol* *2*, 831-844.
- Reddehase, M.J. (2019). Adverse immunological imprinting by cytomegalovirus sensitizing for allergic airway disease. *Med Microbiol Immunol* *208*, 469-473.
- Reddehase, M.J., Baltesen, M., Rapp, M., Jonjic, S., Pavic, I., and Koszinowski, U.H. (1994). The conditions of primary infection define the load of latent viral genome in organs and the risk of recurrent cytomegalovirus disease. *J Exp Med* *179*, 185-193.
- Reddehase, M.J., and Lemmermann, N.A.W. (2018). Mouse Model of Cytomegalovirus Disease and Immunotherapy in the Immunocompromised Host: Predictions for Medical Translation that Survived the "Test of Time". *Viruses* *10*.
- Reddehase, M.J., and Lemmermann, N.A.W. (2019). Cellular reservoirs of latent cytomegaloviruses. *Med Microbiol Immunol* *208*, 391–403.
- Reddehase, M.J., Podlech, J., and Grzimek, N.K. (2002). Mouse models of cytomegalovirus latency: overview. *J Clin Virol* *25 Suppl 2*, S23-36.
- Reddehase, M.J., Weiland, F., Munch, K., Jonjic, S., Luske, A., and Koszinowski, U.H. (1985). Interstitial murine cytomegalovirus pneumonia after irradiation: characterization of cells that limit viral replication during established infection of the lungs. *J Virol* *55*, 264-273.
- Redeker, A., Welten, S. P. and Arens, R. (2014). Viral inoculum dose impacts memory T-cell inflation. *Eur J Immunol* *44*, 1046–1057.
- Reuter, S., Lemmermann, N.A.W., Maxeiner, J., Podlech, J., Beckert, H., Freitag, K., Teschner, D., Ries, F., Taube, C., Buhl, R., *et al.* (2019). Coincident airway exposure to low-potency allergen and cytomegalovirus sensitizes for allergic airway disease by viral activation of migratory dendritic cells. *PLoS Pathog* *15*, e1007595.

- Riddell, S. R., Watanabe, K. S., Goodrich, J. M., Li, C. R., Agha, M. E., and Greenberg, P. D. (1992). Restoration of viral immunity in immunodeficient humans by the adoptive transfer of T cell clones. *Science* 257, 238–241.
- Rifa'i, M., Shi, Z., Zhang, S.Y., Lee, Y. H., Shiku, H., Isobe, K.I., and Suzuki, H. (2008). CD8+CD122+ regulatory T cells recognize activated T cells via conventional MHC class I-alpha/beta-TCR interaction and become IL-10-producing active regulatory cells. *International Immunol* 20, 937–947.
- Robb, R. J., Lineburg, K. E., Kuns, R. D., Wilson, Y. A., Raffelt, N. C., Oliver, S. D., Varelias, A., Alexander, K. A., Teal, B. E., Sparwasser, T., Hammerling, G. J., Markey, K. A., Koyama, M., Clouston, A. D., Engwerda, C. R., Hill, G. R., and MacDonald, K. P. A. (2012). Identification and expansion of highly suppressive CD8(+)FoxP3(+) regulatory T cells after experimental allogeneic bone marrow transplantation. *Blood* 119, 5898–5908.
- Rock, K.L., York, I.A., Saric, T., and Goldberg, A.L. (2002). Protein degradation and the generation of MHC class I-presented peptides. *Adv Immunol* 80, 1-70.
- Roers, A., Siewe, L., Strittmatter, E., Deckert, M., Schlueter, D., Stenzel, W., Gruber, A.D., Krieg, T., Rajewsky, K., and Mueller, W. (2004). T cell-specific inactivation of the interleukin 10 gene in mice results in enhanced T cell responses but normal innate responses to lipopolysaccharide or skin irritation. *J Exp Med* 200, 1289–1297.
- Roetzschke, O., Falk, K., Deres, H., Schild, M., Norda, J., Metzger, G., Jung, and H. G. Rammensee (1990). Isolation and analysis of naturally processed viral peptides as recognized by cytotoxic T cells. *Nature* 348, 252–254.
- Rogers, N. C., Slack, E.C., Edwards, A.D., Nolte, M.A., Schulz, O., Schweighoffer, E., Williams, D.L., Gordon, S., Tybulewicz, V.L., Brown, G.D., and Reis e Sousa, C. (2005). Syk-dependent cytokine induction by Dectin-1 reveals a novel pattern recognition pathway for C type lectins. *Immunity* 22, 507–517.
- Roizman, B. (1979). The structure and isomerization of herpes simplex virus genomes. *Cell* 16, 481-494.
- Roizman, B., and Baines, J. (1991). The diversity and unity of Herpesviridae. *Comp Immunol Microbiol Infect Dis* 14, 63-79.

- Roizman, B., Carmichael, L.E., Deinhardt, F., de-The, G., Nahmias, A.J., Plowright, W., Rapp, F., Sheldrick, P., Takahashi, M., and Wolf, K. (1981). Herpesviridae. Definition, provisional nomenclature, and taxonomy. The Herpesvirus Study Group, the International Committee on Taxonomy of Viruses. *Intervirology* 16, 201-217.
- Roizmann, B., Desrosiers, R.C., Fleckenstein, B., Lopez, C., Minson, A.C., and Studdert, M.J. (1992). The family Herpesviridae: an update. The Herpesvirus Study Group of the International Committee on Taxonomy of Viruses. *Arch Virol* 123, 425-449.
- Rubin, R.H. (1990). Impact of cytomegalovirus infection on organ transplant recipients. *Rev Infect Dis* 12 Suppl 7, S754-766.
- Rudolph, M.G., Stanfield, R.L., and Wilson, I.A. (2006). How TCRs bind MHCs, peptides, and coreceptors. *Annu Rev Immunol* 24, 419-466.
- Saban, D.R. (2014). The chemokine receptor CCR7 expressed by dendritic cells: a key player in corneal and ocular surface inflammation. *Ocul Surf* 12, 87-99.
- Sacher, T., Jordan, S., Mohr, C.A., Vidy, A., Weyn, A.M., Ruszics, Z., and Koszinowski, U.H. (2008). Conditional gene expression systems to study herpesvirus biology in vivo. *Med Microbiol Immunol* 197, 269-276.
- Saeki, H., Moore, A.M., Brown, M.J., and Hwang, S.T. (1999). Cutting edge: secondary lymphoid-tissue chemokine (SLC) and CC chemokine receptor 7 (CCR7) participate in the emigration pathway of mature dendritic cells from the skin to regional lymph nodes. *J Immunol* 162, 2472-2475.
- Sakaguchi, S., Sakaguchi, N., Asano, M., Itoh, M., and Toda, M. (1995). Immunologic self-tolerance maintained by activated T cells expressing IL-2 receptor alpha-chains (CD25). Breakdown of a single mechanism of self-tolerance causes various autoimmune diseases. *J Immunol* 155, 1151-1164.
- Sakaguchi, S., Yamaguchi, T., Nomura, T., and Ono, M. (2008). Regulatory T cells and immune tolerance. *Cell* 133, 775-787.
- Saligrama, N., Zhao, F., Sikora, M. J., Serratelli, W. S., RFernandes, . A., Louis, D. M., Yao, W., Ji, X., Idoyaga, J., Mahajan, V. B., Steinmetz, L. M., Chien, Y.-H., Hauser, S. L.,

- Oksenberg, J. R., Garcia, K. C., and Davis, M. M. (2019). Opposing T cell responses in experimental autoimmune encephalomyelitis. *Nature* 572, 481–487.
- Sallusto, F., Cella, M., Danieli, C., and Lanzavecchia, A. (1995). Dendritic cells use macropinocytosis and the mannose receptor to concentrate macromolecules in the major histocompatibility complex class II compartment: downregulation by cytokines and bacterial products. *J Exp Med* 182, 389-400.
- Sanchez, V., Greis, K.D., Sztul, E., and Britt, W.J. (2000). Accumulation of virion tegument and envelope proteins in a stable cytoplasmic compartment during human cytomegalovirus replication: characterization of a potential site of virus assembly. *J Virol* 74, 975-986.
- Santin, A.D., Hermonat, P.L., Ravaggi, A., Bellone, S., Pecorelli, S., Roman, J.J., Parham, G.P., and Cannon, M.J. (2000). Interleukin-10 increases Th1 cytokine production and cytotoxic potential in human papillomavirus-specific CD8(+) cytotoxic T lymphocytes. *J Virol* 74, 4729-4737.
- Sapozhnikov, A., Fischer, J.A., Zaft, T., Krauthgamer, R., Dzionek, A., and Jung, S. (2007). Organ-dependent in vivo priming of naive CD4+, but not CD8+, T cells by plasmacytoid dendritic cells. *J Exp Med* 204, 1923-1933.
- Saraiva, M., and O'Garra, A. (2010). The regulation of IL-10 production by immune cells. *Nat Rev Immunol* 10, 170-181.
- Sarangi, P.P., Sehrawat, S., Suvas, S., and Rouse, B.T. (2008). IL-10 and natural regulatory T cells: two independent anti-inflammatory mechanisms in herpes simplex virus-induced ocular immunopathology. *J Immunol* 180, 6297-6306.
- Sathe, P., Metcalf, D., Vremec, D., Naik, S.H., Langdon, W.Y., Huntington, N.D., Wu, L., and Shortman, K. (2014). Lymphoid tissue and plasmacytoid dendritic cells and macrophages do not share a common macrophage-dendritic cell-restricted progenitor. *Immunity* 41, 104-115.
- Schlitzer, A., McGovern, N., Teo, P., Zelante, T., Atarashi, K., Low, D., Ho, A.W., See, P., Shin, A., Wasan, P.S., *et al.* (2013). IRF4 transcription factor-dependent CD11b+ dendritic cells in human and mouse control mucosal IL-17 cytokine responses. *Immunity* 38, 970-983.
- Schluns, K.S., Kieper, W.C., Jameson, S.C., and Lefrancois, L. (2000). Interleukin-7 mediates the homeostasis of naive and memory CD8 T cells in vivo. *Nat Immunol* 1, 426-432.

- Schmidt, A., Oberle, N., and Krammer, P.H. (2012). Molecular mechanisms of treg-mediated T cell suppression. *Front Immunol* 3, 51.
- Schneider, C., Nobs, S.P., Heer, A.K., Kurrer, M., Klinke, G., van Rooijen, N., Vogel, J., and Kopf, M. (2014). Alveolar macrophages are essential for protection from respiratory failure and associated morbidity following influenza virus infection. *PLoS Pathog* 10, e1004053.
- Schottstedt, V., Blumel, J., Burger, R., Drosten, C., Groner, A., Gurtler, L., Heiden, M., Hildebrandt, M., Jansen, B., Montag-Lessing, T., *et al.* (2010). Human Cytomegalovirus (HCMV) - Revised. *Transfus Med Hemother* 37, 365-375.
- Schuler, G., and Steinman, R.M. (1985). Murine epidermal Langerhans cells mature into potent immunostimulatory dendritic cells in vitro. *J Exp Med* 161, 526-546.
- Schwele, S., Fischer, A. M., Brestrich, G., Wlodarski, M. W., Wagner, L., Schmueck, M., Roemhild, A., Thomes, S., Hammer, M. H., Babel, N., Kurtz, A., Maciejewski, J.P., Reinke, P., and Volk, H.D. (2012). Cytomegalovirus-specific regulatory and effector T cells share TCR clonality--possible relation to repetitive CMV infections. *J Transplant* 12, 669–681.
- Sebastian, M., Lopez-Ocasio, M., Metidji, A., Rieder, S.A., Shevach, E.M., and Thornton, A.M. (2016). Helios Controls a Limited Subset of Regulatory T Cell Functions. *J Immunol* 196, 144-155.
- Seckert, C.K., Griessl, M., Buttner, J.K., Scheller, S., Simon, C.O., Kropp, K.A., Renzaho, A., Kuhnappel, B., Grzimek, N.K., and Reddehase, M.J. (2012). Viral latency drives 'memory inflation': a unifying hypothesis linking two hallmarks of cytomegalovirus infection. *Med Microbiol Immunol* 201, 551-566.
- Seckert, C.K., Renzaho, A., Tervo, H.M., Krause, C., Deegen, P., Kuhnappel, B., Reddehase, M.J., and Grzimek, N.K. (2009). Liver sinusoidal endothelial cells are a site of murine cytomegalovirus latency and reactivation. *J Virol* 83, 8869-8884.
- Seckert, C.K., Schader, S.I., Ebert, S., Thomas, D., Freitag, K., Renzaho, A., Podlech, J., Reddehase, M.J., and Holtappels, R. (2011). Antigen-presenting cells of haematopoietic origin prime cytomegalovirus-specific CD8 T-cells but are not sufficient for driving memory inflation during viral latency. *J Gen Virol* 92, 1994-2005.

- Shanley, J.D., and Pesanti, E.L., (1985). The Relation of Viral Replication to Interstitial Pneumonitis in Murine Cytomegalovirus Lung Infection. *J Infect Dis* *151*, 454-458.
- Shen, L., and Rock, K.L. (2006). Priming of T cells by exogenous antigen cross-presented on MHC class I molecules. *Curr Opin Immunol* *18*, 85-91.
- Shevach, E. M. (2009). Mechanisms of foxp3+ T regulatory cell-mediated suppression. *Immunity* *30*, 636–645.
- Shevach, E.M., McHugh, R.S., Piccirillo, C.A., and Thornton, A.M. (2001). Control of T-cell activation by CD4+ CD25+ suppressor T cells. *Immunol Rev* *182*, 58-67.
- Shevryev, D., and Tereshchenko, V. (2019). Treg Heterogeneity, Function, and Homeostasis. *Front Immunol* *10*, 3100.
- Shimizu, J., Yamazaki, S., and Sakaguchi, S. (1999). Induction of tumor immunity by removing CD25+CD4+ T cells: a common basis between tumor immunity and autoimmunity. *J Immunol* *163*, 5211–5218.
- Shivkumar, M., Milho, R., May, J.S., Nicoll, M.P., Efstathiou, S., and Stevenson, P.G. (2013). Herpes simplex virus 1 targets the murine olfactory neuroepithelium for host entry. *J Virol* *87*, 10477-88.
- Shouval, D.S., Ouahed, J., Biswas, A., Goettel, J.A., Horwitz, B.H., Klein, C., Muise, A.M., and Snapper, S.B. (2014). Interleukin 10 receptor signaling: master regulator of intestinal mucosal homeostasis in mice and humans. *Adv Immunol* *122*, 177-210.
- Sichien, D., Lambrecht, B.N., Guilliams, M., and Scott, C.L. (2017). Development of conventional dendritic cells: from common bone marrow progenitors to multiple subsets in peripheral tissues. *Mucosal Immunol* *10*, 831-844.
- Simon, C. O., Seckert, C.K., Grzimek, N.K., and Reddehase, M.J. (2006). Murine model of cytomegalovirus latency and reactivation: the silencing/desilencing and immune sensing hypothesis. In *Cytomegaloviruses: molecular biology and immunology*, M.J. Reddehase, ed. (Wymondham, Norfolk, Caister Academic Press), pp. 483-500.

- Sinclair, J., and Sissons, P. (2006). Latency and reactivation of human cytomegalovirus. *J Gen Virol* 87, 1763-1779.
- Singh, N., Dummer, J. S., Kusne, S., Breinig, M. K., Armstrong, A., Makowka, L., Starzl, T. E., and Ho, M. (1988). Infections with cytomegalovirus and other herpesviruses in 121 liver transplant recipients: transmission by donated organ and the effect of OKT3 antibodies. *J Infect Dis* 158, 124–131.
- Snyder, C.M., Cho, K.S., Bonnett, E.L., van Dommelen, S., Shellam, G.R., and Hill, A.B. (2008). Memory inflation during chronic viral infection is maintained by continuous production of short-lived, functional T cells. *Immunity* 29, 650-659.
- Soderberg, C., Larsson, S., Bergstedt-Lindqvist, S., and Moller, E. (1993). Definition of a subset of human peripheral blood mononuclear cells that are permissive to human cytomegalovirus infection. *J Virol* 67, 3166-3175.
- Soderberg-Naucler, C., and Nelson, J.Y. (1999). Human cytomegalovirus latency and reactivation - a delicate balance between the virus and its host's immune system. *Intervirology* 42, 314-321.
- Spencer, S.D., Di Marco, F., Hooley, J., Pitts-Meek, S., Bauer, M., Ryan, A.M., Sordat, B., Gibbs, V.C., and Aguet, M. (1998). The orphan receptor CRF2-4 is an essential subunit of the interleukin 10 receptor. *J Exp Med* 187, 571-578.
- Stahl, F. R., Heller, K., Halle, S., Keyser, K. A., Busche, A., Marquardt, A., Wagner, K., Boelter, J., Bischoff, Y., Kremmer, K.A., Arens, R., Messerle, M. and Foerster, R. (2013). Nodular inflammatory foci are sites of T cell priming and control of murine cytomegalovirus infection in the neonatal lung. *PLoS Pathog* 9, e1003828.
- Stahl, F.R., Keyser, K.A., Heller, K., Bischoff, Y., Halle, S., Wagner, K., Messerle, M.I., and Foerster, M. (2015). M Mck2-dependent infection of alveolar macrophages promotes replication of MCMV in nodular inflammatory foci of the neonatal lung. *Mucosal Immunol* 8, 57-67.
- Steinbrink, K., Wolfl, M., Jonuleit, H., Knop, J., and Enk, A.H. (1997). Induction of tolerance by IL-10-treated dendritic cells. *J Immunol* 159, 4772-4780.

- Steinman, R.M. (1991). The dendritic cell system and its role in immunogenicity. *Annu rev Immunol* *9*, 271-96.
- Steinman, R.M., and Cohn, Z.A. (1973). Identification of a novel cell type in peripheral lymphoid organs of mice. I. Morphology, quantitation, tissue distribution. *J Exp Med* *137*, 1142-1162.
- Steinman, R.M., Pack, M., and Inaba, K. (1997). Dendritic cells in the T-cell areas of lymphoid organs. *Immunol Rev* *156*, 25-37.
- Stemberger, C., Neuenhahn, M., Gebhardt, F.E., Schiemann, M., Buchholz, V.R., and Busch, D.H. (2009). Stem cell-like plasticity of naive and distinct memory CD8⁺ T cell subsets. *Semin Immunol* *21*, 62-68.
- Stern-Ginossar, N., Weisburd, B., Michalski, A., Le, V.T., Hein, M.Y., Huang, S.X., Ma, M., Shen, B., Qian, S.B., Hengel, H. (2012). Decoding human cytomegalovirus. *Science* *338*, 1088-1093.
- Streblow, D.N., S.M. Varnum, R.D. Smith, and J. A. Nelson (2006). A proteomics analysis in human cytomegalovirus particles. In *Cytomegaloviruses: molecular biology and immunology*, M.J. Reddehase, ed. (Wymondham, Norfolk, Caister Academic Press), pp. 91-110.
- Suh, W.K., Cohen-Doyle, M.F., Fruh, K., Wang, K., Peterson, P.A., and Williams, D.B. (1994). Interaction of MHC class I molecules with the transporter associated with antigen processing. *Science* *264*, 1322-1326.
- Sun, J., Madan, R., Karp, C.L., and Braciale, T.J. (2009). Effector T cells control lung inflammation during acute influenza virus infection by producing IL-10. *Nat Med* *15*, 277-284.
- Suryawanshi, A., Manoharan, I., Hong, Y., Swafford, D., Majumdar, T., Taketo, M.M., Manicassamy, B., Koni, P.A., Thangaraju, M., Sun, Z., *et al.* (2015). Canonical wnt signaling in dendritic cells regulates Th1/Th17 responses and suppresses autoimmune neuroinflammation. *J Immunol* *194*, 3295-3304.
- Suvas, S., Azkur, A. K., Kim, B. S., Kumaraguru, U., and Rouse B. T. (2004). CD4⁺CD25⁺ regulatory T cells control the severity of viral immunoinflammatory lesions. *J Immunol* *172*, 4123-4132.

- Swiecki, M., and Colonna, M. (2015). The multifaceted biology of plasmacytoid dendritic cells. *Nat Rev Immunol* 15, 471-485.
- Sylwester, A. W., Mitchell, B. L., Edgar, J. B., Taormina, C., Pelte, C., Ruchti, F., Sleath, P. R., Grabstein, K. H., Hosken, N. A., Kern, F., Nelson, J. A., and Picker, L. J. (2005). Broadly targeted human cytomegalovirus-specific CD4⁺ and CD8⁺ T cells dominate the memory compartments of exposed subjects. *J Exp Med* 202, 673– 685.
- Takemoto, N., Intlekofer, A.M., Northrup, J.T., Wherry, E.J., and Reiner, S.L. (2006). Cutting Edge: IL-12 inversely regulates T-bet and eomesodermin expression during pathogen-induced CD8⁺ T cell differentiation. *J Immunol* 177, 7515-7519.
- Tan, J.C., Indelicato, S.R., Narula, S.K., Zavodny, P.J., and Chou, C.C. (1993). Characterization of interleukin-10 receptors on human and mouse cells. *J Biol Chem* 268, 21053-21059.
- Tanchot, C., Guillaume, S., Delon, J., Bourgeois, C., Franzke, A., Sarukhan, A., Trautmann, A., and Rocha, B. (1998). Modifications of CD8⁺ T cell function during in vivo memory or tolerance induction. *Immunity* 8, 581-590.
- Tang, Q., Murphy, E.A., and Maul, G.G. (2006). Experimental confirmation of global murine cytomegalovirus open reading frames by transcriptional detection and partial characterization of newly described gene products. *J Virol* 80, 6873-6882.
- Taylor-Wiedeman, J., Hayhurst, G.P., Sissons, J.G., and Sinclair, J.H. (1993). Polymorphonuclear cells are not sites of persistence of human cytomegalovirus in healthy individuals. *J Gen Virol* 74 (Pt 2), 265-268.
- Taylor-Wiedeman, J., Sissons, J.G., Borysiewicz, L.K., and Sinclair, J.H. (1991). Monocytes are a major site of persistence of human cytomegalovirus in peripheral blood mononuclear cells. *J Gen Virol* 72 (Pt 9), 2059-2064.
- Terhune, S.S., Schroer, J., and Shenk, T. (2004). RNAs are packaged into human cytomegalovirus virions in proportion to their intracellular concentration. *J Virol* 78, 10390-10398.
- Tessmer, M.S., Fugere, C., Stevenaert, F., Naidenko, O.V., Chong, H.J., Leclercq, G., and Brossay, L. (2007). KLRG1 binds cadherins and preferentially associates with SHIP-1. *Int Immunol* 19, 391-400.

- Thornton, A.M., and Shevach, E.M. (1998). CD4⁺CD25⁺ immunoregulatory T cells suppress polyclonal T cell activation in vitro by inhibiting interleukin 2 production. *J Exp Med* 188, 287-296.
- Tolkoff-Rubin, N.E., Fishman, J.A., and Rubin, R.H. (2001). The bidirectional relationship between cytomegalovirus and allograft injury. *Transplant Proc* 33, 1773-1775.
- Tooze, J., Hollinshead, M., Reis, B., Radsak, K., and Kern, H. (1993). Progeny vaccinia and human cytomegalovirus particles utilize early endosomal cisternae for their envelopes. *Eur J Cell Biol* 60, 163-178.
- Torti, N., and Oxenius, A. (2012). T cell memory in the context of persistent herpes viral infections. *Viruses* 4, 1116-1143.
- Torti, N., Walton, S.M., Brocker, T., Rulicke, T., and Oxenius, A. (2011a). Non-hematopoietic cells in lymph nodes drive memory CD8 T cell inflation during murine cytomegalovirus infection. *PLoS Pathog* 7, e1002313.
- Torti, N., Walton, S.M., Murphy, K.M., and Oxenius, A. (2011b). Batf3 transcription factor-dependent DC subsets in murine CMV infection: differential impact on T-cell priming and memory inflation. *Eur J Immunol* 41, 2612-2618.
- Tovar-Salazar, A., and Weinberg, A. (2020). Understanding the mechanism of action of cytomegalovirus-induced regulatory T cells. *Virology* 547, 1–6.
- Trinchieri, G. (2007). Interleukin-10 production by effector T cells: Th1 cells show self control. *J Exp Med* 204, 239-243.
- Ueno, H., Klechevsky, E., Morita, R., Aspod, C., Cao, T., Matsui, T., Di Pucchio, T., Connolly, J., Fay, J.W., Pascual, V., *et al.* (2007). Dendritic cell subsets in health and disease. *Immunol Rev* 219, 118-142.
- Valenta, T., Hausmann, G., and Basler, K. (2012). The many faces and functions of beta-catenin. *EMBO J* 31, 2714-2736.
- van der Vliet, H.J., and Nieuwenhuis, E.E. (2007). IPEX as a result of mutations in FOXP3. *Clin Dev Immunol* 2007, 89017.

- Velu, V., Titanji, K., Zhu, B., Husain, S., Pladevega, A., Lai, L., Vanderford, T. H., Chennareddi, L., Silvestri, G., Freeman, G. J., Ahmed, R., and Amara R. R. (2009). Enhancing SIV-specific immunity in vivo by PD-1 blockade. *Nature* *458*, 206–210.
- Verma, S., Weiskopf, D., Gupta, A., McDonald, B., Peters, B., Sette, A., Benedict, C.A. (2016). Cytomegalovirus-specific CD4 T cells are cytolytic and mediate vaccine protection. *J Virol* *90*, 650–658.
- Vieyra-Lobato, M. R., Vela-Ojeda, J., Montiel-Cervantes, L., Lopez-Santiago, R., and Moreno-Lafont, M. C. (2018). Description of CD8+ Regulatory T Lymphocytes and Their Specific Intervention in Graft-versus-Host and Infectious Diseases, Autoimmunity, and Cancer. *J Immunol Res* *2018*, 3758713.
- Vignali, D. A. A., Collison, L. W., and Workman C. J. (2008). How regulatory T cells work. *Nat Rev Immunol* *8*, 523–532.
- Vremec, D., Pooley, J., Hochrein, H., Wu, L., and Shortman, K. (2000). CD4 and CD8 expression by dendritic cell subtypes in mouse thymus and spleen. *J Immunol* *164*, 2978-2986.
- Wagner, C.S., Grotzke, J.E., and Cresswell, P. (2012). Intracellular events regulating cross-presentation. *Front Immunol* *3*, 138.
- Wallet, M.A., Sen, P., and Tisch, R. (2005). Immunoregulation of dendritic cells. *Clin Med Res* *3*, 166-175.
- Welsh, R.M., Brubaker, J.O., Vargas-Cortes, M., and O'Donnell, C.L. (1991). Natural killer (NK) cell response to virus infections in mice with severe combined immunodeficiency. The stimulation of NK cells and the NK cell-dependent control of virus infections occur independently of T and B cell function. *J Exp Med* *173*, 1053-1063.
- Welten, S.P.M., Yermanos, A., Baumann, N.S., Wagen, F., Oetiker, N., Sandu, I., Pedrioli, A., Oduro, J.D., Reddy, S.T., Cicin-Sain, L. (2020). Tcf1+ cells are required to maintain the inflationary T cell pool upon MCMV infection. *Nat Commun* *11*, 2295.
- Weninger, W., Manjunath, N., and von Andrian, U.H. (2002). Migration and differentiation of CD8+ T cells. *Immunol Rev* *186*, 221-233.
- Wherry, E.J., and Ahmed, R. (2004). Memory CD8 T-cell differentiation during viral infection. *J Virol* *78*, 5535-5545.

- Wherry, E.J., Teichgraber, V., Becker, T.C., Masopust, D., Kaech, S.M., Antia, R., von Andrian, U.H., and Ahmed, R. (2003). Lineage relationship and protective immunity of memory CD8 T cell subsets. *Nat Immunol* 4, 225-234.
- Wills, M.R., Mason, G.M., and Sissons, J.G.P. (2013). Adaptive cellular immunity to human cy- tomegalovirus. In *Cytomegaloviruses: From Molecular Pathogenesis to Intervention*, M.J. Reddehase, ed. (Wymondham, Norfolk, United Kingdom: Caister Academic Press), pp. 142–172.
- Wirtz, N., Schader, S.I., Holtappels, R., Simon, C.O., Lemmermann, N.A., Reddehase, M.J., and Podlech, J. (2008). Polyclonal cytomegalovirus-specific antibodies not only prevent virus dissemination from the portal of entry but also inhibit focal virus spread within target tissues. *Med Microbiol Immunol* 197, 151-158.
- Wright, J.F., Kurosky, A., and Wasi, S. (1994). An endothelial cell-surface form of annexin II binds human cytomegalovirus. *Biochem Biophys Res Commun* 198, 983-989.
- Xiao, Z., Casey, K.A., Jameson, S.C., Curtsinger, J.M., and Mescher, M.F. (2009). Programming for CD8 T cell memory development requires IL-12 or type I IFN. *J Immunol* 182, 2786-2794.
- Yan, J., Liu, B., Shi, Y., and Qi, H. (2017). Class II MHC-independent suppressive adhesion of dendritic cells by regulatory T cells in vivo. *J Exp Med* 214, 319-326.
- Zanna, M.Y., Yasmin, A.R., Omar, A.R., Arshad, S.S., Mariatulqabtiah, A.R., Nur-Fazila, S.H., and Mahiza, M.I.N. (2021). Review of Dendritic Cells, Their Role in Clinical Immunology, and Distribution in Various Animal Species. *Int J Mol Sci* 22.
- Zhang, X., Sun, S., Hwang, I., Tough, D. F., and Sprent, J. (1998). Potent and Selective Stimulation of Memory-Phenotype CD8+ T Cells In Vivo by IL-15. *Immunity* 8, 591–599.
- Zhang, S., Xiang, J., van Doorselaere, J., and Nauwynck, H.J. (2015). Comparison of the pathogenesis of the highly passaged MCMV Smith strain with that of the low passaged MCMV HaNa1 isolate in BALB/c mice upon oronasal infection. *Vet Res* 46, 94.
- Zheng, S.G., Wang, J., Wang, P., Gray, J.D., and Horwitz, D.A. (2007). IL-2 is essential for TGF-beta to convert naive CD4+CD25- cells to CD25+Foxp3+ regulatory T cells and for expansion of these cells. *J Immunol* 178, 2018-2027.

Zheng, J., Liu, Y., Liu, Y., Liu, M., Xiang, Z., Lam, K.T., Lewis, D. B., Lau, Y.L., and Tu, W. (2013). Human CD8⁺ regulatory T cells inhibit GVHD and preserve general immunity in humanized mice. *Sci Transl Med* 5, 168ra9.

Zhu, B., Wu, Y., Huang, S., Zhang, R., Son, Y.M., Li, C., Cheon, I.S., Gao, X., Wang, M., Chen, Y., Zhou, X., Nguyen, O., Phan, A.T., Behl, S., Taketo, M.M., Mack, M., Shapiro, V.S., Zeng, H., Ebihara, H., Mullo, J.J., Edell, E.S., Reisenauer, J.S., Demirel, N., Kern, R.M., Chakraborty, R., Cui, W., Kaplan, M.H., Zhou, X., Goldrath, A.W., Sun, J. (2021). Uncoupling of macrophage inflammation from self-renewal modulates host recovery from respiratory viral infection. *Immunity* 54, 1200-1218.e9.

7 Curriculum Vitae

8 Scientific Achievements

Oral presentations

3rd AKDC Meeting of the German Society of Immunology

6th – 8th February 2019, Budenheim, Germany

Title: Immunomodulation of cytomegalovirus latency and reactivation by regulatory T cells
and dendritic cells

IMM Retreat

11th – 14th July 2019, Auch, France

Title: Immunomodulation of cytomegalovirus latency and reactivation by regulatory T cells
and dendritic cells

Poster presentations

IRTG Retreat

21st – 23rd November 2019, Deidesheim, Germany

Title: Immunomodulation of cytomegalovirus latency and reactivation by regulatory T cells
and dendritic cells

9 Acknowledgements

10 Eidesstattliche Erklärung

Hiermit versichere ich, dass die vorliegende Arbeit selbstständig und nur mit zur Hilfenahme der angegebenen Quellen angefertigt habe. Weiterhin wurde die Dissertation noch keiner anderen Fakultät oder Universität zur Prüfung vorgelegt.

Datum

J.Schwarz